Theoretical Studies of Reactions Involving Ion-Neutral Complexes

by

Andrew James Chalk

A thesis submitted for the degree of Doctor of Philosophy at the Australian National University

Research School of Chemistry

December 1998

Declaration

The work described in this thesis is my own, except where otherwise stated, and has not been submitted for any other degree. This work was carried out in the Research School of Chemistry at the Australian National University from the period 1995-1998 during the tenure of an Australian Postgraduate Award.

Andrew James Chalk

Acknowledgements

Firstly, my thanks go to my supervisor, Prof. Leo Radom, for his patience, useful suggestions and assistance over the last 4 years.

Thanks also to Dr. Michael Collins and Dr. Paul Mayer for many helpful discussions, especially concerning the work in Chapter 3. Dave Smith, Chris Parkinson and Paul Mayer also deserve thanks for proofreading parts of this thesis. The past and present members of the Radom Group who have not already been mentioned, including 'Astro' Allan East, Athanassios Nicolaides, James 'Jimmy' Gauld, Stefan Senger, Danne Rasumussen, Hans Heuts, Axel Schulz, Micha Hartmann, Theis 'Prince Charnwood' Sølling and Tony Scott have made my stay in the RSC a pleasant and enjoyable experience. Other members of the RSC including Gary Ayton, Ian Hamilton, Vern Cook, Stuart Barrow, Mark McDonald and Owen Jepps and all the Bramley's Bar regulars are also acknowledged.

The ANU Supercomputer Facility has made generous allocations of time on their machines, without which most of this work would not have been possible.

The financial support of an Australian Postgraduate Award is also gratefully acknowledged.

I express my sincere gratitude to my family who have provided me with so much support, both emotionally and financially, during my university career. It would have been impossible to get this far without their help. Finally, to Belinda, thanks for everything, especially for putting up with my many moods during the last few months.

Publications

Parts of the work described in this thesis have been published:

(1) Proton Transport Catalysis: A Systematic Study of the Rearrangement of the Isoformyl Cation to the Formyl Cation.

Chalk, A. J.; Radom L. *J. Am. Chem. Soc.* **1997**, *119*, 7573.

(2) The Importance of Ion-Neutral Complexes in Gas-Phase Ionic Reactions: Fragmentation of $[CH_3CH_2OCH_2]+$ as a Prototypical Case.

Chalk, A. J.; Radom L. *J. Am. Chem. Soc.* **1998**, *120*, 8430.

(3) Ion-Transport Catalysis: Catalyzed Isomerizations of NNH^+ and $NNCH_3^+$.

Chalk, A. J.; Radom L. *J. Am. Chem. Soc.* Accepted for Publication.

(4) Rearrangement and Fragmentation Pathways of $[C_3H_7X]+$ Ions (X = NH and S): Are Ion-Neutral Complexes Important?

Chalk, A. J.; Radom L. Submitted for Publication.

(5) The Involvement of Ion-Neutral Complexes in Ethylene Loss from $[PhC(CH_3)_2]^+$ and Its Isomers.

Chalk, A. J.; Radom L. Submitted for Publication.

Summary

Conventional ab initio molecular orbital calculations have been used to investigate a number of related systems where ion-neutral complexes may play an important role. Particular attention is paid to the characterization of previously proposed mechanisms involving these species.

An overview of the theoretical methods used throughout this thesis is presented in Chapter 1 and a brief discussion of the experimental techniques referred to in this work can be found in Chapter 2.

In Chapter 3, the potential energy surface for rearrangement and fragmentation of $[CH_3CH_2OCH_2]^+$ is characterized. Ion–neutral complexes are found to play a crucial role in the lowest energy decomposition leading to elimination of water. RRKM calculations on the calculated potential energy surface are found to give results consistent with the experimentally observed metastable ion elimination products and with the results of various deuterium- and ^{13}C-labeling experiments. The consequences of producing $[CH_3CH_2OCH_2]^+$ by isomerization from $[CH_3CHOCH_3]^+$ and of producing $[CH_3CH_2CHOH]^+$ by isomerization from $[CH_3C(OH)CH_3]^+$ on the rearrangement/fragmentation behavior are examined and found to be nicely consistent with experimental observations. Experimental thermochemical quantities such as rate-limiting barriers and heats of formation are found generally to be in good agreement with calculated values.

The potential energy surfaces for rearrangement/fragmentation of various $[C_3H_8N]^+$ and $[C_3H_7S]^+$ isomers are examined in Chapter 4. In contrast to the behavior in the corresponding $[C_3H_7O]^+$ system (Chapter 3), it is found that ion-neutral complexes are only of minor importance in determining the fragmentation characteristics. Either

dissociation of such complexes occurs too fast due to a large barrier to their formation ($[C_3H_8N]^+$ system), or alternative lower-energy rearrangement routes that do not involve ion-neutral complexes are available ($[C_3H_7S]^+$ system). Calculated thermochemical quantities such as heats of formation and reaction barriers are found to be in reasonable agreement with experimental results. Metastable ion product abundances and results of both deuterium- and ^{13}C-labeling experiments are rationalized in terms of the calculated potential energy surfaces and rate constants obtained using RRKM theory.

The potential energy surfaces for ethylene loss from various $[C_9H_{11}]^+$ ions are examined in Chapter 5. Good agreement between the theoretical predictions and available experimental thermochemical data is found. We characterize an alternative pathway to the 'phenylated cyclopropane' mechanism originally proposed to explain the results of ^{13}C-labeling studies of ethylene elimination from $[PhC(CH_3)_2]^+$. This alternative mechanism is found to be consistent with experimental results of both ^{13}C- and deuterium-labeling experiments. We also examine the mechanism for ethylene loss and label exchange for several other isomeric $[C_9H_{11}]^+$ ions. It is found that the ^{13}C-label exchange observed in protonated allylbenzene and some of the deuterium-labeling results for other ions can be explained by the intervention of intermediate ion-neutral complexes. Comparisons are made with the work on related $[C_3H_6X]^+$ ions (X= OH, SH and NH_2) presented in Chapters 3 and 4.

The effect of interaction with a series of small neutral molecules (X = He, Ne, Ar, CO, HF, N_2, H_2O and NH_3) on the barrier for rearrangement of the isoformyl cation (HOC^+) to the formyl cation (HCO^+) is examined in Chapter 6. Interaction with species (He, Ne and Ar) whose proton affinities are *less than* that of CO at oxygen leads to a reduction in the barrier from the value (147 kJ mol^{-1}) in the isolated system, but the barrier remains positive. Interaction with molecules (HF and N_2) whose proton affinities lie *between* the proton affinities of CO at O and at C leads to the barrier becoming negative, thus allowing proton migration to take place without an overall barrier. Finally,

interaction with molecules (H_2O and NH_3) whose proton affinities are *greater than* that of CO at C leads to a further lowering of the barrier; however, proton transfer to X rather than proton migration from O to C becomes energetically preferred. The most effective proton-transport catalysts for the rearrangement of HOC^+ to HCO^+ are thus molecules whose proton affinities lie between those of CO at O and at C.

In Chapter 7, the effect of interaction with a range of neutral molecules (X) on the barrier to the degenerate proton-transport reactions in NNH^+ (X = Ar, HF, CO, N_2 and H_2O) and methyl-cation-transport reactions in $NNCH_3^+$ (X = HF, H_2, N_2, HCl and H_2O) is examined. It is found that the barriers to both proton and methyl-cation transport are lowered from their values in the isolated ions of 182 kJ mol^{-1} and 152 kJ mol^{-1}, respectively, by interaction with species having values of the proton or methyl-cation affinity, respectively, lower than that of molecular nitrogen. Interaction with species that have larger values of proton or methyl-cation affinities leads to a further lowering of the barrier but transfer to the neutral molecule X becomes the more energetically favorable process in such cases. It is found that the ideal catalyst for ion transport should have an ion affinity close to but less than that of molecular nitrogen and have a large dipole moment.

Table of Contents

Introduction

The main aim of this thesis is to use ab initio molecular orbital theory to examine the involvement of ion-neutral complexes in a number of systems. An ion-neutral complex is a weakly-bound species in which a neutral molecule and an ion are held together by attractive electrostatic interactions. The interaction energy of an ion-neutral complex, ignoring rotational effects, is given approximately by the following expression,

$$V(r) = -\frac{\mu q \cos\theta}{r^2} - \frac{\alpha q^2}{2r^4}$$

where the two components are separated by a distance r, q is the charge of the ion, μ and α are the dipole moment and polarizability of the neutral, respectively, and θ is the angle of the dipole with respect to the charge. The first term represents the interaction with the charge and the permanent dipole of the neutral, while the second term is the charge–induced-dipole interaction.

Since the first proposal of an ion-neutral complex as an intermediate over 40 years ago, many studies have been made as to the importance of these species in ionic reactions. The electrostatic interactions described above often allow formation of a complex from a conventionally bonded ion, and subsequent rearrangement, to occur below the energy required for dissociation of the complex. In addition, the loose nature of the bonding can allow reactions, such as reorientation of the two species, to occur that would be impossible via conventionally bonded intermediates.

The experimental study of ion-neutral complexes can be rather difficult. The intermediacy of ion-neutral complexes can be inferred from various experimental results, but the direct observation of these species as intermediates is not easy. By the use of ab initio calculations, it is relatively straightforward to examine mechanisms involving ion-

neutral complexes and to characterize any intermediates in detail. Since the species exist in the gas-phase, ab initio calculations are ideally suited to their study and are becoming an increasingly important tool in the field of ion chemistry.

High-level ab initio calculations are used to study the involvement of ion-neutral complexes in a number of separate, though related, systems. Mechanisms that have previously been proposed based on experimental data are examined by ab initio calculations and in some cases these mechanisms are modified, or new ones suggested, in light of the calculated results. We also make comparisons between the various systems in order to examine some of the factors determining the involvement of ion-neutral complexes as intermediates and examine how the properties of the neutral can affect the structures and stabilization energies of these species.

Chapter 1

Theoretical Methods

1.1 Introduction

Any system of particles can be described by the laws of quantum mechanics and, in principle, it is possible to calculate any observable property of the system using these laws. However, in practice, the resulting equations are intractable for all but the simplest systems, e.g. the hydrogen atom. In order for these equations to be soluble, they must be simplified by the use of various approximations. The so-called ab initio methods achieve this using only the laws of quantum mechanics, along with the fundamental constants of nature, e.g. the speed of light and Planck's constant, and various rigorously defined mathematical approximations.

Ab initio methods are becoming an increasingly important tool in the study of chemical systems since they do not suffer from problems that can make experimental study of certain systems extremely difficult or impossible. Systems involving highly reactive species or transition structures, for example, can be relatively simply studied by ab initio calculations. The ion-neutral complexes studied in this thesis fit into this category. It is quite difficult to confirm the involvement of ion-neutral complexes in ionic reaction mechanisms by experimental means, but relatively simple to do so by the use of ab initio calculations. Continued advances in computer technology has meant that larger molecules than ever before can be investigated by the methods described in this chapter.

This chapter presents a brief overview of the theoretical methods used in this thesis. More detailed discussions of these and other methods can be found elsewhere.[1–4]

1.2 The Schrödinger Equation

The state of almost any system can be described by the time-independent Schrödinger equation,[5] which is most simply written as,

$$H\Psi = E\Psi \tag{1.1}$$

where H is the Hamiltonian operator (described below), Ψ is the wavefunction and E is the total energy of the system. The Hamiltonian operator (H) can be divided into two components, corresponding to the kinetic and potential energy, i.e.

$$H = T + V \tag{1.2}$$

where T and V are the kinetic and potential energy operators, respectively.

For a molecular system, the Hamiltonian operator can be written in atomic units as follows,[3]

$$H = -\sum_{i=1}^{N_e}\frac{\nabla_i^2}{2} - \sum_{a=1}^{N_n}\frac{\nabla_a^2}{2M_a} - \sum_{i=1}^{N_e}\sum_{a=1}^{N_n}\frac{Z_a}{r_{ia}} + \sum_{i=1}^{N_e}\sum_{j>i}^{N_e}\frac{1}{r_{ij}} + \sum_{a=1}^{N_n}\sum_{b>a}^{N_n}\frac{Z_a Z_b}{r_{ab}} \tag{1.3}$$

where i and j represent the ith and jth electrons, a and b are the ath and bth nuclei, M_a is the mass of the ath nucleus relative to that of an electron, Z_a is the charge on nucleus a and r_{xy} is the distance between the particles x and y. The first two terms represent the kinetic energy of the electrons and nuclei, respectively, while the remainder represent the potential energy.

1.3 The Born-Oppenheimer Approximation

The complexity of Equation 1.3 can be reduced somewhat by employing a simple approximation, known as the Born-Oppenheimer approximation.[6] Since the nuclei are much heavier than the electrons, it is reasonable to suggest that the electrons can adjust rapidly to any change of the nuclear configuration. Hence, we can separate the Hamiltonian (1.3) into nuclear and electronic components, allowing the calculation of the energy at a fixed nuclear configuration. The electronic Hamiltonian is shown in Equation 1.4 below,

$$H = -\sum_{i=1}^{N_e} \frac{\nabla_i^2}{2} - \sum_{i=1}^{N_e} \sum_{a=1}^{N_n} \frac{Z_a}{r_{ia}} + \sum_{i=1}^{N_e} \sum_{j>i}^{N_e} \frac{1}{r_{ij}} \qquad (1.4)$$

The hypersurface describing the variation of energy with nuclear position for a given electronic state is known as the potential energy surface (PES).

This approximation allows the nuclear motion to be ignored, but the equations still have no analytic solutions except for one-electron systems (e.g. H_2^+). In order to make these methods generally applicable, approximations for treating the electron many-body problem must also be included.

1.4 Orbitals and the Basis Set Expansion

1.4.1 The Orbital Approximation

The Schrödinger equation (1.1) can be further simplified by assuming that the motion of each electron is independent. Hence, the wavefunction of the system can be expressed as a product of one-electron wavefunctions, referred to as spin-orbitals. Each

spin-orbital χ, is a product of a spatial function (molecular orbital) (ψ), which is dependent on the position of the electron, and a spin function, indicating the spin state of the electron.

In order that the wavefunction obey the Pauli exclusion principle, certain restrictions must be made. According to the exclusion principle, the wavefunction must be antisymmetric with respect to the interchange of electrons. A simple product of spin-orbitals is not adequate, since the resulting wavefunction is symmetric with respect to electron interchange. A wavefunction that does obey the exclusion principle can be formed from the determinant of the n-electron spin-orbital matrix,

$$\Psi = \frac{1}{\sqrt{n!}} \begin{vmatrix} \chi_1(1) & \chi_2(1) & \cdots & \chi_n(1) \\ \chi_1(2) & \chi_2(2) & \cdots & \chi_n(2) \\ \vdots & \vdots & & \vdots \\ \chi_1(n) & \chi_2(n) & \cdots & \chi_n(n) \end{vmatrix} \qquad (1.5)$$

where $\chi_i(j)$ indicates electron j occupying the spin orbital χ_i and the prefactor is a normalization constant. This expression is commonly referred to as a Slater determinant.[7]

1.4.2 The Basis Set Expansion

In practice, the spatial component of a spin-orbital is expanded in terms of a set of one-electron functions (ϕ_μ). Hence, the molecular orbitals can be written as,

$$\psi_i = \sum_{\mu=1}^{N} c_{\mu i}\phi_\mu \qquad (1.6)$$

where $c_{\mu i}$ are the molecular orbital coefficients. These functions ϕ_μ are known as basis functions. When the atomic orbitals of the substituent atoms are used as basis functions, the method is known as a linear combination of atomic orbitals (LCAO).

1.5 The Variational Theorem

An important theorem in quantum mechanics is the variational theorem,[1-4] which states that the energy (E_{approx}) of an approximate wavefunction (Ψ_{approx}) is an upper bound to the exact energy (E_{exact}), i.e.

$$E_{approx} = \frac{\int \Psi^*_{approx} \mathbf{H} \Psi_{approx}\, d\tau}{\int \Psi^*_{approx} \Psi_{approx}\, d\tau} \geq E_{exact} \qquad (1.7)$$

By the use of this theorem, it is possible to optimize the molecular orbital coefficients ($c_{\mu i}$) in order to obtain the minimum total energy. This will give the best wavefunction possible within the constraints of the approximations used. Methods that give wavefunctions obeying Equation 1.7 are said to be variational.

1.6 Hartree-Fock (HF) Theory

After applying the variational theorem to an approximate N-electron wavefunction formed by the methods described above, we obtain the Roothaan-Hall equations,[8,9]

$$\sum_{\mu=1}^{N} c_{\mu i}(F_{\mu v} - \varepsilon_i S_{\mu v}) = 0 \qquad (1.8)$$

where $F_{\mu v}$ is the Fock matrix, ε_i is the energy of the molecular orbital ψ_i and $S_{\mu v}$ is the overlap matrix. Since the Fock matrix $F_{\mu v}$ is also dependent on the orbital coefficients $c_{\mu i}$, this equation must be solved iteratively until convergence of the energy and the orbital coefficients is achieved. Since this method treats each electron in a 'field' generated by all the other electrons, we can view this procedure in a more intuitive way. In effect, on each iteration, we are adjusting the field that each electron 'sees.' Convergence is achieved

when all electrons see the same field. This approach was first proposed by Hartree[10] and Fock[11] and is referred to as Hartree-Fock (HF) or self-consistent field (SCF) theory. The HF method is not only variational but it also correctly describes the behavior of molecules at large separation. The energy of two or more infinitely separated species calculated by this method will be equal to the sum of the energies of the isolated species. Methods exhibiting this property are known as size-consistent.

There are several variations of the HF method which deal with the treatment of open-shell systems. Since we are only concerned with closed-shell systems in this work, the reader is referred to standard texts for a discussion of the treatment of such systems.[1-4]

There are two fundamental limitations to the Hartree-Fock method. It ignores relativistic effects, but since these effects are only important for heavier atoms (e.g transition metals) they need not concern us here. The second, more serious limitation, is its neglect of electron correlation. Methods for including this are discussed below.

1.7 Electron Correlation

Although we can increase the number of basis functions in a Hartree-Fock calculation in order to obtain better results, there is a fundamental limitation to the accuracy of calculations based on this method. This deficiency occurs because of the assumption that the electrons are independent of one another. In a real system, the motion of electrons will be correlated to a certain extent. Hartree-Fock does include the small amount of electron correlation that results from electrons of like spins avoiding each other according to the Pauli exclusion principle. However, this is insufficient to properly describe a system. There are several approaches for the inclusion of electron correlation

into a wavefunction. For a recent review of the importance of electron correlation and methods for including it, see reference 12.

1.7.1 Full Configuration Interaction (FCI)

The solution to the Hartree-Fock equations for an n-electron and N-basis function system is a set of N spin orbitals (χ_i). Only the lowest n of these orbitals are occupied, the remainder being known as virtual orbitals. This set of occupied orbitals, or configuration as it is commonly referred to, is only one of a set of N!/((N-n)!n!) possible configurations. Other configurations can be obtained by exciting electrons from occupied to virtual orbitals, resulting in singly, doubly or higher excited configurations. These excitations are usually abbreviated to singles, doubles etc.

In order to improve the Hartree-Fock wavefunction, the full configuration interaction (FCI) method adds variationally determined amounts of all possible configurations to the Hartree-Fock wavefunction,

$$\Psi_{FCI} = \sum a_i \Psi_i \qquad (1.9)$$

where Ψ_0 represents the Hartree-Fock wavefunction, Ψ_i ($i > 0$) represent the various excitations of this wavefunction and a_i is known as the amplitude of the configuration. This wavefunction represents the most accurate that is possible within the limits of the basis set used. The FCI wavefunction is variational and size-consistent. In the limit of an infinite basis set, the FCI method gives the exact solution to the time independent Schrödinger equation. However, in practice, the computational cost of this method makes it impractical for treatment of all but the smallest systems.[13]

1.7.2 Quadratic Configuration Interaction

In light of the problems discussed above, it is desirable to truncate the CI expansion so that reasonable computation times can be obtained. This results in methods such as CIS (single excitations), CISD (single and double excitations) etc. However, it introduces another problem, in that the resulting methods are no longer size consistent. In order to eliminate this problem, the quadratic configuration interaction (QCI) family of methods was introduced.[14] They achieve size consistency by adding various terms to the CISD wavefunction. The resulting QCISD wavefunction contains contributions from single and double, as well as some quadruple excitations. Although this method is size consistent, it is not variational.

The QCISD wavefunction does not consider triple excitations, which can be important in some systems. The direct inclusion of triples (QCISDT) would make the calculation prohibitively expensive for larger systems. Hence, in the QCISD(T) method, the triple excitations are included in an approximate, and much cheaper, perturbative treatment.

In order to minimize the cost of QCISD(T) calculations, the core orbitals are often ignored for the purposes of correlation. Although core correlation will affect the total energy, it generally does not affect energy comparisons to any great extent. This so-called frozen-core approximation is used for all QCISD calculations in this work.

1.7.3 Møller-Plesset Perturbation Theory

Another common method for including electron correlation is perturbation theory, the most common form being Møller-Plesset perturbation theory.[15] Perturbation theory is concerned with finding the change in the energy that occurs when the wavefunction is

perturbed slightly. The wavefunction is written as a sum of the Hartree-Fock wavefunction and a perturbation,

$$H(\lambda) = H_0 + \lambda V \tag{1.10}$$

where λ is a dimensionless expansion parameter. We then write the perturbation (λV) as the difference between the Hartree-Fock Hamiltonian (H_0) and the exact Hamiltonian (H),

$$V = H - H_0 \tag{1.11}$$

According to Rayleigh-Schrödinger perturbation theory,[1-4] the wavefunction and energy are expanded as a Taylor series,

$$\Psi(\lambda) = \Psi^{(0)} + \lambda\Psi^{(1)} + \lambda^2\Psi^{(2)} + \ldots \tag{1.12}$$

$$E(\lambda) = E^{(0)} + \lambda E^{(1)} + \lambda^2 E^{(2)} + \ldots \tag{1.13}$$

With λ set to one, these expressions are truncated to various levels, giving the MPn series, e.g energy terms up to second order are included for MP2.

From an *n*th order wavefunction it is possible to calculate the energy up to order $2n+1$.[4] Hence, the MP2 and MP3 energies can be calculated from the first-order wavefunction and include only double excitations.[16] The MP4 energy must be calculated from the second-order wavefunction, which includes single, double, triple and quadruple excitations, with the triples contribution being the most time consuming part.[17] The MPn methods have the advantage of being size consistent but they are not variational.

1.8 Basis Sets

In section 1.4.2 the concept of basis functions was mentioned briefly. Here we go into more detail. Typically, basis functions are atom centered, i.e. atomic orbitals, although this isn't always the case. Two types of atom-centered functions are commonly used. Slater-type orbitals[18] (STOs) are characterized by an $\exp(-\zeta r)$ radial dependence. STOs are the exact solutions to the hydrogen atom problem and therefore provide a good description of atomic wavefunctions, properly reproducing the cusp at the nucleus for example. However, gaussian-type orbitals (GTOs), which are characterized by an $\exp(-\zeta r^2)$ radial dependence,[19] are the most commonly used basis functions. The main reason for this is that the calculation of the two-electron integrals for GTOs is much more efficient than for STOs. Although more gaussian functions will be needed to properly describe a given wavefunction, the efficient integral evaluation makes them the basis functions of choice. Gaussian-type basis functions are often expressed as a linear combination of primitive gaussian functions, g_i:

$$\phi_\mu = \sum_i d_{\mu i} g_i \qquad (1.14)$$

This type of basis function, known as a contracted gaussian, is used exclusively in this work.

1.8.1 Split-Valence Basis Sets

Split-valence basis sets are divided into core and valence components. This allows more basis functions, and therefore flexibility, to be given to the chemically important valence orbitals while keeping the number of basis functions to a minimum. Double-split-valence basis sets such as 6-31G[20] have one basis function per core orbital and two basis functions per valence orbital, while triple-split-valence basis sets (e.g. 6-

311G)[21] have one basis function for each core orbital and three basis functions per valence orbital. The notation 6-31G means that 6 primitive gaussians are used for each core orbital and sets containing three and one primitives are used for the valence orbitals. Several basis sets of this type are described below.

1.8.2 Polarization and Diffuse Functions

For the basis set types discussed above, the functions are all centered at the nucleus. However, in a molecule, the electron distribution around the nucleus can be polarized by interactions with other atoms, so that it is no longer centered at the nucleus. In order that the basis set is flexible enough to accurately describe any charge polarization, so-called polarization functions are employed. Polarization functions are higher angular momentum functions, which can combine with other functions in the basis set to allow charge polarization.

Diffuse functions are used to properly describe the outlying regions of the molecule. These functions are low angular momentum functions (*s* and *p*) with low exponents, i.e. they extend further away from the nucleus. Diffuse functions are needed to properly describe species with loosely bound electrons such as anions or species containing lone pairs.

1.8.3 Pople Basis Sets

The Pople basis sets used in this work have a rather simple nomenclature scheme that is illustrated by a number of examples below.

6-31G(d):[20] As for 6-31G described above with the addition of *d* polarization functions on heavy atoms (i.e non-hydrogen atoms).

6-311G(d,p):[21] The 6-311G basis with addition of *d* functions on heavy atoms and *p* functions on hydrogen.

6-311+G(d,p):[21] As above with the addition of diffuse (*s* and *p*) functions on heavy atoms.

6-311G(2df,p):[21,22] The 6-311G basis with two sets of *d* functions and a set of *f* functions on heavy atoms and one set of *p* functions on hydrogen.

1.8.4 Basis Set Superposition Error

Basis set superposition error (BSSE) is commonly thought to be only important in weakly interacting species. However, it occurs in any energy comparison using a finite basis set.[23] This work is most concerned with weakly interacting systems (ion-neutral complexes), hence, we restrict the discussion to such systems. There have been many studies concerning BSSE in the literature to date, and some recent examples are listed.[24]

BSSE is a consequence of the finite nature of the basis set used. It is manifested in complexes as an overestimation of the binding energy. This occurs since in a complex [A B], the basis set of A is supplemented by functions from B and vice versa. This means that each component will have its energy artificially lowered with respect to the isolated species, resulting in an overestimation of the binding energy. Several methods to overcome this problem have been proposed, but the simplest is the counterpoise method (CP) of Boys and Bernardi.[25] This method is illustrated below. The standard interaction energy can be written as follows,

$$\Delta E(AB) = E(AB) - E(A) - E(B) \qquad (1.15)$$

where all three species are in their equilibrium geometries. The BSSE correction is then written as,

$$BSSE = [E^B(A) - E(A)] + [E^A(B) - E(B)] \quad (1.16)$$

where $E^B(A)$ is the energy of A and both A and B are in their geometry within the complex. The corrected interaction energy can then be written as,

$$\Delta E_{corr}(AB) = \Delta E(AB) - BSSE \quad (1.17)$$

Although this treatment is simple, it does present some problems. The BSSE calculated by this method, although useful, is only an approximation to the true result. It can also be difficult to identify the two components of the complex, as discussed in more detail in Chapter 6. Many ways have been proposed to circumvent the problems of the counterpoise correction,[24] but the only sure method is to use a very large basis set.

Although many ion-neutral complexes are examined in this thesis, it is not essential that accurate interaction energies be known. Since we are examining the role of ion-neutral complexes as intermediates, it is the energy of the complex relative to other species that is important. In Chapter 6 it is shown that the effect of BSSE on potential energy surfaces is minor. Hence, we neglect the effects of BSSE for all but this test case.

1.9 Hierarchy of Methods

The relationship between basis set and electron correlation level is summarized in the Pople diagram[3] shown in Figure 1.1

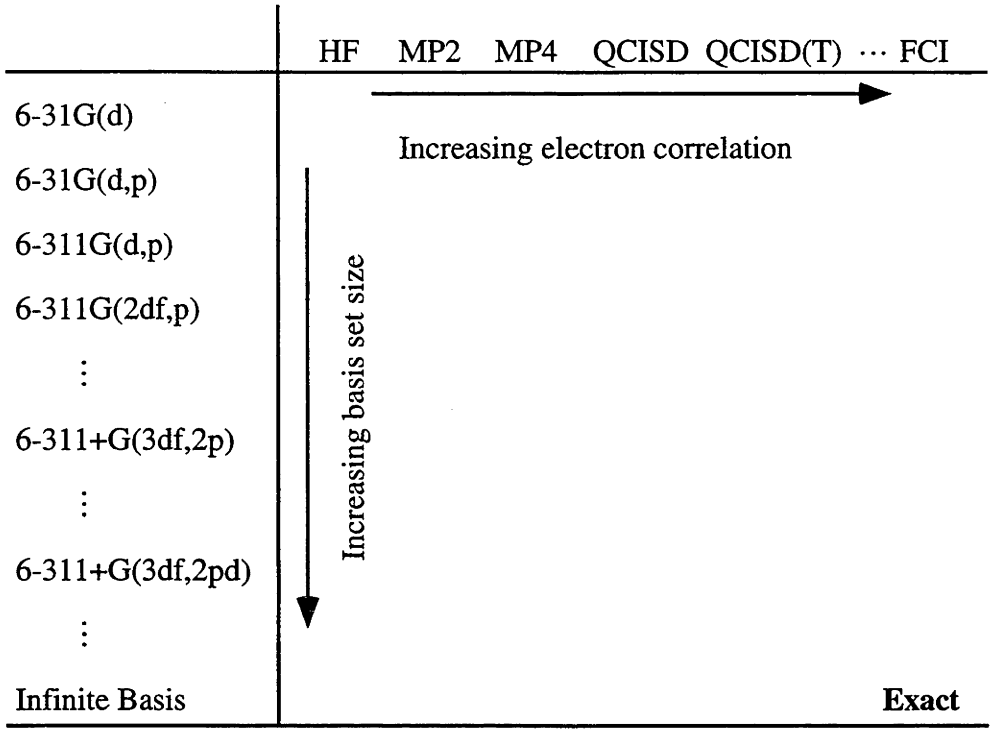

Figure 1.1 Pople diagram of ab initio methods.

At the top of Figure 1.1 are various treatments of electron correlation, with Hartree-Fock, which includes virtually no electron correlation, at the far left. Successively more accurate treatments of electron correlation are shown from left to right until FCI, which takes into account all the electron correlation within the limits of the basis set used, is reached. Going downwards, the basis sets become successively larger until an infinite basis set is reached. As we go down the diagonal of the figure, the calculations become more accurate until the exact solution to the non-relativistic Schrödinger equation is reached at the bottom right-hand corner. Since the increased accuracy also results in a greater computational cost, a balance must be struck between the desired accuracy and computational cost.

1.10 Geometry Optimization

For almost all computational problems, it is impractical to calculate the entire potential energy surface. It is often more convenient to locate points of interest on the surface, which are usually stationary points. These points are characterized by all the derivatives with respect to the 3N-6 (for a non-linear molecule) internal coordinates being equal to zero, i.e.

$$\frac{\partial E}{\partial r_i} = 0 \qquad \text{where i = 1, 2, 3 ... 3N-6.} \qquad (1.18)$$

There are two types of stationary points that are generally of interest to chemists. The first are local minima, corresponding to equilibrium structures. The second are first-order saddle points, which correspond to transition structures. The two types of stationary points can be distinguished by examining the eigenvalues of the Hessian, or force-constant matrix, formed by the second derivatives of the energy with respect to the coordinates,

$$\frac{\partial^2 E}{\partial r_i \partial r_j} \qquad \text{where i, j = 1, 2, 3 ... 3N-6.} \qquad (1.19)$$

Equilibrium structures are characterized by no negative eigenvalues of the Hessian, while first-order saddle points have one negative eigenvalue.

Efficient geometry optimization techniques,[4,26,27] for both minima and saddle points, are implemented into the Gaussian 94 program.[28] These allow stationary points to be located in a relatively straightforward manner for methods that have readily available analytic derivatives (HF, MP2, QCISD etc). Saddle-point optimizations usually require accurate knowledge of the potential energy surface and a good starting guess to converge to the correct structure. Hence, calculation of the second derivatives at the guess

geometry is usually necessary. The HF and MP2 methods are among those implemented in Gaussian 94 allowing the location of both stable geometries and transition structures using these methods to be relatively routine.

1.11 Vibrational Frequencies and Zero-Point Energies

Vibrational frequencies can be calculated by diagonalization of the force constant matrix (1.19), calculated by analytic or numerical second derivatives. The resulting values are known as normal-mode frequencies. An equilibrium structure is characterized by all frequencies being real while a first-order saddle point or transition structure has one imaginary frequency.

The harmonic approximation used in the calculation of normal mode frequencies leads to systematic errors, the calculated results usually being larger than the experimental fundamental frequencies.[29,30] Hence, the calculated frequencies are often scaled to take into account the effects of the neglect of anharmonicity, incomplete electron correlation and basis set deficiencies. Scaling factors for many methods and basis sets are available.[29]

These harmonic vibrations have a zero-point energy that is ignored in the calculation of the electronic energy of a species. Hence, this correction must be made if meaningful comparison with experimental energy differences is to be made. The zero-point vibrational energy (ZPVE) is given by:

$$\mathrm{ZPVE} = \frac{1}{2}\sum_i \nu_i \qquad (1.20)$$

where ν_i are the scaled vibrational frequencies in appropriate units. It should be noted that the optimum scaling factors for frequencies and zero-point energies often differ.[29]

1.12 Notation

In the remainder of this discussion, standard notation for describing a particular method will be used such as,

Method 1/Basis 1//Method 2/Basis 2

This means that a single-point energy calculation using Method 1 and Basis 1 (the Method 1/Basis 1 level) is performed on a geometry optimized using Method 2 and Basis 2 (the Method 2/Basis 2 level).

1.13 Compound Methods

1.13.1 Gaussian-2 (G2)

The Gaussian-2 (G2)[31] method aims to approximate the QCISD(T)/6-311+G(3df,2p)//MP2/6-31G(d) level of theory, with the addition of a zero-point energy correction. It achieves this by assuming the additivity of basis set and correlation effects as given by the following expressions:

$$E(G2) = E[MP4/6\text{-}311G(d,p)] + \Delta E(+) + \Delta E(2df) + \Delta E(QCI) + \Delta + HLC + ZPVE \quad (1.21)$$

where $\Delta E(+) = E[MP4/6\text{-}311+G(d,p)] - E[MP4/6\text{-}311G(d,p)]$,

$\Delta E(2df) = E[MP4/6\text{-}311G(2df,p)] - E[MP4/6\text{-}311G(d,p)]$,

$\Delta E(QCI) = E[QCISD(T)/6\text{-}311G(d,p)] - E[MP4/6\text{-}311G(d,p)]$,

$\Delta = E[MP2/6\text{-}311+G(3df,2p)] - E[MP2/6\text{-}311G(2df,p)] - E[MP2/6\text{-}311+G(d,p)] + E[MP2/6\text{-}311G(d,p)]$

and the higher level correction (HLC) is given by -0.005n Hartree for a closed-shell system, where n is the number of valence electron pairs. The zero-point vibrational energy correction (ZPVE) uses HF/6-31G(d) frequencies scaled by 0.8929.

The G2 method has been shown to generally perform to chemical accuracy (± 10 kJ mol^{-1}) for a range of thermochemical quantities, such as ionization energies, heats of formation and proton affinities.[32]

Several other variations of the G2 method are used in this work. In some circumstances, the standard level of optimization or ZPVE calculation may be inadequate for the task at hand. In several circumstances, we have altered G2 slightly to suit our needs, for example using MP2/6-31G(d,p) geometries to provide a better description of proton transport (Chapter 6). These variations are described in the relevant chapters.

1.13.2 G2(MP2,SVP)

The G2(MP2,SVP)[33] method is tailored towards larger systems where standard G2 methods would not be computationally feasible. The G2(MP2,SVP) method is formulated as follows,

$$E(G2(MP2,SVP)) = E[QCISD(T)/6\text{-}31G(d)] + E[MP2/6\text{-}311+G(3df,2p)] - E[MP2/6\text{-}31G(d)] + HLC + ZPVE \quad (1.22)$$

where HLC = –0.00532n Hartree and the ZPVE is the same as for G2.

This method takes out many of the most time-consuming calculations that are present in G2 so that larger systems can be studied. The much simpler additivity scheme also means that this method is generally not as accurate as G2. The G2(MP2,SVP)

method has been shown, however, to be more accurate than G2 for the calculation of heats of formation of hydrocarbons.[34]

1.14 Heats of Formation

The method used for the calculation of heats of formation in this work is based on that of Nicolaides et al.[35] This method is best illustrated by the example of the heat of formation of methane.

In this approach, the atomization energy (ΔH_0^{at} at 0 K) is calculated using the atomization reaction shown in Equation 1.23,

$$CH_{4(g)} \longrightarrow C_{(g)} + 4H_{(g)} \qquad \Delta H_0^{at} \qquad (1.23)$$

This can then be combined with experimental values for the heats of formation of $C_{(g)}$ and $H_{(g)}$ to give the heat of formation of methane at 0 K,

$$\Delta H_{f\,0}(CH_4) = \Delta H_{f\,0}^{exp}(C_{(g)}) + 4\Delta H_{f\,0}^{exp}(H_{(g)}) - \Delta H_0^{at} \qquad (1.24)$$

Often heats of formation are quoted at other temperatures, most notably 298 K. In order to calculate heats of formation at other temperatures, standard equations[35,36] can be used to calculate the temperature correction for the molecule in question. Temperature corrections for elements in their standard states are obtained from experimental results.

1.15 RRKM Theory

Several chapters in this work employ RRKM theory, named after Rice, Ramsperger, Kassel and Marcus. RRKM theory is also referred to as quasi-equilibrium

theory in the mass spectrometry literature. RRKM theory is similar to the more widely known transition state theory except that it is formulated in the microcanonical ensemble, i.e fixed energy, rather than the fixed temperature (canonical ensemble) used in transition state theory. A Boltzmann average of the RRKM rate constants will result in the transition state theory rate constant expression. RRKM theory is well suited to the study of metastable ions since they often have well defined energies (See Chapter 2), making RRKM theory a useful tool in the study of the kinetics of these ions. Here we present a brief overview of the RRKM method. More details can be found elsewhere.[37,38]

Before we discuss the RRKM formula, the two major assumptions it uses will be examined. The first is sometimes called the ergodicity assumption, which means that vibrational energy is rapidly (on the reaction time scale) spread amongst all modes. The second, known as the transition state assumption, is that one can choose a dividing surface separating reactants and products such that all trajectories passing through this surface go on to form products. The expression for the RRKM rate constant can be written as,

$$k(E) = \frac{\sigma N^{\dagger}(E - E_0)}{h\rho(E)} \qquad (1.25)$$

where E is the internal energy (relative to the reactant), E_0 is the energy of the transition structure, σ is the reaction path degeneracy, $N^{\dagger}(E\text{-}E_0)$ is the number of states in the transition structure with energy less than or equal to E, $\rho(E)$ is the density of states of the reactant at energy E and h is Planck's constant. The sum and density of states in this work have been calculated by a direct count of the vibrational states using the Beyer-Swinehart algorithm.[39]

Equation 1.25 is more easily understood by examining the effects responsible for determining the values of the numerator and denominator. The numerator represents the number of states in the transition structure at the given energy, which can be thought of as

the number of possible pathways through the transition structure. Hence, an increase in the number of states means that there are more ways to go through the transition structure and the rate is therefore increased. The denominator represents how dense the states are in the reactant at the given energy. A higher density of states in the reactant means that it will take longer for sufficient energy to reach the reaction coordinate and the reaction will therefore be slower.

In the dissociation reactions of ions or ion-neutral complexes, there is often no reverse barrier to dissociation and therefore no formal transition structure. It is possible to locate the transition structure variationally, but for the present studies it is sufficient to approximate the transition structure. This can be done in two ways depending on the situation. For dissociation of an ion-neutral complex, one can estimate the vibrational frequencies of the transition structure by scaling the lowest five or so frequencies of the complex to obtain a value of $\Delta S^{\dagger}$ expected for typical dissociation reactions (~ 12 J K^{-1} mol^{-1}). The value of $\Delta S^{\dagger}$ is not explicitly needed in the calculation of the rate constant, but allows us to guess frequencies corresponding to a 'loose' transition structure expected for these reactions.[38]

In a situation where an ion dissociates via an intermediate ion-neutral complex, the second method in which we simply assume that the transition structure for formation of the product complex is the same as that for dissociation can be used. Both these methods have been employed in this work.

1.16 Software and Units

All calculations in this work were performed using the VP-2200, VPP-300 and SGI Power Challenge of the Australian National University Supercomputing Centre and various IBM RS/6000 workstations using Gaussian 94[28] and MOLPRO.[40] All bond

lengths are measured in Ångstrom and all angles in degrees unless otherwise noted. All relative energies are in kJ mol^{-1} unless otherwise noted.

1.17 References

(1) Levine, I. N. *Quantum Chemistry;* 4th ed. ed.; Prentice-Hall: Englewood Cliffs, 1991.

(2) Szabo, A.; Ostlund, N. S. *Modern Quantum Chemistry: Introduction to Advanced Electronic Structure Theory*; Macmillan: New York, 1982.

(3) Hehre, W. J.; Radom, L.; Schleyer, P. v. R.; Pople, J. A. *Ab Initio Molecular Orbital Theory*; Wiley: New York, 1986.

(4) Jensen, F. *Introduction to Computational Chemistry*; John Wiley & Sons: Chichester, 1998.

(5) Schrödinger, E. *Phys. Rev.* **1926**, *28*, 1049.

(6) Born, M.; Oppenheimer, J. R. *Ann. Physik* **1927**, *84*, 457.

(7) Slater, J. C. *Phys. Rev.* **1929**, *34*, 1293.

(8) Roothaan, C. C. *Rev. Mod. Phys.* **1951**, *23*, 161.

(9) Hall, G. G. *Proc. Roy. Soc. London A* **1951**, *205*, 541.

(10) Hartree, D. R. *Proc. Cam. Phil. Soc.* **1928**, *24*, 89.

(11) Fock, V. Z. *Z. Phys.* **1930**, *61*, 126.

(12) Raghavachari, K.; Anderson, J. B. *J. Phys. Chem.* **1996**, *100*, 12960.

(13) Evangelisti, S.; Bendazzoli, G. L.; Ansaloni, R.; Durì, F.; Rossi, E. *Chem. Phys. Lett.* **1996**, *252*, 437.

(14) Pople, J. A.; Head-Gordon, M.; Raghavachari, K. *J. Chem. Phys.* **1987**, *87*, 5968.

(15) Møller, C.; Plesset, M. S. *Phys. Rev.* **1934**, *46*, 618.

(16) Krishnan, R.; Pople, J. A. *Int. J. Quantum Chem.* **1978**, *14*, 91.

(17) Krishnan, R.; Frisch, M. J.; Pople, J. A. *J. Chem. Phys.* **1980**, *72*, 4244.

(18) Slater, J. C. *Phys. Rev.* **1930**, *36*, 57.

(19) Boys, S. F. *Proc. Roy. Soc. London A* **1950**, *26*, 57.

(20) Ditchfield, R.; Hehre, W. J.; Pople, J. A. *J. Chem. Phys.* **1971**, *54*, 724.

(21) Krishnan, R.; Binkley, J. S.; Seeger, R.; Pople, J. A. *J. Chem. Phys.* **1980**, *72*, 650.

(22) Frisch, M. J.; Pople, J. A.; Binkley, J. S. *J. Chem. Phys.* **1984**, *80*, 3265.

(23) Jensen, F. **1996**,

(24) For recent examples, see: (a) Mayer, I.; Vibók, Á. *Mol. Phys.* **1997**, *92*, 503. (b) Tao, F-U. *J. Mol. Struct. (Theochem),* **1996**, *367*, 55. (c) Halàsz, G.; Vibók, Á.; Valiron, P.; Mayer, I. *J. Phys. Chem.* **1996**, *100*, 6332. (d) Abkowicz, J. A.; Latajka, Z.; Scheiner, S.; Chalasiñski G. *J. Mol. Struct. (Theochem),* **1995,** *342*, 153.

(25) Boys, S. F.; Bernardi, F. *Mol. Phys.* **1970**, *19*, 553.

(26) Schlegel, H. B. In *Modern Electronic Structure Theory, Part I*; D. R. Yarkony, Ed.; World Scientific Publishing: Singapore, 1995; Vol. 2.

(27) Peng, C. Y.; Ayala, P. Y.; Schlegel, H. B.; Frisch, M. J. *J. Comp. Chem.* **1996**, *17*, 49.

(28) Frisch, M. J.; Trucks, G. W.; Schlegel, H. B.; Gill, P. M. W.; Johnson, B. G.; Robb, M. A.; Cheeseman, J. R.; Keith, T. A.; Petersson, G. A.; Montgomery, J. A.; Raghavachari, K.; Al-Laham, M. A.; Zakrzewski, V. G.; Ortiz, J. V.; Foresman, J. B.; Cioslowski, J.; Stefanov, B. B.; Nanayakkara, A.; Challacombe M.; Peng, C. Y.; Ayala, P. Y.; Chen, W.; Wong, M. W.; Andres, J. L.; Replogle, E. S.; Gomperts, R.; Martin, R. L.; Fox D. J.; Binkley, J. S.; Defrees, D. J.; Baker, J.; Stewart J. P. P.; Head-Gordon, M.; Gonzalez, C.; Pople, J. A. GAUSSIAN 94, Revision D.1; Gaussian Inc.; Pittsburgh PA, 1995.

(29) (a) Pople, J. A.; Scott, A. P.; Wong, M. W.; Radom, L. *Isr. J. Chem.* **1993**, *33*, 345. (b) Scott, A. P.; Radom, L. *J. Phys. Chem.* **1996**, *100*, 16502.

(30) Schaefer, H. F.; Thomas, J. R.; Yamaguchi, Y.; DeLeeuw, B. J.; Vacek, G. In *Modern Electronic Structure Theory, Part I*; D. R. Yarkony, Ed.; World Scientific Publishing: Singapore, 1995; Vol. 2.

(31) Curtiss, L. A.; Raghavachari, K.; Trucks, G. W.; Pople, J. A. *J. Chem. Phys.* **1991**, *94*, 7221.

(33) For recent reviews on G2 theory, see: (a) Curtiss, L. A.; Raghavachari, K. In *Quantum Mechanical Electronic Structure Calculations with Chemical Accuracy*, (Ed.: Langhoff, S. R.), Kluwer Academic Publishers, Dordrecht, 1995. (b) Raghavachari, K.; Curtiss, L. A. In *Modern Electronic Structure Theory*, (Ed.: Yarkony, D. R.), World Scientific, Singapore, 1995.

(33) Curtiss, L. A.; Redfern, P. C.; Smith, B. J.; Radom, L. *J. Chem. Phys.* **1996**, *104*, 5148.

(34) (a) Nicolaides, A.; Radom, L. *Mol. Phys.* **1996**, *88*, 759. (b) Curtiss, L. A.; Raghavachari, K.; Redfern, P. C.; Pople, J. A. *J. Chem. Phys.* **1997**, *106*, 1063.

(35) Nicolaides, A.; Rauk, A.; Glukhovtsev, M. N.; Radom, L. *J. Phys. Chem.* **1996**, 17460.

(36) MacQuarrie, D. A. *Statistical Mechanics*; Harper & Row: New York, 1976.

(37) Gilbert, R. G.; Smith, S. C. *Theory of Unimolecular and Recombination Reactions*; Blackwell Scientific Publications: Oxford, 1990.

(38) Baer, T.; Mayer, P. M. *J. Am. Soc. Mass Spectrom.* **1997**, *8*, 103.

(39) Beyer, T.; Swineheart, D. F. *Comm. Assoc. Comput. Machines* **1973**, *16*, 379.

(40) MOLPRO is a package of *ab initio* programs written by H. J. Werner and P. J. Knowles with contributions from J. Almlof, R. D. Amos, M. J. O. Deegan, S. T. Elbert, C. Hampel, W. Meyer, K. Peterson, R. Pitzer, A. J. Stone, P. R. Taylor and R. Lindh.

Chapter 2

Experimental Gas-Phase Ion Chemistry

2.1 Introduction

Although the work in this thesis is entirely theoretical, much of it aims to rationalize results obtained by various experimental techniques. In later Chapters, the results of experimental studies are referred to frequently, so it is important to examine the methods employed to obtain these experimental results. Hence, an overview of the relevant experimental techniques is now presented.

2.2 Metastable Ions

Metastable ions are one of three types of ions that can be formed in the ion source of a mass spectrometer (See Figure 2.1). Stable ions leave the ion source and reach the detector without dissociation occurring. These are the ions typically observed in a normal mass spectrum. Unstable ions dissociate in the ion source, resulting in product ions in the normal mass spectrum. Metastable ions result from dissociations that occur on the microsecond timescale, i.e. outside the ion source. Product ions generated in the ion source can also be any of the three types. A large portion of this thesis focuses on the reactions of metastable ions, so here we examine commonly used experimental methods for examining these ions and the important results that can be obtained from their study. More detailed discussions on the subject of metastable ions can be obtained elsewhere.[1-5]

Metastable ions were originally observed as diffuse peaks in normal mass spectra, corresponding to non-integer *m/z* values. However, they can more conveniently be

examined in a double focussing mass spectrometer. An example of such an instrument, the Mass-Analyzed Ion Kinetic Energy (MIKE) Spectrometer, is shown schematically in Figure 2.1. Instruments where the electrostatic analyzer precedes the magnetic analyzer also exist.

A sequence of reactions that will result in the formation of a closed-shell metastable ion is summarized below,

$$AB \longrightarrow AB^{+\bullet} + e^- \qquad (2.1)$$

$$AB^{+\bullet} \longrightarrow A^+ + B^\bullet \qquad (2.2)$$

$$A^+ \longrightarrow C^+ + D \qquad (2.3)$$

Molecular ions ($AB^{+\bullet}$) are formed in the ion source via electron impact (Reaction 2.1) and dissociate to form the product ion A^+ via Reaction 2.2. This product ion leaves the ion source after about 10^{-6} s and is mass selected in the magnetic analyzer. The metastable ion A^+ fragments in the second field-free region via reactions such as 2.3, and the resulting ions (e.g. C^+) can be examined by the electrostatic analyzer. The electrostatic analyzer acts as a kinetic energy filter, with any ion having a specific kinetic energy

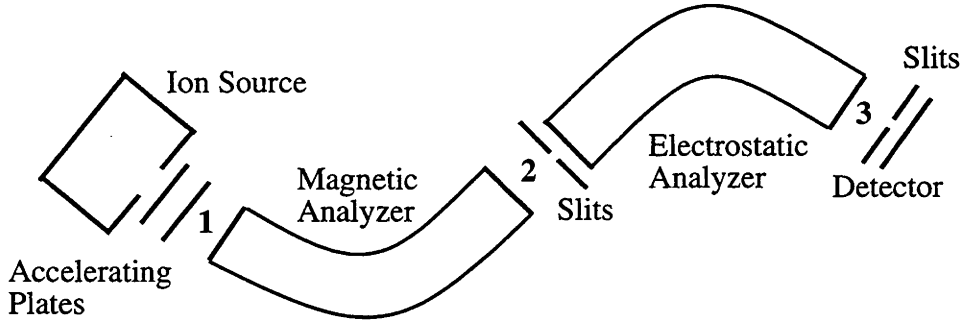

Figure 2.1 Schematic diagram of a Mass-Analyzed Ion Kinetic Energy (MIKE) Spectrometer. The numbers 1, 2 and 3 refer to field-free regions.

(proportional to the voltage applied across the analyzer) being focussed on the detector slits. The electrostatic analyzer voltage is scanned in order to obtain information about the fragmentation reactions occurring in the second-field free region from the metastable ion of interest.

The lifetime of a metastable ion is determined by the time it takes the ion to reach the second field-free region. Hence, it corresponds to a well-defined value, typically around 10^{-5} seconds, or a dissociation rate constant of $10^4 - 10^6$ s^{-1}. The long lifetime of

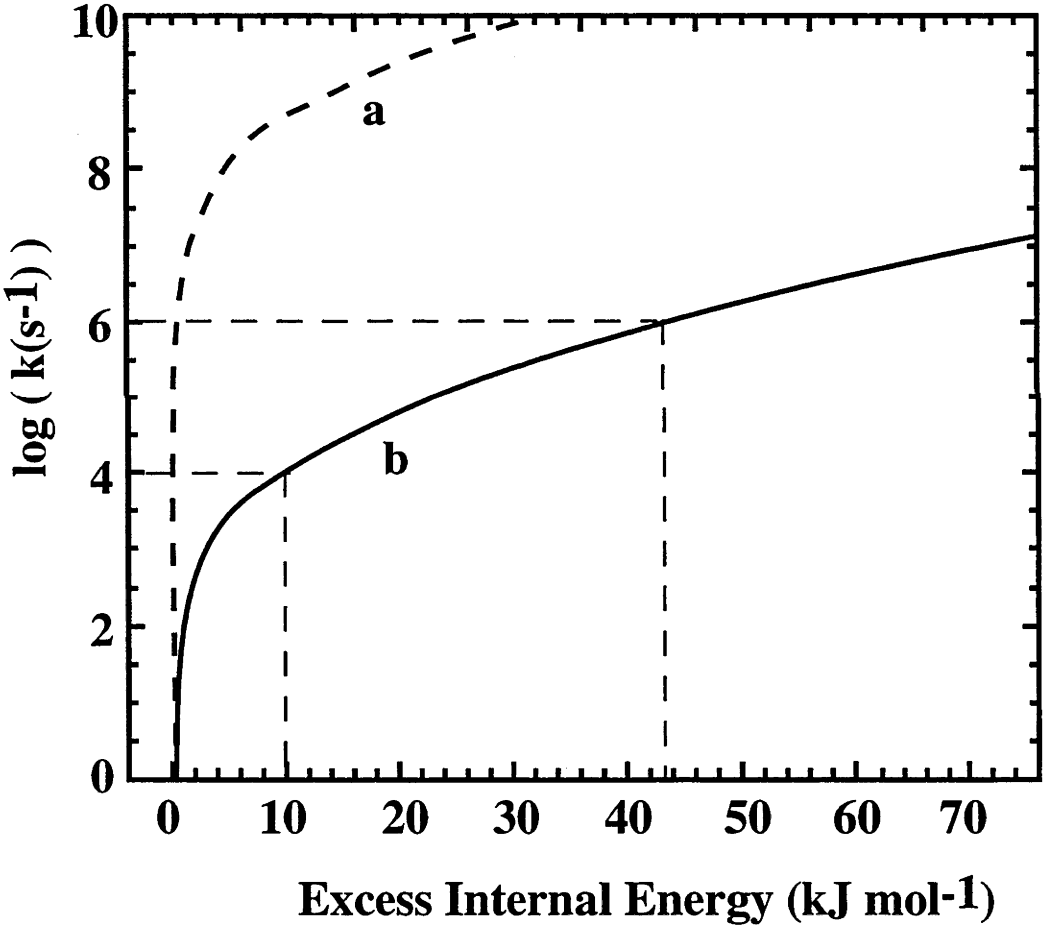

Figure 2.2 Log rate constant versus excess internal energy for processes involving (a) a loose transition structure and (b) a tight transition structure, having the same activation energy. The energy region corresponding to dissociation rates of $10^4 - 10^6$ s^{-1} is denoted by dashed lines.

a metastable ion has two important consequences. Dissociation of metastable ions will typically occur close to the threshold, i.e. the internal energy present in the ion will be only slightly greater than that required for dissociation. It can be seen from Figure 2.2 that for curve (a), which is representative of a dissociation reaction, the energy required to reach the relevant rate constant region is very close to the threshold at 0 kJ mol^{-1}. However, this is not always the case. Curve (b) in Figure 2.2 represents a situation where isomerization via a 'tight' transition structure (i.e. $\Delta S^{\dagger} < 0$) is the rate-limiting step. For the situation where isomerization to another ion, rather than dissociation, is the rate-limiting step, energies significantly above the threshold may be present in metastable ions. However, although the spread of energies in this case is larger, their range is still reasonably well defined. The long lifetime of a metastable ion also means that there is enough time to allow all energetically accessible configurations to be sampled, implying that only the lowest energy pathways will be observed.

2.2.1 Product Abundances

The relative abundances of metastable ion elimination products can be a useful tool in examining the mechanism and energetics of metastable ion dissociations. Since the lowest energy pathways usually dominate, insights into the nature of the potential energy surface can be gained by examining the product distributions. Several possible potential surfaces for the fragmentation and rearrangement of two metastable ions X^+ and Y^+ are presented in Figure 2.3. Figure 2.3a shows a potential energy surface where the two ions can interconvert prior to dissociation (arrows). In this situation, the metastable product abundances for ions formed initially as X^+ will be the same as those for ions formed as Y^+. In Figure 2.3b, a case where the energy of the barrier for interconversion of the two ions is greater than that required for dissociation is shown. In this situation, the two ions will have different product abundances. Finally, a rate-limiting isomerization of X^+ to Y^+, as shown in Figure 2.3c, will result in the two ions having the same elimination

product, but it will have greater internal energy when formed from X^+. This effect is discussed further in Section 2.2.3.

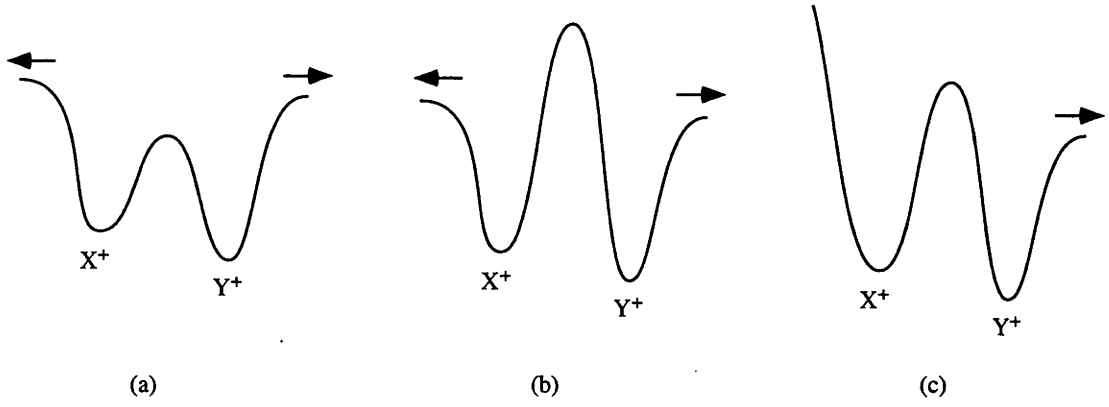

Figure 2.3 Schematic energy profiles for possible fragmentation and rearrangements of two ions.

Information on the nature of the rate-limiting step can be gained by examining product abundances in different field-free regions. Ions dissociating in the first field-free region do so with higher rate constants, and therefore internal energy, than ions in the second field-free region. The usefulness of this method is best illustrated by an example, the metastable ion $[CH_3CH_2OCH_2]^+$, which is discussed in further detail in Chapter 3. In the second field-free region, the metastable ion $[CH_3CH_2OCH_2]^+$ loses 95% water and 5% ethylene.[6] However, in the first field-free region, loss of 70% water and 30% ethylene is observed.[6] This indicates a situation where water loss is energetically favored but there is a 'tight' transition structure along the pathway to its formation, making it slower in the first field-free region.

2.2.2 Appearance Energies

The appearance energy corresponds to the energy required to reach the onset of a particular dissociation pathway. Using photoionization mass spectrometry or conventional mass spectrometers with monoenergetic electron sources, an accuracy of around ±5 kJ mol^{-1} can be obtained.[4] However, the experiments examined in later chapters generally use older methods that give less accurate results.

The factors determining the appearance energy (AE) are summarized in Figure 2.4. The appearance energy of the fragment ion (A^+) (see Equations 2.1-2.3) is the sum of the ionization energy of the neutral species (AB), plus the barrier to formation of A^+ (E_a) from AB, and the kinetic shift (E_s). Assuming that E_s is zero, in the absence of a reverse barrier (E_a^r) the appearance energy corresponds to the difference between the heats of formation of A^+ plus $B^\bullet$ and AB, allowing the derivation of unknown heats of formation from appearance energies. The kinetic shift (E_s) results from the fact that the fragmentation of an ion must occur with a particular rate constant, and therefore ion internal energy, to be observed on the timescale of the experiment. For reactions where the increase of rate constant with internal energy is slow, sufficient rates may not be reached until well above the threshold. Such processes include reactions having large barriers, 'tight' transition structures or large reactant molecules having many degrees of vibrational freedom. An example of the dependence of the rate constant on energy for a tight transition structure is shown as curve (b) in Figure 2.2. Examples of similar curves for other situations can be found elsewhere.[1,5,7] It can be seen from curve (b) in Figure 2.2 that a rate constant of 10^4 s^{-1} will not be achieved until an internal energy of about 10 kJ mol^{-1} above the threshold is reached. The kinetic shift results in the measured appearance energy being higher than it should be. Hence, quantities derived from appearance energies are an upper bound to the true value. Many examples of the consequences of chemical shift are discussed in Chapters 3 and 4.

If it is assumed that the reverse barrier (E_a^r) is small, it is also possible to use appearance energies to determine barriers for the dissociation processes of A^+. The appearance energy of the ion C^+ (Reaction 2.3) can be measured and combined with the heats of formation of AB, A^+ and $B^\bullet$, to derive the barrier for the production of C^+ from the metastable ion A^+. Inaccuracies in these heats of formation are an additional source of error in experimental barriers derived in such a manner.

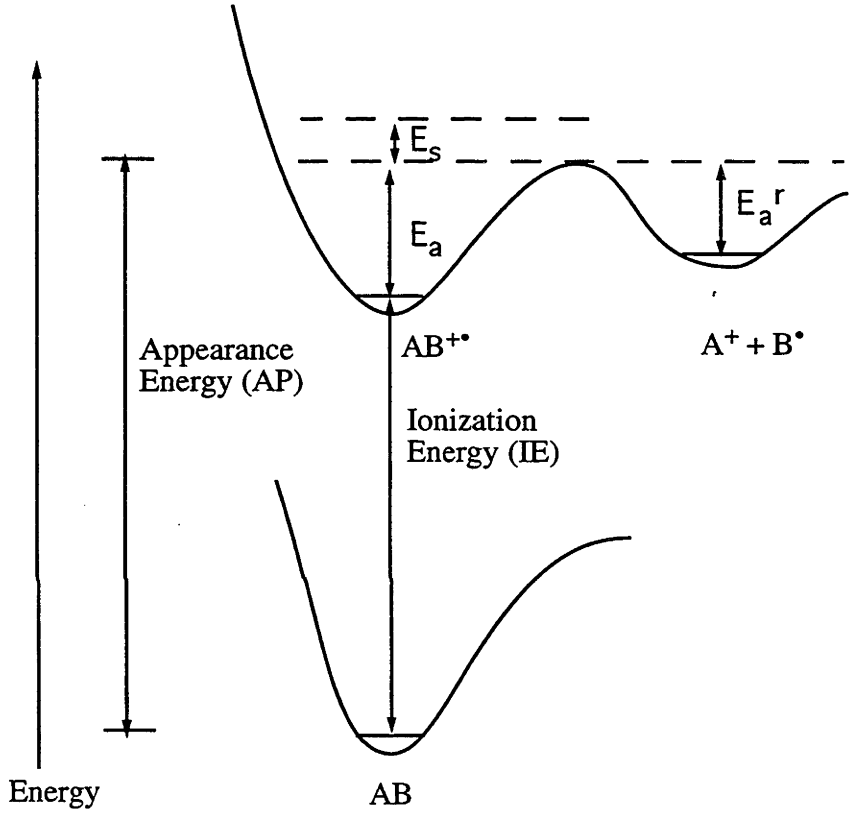

Figure 2.4 Schematic energy profile of ionization and dissociation of AB.

2.2.3 Kinetic Energy Release

A schematic potential energy surface for a dissociation reaction with a reverse barrier is shown schematically in Figure 2.5. The energy in the products resulting from the reverse barrier E_a^r will be partitioned into their internal energy (E_i), consisting of

vibrational and rotational components and translational energy (E_t). This translational energy is manifested in the relative kinetic energy of B^+ and C, with the energy of the former being observable in the mass spectrometer.

The decomposition of A^+ will result in the expulsion of the products in random directions, resulting in a broadening of the relevant peak. Broad flat-topped or 'dish' shaped peaks are often associated with large kinetic energy releases while thin gaussian shaped peaks indicate small amounts of kinetic energy release.[1-5] Hence, the width of the metastable peak can give an indication of the kinetic energy release accompanying a fragmentation reaction.

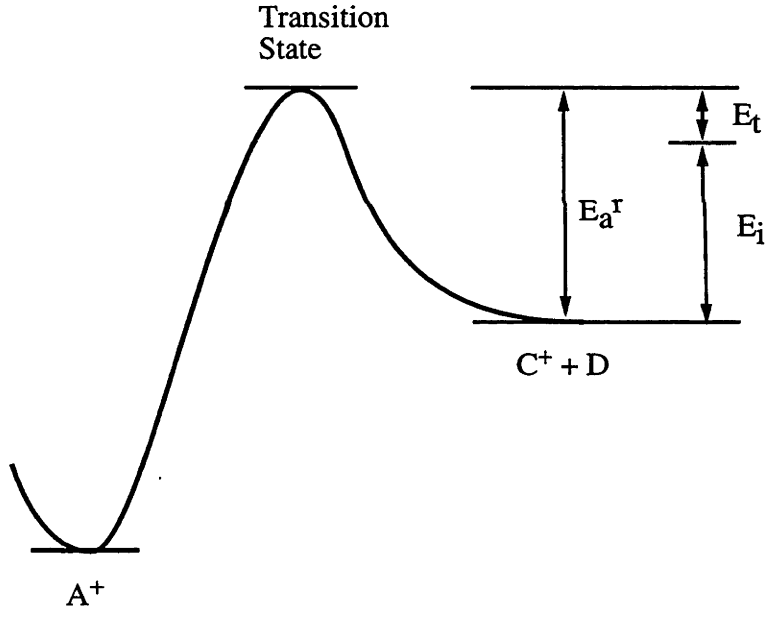

Figure 2.5 Schematic potential energy surface for a dissociation reaction having a reverse barrier.

Examination of the peak width can also give mechanistic information. The fact that two ions produce the some product with the same kinetic energy release provides evidence that they do so via a common intermediate.

2.2.4 Isotope Labeling

A powerful tool in mechanistic studies of metastable ions is isotope labeling. Parts of the molecule are labeled with heavy isotopes (usually deuterium or ^{13}C) and the isotope distribution in the product ions is examined. Labeling results may indicate that certain atoms become equivalent via reversible isomerization processes prior to dissociation. A common mechanism for hydrogen exchange in cations is 1,2-hydrogen shifts. Methyl and even phenyl-cation shifts can result in exchange of carbon atoms. Many examples of such processes can be found in Chapters 3, 4 and 5.

Isotope effects can also provide insight into the nature of the rate-determining step of a reaction. Since there will often be only small amounts of excess energy in the transition state, isotope effects can be quite large in metastable ions. Hence, the fact that $CH_3CD_3^{+\bullet}$ looses $H^\bullet$ and $D^\bullet$ in the ratio of 600:1[8] provides strong evidence that cleavage of a C–H bond is the rate-determining step for this reaction.

2.3 The Selected Ion Flow Tube

The selected ion flow tube, first introduced by Adams and Smith[9] in 1976 is a powerful tool in the study of ion reactivity.[10] The experimental studies of the proton-[10,11] and methyl-cation–transport[12] reactions discussed in Chapters 6 and 7 utilized the SIFT technique, so a brief overview of the flow tube and its use in the study of isomeric ions is now presented. The use of the SIFT technique for studies of isomeric ions has recently been reviewed.[10]

2.3.1 Instrumentation

A schematic diagram of the SIFT apparatus is shown in Figure 2.6.[9,10] The source gas is injected through the port on the left-hand side and ions are formed by electron impact. The ion of interest is selected in the mass filter and transmitted through the Venturi orifice, which maintains the pressure differential between the two chambers, into the flow tube. The helium buffer gas then carries the ions of interest to the right through the flow tube, where they can react with reactant gases injected through the inlets. The resulting ions are drawn in to the mass filter on the right and the product ion of interest is detected. Diffusion pumps allow each section to remain at the correct pressure.

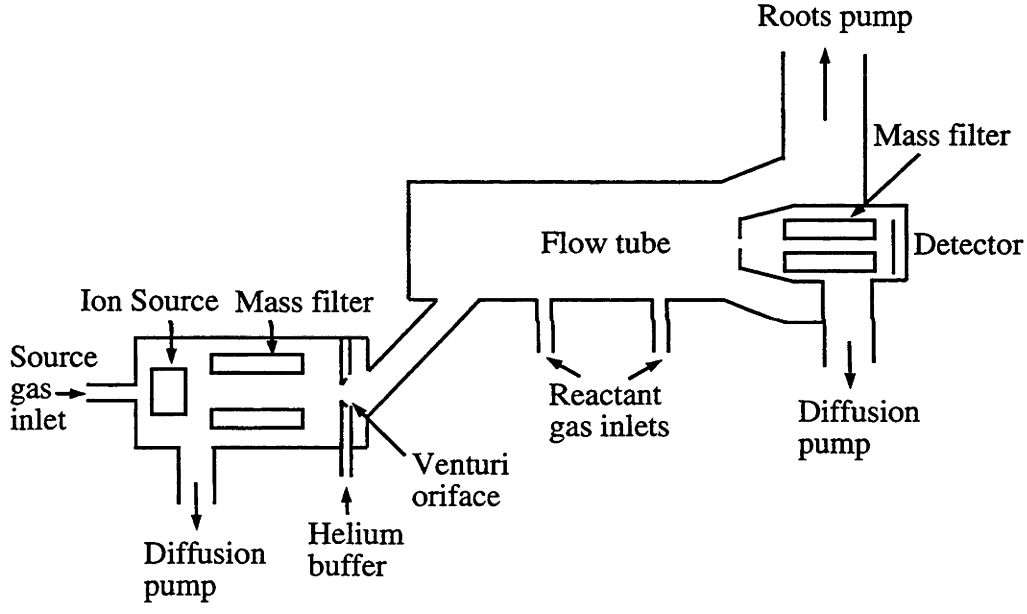

Figure 2.6 Schematic Diagram of a Selected Ion Flow Tube (SIFT)

The rate constant for a particular reaction can be obtained by plotting the log of the ion count for the reactant ion versus the flow rate of the neutral reactant gas. This usually results in a linear relation, with the slope being proportional to the rate constant for the reaction.

2.3.2 Isomer Identification

The instrument described above can only discriminate product ions by their *m/z* ratios and therefore cannot distinguish between isomers such as HOC^+ and CHO^+, since they have the same *m/z* ratio. However, it is possible to distinguish the different reactivities of such ions.[10] One such method is to choose a neutral reactant gas such that it reacts with the two isomers at different rates. The flow rate of the injected neutral is varied and the signal from the reactant ion is monitored. This results in a plot such as shown in Figure 2.7. The initial steep linear falloff of the ion signal results from the reaction of the monitor gas with the most reactive isomer. The reaction with the less reactive species results in the shallow falloff at the right of the plot. Analysis of these results can give both the rate constants for the two reactions and the relative abundances of the isomers involved. Now that the isomers can be discriminated, further reactions can be examined. For example, other reactant gases (e.g. proton-transport catalysts) can be injected and their effect on the ratio of the two isomers as a function of flow rate studied.

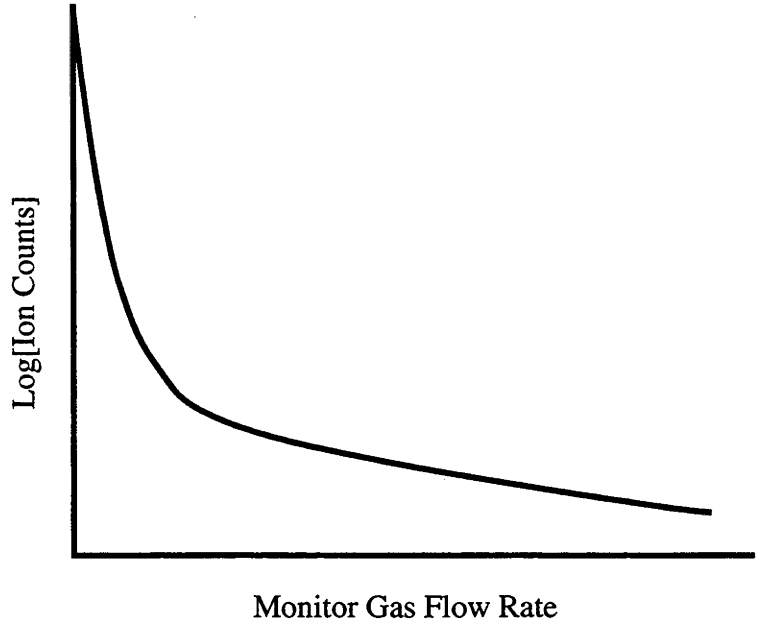

Figure 2.7 Monitor gas flow rate vs log[Ion Counts] for a mixture of two isomers

2.4 References

(1) Cooks, R. G.; Beynon, J. H.; Caprioli, R. M.; Lester, G. R. *Metastable Ions*; Elsevier: Amsterdam, 1973.

(2) Bowen, R. D.; Williams, D. H.; Schwarz, H. *Angew. Chem. Int. Ed. Engl.* **1979**, *18*, 451.

(3) Holmes, J. L.; Terlouw, J. K. *Org. Mass Spectrom.* **1980**, *15*, 383.

(4) Holmes, J. L. *Org. Mass Spectrom.* **1985**, *20*, 169.

(5) Levson, K. *Fundamental Aspects of Mass Spectrometry*; Verlag Chemie: Weinheim, 1978.

(6) Hvistendahl, G.; Williams, D. H. *J Am. Chem. Soc.* **1975**, *97*, 3097.

(7) Baer, T.; Mayer, P. M. *J. Am. Soc. Mass Spectrom.* **1997**, *8*, 103.

(8) Lohle, U.; Ottinger, C. *J. Chem. Phys.* **1969**, *51*, 3097.

(9) Adams, N. G.; Smith, D. *Int. J. Mass Spectrom. Ion Phys.* **1976**, *21*, 349.

(10) McEwan, M. J. In *Advances in Gas-Phase Ion Chemistry*; N. G. Adams and L. M. Babcock, Ed.; JAI Press: Greenwich, 1992.

(11) Freeman, C. G.; Knight, J. S.; Love, J. G.; McEwan, M. J. *Int. J. Mass Spectrom. Ion Proc.* **1987**, *80*, 255.

(12) Baranov, V.; Petrie, S.; Bohme, D. K. *J. Am. Chem. Soc.* **1996**, *118*, 4500.

Chapter 3

The Importance of Ion-Neutral Complexes in Gas-Phase Ionic Reactions: Fragmentation of $[CH_3CH_2OCH_2]^+$ as a Prototypical Case

3.1 Introduction

It is more than 40 years since Myerson invoked ion–neutral complexes to explain the loss of identity of labels in the benzyl ions produced from *t*-butylbenzene (see Chapter 5 for details).[1] Since that time, ion-neutral complexes have been found to be ubiquitous in gas-phase ionic reactions.[2] Simple electrostatics *demands* that when an ion encounters a neutral species in the gas phase, the energy initially decreases. This means that either the product is formed directly without a barrier, or there is the initial involvement of an ion–neutral complex before a barrier is surmounted on the way to the product. A classical example is the S_N2 reaction of X^- with CH_3Y for which the gas-phase reaction profile involves a reactant ion–neutral complex $[X\cdots CH_3Y]^-$ leading to a transition structure $[X\cdots CH_3\cdots Y]^-$ and then a product ion–neutral complex $[XCH_3\cdots Y]^-$.[3] In contrast, the text-book reaction profile of the S_N2 reaction in solution does not involve ion–neutral complexes but proceeds simply from reactants to the transition structure $[X\cdots CH_3\cdots Y]^-$ and then to products. The ion–neutral complexes lose their relevance when complexation with solvent, i.e. solvation, is possible.

Ion-neutral complexes have been postulated as intermediates in elaborate mechanisms that attempt to explain the formation of unusual products in gas-phase ionic reactions.[2] For example, the means by which H_2O is lost from $[CH_3CH_2OCH_2]^+$ is not at all obvious. However, its formation has been rationalized in terms of an imaginative

mechanism involving the participation of a series of ion–neutral complexes (Scheme 3.1).[4] It is not straightforward to experimentally verify the involvement of the postulated ion–neutral complexes and to characterize them in detail. In addition, it is not clear which species in mechanistic schemes such as Scheme 3.1 represent true intermediates on the potential energy surface, as opposed, for example, to transition structures. The term "transitional species" has been used to describe some of the less well defined entities.[2a] Although difficult to answer experimentally, such issues *can* be addressed theoretically. Both the ion–neutral complexes and the transition structures of Scheme 3.1 can be fully characterized and the reaction path joining the individual species can be followed.

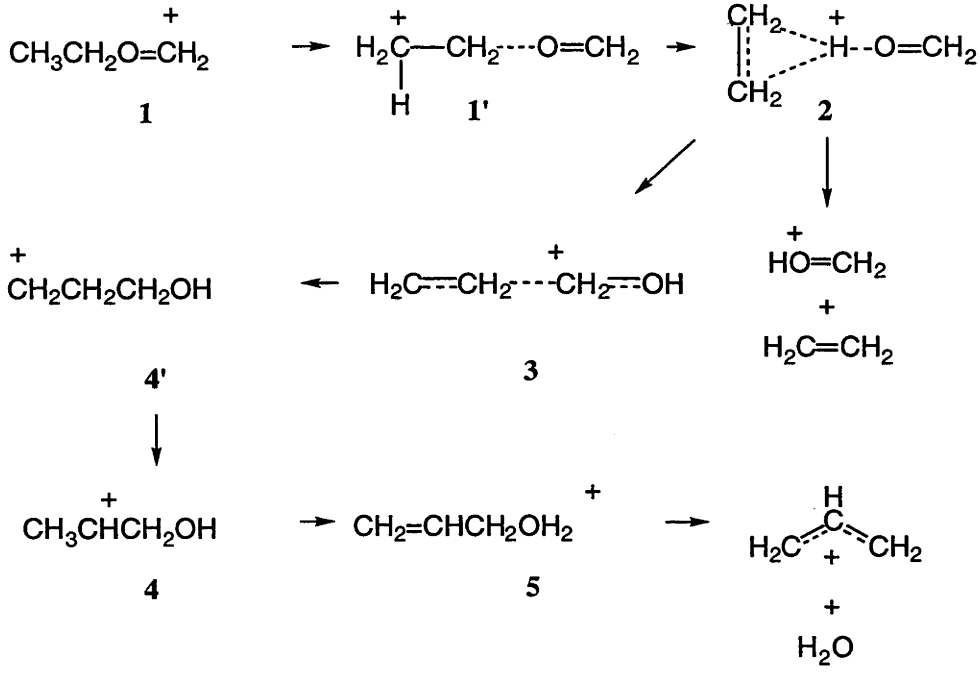

Scheme 3.1

The dissociation of the $[CH_3CH_2OCH_2]^+$ cation represents an attractive prototype for the study of the involvement of ion–neutral complexes in gas-phase chemical reactions. There have been a number of relevant experimental studies on this system. Tsang and Harrison reported the metastable mass spectrum of $[CH_3CH_2OCH_2]^+$ and $[CH_3CHOCH_3]^+$ ions in 1970.[5] After several other studies,[6,7a,8] including an experimental determination of energy barriers,[6] the rearrangement and dissociation mechanism of Scheme 3.1 was proposed by Bowen and Williams in 1978.[4] Extensive

labeling experiments and studies of other $[C_3H_7O]^+$ isomers have been performed[7b,9–12] and alternatives to Scheme 3.1 have also been proposed.[10] Theoretical work reported on these systems includes calculations of the structures and energies of many of the $[C_3H_7O]^+$ isomers at the MP3/6-31G(d)//HF/3-21G level[13] while a recent important study[12] has examined in detail the rearrangement and dissociation processes at the MP2/6-31G(d)//HF/6-31G(d) level.

The present study aims to examine the mechanism of Scheme 3.1 and other related processes using levels of theory higher than those previously applied to the problem. We characterize rigorously the various species encountered on the potential energy surface as equilibrium structures or transition structures and, with the aid of RRKM calculations, compare our results with available experimental information.

3.2 Methods and Results

Standard ab initio molecular orbital calculations have been carried out using a modified version of the G2 method (see 1.13.1). For the potential surface examined in the present study, we have found some significant differences between the HF/6-31G(d) and MP2/6-31G(d) results and we have therefore used MP2/6-31G(d) frequencies (scaled by 0.9646)[14] in place of HF/6-31G(d) (scaled by 0.8929) in the G2 analysis. This procedure (which requires a modified HLC) has been referred to as G2(ZPE=MP2)[15] but for brevity we simply use the G2 label in the present chapter. The MP2 geometry and frequency calculations are performed with all electrons correlated, i.e. MP2(full).

Heats of formation at 298 K have been calculated by the atomization method, as described in Section 1.14, using scaled (by 1.0084[16]) MP2/6-31G(d) frequencies.

The dependence of the rate constant $k(E)$ of a unimolecular reaction on the internal

energy (E) of a species have been calculated using RRKM theory (see Section 1.15). These calculations employed calculated MP2/6-31G(d) frequencies scaled by a factor of 0.9427.[16] Because there is no formal transition structure for direct formaldehyde elimination from $[CH_3CH_2OCH_2]^+$ or ethylene elimination from the ion-neutral complexes, the transition structure frequencies for these dissociations were obtained from the calculated frequencies for the appropriate reactant by removing one frequency corresponding to the reaction coordinate and scaling the lowest 5 frequencies to give a value for $\Delta S^{\ddagger}$ (600 K) of approximately +15 J K^{-1} mol^{-1}.[17,21]

Optimized MP2/6-31G(d) geometries are shown in Figure 3.1 while a schematic potential energy profile is shown in Figure 3.2. Total G2 energies and complete geometries in the form of GAUSSIAN 94 archive entries are shown in Tables A1.1 and A1.2, respectively, in Appendix 1.

3.3 Discussion

3.3.1 Structural and Energetic Features of the Potential Surface

The most notable geometrical feature for the starting $[CH_3CH_2OCH_2]^+$ cation (**1**) is a C–O bond length (1.522 Å, Figure 3.1) which is significantly greater than that of typical C–O bonds (e.g. 1.424 Å in CH_3OH at MP2/6-31G(d)). In this sense, the geometry is part of the way towards a $[CH_3CH_2\cdots OCH_2]^+$ structure, i.e. it is intermediate between **1** and **1'** of Scheme 3.1. We do not find a separate minimum corresponding to **1'** although **TS:1→2** resembles the proposed structure of **1'**.

A 1,3-hydrogen migration via **TS:1→2** at 109 kJ mol^{-1} (Figure 3.2) leads to structure **2** which is best described as a complex between protonated formaldehyde and

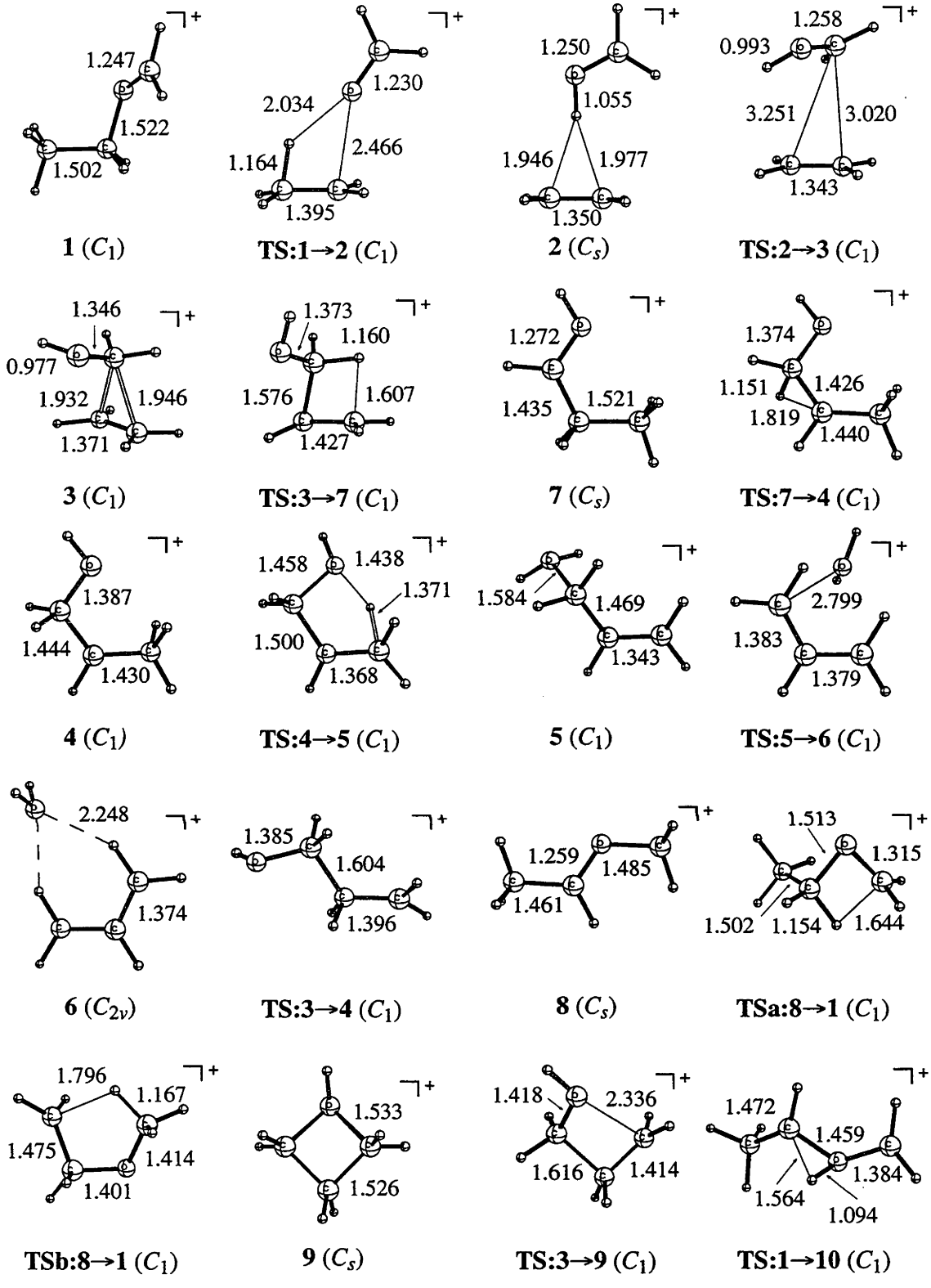

Figure 3.1 Selected MP2/6-31G(d) Bond Lengths (Å).

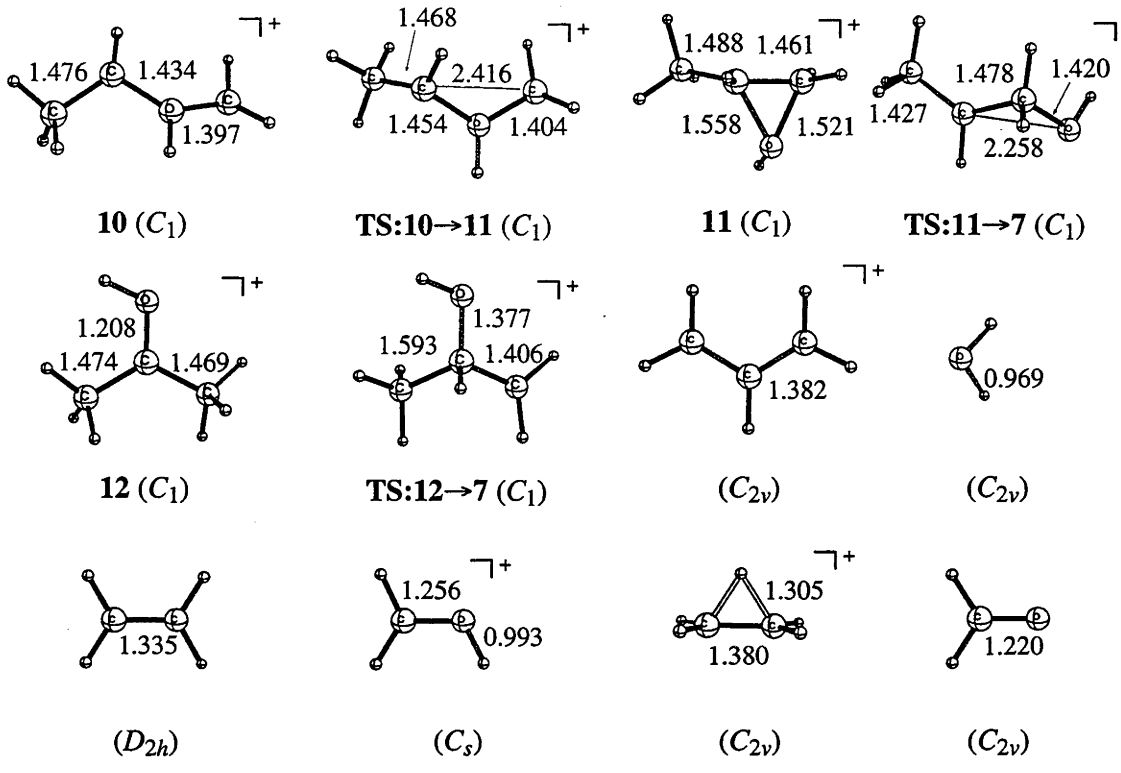

Figure 3.1 (Cont.) Selected MP2/6-31G(d) Bond Lengths (Å).

ethylene. Ion **2** is characterized by long C•••H bonds, the hydroxyl hydrogen atom of the $[CH_2OH]^+$ fragment bridging the ethylene unit. The C•••H bonds (1.946 Å and 1.977 Å) are significantly longer than in the nonclassical ethyl cation (1.305 Å at MP2/6-31G(d)) while the $[CH_2OH]^+$ and C_2H_4 moieties are only slightly perturbed from their structures as isolated species. Complex **2** is bound with respect to $[CH_2OH]^+$ plus C_2H_4 by 73 kJ mol^{-1} and it lies 65 kJ mol^{-1} higher in energy than **1**.

Rotation of the $[CH_2OH]^+$ moiety in **2** leads to structure **3** via **TS:2→3** at 104 kJ mol^{-1}. Ion **3** may also be described as an ion–neutral complex between protonated formaldehyde and ethylene but now the bridge is provided by the carbon atom of $[CH_2OH]^+$ rather than the hydroxyl hydrogen, leading to long bridging C•••C bonds. Structure **3** lies 75 kJ mol^{-1} above **1** and 10 kJ mol^{-1} above **2**.

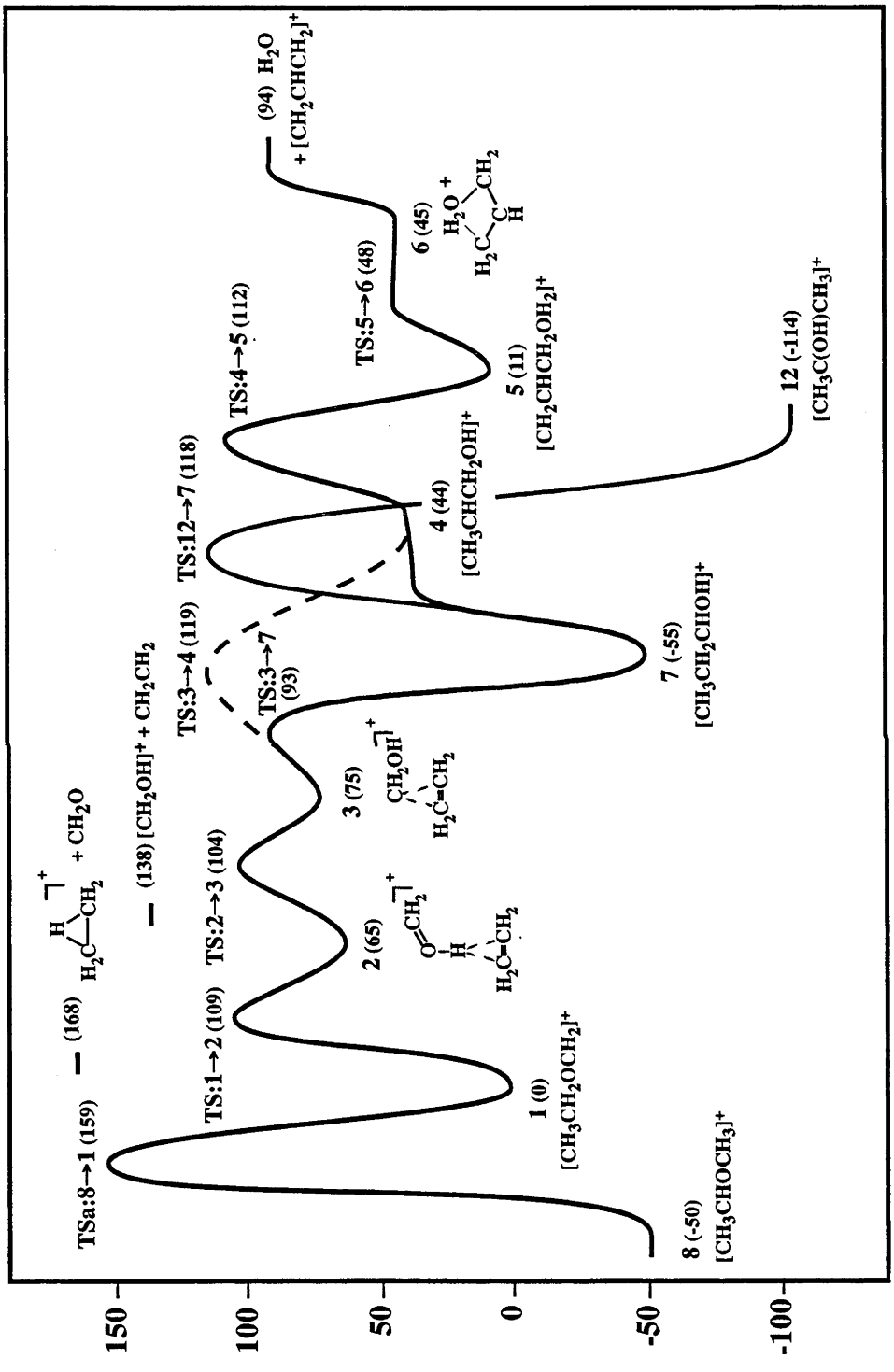

Figure 3.2 Schematic energy profile for water elimination from $CH_3CH_2OCH_2^+$ (**1**). Relative energies (kJ mol^{-1}) given in parenthesis.

We do not find any evidence for the discrete involvement of the primary 3-hydroxyprop-1-yl cation, $[CH_2CH_2CH_2OH]^+$ (**4'**, Scheme 3.1). Instead, the lowest energy path consists of a concerted ring opening and 1,3-hydrogen shift via **TS:3→7** at 93 kJ mol^{-1}, forming protonated propionaldehdye, $[CH_3CH_2CHOH]^+$ (**7**), which lies 55 kJ mol^{-1} below **1**. A 1,2-hydrogen shift in **7** results in the secondary 1-hydroxyprop-2-yl cation, $[CH_3CHCH_2OH]^+$ (**4**) which lies 44 kJ mol^{-1} above **1**. Although **4** is located at a potential minimum on the MP2/6-31G(d) surface (as reflected in all the vibrational frequencies being real), the energy of **TS:7→4** drops below that of **4** at the G2 level (including zero-point vibrational energy). This suggests that **4** at best lies in a very shallow potential well. An alternative direct pathway from **3** to **4** involves concerted ring-opening and a 1,2-hydrogen shift. This proceeds via **TS:3→4** at 119 kJ mol^{-1} and thus is energetically less favorable than the pathway via **7**.

A 1,4-hydrogen migration in **4** leads, via **TS:4→5** at 112 kJ mol^{-1}, to protonated allyl alcohol, $[CH_2{=}CHCH_2OH_2]^+$ (**5**). This structure is characterized by a long C•••O bond (1.584 Å). However, the C–C bonds in the allyl moiety of **5** may be distinctly recognized as single (1.469 Å) and double (1.343 Å) so that **5** cannot really be described as a complex between allyl cation and water. Isomer **5** lies just 11 kJ mol^{-1} above **1**.

The H_2O component of **5** can move to a bridging position, as in **6**, via **TS:5→6** at 48 kJ mol^{-1}. Complex **6** corresponds to an ion–neutral complex between the allyl cation and water. It is bound with respect to these species by 49 kJ mol^{-1}. The energy of **6** is just 45 kJ mol^{-1} above **1**, but **6** lies in a very shallow potential well, being separated from **5** by a barrier (via **TS:5→6**) of just 3 kJ mol^{-1}. Because of the shallowness of the potential well in which it resides, it is not clear whether **6** plays a significant role in the rearrangement/fragmentation of $[CH_3CH_2OCH_2]^+$.

Dissociation from either **5** or **6** leads to the allyl cation plus water at an energy of 94 kJ mol^{-1}. This is the lowest energy pair of dissociation products. The highest energy

point on the reaction path leading from $[CH_3CH_2OCH_2]^+$ (**1**) to these products is **TS:4→5** at 112 kJ mol^{-1}, i.e. their formation involves a reverse barrier of 18 kJ mol^{-1}.

The potential surface of Figure 3.2 reflects the reaction mechanism displayed in Scheme 3.2. There are only minor differences between Scheme 3.2 and the originally postulated mechanism[4] of 3.1. The main differences are the non-involvement as discrete species of **1'** and **4'**, as noted above, and the bridged (rather than open-chain) structure for **3**. The slightly lower energy pathway made possible by the involvement of **7** in the transformation of **3** to **4** was also not included in Scheme 3.1. Our potential surface is very similar to that obtained by Bouchoux et al.[12] at the MP2/6-31G(d)//HF/6-31G(d) level. There are no qualitative differences and even the quantitative agreement is very good, despite a significantly higher level of theory being used in the present study. It is very satisfying that the intricate rearrangements postulated by Bowen and Williams[4] on the basis of a limited amount of experimental data are essentially confirmed by the theoretical calculations.

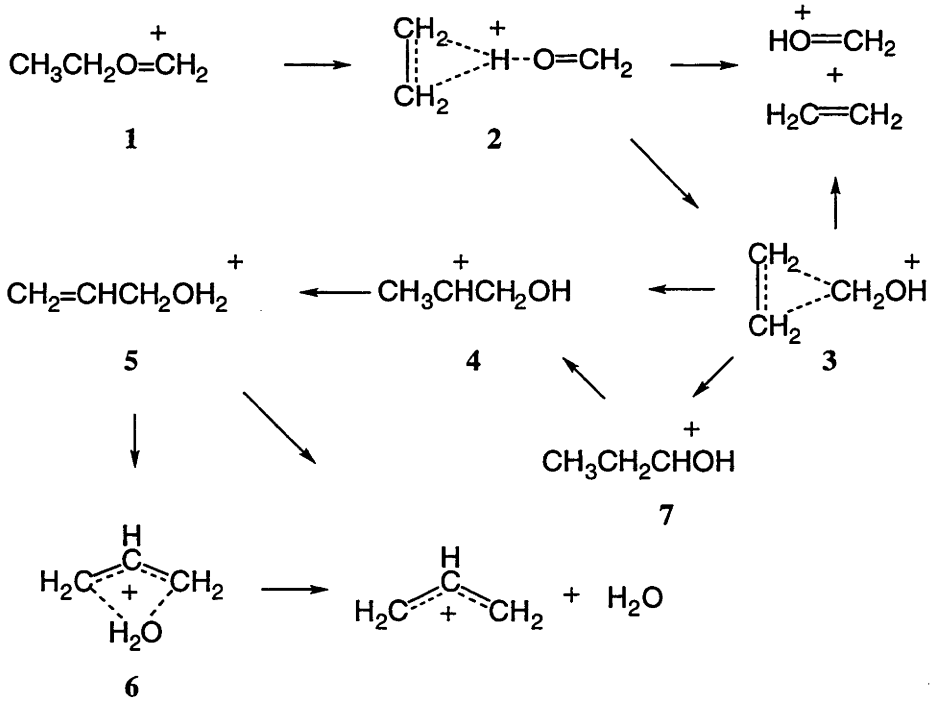

Scheme 3.2

3.3.2 Related Mechanisms

An additional isomer not included in Schemes 3.1 or 3.2 but which is very relevant to the rearrangement and dissociation pathways, as discussed below, is $[CH_3CHOCH_3]^+$ (**8**). This is found to lie 50 kJ mol^{-1} below **1**. Two possible isomerization pathways have been postulated from **8** to **1**,[7a] namely a direct 1,3-hydrogen shift or a two-step process involving a 1,2-hydrogen shift to give $[CH_2CH_2OCH_3]^+$ followed by a 1,4-hydrogen shift. We find that the 1,3-hydrogen shift occurs via **TSa:8→1** at 159 kJ mol^{-1} (relative to **1**), corresponding to a barrier for **8→1** of 209 kJ mol^{-1}. Our calculations indicate that in the second pathway, the 1,2- and 1,4-hydrogen shifts can occur in a concerted manner via **TSb:8→1** at a considerably higher energy, corresponding to a barrier of 275 kJ mol^{-1}. There is no involvement of $[CH_2CH_2OCH_3]^+$ as a discrete intermediate (minimum energy structure) but **TSb:8→1** does resemble such a structure.

Another $[C_3H_7O]^+$ isomer not included in Schemes 3.1 or 3.2 is protonated oxetane (**9**). It is characterized by quite long C–O bonds (1.533 Å) and lies 20 kJ mol^{-1} above **1**. It is of relevance to labeling experiments since it could allow exchange of hydrogen and carbon labels in 3 via the transition structure **TS:3→9** at 118 kJ mol^{-1}. This is also discussed below.

It has been suggested[10] that it may be possible for **1** to isomerize to **4** via protonated methyloxirane (**11**) in a pathway involving no ion-neutral complexes. The pathway that we have characterized for this transformation begins with a 1,2-hydrogen shift via **TS:1→10** with a barrier of 396 kJ mol^{-1} to form the high energy species $[CH_3CHOHCH_2]^+$ (**10**) at 332 kJ mol^{-1}, followed by ring closure to give protonated methyloxirane (**11**). Although **10** is a true minimum on the MP2/6-31G(d) potential surface, the energy of **TS:10→11** drops below that of **10** at the G2 level (including ZPE), indicating little or no barrier for the **10→11** cyclization. Thus **TS:1→10** is

effectively the transition structure for the transformation from **1** to **11**. Protonated methyloxirane (**11**) lies 26 kJ mol^{-1} above **1**. A ring opening via **TS:11→7** at 83 kJ mol^{-1} yields **7** which can isomerize to **4** and then continue as described above. However, due to the very high energy of **10**, this mechanism is not competitive with that of Scheme 3.2 involving ion-neutral complexes.

Finally, it has been suggested that it is possible for protonated acetone ($[CH_3C(OH)CH_3]^+$, (**12**)) to rearrange to **7**. We find that protonated acetone, which lies 114 kJ mol^{-1} below **1**, can isomerize directly to **7** via **TS:12→7** at 118 kJ mol^{-1}. We find no evidence for the existence of $[CH_3CH(OH)CH_2]^+$, which was proposed as an intermediate for this isomerization,[7b] although **TS:12→7** bears a strong resemblance to such a structure. The consequences of forming **7** from **12** are discussed below.

3.3.3 Comparisons with Experimental Thermochemical Data

Calculated heats of formation at 298 K ($\Delta_f H^\circ_{298}$) are compared with available experimental data[9,18] in Table 3.1. The agreement between theory and experiment is generally within the G2 target accuracy of ± 10 kJ mol^{-1}. Two species for which directly measured experimental values are available that show somewhat larger discrepancies are **1** and **11**, the differences being 19 and 13 kJ mol^{-1}, respectively, in these cases. The heats of formation for **4** and **5** are only estimated quantities[9] and these differ by larger amounts from the G2 values.

The calculated barriers for the formation of the various fragmentation products may be compared with values determined from measured appearance energies. The calculated values for the barriers for the formation of H_2O and C_2H_4 are 112 and 138 kJ mol^{-1}, which are somewhat higher than the reported experimental values[7a] of 96 ± 13 and 117 ± 13 kJ mol^{-1}, respectively. As noted in Chapter 2, however, obtaining the experimental values requires the use of heats of formation of the precursor neutral and the

relevant parent ion, so the results would be changed by employing updated values for these quantities (see Chapter 2).

Table 3.1 Theoretical and Experimental Heats of Formation ($\Delta_f H^\circ_{298}$)

Species		G2	Experiment[a]
$[CH_3CH_2OCH_2]^+$	(**1**)	612	593
$[CH_2CH_2\ HOOCH_2]^+$	(**2**)	678	
$[CH_2CH_2\ CH_2OH]^+$	(**3**)	684	
$[CH_3CHCH_2OH]^+$	(**4**)	654	(673)[b]
$[CH_2CHCH_2OH_2]^+$	(**5**)	620	(602)[b]
$[CH_2CHCH_2\ OH_2]^+$	(**6**)	659	
$[CH_3CH_2CHOH]^+$	(**7**)	554	550
$[CH_3CHOCH_3]^+$	(**8**)	561	562
$[CH_2CH_2CH_2OH]^+$	(**9**)	626	625
$[CH_3CHOHCH_2]^+$	(**10**)	942	
$[CH_3CHCH_2OH]^+$	(**11**)	633	620
$[CH_3C(OH)CH_3]^+$	(**12**)	495	490
$H_2O + [CH_2CHCH_2]^+$		709	709
$CH_2CH_2 + [CH_2OH]^+$		752	755
$CH_2O + [CH_3CH_2]^+$		784	793

[a] All experimental values are taken from reference 18 unless otherwise noted. [b] Estimated in reference 9.

The experimental appearance energies for the elimination of H_2O and C_2H_4 from **8** are each found to be 249 ± 13 kJ mol^{-1}.[7a] The coincidence of these values is consistent

with the fact that the energy barriers for both of these processes is determined by the energy of **TSa:8→1** (Figure 3.2). Quantitatively, the experimental barrier (249 kJ mol^{-1}) is somewhat higher than the calculated value of 209 kJ mol^{-1}, as found also in other recent theoretical work.[20]

Experimental appearance energies for the elimination of H_2O and C_2H_4 from **12** are found to coincide at a value of 268 ± 20 kJ mol^{-1},[7b] again consistent with the fact that both are determined by the energy of **TS:12→7**. The experimental barrier is again somewhat higher than the calculated value of 232 kJ mol^{-1}.

3.3.4 Relationship to Observed Rearrangement/Fragmentation Behavior

The calculated potential energy profile (Figure 3.2) and the results of RRKM calculations of rate constants for the loss of ethylene from the ion-neutral complexes **2** and **3** and for the rate-determining step (**7** → **5**) for loss of water from $[CH_3CH_2OCH_2]^+$ (**1**) (Figure 3.2) can be used to rationalize a number of experimental observations. Firstly, it is clear from Figure 3.2 that the lowest energy fragmentation process for **1** corresponds to the loss of a water molecule, requiring 112 kJ mol^{-1}. This is consistent with the observation that water elimination is the dominant reaction of the metastable ion **1**.[5,6,9] In addition, the results of Figure 3.3 show that, within the metastable time frame ($k \approx 10^4 - 10^6$ s^{-1}), water loss should take place over a much wider energy range than ethylene loss, again consistent with the dominance of water elimination. Figure 3.3 also shows that as the time frame is changed to encompass larger values of k, water loss becomes slow relative to ethylene loss. This is reflected in the ratio of water loss to ethylene loss increasing significantly in going from the first field-free region to the second field-free region of the mass spectrometer.[7a]

The rate constant curves in Figure 3.3 are characteristic of a situation in which

there is a lower-energy rearrangement process (water loss) and a higher-energy direct dissociation (ethylene loss). Under these circumstances, the rearrangement process is favored by low-energy ions and the direct dissociation is favored by high-energy ions. It is therefore not surprising that, in contrast to the dominant water loss in the metastable ion spectrum of **1**, the collision-induced dissociation spectrum is dominated by ethylene loss and also shows some formaldehyde loss,[6c,7a] even though these last two processes require 26 and 56 kJ mol^{-1}, respectively, more energy than water loss.

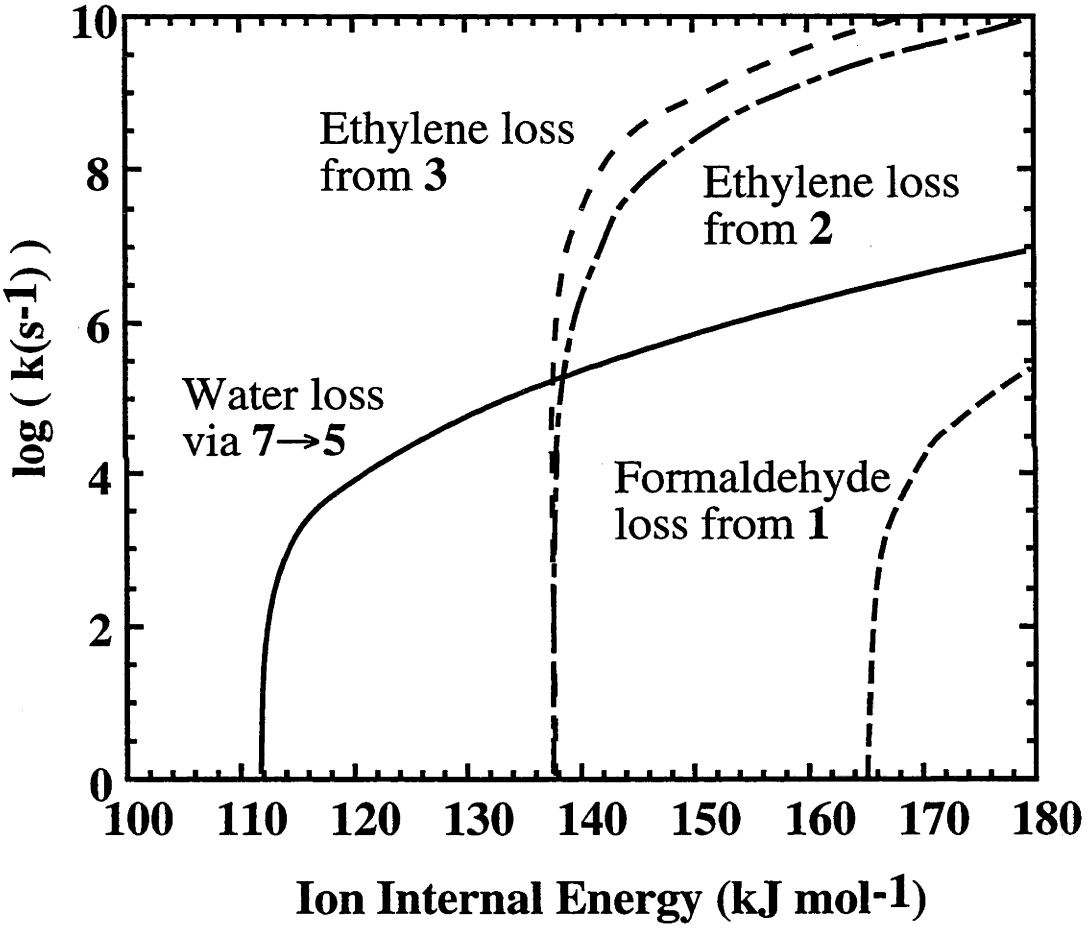

Figure 3.3 RRKM rate constants (log k) calculated as a function of internal energy (E) for ethylene loss from **2** and **3**, formaldehyde loss from **1** and the rate-determining step (**7** → **5**) for water loss. Energy is measured relative to **1**.

The decomposition of the metastable $[CH_3CHOCH_3]^+$ ion (**8**) results in elimination of ethylene, formaldehyde and small amounts of water,[5,6b,7a] all of which may be lost after rearrangement to $[CH_3CH_2OCH_2]^+$ (**1**). It has been observed that the metastable spectrum of **8** shows some similarity to the collision-induced dissociation mass spectrum of **1**.[6c,7a] This result can be readily rationalized by noting that the existence of a substantial barrier (209 kJ mol^{-1}) for isomerization of **8** to **1** will result in the formation of **1** with considerable excess energy. The energy of **TS:8→1** is above that required for ethylene elimination and is only marginally (9 kJ mol^{-1}) below that required for formaldehyde elimination. In fact, due to the large barrier, it would be expected that the isomerization of **8** to **1** would not occur on the metastable time frame until energies significantly above threshold have been reached. Thus, RRKM calculations indicate that metastable isomerization will not begin until about 35 kJ mol^{-1} above the threshold, well in excess of the energy needed to eliminate formaldehyde. Hence our calculated barrier is consistent with significant loss of formaldehyde from **8**.

Metastable protonated acetone ($[CH_3C(OH)CH_3]^+$, (**12**)) also loses water and ethylene.[6,7b] However, the abundances are different to those observed for ion **1**, ethylene elimination being slightly favored over water elimination.[6,7b] This is again readily explained by the fact that ions that have isomerized from **12** to **7** will have surmounted a large barrier (118 kJ mol^{-1} relative to **1**) and hence have a significant amount of internal energy. As noted above for the isomerization of **1** to **8**, the ions will actually have significantly more energy than this barrier suggests, RRKM calculations indicating that metastable isomerization of **7** to **12** will not occur until an energy of about 165 kJ mol^{-1} above **1** is reached. Because higher internal energies favor ethylene elimination, metastable **12** thus shows a greater proportion of ethylene elimination than does **1**. It should also be noted that metastable **12** has sufficient energy to eliminate formaldehyde. However, formaldehyde elimination is generally slow relative to ethylene and water elimination (Figure 3.3) and is therefore not observed in metastable ion decompositions. At the higher internal energies represented in the first field-free region,

formaldehyde elimination becomes more competitive and a small extent of formaldehyde elimination is observed.[6b]

3.3.5 Label Exchange Mechanisms and Kinetic Analysis

Extensive labeling studies have been reported for various deuterated analogues of **1**.[9–12] It has been found that exchange of the hydrogen atoms within the ethyl group of **1** (henceforth referred to as ethyl hydrogens) and exchange of the ethyl hydrogens with those in the OCH_2 group (referred to as methylene hydrogens) occur at different rates,[12] suggesting differing mechanisms for the two processes. Exchange of the ethyl hydrogens is straightforward and can be attributed to reversible isomerization of **1** and **2**. Methylene exchange can be caused either by reversible isomerization between **3** and **7** or between **3** and **9**. The intervention of **7** or **9** can be distinguished by noting that the latter would have the added effect of causing loss of identity of ^{13}C-labels. Early experiments by Bowen et al. indicated that significant amounts of ^{13}C-label exchange occurs during ethylene elimination from labeled analogues of **1**[9] and **7**.[8b] However, later labeling experiments on **1**[11] and **7**[10] and ICR experiments on mixtures of $[^{13}CH_2OH]^+$ and CH_2CH_2 have failed to observe significant ^{13}C-label exchange.[12,19]

Our RRKM calculations of reaction rates assist in the understanding of the label-exchange processes. A plot of the log of the calculated rate constants versus internal energy for the possible isomerization processes of ion **3** is shown in Figure 3.4. It can be seen that at energies appropriate to metastable ethylene elimination (~138 kJ mol^{-1}), the rate constant for isomerization of **3** to **9** is roughly an order of magnitude slower than isomerization to **7** and approximately three orders of magnitude slower than isomerization back to **2**. The isomerization of **3** to **4** is found to be comparably slow. Our calculations thus support the conclusion that isomerization of **3** to **9** does not occur to any great extent and hence only small amounts of ^{13}C-label exchange should take place. Label exchange between the methylene hydrogens and the ethyl hydrogens is predicted to be

predominantly caused by the reversible isomerization of **3** and **7**.

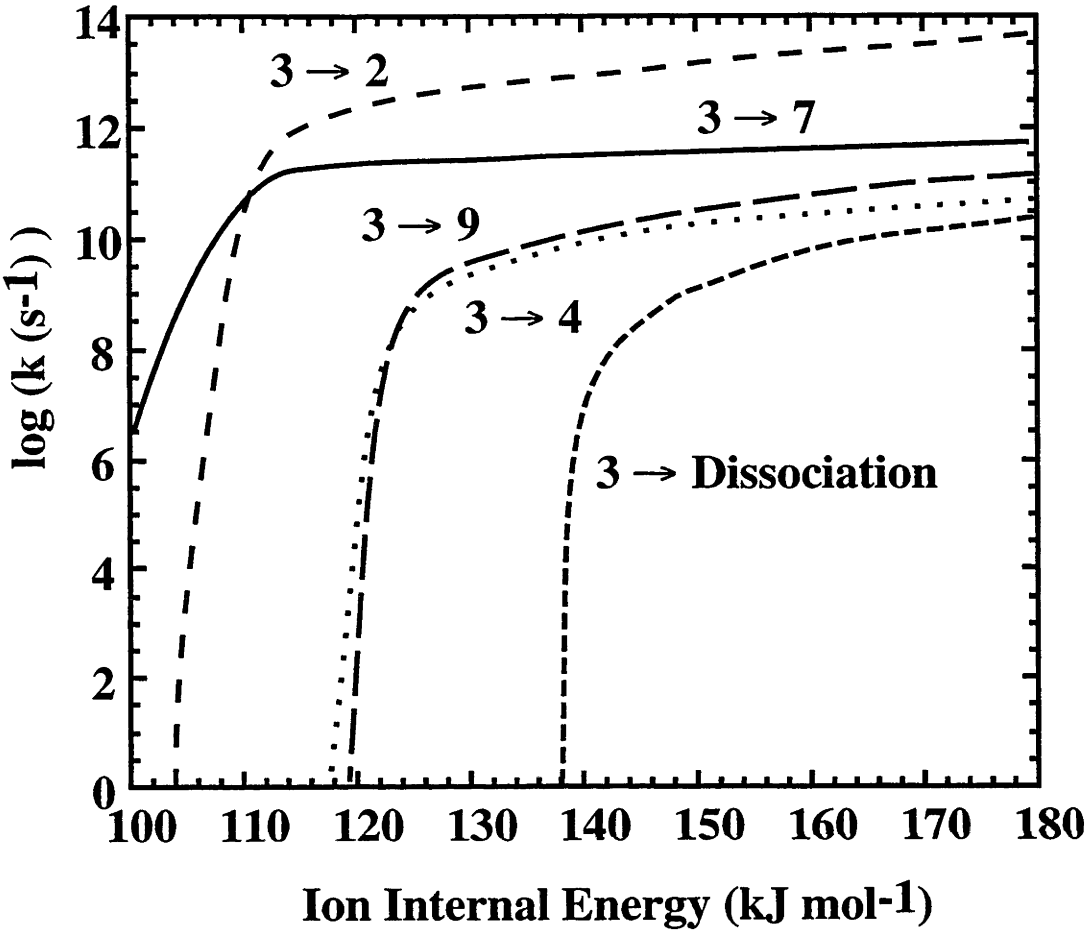

Figure 3.4 RRKM rate constants (log *k*) calculated as a function of internal energy (*E*) for the isomerization processes of **3**. Energy is measured relative to **1**.

The labeling experiments show that during water elimination there is a pronounced tendency for β-hydrogen transfer to oxygen to occur whereas during ethylene elimination the labels are distributed almost statistically amongst all the available sites.[9,11,12] Interesting labeling behavior, which will be discussed later, is also observed for **7** and **12**. In order to address these issues, we have carried out an analysis of the reaction kinetics. Assuming as before that ethylene elimination occurs only from **2** and **3** and that

the rate-limiting step to water elimination from **1** is isomerization of **7** to **5** (via TS:**4**→**5**), which is consistent with recent experiments,[12] we can write the rate equations for the processes involved in label exchange as follows.

$$\frac{d[\mathbf{1}]}{dt} = -k_{12}[\mathbf{1}] + k_{21}[\mathbf{2}] \tag{3.2}$$

$$\frac{d[\mathbf{2}]}{dt} = -(k_{21} + k_{23} + k_{2d})[\mathbf{2}] + k_{12}[\mathbf{1}] + k_{32}[\mathbf{3}] \tag{3.3}$$

$$\frac{d[\mathbf{3}]}{dt} = -(k_{32} + k_{37} + k_{3d})[\mathbf{3}] + k_{23}[\mathbf{2}] + k_{73}[\mathbf{7}] \tag{3.4}$$

$$\frac{d[\mathbf{7}]}{dt} = -(k_{73} + k_{7d})[\mathbf{7}] + k_{37}[\mathbf{3}] + k_{12-7}[\mathbf{12}] \tag{3.5}$$

$$\frac{d[\mathbf{12}]}{dt} = -k_{12-7}[\mathbf{12}] \tag{3.6}$$

$$\frac{d[H_2O]}{dt} = k_{7d}[\mathbf{7}] \tag{3.7}$$

$$\frac{d[C_2H_4]}{dt} = k_{2d}[\mathbf{2}] + k_{3d}[\mathbf{3}] \tag{3.8}$$

where k_{xy} is the rate constant for isomerization of **x** to **y** and k_{xd} is the rate of dissociation of **x**. It is possible to solve these equations and hence obtain the abundances of all species involved at any specified time. However, this does not tell us anything about the behavior of labeled species.

In order to examine the isotope distribution patterns, we have extended the system of rate equations to describe the behavior of all the possible singly-deuterated analogues of **1**, **2**, **3**, **7** and the O-deuterated analogue of **12** (see Figure 3.5 and Appendix A1). We have made the additional assumption that there are no isotope effects. The equations A1.1–A1.18 have been solved numerically and the results used to make quantitative

predictions of the abundances for the eliminated species from the metastable singly-deuterated ions. Since the decomposition of metastable ions occurs in a fairly narrow time window (10^{-6}–10^{-5} s), we are interested in the change in abundance that occurs during this time interval. We must also choose an appropriate energy at which to calculate the unimolecular rate constants. Because the rate-limiting steps for ethylene elimination, namely dissociation of either complex **2** or complex **3**, have no reverse barrier, the metastable elimination of ethylene will occur near threshold. Hence, for ethylene we have calculated the rates for an internal energy just above the thermochemical threshold (138.1 kJ mol^{-1}). For water elimination, however, the choice is not so obvious. Our RRKM calculations indicate that metastable water elimination can occur

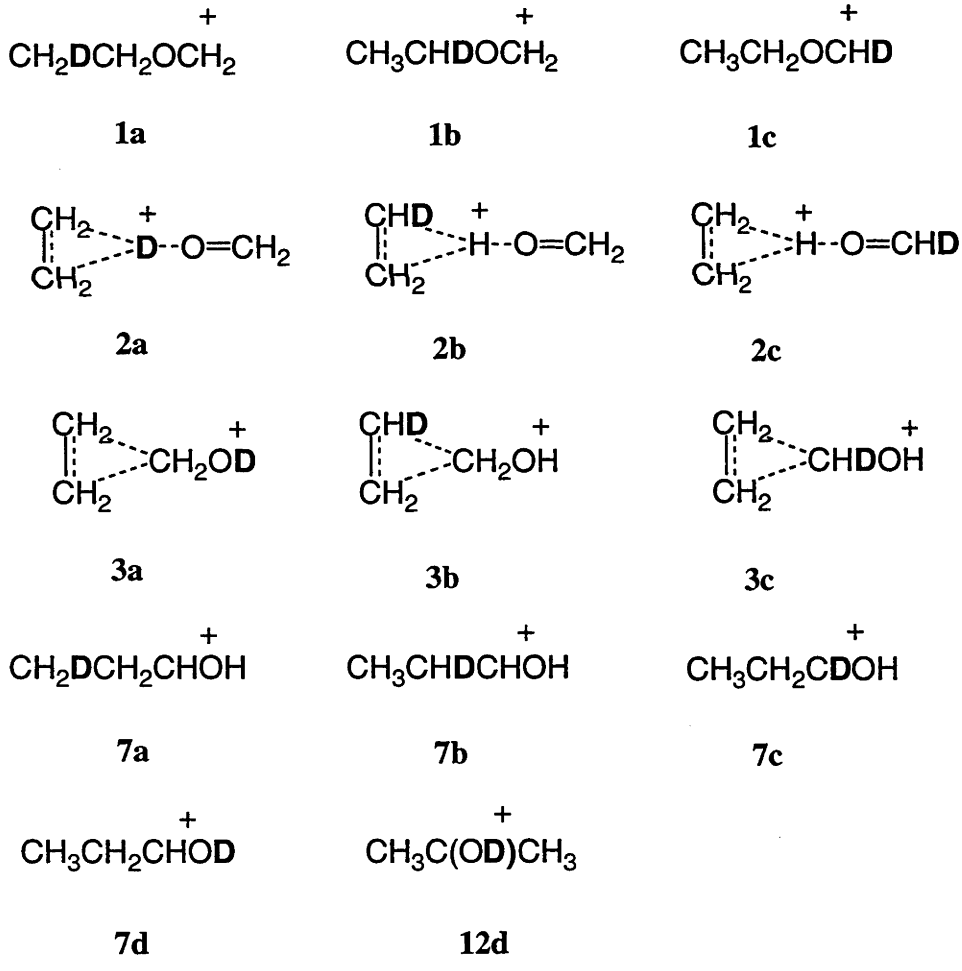

Figure 3.5 Singly-deuterated analogues of ions **1**, **2**, **3**, **7** and **12**.

over a range of internal energies of **1**, ranging from approximately 120 kJ mol^{-1} to 138 kJ mol^{-1}, at which stage ethylene elimination becomes more favorable (see Figure 3.3). It is likely that significant changes in the isotope distribution will occur over this energy range, so the rate constants have been calculated at two internal energies, 120 kJ mol^{-1} and 128 kJ mol^{-1}. Isotope distributions for both water and ethylene elimination have also been calculated at 170 kJ mol^{-1}, just above the onset calculated for metastable isomerization (see above), to examine label exchange in the dissociation of metastable **12**.

Table 3.2 Calculated and Experimental Isotope Distributions for Water Elimination[a]

	H_2O				HOD			
Species	$E = 120$	$E = 128$	$E = 170$	Expt[b]	$E = 120$	$E = 128$	$E = 170$	Expt[b]
1a	65	69	-	-	34	31	-	-
1b	74	71	-	-	26	29	-	-
1c	78	75	-	-	22	25	-	-
7c	83	77	-	88	17	23	-	12
7d	32	60	-	31	68	40	-	69
12d	-	-	9	10[c]	-	-	91	90[c]
Statistical	71	71	71	71	29	29	29	29

[a] Calculated values obtained using rate constants derived for ions **1** with internal energy E (kJ mol^{-1}). Isotopomers displayed in Figure 3.5. [b] Average of experimental values from references 9, 11 and 12 unless otherwise noted. [c] From reference 6c.

Calculated isotope distributions for water elimination from the deuterated analogues of **1** and for **7c**, **7d** and **12d** (see Figure 3.5) are compared with available experimental data in Table 3.2. Statistical results are also shown for comparison. It can be seen that at an energy of 120 kJ mol^{-1}, **1a** displays a greater than statistical loss of

HOD while **1b** and **1c** show less than statistical loss, consistent with β-transfer to oxygen being favored, as experimentally observed.[9,11,12] When the energy is increased to 128 kJ mol^{-1}, the abundances approach their statistical value but still display a slight tendency for β-transfer. At 120 kJ mol^{-1}, **7d** shows a much greater than statistical loss of HOD while **7c** shows a greater than statistical loss of H_2O, consistent with a tendency for retention of the oxygen-bound hydrogen during water elimination, as is observed experimentally.[9,11,12] The calculated abundance of HOD elimination from **7c** (17%) is the same as that which would result from retention of the oxygen-bound hydrogen along with random selection of the second water hydrogen from the six other hydrogens, i.e. significant exchange of the carbon-bound hydrogens occurs, again in agreement with experiment.[9,11,12] At the higher energy of 128 kJ mol^{-1} the abundances for water elimination from **7c** and **7d** also approach the statistical result but the trends observed at lower energies still remain to a lesser extent. At the energies appropriate to water elimination from **12** (170 kJ mol^{-1}), there is a very pronounced tendency for retention of deuterium on oxygen, i.e. dominant loss of partially deuterated water is observed. At these high energies, isomerization of **7** to **5**, which leads to water loss, is of comparable rate to isomerization of **7** to **3**. Hence, dissociation occurs before significant label exchange can occur and the label remains predominantly attached to oxygen. In the cases where experimental labeling data for water loss from **1** and **7** exist, good agreement between theory and experiment is seen at the lower internal energy. Good agreement with experimental labeling results is also observed for **12d**. The calculated distribution for elimination from **12** of 29% H_2O and 71% ethylene are also in satisfactory agreement with the experimental results, ranging from 31-46% H_2O and 69-54% CH_2CH_2.[6,7b]

For ethylene elimination, our calculations (Table 3.3) predict a statistical distribution of labels for all species shown, which is consistent with experiment for all but two related cases. In contrast to the predicted statistical behavior, **7d** is found experimentally to show a much greater than statistical loss of CH_2CH_2. A possible

explanation for this behavior is that some other pathway is in operation that allows ion **7** to eliminate ethylene with retention of the deuterium label on oxygen. This is supported by experiments,[10] which suggest an additional pathway for ethylene elimination for **7d** ions, with the measured kinetic energy release for ions where label exchange has occurred being different from those that retain the label. These experiments also show that the kinetic energy release of those ions that exhibit label exchange is the same as that for ethylene elimination from ion **1**.[10] This suggests that label exchange in ions **7d** occurs via a common intermediate to **1** (i.e. via **2** or **3**) while a separate mechanism applies for eliminations of ethylene where the label is retained on oxygen. It has previously been suggested[9] that a competing mechanism for ethylene elimination from **7** is sequential 1,2-hydrogen shifts from **7** to form $[CH_3CHCH_2OH]^+$ (**4**) and then $[CH_2CH_2CH_2OH]^+$ (**4'**), with the latter dissociating by a simple bond cleavage resulting in loss of (label-retaining) ethylene. This mechanism would result in an increase in label-retaining

Table 3.3 Calculated and Experimental Isotope Distributions for Ethylene Elimination[a]

	CH_2CH_2			$CHDCH_2$		
Species	E = 138.1	E=170	Expt[b]	E = 138.1	E=170	Expt[b]
1a	43	-	-	57	-	-
1b	43	-	-	57	-	-
1c	43	-	-	57	-	-
7c	43	-	42	57	-	58
7d	43	-	66	57	-	34
12d	-	38	66[c]	-	62	34[c]
Statistical	43	43	43	57	57	57

[a] Calculated values obtained using rate constants derived for ions **1** with internal energy E (kJ mol^{-1}). Isotopomers displayed in Figure 3.5. [b] Average of experimental values from references 9, 11 and 12 unless otherwise noted. [c] From reference 6c.

eliminations for **7d** and would also account for the different kinetic energy release value for ethylene eliminated with the label retained on oxygen. A similar argument can account for the difference between our calculated results and experiment for **12d**. Thus, since **12d** initially isomerizes to **7d**, the above mechanism would also be consistent with the observed preference for label-retaining eliminations.

3.4 Concluding Remarks

The decomposition of $[CH_3CH_2OCH_2]^+$ proceeds via a mechanism in which the involvement of ion-neutral complexes as intermediates plays a crucial role. Mutual reorientation of the two components of the ion-neutral complex **2** to form **3** allows a rearrangement that would be considerably more difficult via conventionally bonded species. Our proposed mechanism (Scheme 3.2) is very similar to that originally proposed by Bowen and Williams (Scheme 3.1) and strongly supports the results of recent calculations carried out at a somewhat lower level of theory. The reaction profile, along with an RRKM study of the reaction kinetics, shows that Scheme 3.2 can account for the results of extensive deuterium and ^{13}C-labelling experiments. There is generally good agreement with available experimental thermochemical data.

3.5 References

(1) Rylander, P. N.; Meyerson, S. *J. Am. Chem. Soc.* **1956**, *78* , 5799.

(2) For recent reviews on ion-neutral complexes see, for example: (a) Bowen, R. D. *Acc. Chem. Res.*, **1991**, *24*, 364. (b) Longevialle, P. *Mass Spectrom. Rev.* **1992**, *11*, 157. (c) McAdoo, D. J.; Morton, T. H. *Acc. Chem. Res.* **1993**, *26*, 295.

(3) See, for example: Shaik, S.; Schlegel, H. B.; Wolfe, S. *Theoretical Aspects of Physical Organic Chemistry: The S_N2 Mechanism*; Wiley: New York, 1992.

(4) Bowen, R. D.; Williams, D. H. *J. Am Chem. Soc.* **1978**, *100*, 7454.

(5) Tsang, C. W.; Harrison, A. G. *Org Mass. Spectrom.* **1970**, *3*, 647.

(6) (a) Yeo, A. N. H.; Williams, D. H. *J. Am. Chem. Soc.* **1971**, *93*, 395. (b) Tsang, C. W.; Harrison, A. G. *Org Mass Spectrom.* **1973**, *7*, 1377. (c) McLafferty, F. W.; Sakai, I. *Org. Mass Spectrom.* **1973**, *7*, 971.

(7) (a) Hvistendahl, G.; Williams, D. H. *J. Am. Chem. Soc.* **1975**, *97*, 3097. (b) Hvistendahl, G; Bowen, R. D.; Williams, D. H. *J. Chem. Soc. Chem. Comm.* **1976**, 294.

(8) (a) Williams, D. H.; Bowen, R. D. *J. Am. Chem. Soc.* **1977**, *99*, 3192. (b) Bowen, R. D.; Kalman, J. R.; Williams, D. H.; *J. Am. Chem. Soc.* **1977**, *99*, 5481.

(9) Bowen, R. D.; Williams, D. H.; Hvistendahl, G.; Kalman, J. R. *Org. Mass Spectrom.* **1978**, *13*, 721.

(10) Holmes, J. L.; Rye, R. T. B.; Terlouw, J. K. *Org. Mass. Spectrom.* **1979**, *14*, 606.

(11) McAdoo, D. J.; Hudson, C. E. *Int. J. Mass Spectrom. Ion Proc.* **1989**, *88*, 133.

(12) Bouchoux, G.; Penaud-Berruyer, F.; Audier, H. E.; Mourgues, P.; Tortajada, J. *J. Mass Spectrom.* **1997**, *32*, 188.

(13) Nobes, R. H.; Radom, L. *Org. Mass Spectrom.* **1984**, *19*, 385.

(14) Pople, J. A.; Scott, A. P.; Wong, M. W.; Radom, L. *Isr. J. Chem.* **1993**, *33*, 345.

(15) Curtiss, L. A.; Raghavachari, K.; Pople, J. A. *J. Chem. Phys.* **1995**, *103*, 4192.

(16) Scott, A. P.; Radom, L. *J. Phys. Chem.* **1996**, *100*, 16502.

(17) The entropy of activation ($\Delta S^{\ddagger}$) for the dissociation process should be positive because of the expected loose transition structure. The actual magnitude of $\Delta S^{\ddagger}$ is chosen to be typical of bond cleavage reactions.[21] The $\Delta S^{\ddagger}$ is not explicitly required but the frequencies obtained by this fitting procedure are used in the RRKM calculations.

(18) Lias, S. G.; Bartmess, J. E.; Liebman, J. F.; Holmes, J. L.; Levin, R. D.; Mallard, W. G. *J. Phys. Chem. Ref. Data Suppl.* **1988**, *17*.

(19) Tortajada, J.; Audier, H. E.; Monteiro, C.; Mourgues, P. *Org. Mass Spectrom.*

1991, *26*, 913.

(20) Hudson, C. E.; McAdoo, D.J. *J. Am. Soc. Mass Spectrom.* **1998**, *9*, 130.

(21) Baer, T.; Mayer, P.M. *J. Am. Soc. Mass Spectrom.* **1997**, *8*, 103.

Chapter 4

Rearrangement and Fragmentation Pathways of $[C_3H_7X]^+$ Ions (X = NH and S): Are Ion-Neutral Complexes Important?

4.1 Introduction

In 1978, Bowen and Williams proposed that elimination of water from the $[CH_3CH_2OCH_2]^+$ metastable ion occurs via a mechanism involving ion-neutral complexes as intermediates.[1] Since that time, numerous examples of the intermediacy of ion-neutral complexes have been discussed[2] and explicit support for their involvement in the rearrangement/fragmentation of $[CH_3CH_2OCH_2]^+$ has come from high-level ab initio studies (see Chapter 3).[3] Interestingly, experiments on the isoelectronic ions $[CH_3CH_2NHCH_2]^+$ and $[CH_3CH_2SCH_2]^+$ have found that their behavior is quite different from that of the corresponding $[CH_3CH_2OCH_2]^+$ ion.[4,5] In particular, these experiments suggest that ion-neutral complexes may be less important in the decomposition of the former pair of ions.[4b,4c,4f,5]

Experimental studies of the metastable decomposition of the $[CH_3CH_2NHCH_2]^+$ ion have found that, in contrast to the behavior of $[CH_3CH_2OCH_2]^+$, only ethylene loss is observed, with exclusive occurrence of β-hydrogen transfer to nitrogen. On the other hand, $[CH_3CH_2SCH_2]^+$ is found to behave more similarly to $[CH_3CH_2OCH_2]^+$, in that both hydrogen sulfide and ethylene are lost during metastable decomposition. However, again in contrast to the situation for $[CH_3CH_2OCH_2]^+$, the mechanism proposed to explain this observation does not involve the participation of any ion-neutral complexes.[5]

Relevant experimental studies of the fragmentation of other metastable $[C_3H_8N]^+$ and $[C_3H_7S]^+$ ions, including several labeling studies, have also been performed,[4,5] and detailed mechanisms have been proposed to explain the results of the various experiments (Schemes 4.1 and 4.2).[4c,5] There have also been theoretical investigations on aspects of the potential energy surface for the decomposition of several of the $[C_3H_8N]^+$ isomers.[4a,6] We are not aware, however, of any relevant theoretical studies reported to date on the $[C_3H_7S]^+$ system.

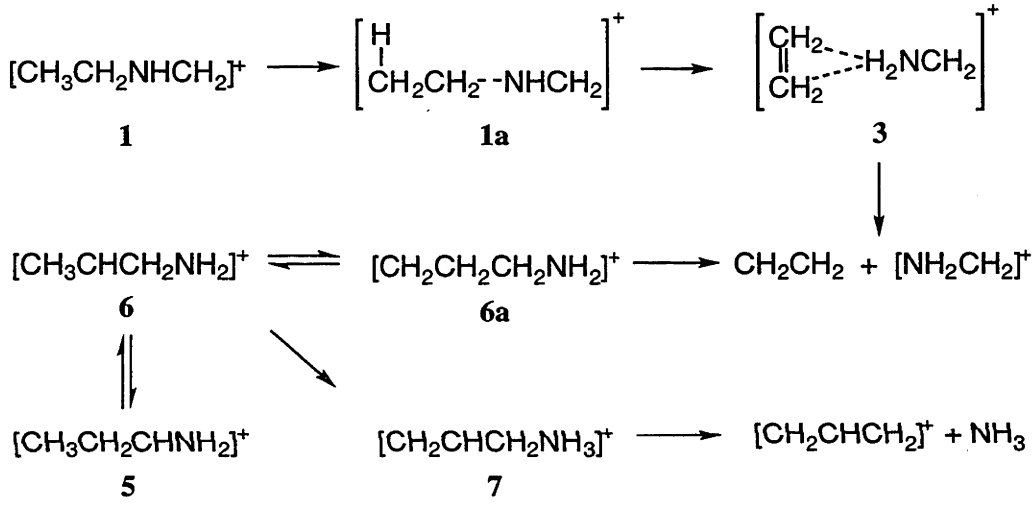

Scheme 4.1

The present work aims to characterize the potential energy surfaces for rearrangement/fragmentation of several $[C_3H_8N]^+$ and $[C_3H_7S]^+$ isomers. Along with RRKM calculations, these results are used to rationalize the experimentally observed product abundances and labeling patterns, as well as to make comparisons with experimental thermochemical information. The potential surfaces for the systems examined here and the work on $[C_3H_7O]^+$ ions[3b] presented in Chapter 3 allow us to identify some of the key factors that determine the importance of ion-neutral complexes in the rearrangement/fragmentation processes.

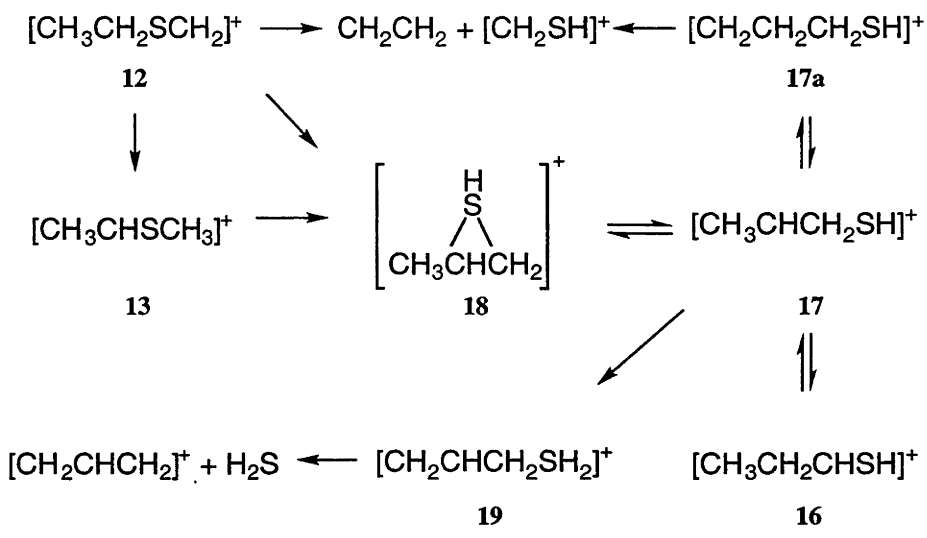

Scheme 4.2

4.2 Methods and Results

Standard ab initio molecular orbital calculations have been performed using a modification of the G2 method (see 1.13). We have used a modified version of G2, namely G2(ZPE=MP2),[7] which employs scaled MP2/6-31G(d) frequencies rather that HF/6-31G(d). We will refer to G2(ZPE=MP2) simply as G2 for the sake of brevity. MP2 calculations are performed with correlation of all electrons, i.e. MP2(full).

Heats of formation at 298 K have been calculated using the atomization method, with temperature corrections applied as described in Section 1.14, using scaled (by 1.0084)[8] MP2/6-31G(d) frequencies.

The energy dependence of the unimolecular rate constant $k(E)$ of a species has been calculated using RRKM theory (see Section 1.15), employing scaled (by 0.9427)[8] MP2/6-31G(d) frequencies. For fragmentation reactions, where no formal transition

structure exists, the transition structure for formation of the product complex has been substituted.

Calculated G2 total energies relevant to the $[C_3H_8N]^+$ and $[C_3H_7S]^+$ are listed in Tables A2.1 and A2.2 in Appendix 2. Selected bond lengths from MP2/6-31G* optimized are displayed in Figures 4.1 and 4.3 while complete geometries, in the form of Gaussian 94 archive entries, are shown in Tables A2.3 and A2.4. Schematic energy profiles for the $[C_3H_8N]^+$ and $[C_3H_7S]^+$ systems are displayed in Figures 4.3 and 4.4, respectively. Unless otherwise noted, all relative energies refer to G2 values at 0 K and structural data refer to MP2/6-31G(d) optimized geometries.

4.3 Discussion

4.3.1 Structural and Energetic Features of the $[C_3H_8N]^+$ Surface

The lowest energy conformer of the species $[CH_3CH_2NHCH_2]^+$ (**1**) is shown in Figure 1. All energies in the following section are given relative to that of **1**, unless otherwise noted.

We find two possible transition structures for the rearrangement of $[CH_3CH_2NHCH_2]^+$ (**1**) to $[CH_3CHNHCH_3]^+$ (**2**), which lies 38 kJ mol^{-1} below **1**. The first, lower-energy structure (**TSa:1→2**) corresponds to a 1,3-hydrogen shift and has a relative energy of 234 kJ mol^{-1}. The second (**TSb:1→2**) involves concerted 1,4- and 1,2-hydrogen shifts and lies at 289 kJ mol^{-1}.

Loss of molecular hydrogen from $[CH_3CHNHCH_3]^+$ (**2**) can occur via **TS:2→9**, which has an energy of 231 kJ mol^{-1}, leading to **9**. Ion **9** is a weak complex

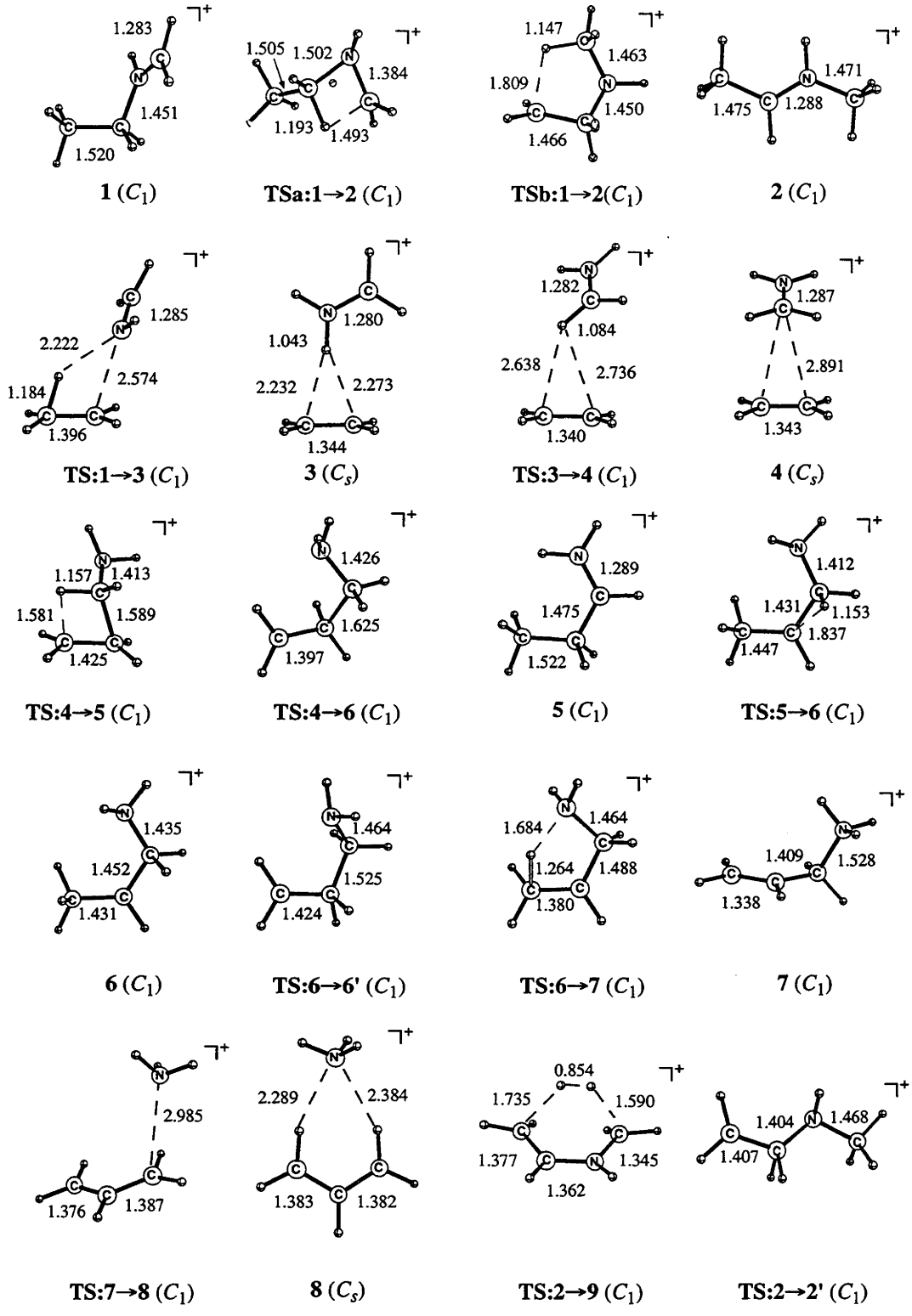

Figure 4.1 Selected MP2/6-31G(d) bond lengths (Å) relevant to $[C_3H_8N]^+$ ions.

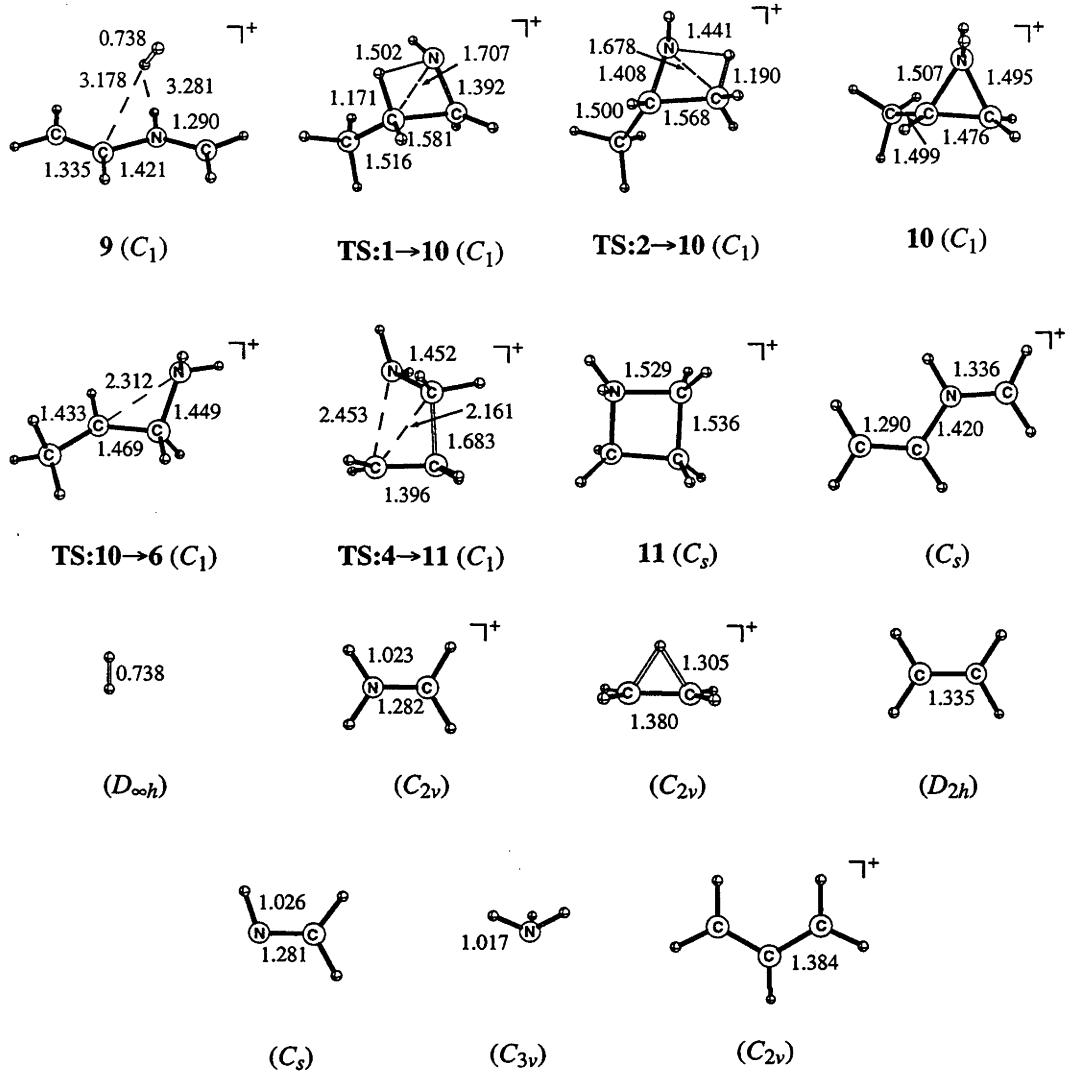

Figure 4.1 (Cont.) Selected MP2/6-31G(d) bond lengths (Å) relevant to $[C_3H_8N]^+$ ions.

between molecular hydrogen and $[CH_2CHNHCH_2]^+$ that is bound by less than 1 kJ mol^{-1}. It dissociates to give these species, with a relative energy of 125 kJ mol^{-1}. We also find a transition structure (**TS:2→2'**) at 268 kJ mol^{-1} that will result in hydrogen exchange within the CH_3CH group of **2**, as discussed further below.

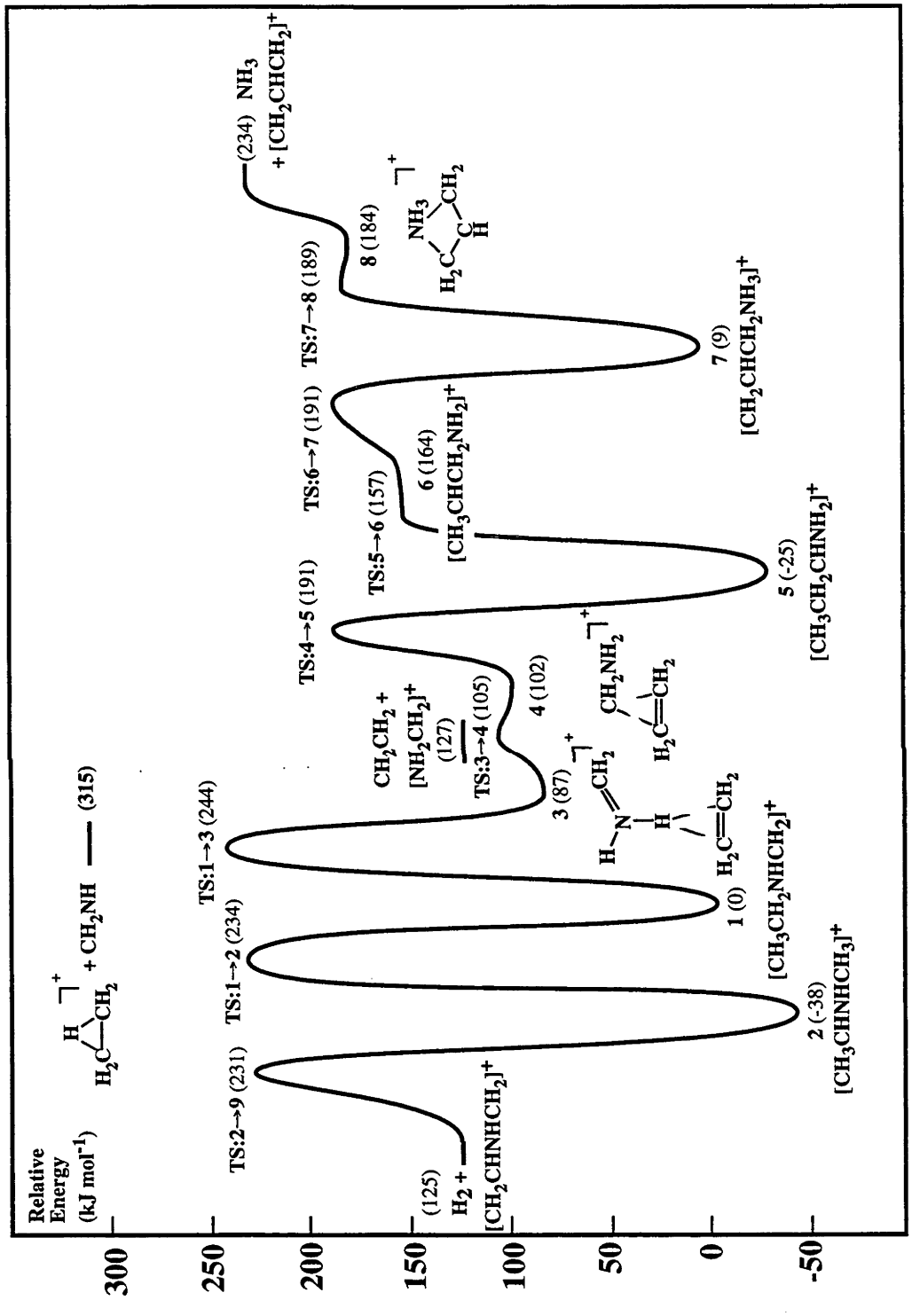

Figure 4.2 Schematic energy profile for rearrangement/fragmentation of $[C_3H_8N]^+$ ions. Relative energies (kJ mol^{-1}) given in parentheses.

The $[CH_3CH_2NHCH_2]^+$ ion (**1**) can also rearrange to **3** via a 1,3-hydrogen shift (**TS:1→3**), with a barrier of 244 kJ mol^{-1}. Although we find no evidence for the existence of the previously proposed intermediate **1a** (Scheme 4.1), **TS:1→3** does bear some resemblance to such a structure. The resulting ion **3** is best represented as the proton-bound complex $[CH_2CH_2{\bullet\bullet\bullet}H_2NCH_2]^+$. This complex contains very long C–H bonds (2.232 Å and 2.273 Å), which are significantly stretched compared with those in the isolated (bridged) ethyl cation (1.305 Å at MP2/6-31G(d)). Ion **3** is stabilized by 40 kJ mol^{-1} with respect to its isolated components CH_2CH_2 and $[NH_2CH_2]^+$ and lies 87 kJ mol^{-1} above **1**.

Re-orientation of the two components of the complex $[CH_2CH_2{\bullet\bullet\bullet}H_2NCH_2]^+$ (**3**) can occur via **TS:3→4**, with a relative energy of 105 kJ mol^{-1}, corresponding to a barrier from **3** of only 18 kJ mol^{-1}. The resulting ion-neutral complex **4**, which is best described as $[CH_2CH_2{\bullet\bullet\bullet}CH_2NH_2]^+$, now has the ethylene carbons weakly bonded to the carbon atom from the $[NH_2CH_2]^+$ moiety, with long C–C bonds (2.891 Å). Ion **4** is stabilized by 25 kJ mol^{-1} with respect to CH_2CH_2 and $[NH_2CH_2]^+$ and lies 102 kJ mol^{-1} above **1**. Dissociation of either **3** or **4** results in ethylene plus $[CH_2NH_2]^+$ at 127 kJ mol^{-1}.

The complex **4** can undergo a concerted ring opening and 1,3-hydrogen shift to give $[CH_3CH_2CHNH_2]^+$ (**5**) at –25 kJ mol^{-1}. The transition structure (**TS:4→5**) for this process has an energy 191 kJ mol^{-1} above **1**.

Ion **5** can rearrange to $[CH_3CHCH_2NH_2]^+$ (**6**) via **TS:5→6** at a relative energy of 157 kJ mol^{-1}. The energy of **6** (164 kJ mol^{-1}), is actually higher than that of the transition structure for isomerization to **5** once zero-point vibrational energies are included, indicating that at best **6** lies in a shallow potential well. It is also possible for **4** to isomerize directly to **6** via **TS:4→6**, corresponding to a concerted ring opening and 1,2-hydrogen shift, with a relative energy of 222 kJ mol^{-1}.

Another possible rearrangement of $[CH_2CH_2{\bullet\bullet\bullet}CH_2NH_2]^+$ (**4**) leads to protonated azetidine (**11**) with a relative energy of 23 kJ mol^{-1}. The transition structure for this process (**TS:4→11**) lies at 226 kJ mol^{-1}. The role of **11** in labeling experiments will be discussed later.

More direct routes to the formation of $[CH_3CHCH_2NH_2]^+$ (**6**) from both **1** and **2** are also possible. Ions **1** and **2** can rearrange via 1,2-hydrogen shifts to form protonated methylaziridine (**10**) at 29 kJ mol^{-1}. Subsequent ring opening via **TS:10→6** at 176 kJ mol^{-1} results in the formation of **6**. However, the transition structures for these pathways have relative energies of 299 kJ mol^{-1} (**TS:1→10**) and 290 kJ mol^{-1} (**TS:2→10**) that are significantly higher than that required (244 kJ mol^{-1}) for formation of **6** from **1** and **2** via **4** and **5**, and will therefore most likely not be competitive.

Isomerization of $[CH_3CHCH_2NH_2]^+$ (**6**) to $[CH_2CHCH_2NH_3]^+$ (**7**) can occur via a 1,4-hydrogen shift (i.e. via **TS:6→7**) with an energy of 191 kJ mol^{-1}. Ion **7** is characterized by a long C–N bond (1.528 Å) and therefore already resembles in some respects a complex between the allyl cation and ammonia. However, the C–C bond lengths in **7** are still identifiable as single (1.409 Å) and double (1.338 Å), indicating a strongly distorted allyl cation. Although we find no evidence for the intermediate **6a** of Scheme 4.1, we do find a transition structure **TS:6→6'** at 236 kJ mol^{-1} that resembles **6a**. This transition structure results in exchange of hydrogens within the ethylidene (CH_3CH) group of **6**.

Migration of the ammonia moiety in $[CH_2CHCH_2NH_3]^+$ (**7**) to a bridging position via **TS:7→8** at 189 kJ mol^{-1} gives **8**. Ion **8** can indeed be described as an ion-neutral complex between the allyl cation and ammonia. It lies 184 kJ mol^{-1} above **1** and is stabilized by 50 kJ mol^{-1} with respect to the separated species. Dissociation of the complex **8** or direct loss of ammonia from **7** results in the allyl cation plus ammonia,

lying 234 kJ mol^{-1} above **1**.

The mechanism shown in Scheme 4.3 reflects the potential energy profile of Figure 4.2. Apart from the fact that the species **1a** and **6a** that were postulated to be intermediates in Scheme 4.1 are actually transition structures, with **6a** having a relatively high energy, our calculations provide strong support for the mechanism proposed by Bowen at al.[4c] Our calculated surface is also found to be in good agreement with previous theoretical work.[4a,

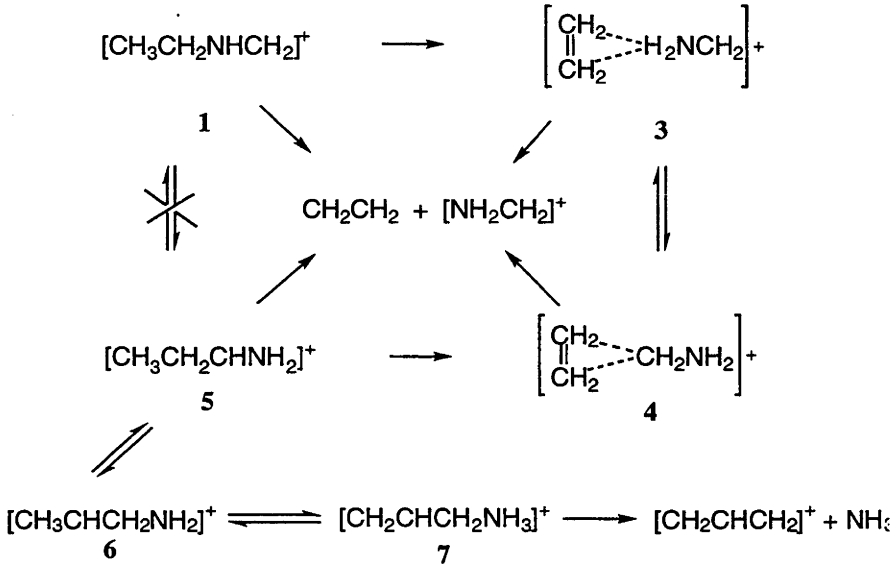

Scheme 4.3

4.3.2 Structural and Energetic Features of the $[C_3H_7S]^+$ Surface

The lowest energy conformer of $[CH_3CH_2SCH_2]^+$ (**12**) is shown in Figure 4.3. All energies in the following section are given relative to that of **12**, unless otherwise stated.

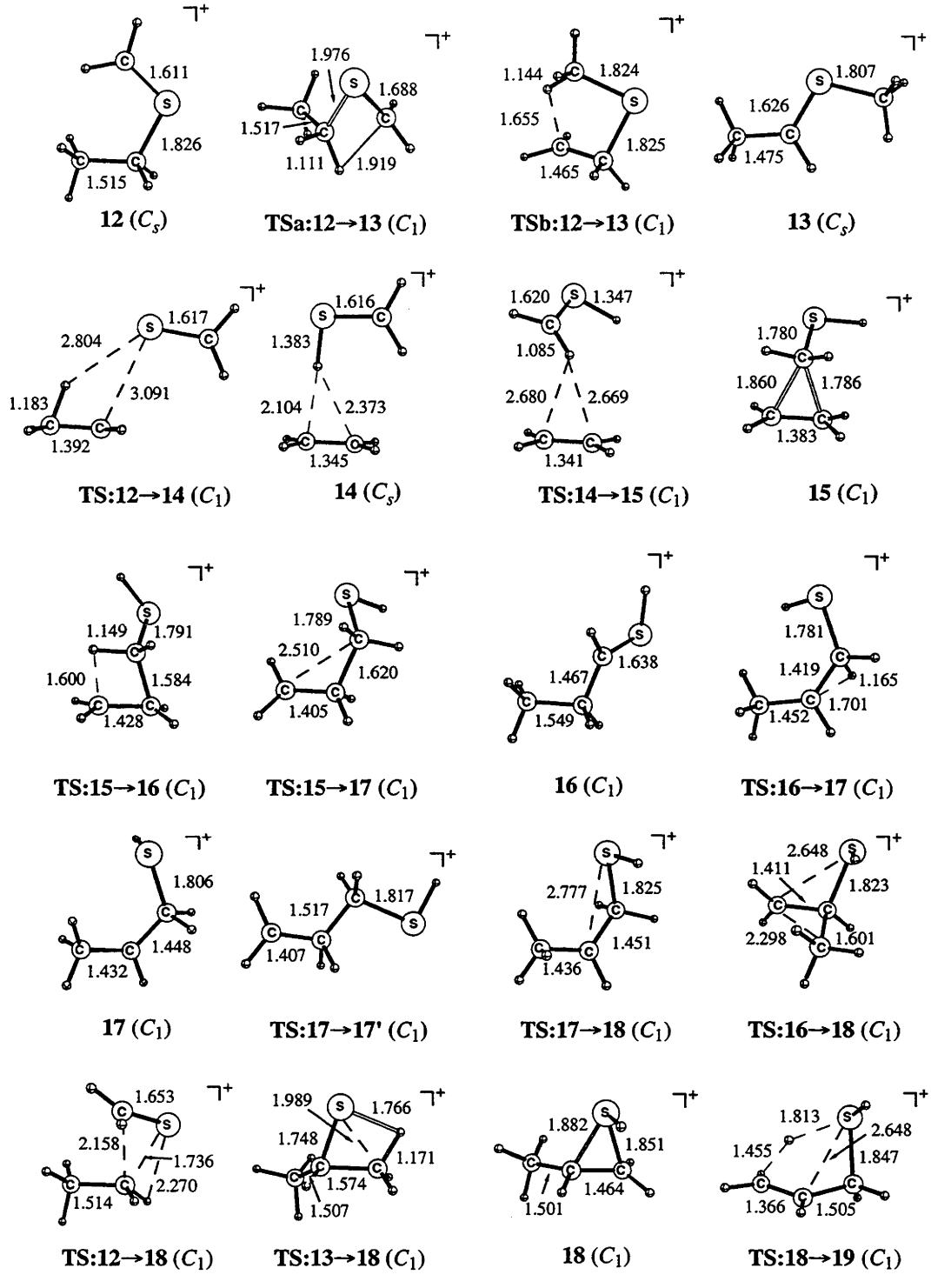

Figure 4.3 Selected MP2/6-31G(d) bond lengths (Å) relevant to $[C_3H_7S]^+$ ions.

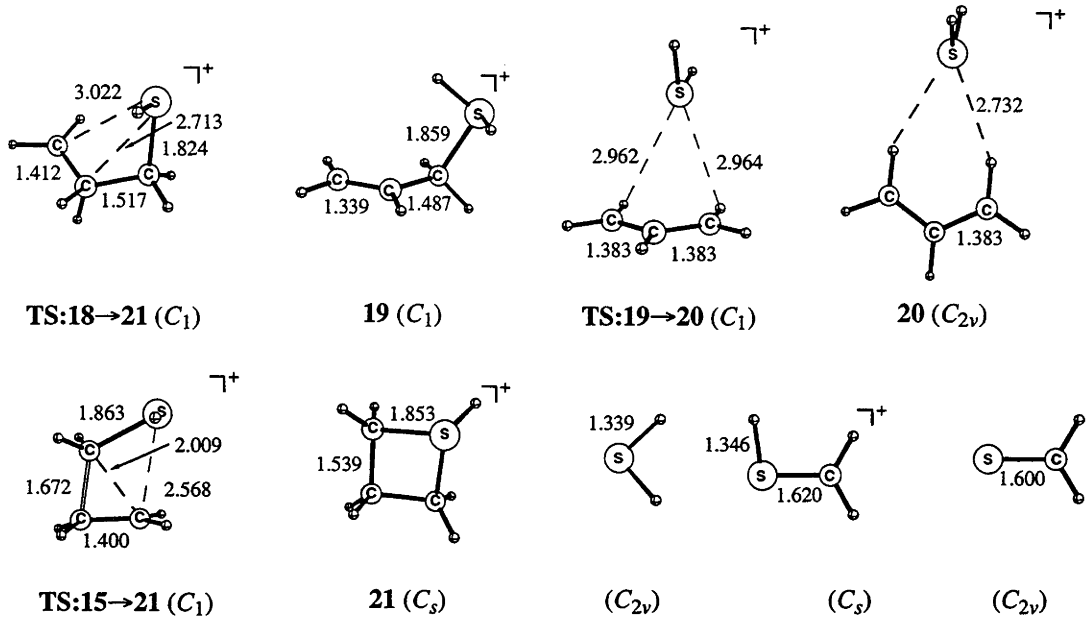

TS:18→21 (C_1) **19** (C_1) **TS:19→20** (C_1) **20** (C_{2v})

TS:15→21 (C_1) **21** (C_s) (C_{2v}) (C_s) (C_{2v})

Figure 4.3 (Cont.) Selected MP2/6-31G(d) bond lengths (Å) relevant to $[C_3H_7S]^+$ ions.

We find two possible pathways for the isomerization of $[CH_3CH_2SCH_2]^+$ (**12**) to $[CH_3CHSCH_3]^+$ (**13**), which lies at –40 kJ mol^{-1} (Figure 4.4). The first occurs via a 1,3-hydrogen shift (**TSa:12→13**) at 172 kJ mol^{-1} and the second occurs via concerted 1,4- and 1,2-hydrogen shifts (**TSb:12→13**) at 207 kJ mol^{-1}.

Alternatively, a 1,3-hydrogen shift in **12** can occur via **TS:12→14** at 204 kJ mol^{-1}, resulting in **14**. This species is best described as an ion-neutral complex $[CH_2CH_2{\bullet\bullet\bullet}HSCH_2]^+$, in which the ethylene is bridged by a proton, with long C–H bonds (2.104 Å and 2.373 Å). Ion **14** has a relative energy of 117 kJ mol^{-1} and is stabilized by 41 kJ mol^{-1} with respect to the isolated species.

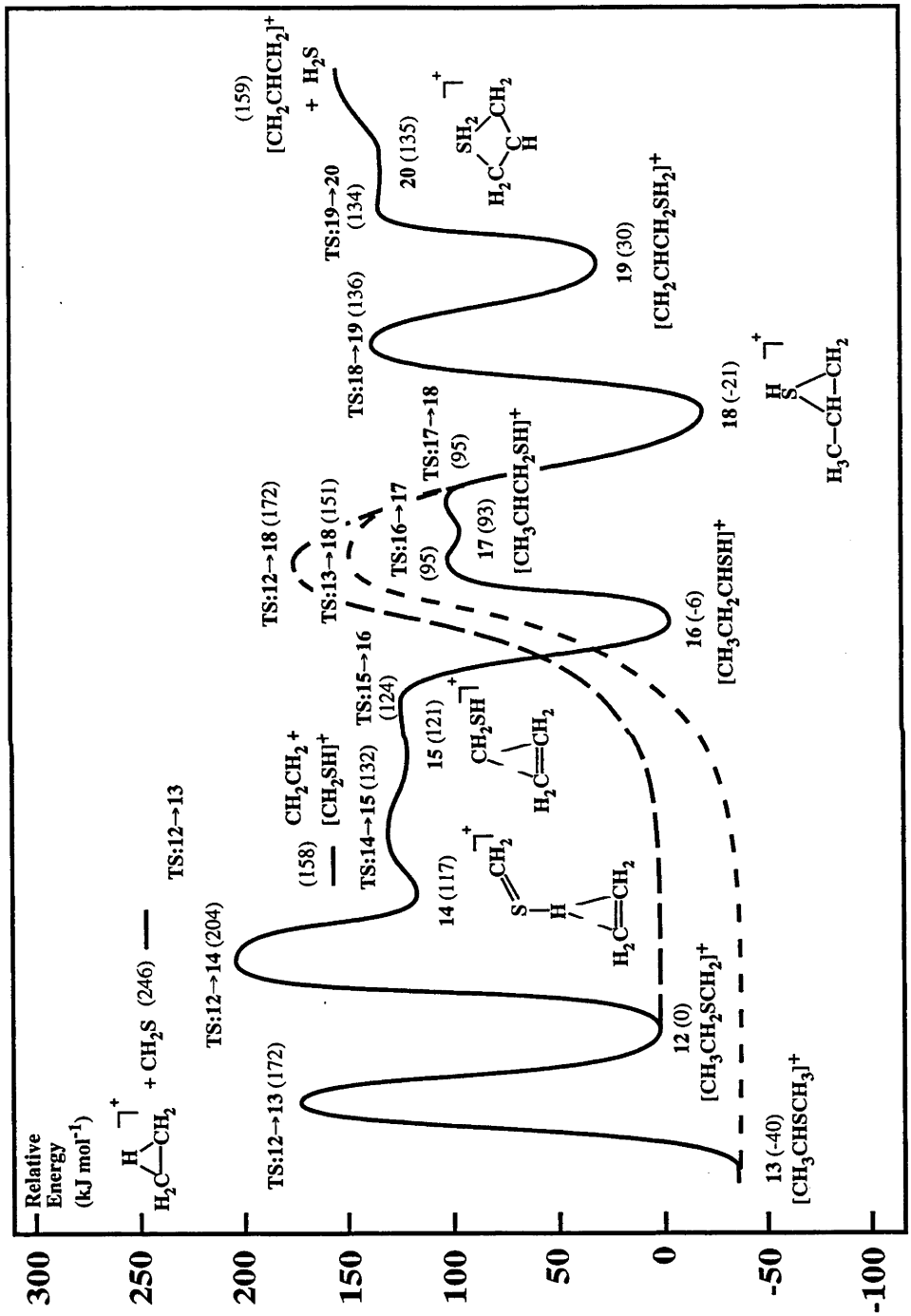

Figure 4.4 Schematic energy profile for rearrangement/fragmentation of $[C_3H_7S]^+$ ions. Relative energies (kJ mol^{-1}) given in parentheses.

Reorientation within the complex $[CH_2CH_2{\bullet\bullet\bullet}HSCH_2]^+$ (**14**) can occur via **TS:14→15** to form **15**, which has an energy of 121 kJ mol^{-1}. Ion **15** is also an ion-neutral complex, but in this case is best described as $[CH_2CH_2{\bullet\bullet\bullet}CH_2SH]^+$ in which the ethylene is bridged by a carbon atom, with elongated C–C bonds of 1.860 Å and 1.786 Å. The C–S bond is also extended by 0.160 Å, indicating a strong interaction between the two components of this complex. Ion **15**, lying at 121 kJ mol^{-1}, is stabilized by 37 kJ mol^{-1} relative to the isolated species. Dissociation of either **14** or **15** results in ethylene plus $[CH_2SH]^+$, with a relative energy of 158 kJ mol^{-1}.

The $[CH_2CH_2{\bullet\bullet\bullet}CH_2SH]^+$ complex (**15**) lies in a very shallow well with a barrier of only 3 kJ mol^{-1} for its rearrangement (via **TS:15→16**) to $[CH_3CH_2CHSH]^+$ (**16**) at –6 kJ mol^{-1}.

Ion **15** can also rearrange to form protonated thietane (**21**) via **TS:15→21** at 157 kJ mol^{-1}. Protonated thietane (**21**) lies at an energy of 1 kJ mol^{-1} and is important in ^{13}C-label exchange as discussed below.

We find two pathways for the rearrangement of $[CH_3CH_2CHSH]^+$ (**16**) to protonated methylthiirane (**18**), which has a relative energy of –21 kJ mol^{-1}. The first is a stepwise route involving an initial 1,2-hydrogen shift (via **TS:16→17** at 95 kJ mol^{-1}) to form $[CH_3CHCH_2SH]^+$ (**17**) at 93 kJ mol^{-1}. Ion **17** can also be formed directly from **15** via **TS:15→17** at 159 kJ mol^{-1}. Subsequent ring closure in **17** via **TS:17→18** at 95 kJ mol^{-1} results in **18**. The second pathway via **TS:16→18** involves a 1,2-methyl shift and is distinguished firstly by its higher energy (154 kJ mol^{-1}) and secondly by the fact that it will result in exchange of ^{13}C-labels. This is discussed further below.

The ion **17a** from Scheme 4.2 corresponds to the transition structure **TS:17→17'**, which could contribute to hydrogen exchange within **17** and lies at an

energy of 173 kJ mol^{-1}.

An alternative pathway for the formation of protonated methylthiirane (**18**) has previously been suggested starting from **13** and involving a 1,2-hydrogen shift from carbon to sulfur and ring closure.[5] We find that this reaction can indeed occur, via **TS:13→18**, with a barrier of 151 kJ mol^{-1}. We also find a pathway whereby **12** can directly rearrange to **18** as previously suggested.[5] This also occurs via a 1,2-hydrogen shift (**TS:12→18**), having a relative energy of 193 kJ mol^{-1}. The energies of the rate-limiting steps to direct isomerization to **18** from either **12** (via **TS:12→18**) of 172 kJ mol^{-1} or **13** (via **TS:13→18**) of 151 kJ mol^{-1} are actually lower than that for the rate-limiting step (via **TS:12→14**) for the ion-neutral complex mechanism discussed above of 204 kJ mol^{-1}.

A 1,4-hydrogen shift in protonated methylthiirane (**18**) via **TS:18→19** at 136 kJ mol^{-1} results in protonated allyl thiol $[CH_2CHCH_2SH_2]^+$ (**19**) with an energy of 30 kJ mol^{-1}. As for the analogous $[C_3H_8N]^+$ ion , we observe a long C–S bond (1.859 Å), suggesting a structure with ion-neutral-complex character. However, the C–C bonds in **19** are still recognizable as single (1.487 Å) and double (1.339 Å), indicating considerable distortion in the complex between H_2S and the allyl cation. Ion **18** can also isomerize via **TS:18→21** (152 kJ mol^{-1}) to form protonated thietane (**21**) which is important in ^{13}C-label exchange.

Migration of the H_2S moiety in **19** yields the H_2S-allyl cation complex (**20**) at 135 kJ mol^{-1} via the transition structure **TS:19→20** at 134 kJ mol^{-1}. Dissociation of **20** or direct H_2S loss from **19** leads to H_2S plus $[CH_2CHCH_2]^+$, with a relative energy of 159 kJ mol^{-1}.

The mechanism shown in Scheme 4.4 is representative of the potential energy profile shown in Figure 4.4. The main difference that we observe between the

previously proposed mechanism of Scheme 4.2 and that reflecting our calculations and shown in Scheme 4.4 is the fact that **16a** corresponds not to a minimum but to a relatively high energy transition structure. We find that the "direct" pathways shown in Schemes 4.2 and 4.4 are actually lower in energy than the ion-neutral-complex–mediated mechanism (i.e. isomerization via **14** and **15**).

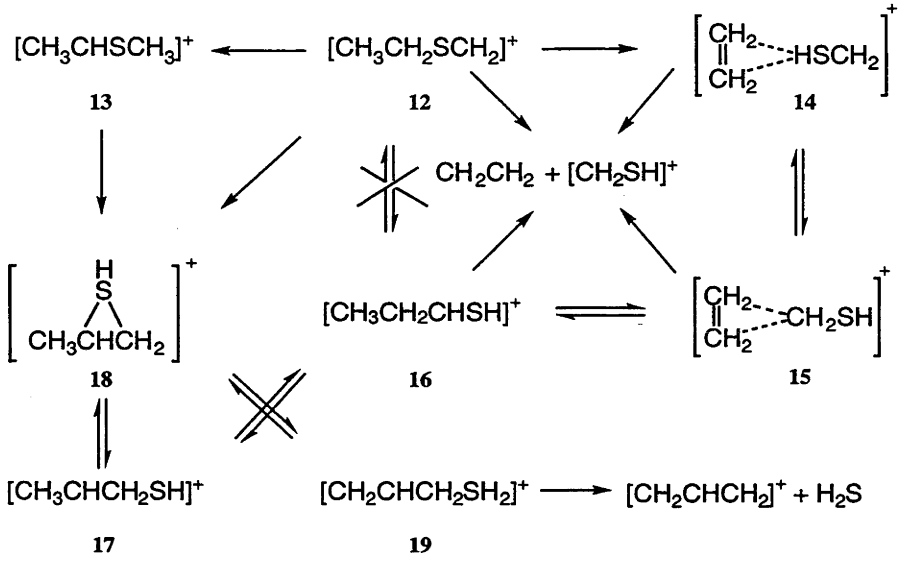

Scheme 4.4

4.3.3 Comparisons With Experimental Thermochemical Data

Calculated and experimental heats of formation ($\Delta_f H^\circ_{298}$) for $[C_3H_8N]^+$ ions and related species are presented in Table 4.1. Agreement between our calculated results and the experimental values from Lias et al.[9] is generally good but in some cases there are differences greater than 10 kJ mol^{-1}. Comparison with the rederived experimental values of Hammerum and Sølling[10] shows improved agreement, with all values but one now being within the accepted error margin. For the CH_2NH plus $[NH_2CH_2]^+$ pair, the discrepancy is 48 kJ mol^{-1} but this is reduced to just 6 kJ mol^{-1} when a more recent value[11] for the heat of formation of CH_2NH is used.

Heat of formation data relevant to the dissociation of $[C_3H_7S]^+$ ions and related species is listed in Table 2. Agreement between theory and the values from Lias et al.[17] is within the accepted limits (± 10 kJ mol^{-1}) for the product pair H_2S and $[CH_2CHCH_2]^+$ only. The calculated heats of formation show greater discrepancies when compared with experimental results from Broer et al.,[5a] the differences being as large as 47 kJ mol^{-1}, suggesting that re-examination of the experimental data is desirable.

Comparisons with experimentally determined barrier heights can also be made. The barriers obtained[4c] from the appearance energies for ethylene loss from **1** and **5** of 293 kJ mol^{-1} and 296 kJ mol^{-1}, respectively, are significantly higher than the calculated values of 244 kJ mol^{-1} and 216 kJ mol^{-1}. However, since appearance energies provide an upper bound to the true barriers, our results could be taken as being consistent with experiment. The barrier to ammonia loss from **7** is found experimentally to have a value of 255 kJ mol^{-1}, again somewhat higher than our calculated value of 225 kJ mol^{-1}.

Experimental barriers[5a] to ethylene loss from both **12** and **13** correspond to a relative energy of 222 kJ mol^{-1}, again higher than the calculated barrier of 172 kJ mol^{-1} for the rate-limiting steps from **12** and **13** (via **18**). Ethylene loss from **16** is found experimentally to have a barrier[5a] of 155 kJ mol^{-1}, quite close to the calculated value of 164 kJ mol^{-1}. It should be noted that these barriers were derived using the heats of formation from Broer et al.[5a] with which we have noted significant disagreement, and they would be altered by employing more accurate heats of formation for the relevant ions.

Table 4.1 Calculated and Experimental Heats of Formation for $[C_3H_8N]^+$ Ions and Related Species (kJ mol^{-1})

Species		G2	Experiment[a]
$[CH_3CH_2NHCH_2]^+$	**1**	671	653, 666[b]
$[CH_3CHNHCH_3]^+$	**2**	632	615, 631[b]
$[CH_2CH_2\bullet\bullet\bullet H_2NCH_2]^+$	**3**	762	
$[CH_2CH_2\bullet\bullet\bullet CH_2NH_2]^+$	**4**	776	
$[CH_3CH_2CHNH_2]^+$	**5**	644	636, 652[b]
$[CH_3CHCH_2NH_2]^+$	**6**	835	
$[CH_2CHCH_2NH_3]^+$	**7**	679	
$[CH_2CHCH_2\bullet\bullet\bullet NH_3]^+$	**8**	860	
$[CH_2CHNHCH_2\bullet\bullet\bullet H_2]^+$	**9**	804	
$[CH_2CH_2CH_2NH_2]^+$	**10**	690	698
$[CH_3CHCH_2NH_2]^+$	**11**	697	704
$NH_3 + [CH_2CHCH_2]^+$		910	900
$CH_2CH_2 + [NH_2CH_2]^+$		801	797, 804[b]
$CH_2NH + [CH_3CH_2]^+$		989	1037, 995[c]
$H_2 + [CH_2CHNHCH_2]^+$		802	

[a] All experimental values are taken from ref. 9 unless otherwise noted. [b] Values rederived in Hammerum et al.[10] [c] Heat of formation for CH_2NH from ref. 11.

Table 4.2 Calculated and Experimental Heats of Formation for $[C_3H_7S]^+$ Ions and Related Species (kJ mol^{-1})

Species		G2	Experiment[a]
$[CH_3CH_2SCH_2]^+$	**12**	770	803[b]
$[CH_3CHSCH_3]^+$	**13**	731	778[b]
$[CH_2CH_2\bullet\bullet\bullet HSCH_2]^+$	**14**	892	
$[CH_2CH_2\bullet\bullet\bullet CH_2SH]^+$	**15**	891	
$[CH_3CH_2CHSH]^+$	**16**	765	799[b]
$[CH_3CHCH_2SH]^+$	**17**	865	879[b]
$[CH_3\overline{CHCH_2SH}]^+$	**18**	749	737, 774[b]
$[CH_2CHCH_2SH_2]^+$	**19**	801	
$[CH_2CHCH_2\bullet\bullet\bullet SH_2]^+$	**20**	912	
$[\overline{CH_2CH_2CH_2SH}]^+$	**21**	769	749, 799[b]
$H_2S + [CH_2CHCH_2]^+$		935	925, 920[b]
$CH_2CH_2 + [CH_2SH]^+$		933	914, 946[b]
$CH_2S + [CH_3CH_2]^+$		1020	1007

[a] All experimental values are taken from ref. 9 unless otherwise noted. [b] From Broer et al.[5a]

4.3.4 Rationalization of Fragmentation Behavior

There is extensive experimental information available concerning the fragmentation behavior of the $[C_3H_8N]^+$ and $[C_3H_7S]^+$ ions.[4,5] By examining the calculated potential energy surfaces and results of RRKM calculations, we attempt to rationalize the various observations.

4.3.4.1 $[CH_3CH_2NHCH_2]^+$ (1)

The only observed metastable elimination product from $[CH_3CH_2NHCH_2]^+$ (**1**) is ethylene.[4] This can be readily explained by examining the schematic energy profile shown in Figure 4.2. A substantial barrier exists for isomerization of **1** to the ion-neutral complex **3**, and hence **3** will be formed with significant excess energy. In a situation such as this, dissociation will be favored over isomerization. Hence, fragmentation of the complex leading to the elimination of ethylene, takes place before rearrangements that would result in the loss of other species can occur.

From the energy profile shown in Figure 4.2 it would be reasonable to conclude that loss of molecular hydrogen from **1** could occur after isomerization to **2**. However, no such loss is observed experimentally.[4f] Although the calculated barrier for isomerization of **1** to **2** is lower than the barrier for loss of ethylene, the transition structure is fairly tight (Figure 4.1), suggesting the possibility of an opposing entropy contribution to the relative reaction rates. Indeed, examination of calculated rate constants (Figure 4.5) shows that rearrangement of **1** to **3**, leading to ethylene elimination, is significantly faster then rearrangement of **1** to **2**, leading to H_2 loss. This is now consistent with the absence of H_2 elimination from **1** observed experimentally.

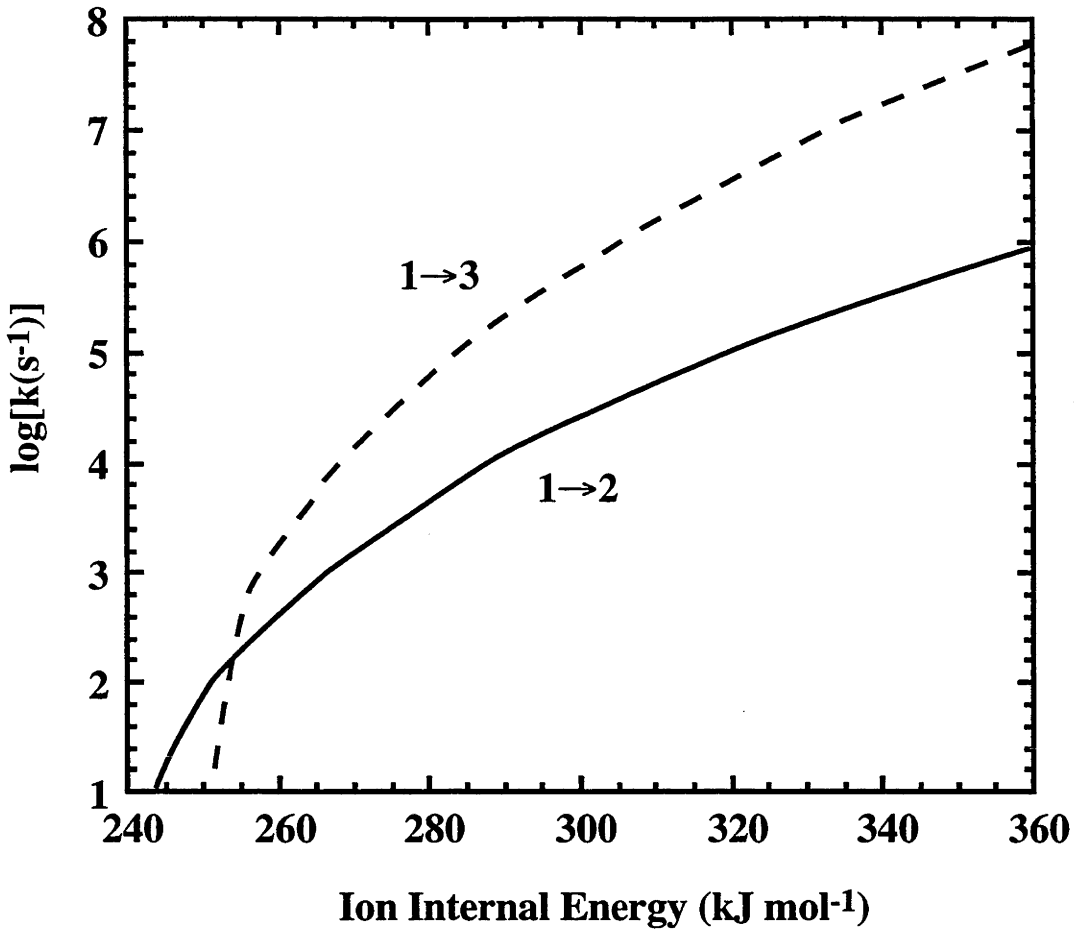

Figure 4.5 RRKM rate constants (log *k*) calculated as a function of internal energy (*E*) for rearrangement processes of **1**. Energy is measured relative to **1**.

4.3.4.2 $[CH_3CHNHCH_3]^+$ (2)

The metastable ion $[CH_3CHNHCH_3]^+$ (**2**) exhibits a competition between elimination of ethylene (~70%) and hydrogen (~30%).[4b,4f] This is consistent with the similar barriers calculated for elimination of ethylene (via **TS:1→3**) and hydrogen (via **TS:2→9**) (244 and 231 kJ mol^{-1}, respectively, Figure 4.2). In addition, RRKM calculations indicate that these reactions occur with rate constants that are very similar.

4.3.4.3 $[CH_3CH_2CHNH_2]^+$ (5)

Yet another distinct fragmentation pattern is shown by the metastable ion $[CH_3CH_2CHNH_2]^+$ (**5**), which eliminates both ethylene and ammonia, with the latter dominating.[4] It can be seen from Figure 4.6 that the rates of ammonia elimination from **7** and ethylene loss from **5** (via **TS:4→5**) are similar in the rate constant region appropriate to metastable ions ($k = 10^4 - 10^6$ s^{-1}). Although this does not indicate preferential ammonia loss, it is consistent with both ethylene and ammonia loss being observed. It can also be seen from Figure 4.6 that at increased energies, ammonia elimination becomes more favorable, despite the fact that ethylene is a lower-energy elimination product. This result is consistent with the greater proportion of ammonia loss observed when **5** is examined under the higher internal energy conditions present in the first field-free region of the mass spectrometer.[4f]

4.3.4.4 $[CH_3CHSCH_3]^+$ (13) and $[CH_3CH_2CHSH]^+$ (16)

The metastable ions $[CH_3CHSCH_3]^+$ (**13**) and $[CH_3CH_2CHSH]^+$ (**16**) both eliminate roughly 38% ethylene and 62% hydrogen sulfide.[5c] However, different kinetic energy releases are observed, suggesting different rate-limiting steps for the elimination from the two ions. At first glance, it seems that this latter observation conflicts with our calculated surface (Figure 4.4), which shows that **13** can rearrange to **18** below the threshold for ethylene elimination, thereby suggesting that the kinetic energy released during ethylene elimination should be the same for both these species. However, we find that metastable isomerization of **13** to **18** does not occur with a sufficient rate to be observed experimentally ($\sim 10^4$ s^{-1}) until an energy of about 190 kJ mol^{-1} is reached. This results in elimination from the two ions having different rate-limiting steps and hence the kinetic energy releases for these two species are indeed different.

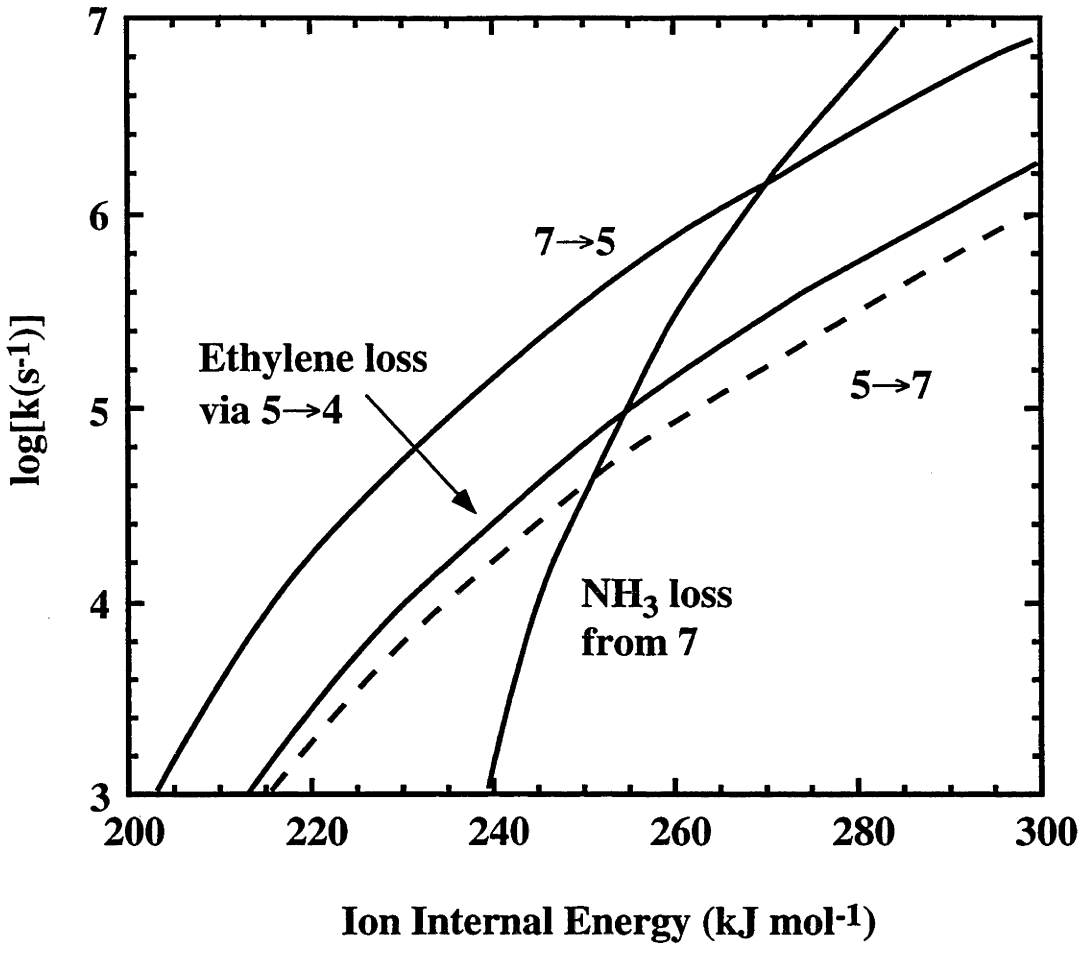

Figure 4.6 RRKM rate constants (log *k*) calculated as a function of internal energy (*E*) for rearrangement/fragmentation processes from **5** and **7**. Energy is measured relative to **1**.

It remains to explain why **13** and **16** have similar fragmentation patterns[5c] despite the difference in their rate-limiting steps. The formation of ion **18** from **13** will result in **18** (or **16**) being produced with excess internal energy, which would normally be expected to affect the product distributions. However, since the rate-limiting steps for elimination of ethylene and hydrogen sulfide from **16** both involve dissociation of a complex, they will have similar frequency factors. In addition, the fragmentation products have similar energies. We might therefore expect that the relative rate constants would be similar, regardless of ion internal energy, consistent with **13** and **16** showing

similar fragmentation patterns, despite the greater internal energy present in **16** produced by rearrangement of **13**.

4.3.4.5 $[CH_3CH_2SCH_2]^+$ (12)

The metastable ion $[CH_3CH_2SCH_2]^+$ (**12**) eliminates both ethylene (57%) and hydrogen sulfide (43%).[5c] The rearrangement of **12** to **14** has a substantial barrier and, for reasons similar to those presented for the analogous $[CH_3CH_2NHCH_2]^+$ ion (**1**), we might have expected only to observe ethylene elimination if the other possible fragmentation pathways were required to proceed via **TS:12→14**. However, as discussed in Section 4.3.2, there are lower-energy routes that could allow the formation of hydrogen sulfide via conventionally-bonded intermediates without the involvement of **TS:12→14**. In the metastable time frame ($k = 10^4 - 10^6$ s^{-1}), we find that rearrangement of **12** to **13** and **12** to **14** have approximately equal rates, with direct isomerization of **12** to **18** being somewhat slower (Figure 4.7). We could therefore expect that approximately 50% of **12** would lose ethylene only (via **TS:12→14**) while the remainder would rearrange via **13** to **18** and then **16**, resulting in loss of ethylene and hydrogen sulfide in the ratios discussed for ion **16** in Section 4.3.4.4. This would then be consistent with the greater abundance of ethylene loss observed from **12** relative to that from **16**.[5c]

To our knowledge, no experiments have examined the decomposition of $[C_3H_7S]^+$ ions in different energy regimes (field-free regions) but we can make predictions based on the results discussed above. We would expect little variation in the relative abundances of the elimination products from ions **13**, **16** and **18** since we have shown that these are insensitive to internal energy. On the other hand, because rearrangement of **12** to **14** becomes more favorable than rearrangement of **12** to **13** at higher energies (Figure 4.7), we would expect a greater proportion of ethylene

elimination to occur when ion **12** has larger internal energies.

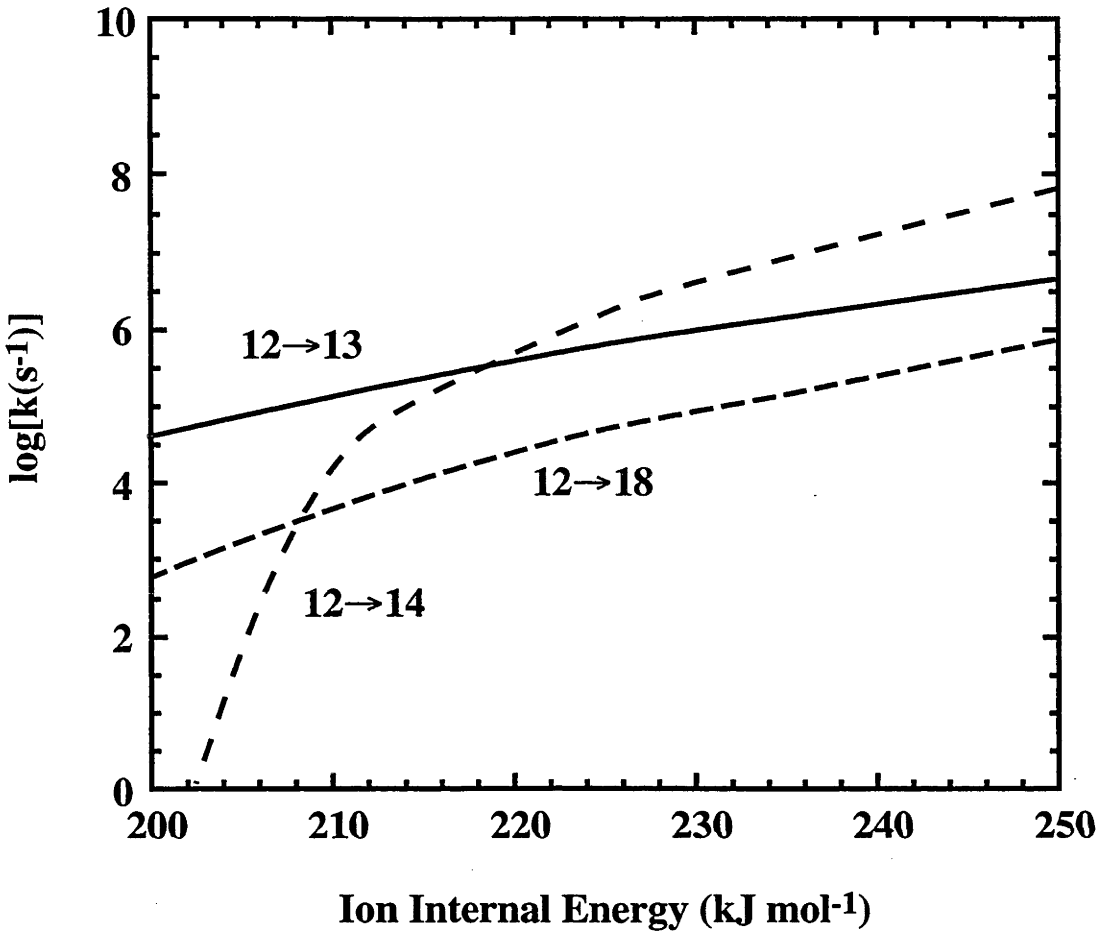

Figure 4.7 RRKM rate constants (log *k*) calculated as a function of internal energy (*E*) for the rearrangement processes of **12**. Energy is measured relative to **12**.

4.3.5 Labeling Experiments

Numerous labeling studies have been carried out on both deuterated and ^{13}C-substituted isotopomers of the $[C_3H_7X]^+$ ions. Our calculations can assist in the understanding of such experiments.

4.3.5.1 $[CH_3CH_2NHCH_2]^+$ (1)

Labeling experiments have shown that during ethylene elimination from $[CH_3CH_2NHCH_2]^+$ (**1**), β-hydrogen transfer to nitrogen occurs exclusively.[4] This is not surprising considering the mechanism discussed in Section 4.3.4.1. The initial isomerization step (**TS:1→3**) involves transfer of a β-hydrogen to nitrogen (Figure 4.1) and due to its high internal energy, the resulting complex will dissociate almost immediately. Hence, no further reactions that could result in label exchange occur.

4.3.5.2 $[CH_3CHNHCH_3]^+$ (2)

Based on labeling experiments for ethylene and hydrogen elimination from $[CH_3CHNHCH_3]^+$ (**2**), a mechanism suggesting complete exchange of the hydrogens within the CH_3CH group has been proposed.[4f] The transition structure for this exchange (**TS:2→2'**) has an energy of 268 kJ mol^{-1}, which is somewhat higher than the energies of the energy-determining steps for isomerization of either **2** to **3** or **2** to **9** (**TS:1→3** at 244 kJ mol^{-1} and **TS:2→9** at 231 kJ mol^{-1}, respectively). However, our calculated rate constants for exchange within **2** and rearrangement of **2** to either **3** or **9** are comparable in the metastable region, consistent with the observed labeling results.

Loss of molecular hydrogen from **2** involves abstraction of one hydrogen atom from each of the methyl groups (see **TS:2→9**, Figure 4.1). If the exchange mechanism **2→2'** discussed above is operating, it would be expected that the N-methyl group would contribute one hydrogen while the other hydrogen would come randomly from the CH_3CH group. Such a mechanism has previously been shown to agree well with the experimental results.[4f]

4.3.5.3 $[CH_3CH_2CHNH_2]^+$ (5)

For the metastable ion $[CH_3CH_2CHNH_2]^+$ (**5**), labeling experiments suggest that in the first field-free region the nitrogen-bound hydrogens retain their identity but the remaining six hydrogens show complete exchange.[4f] For example, during ethylene loss from metastable $[CH_3CD_2CHNH_2]^+$ the observed abundances are 5% CH_2CH_2, 52% C_2H_3D and 43% $C_2H_2D_2$[4f] compared with the values of 7%, 54% and 40%, respectively, expected for statistical exchange of all the alkyl hydrogens. Labeling experiments suggest a different behavior in the lower-energy second field-free region, with ethylene loss from $[CH_3CD_2CHNH_2]^+$ occurring in the ratios, 0% CH_2CH_2, 63% C_2H_3D and 37% $C_2H_2D_2$.[4f] This is close to the values of 0%, 67% and 33%, respectively, predicted if exchange is restricted to the CX_2CX moiety.

The mechanism proposed to explain the observed label exchange in **5** involves sequential hydrogen shifts,[4c,4d] and can be rationalized in terms of our calculated potential energy surface (Figure 4.4). Reversible rearrangement of **5** and **6** results in exchange within the CH_2CH group. This occurs below the dissociation threshold and would therefore be expected to be rapid. In the lower-energy second field-free region, exchange is restricted to the CH_2CH group. Further exchange within **6**, occurring via **TS:6→6'**, which would result in a statistical distribution of carbon-bound hydrogens in **5**, would require a relative energy of 235 kJ mol^{-1}, or 44 kJ mol^{-1} more than that required for ethylene elimination. Although such exchange does not take place in the second field-free region, rearrangement via **TS:6→6'** becomes more favorable with the higher internal energies characteristic of the first field-free region, and exchange of all carbon-bound hydrogens is observed.

Now we must address the question of label retention of nitrogen-bound hydrogens in the loss of ethylene from **5**. We find that rearrangement of **7** to **5** is faster than ammonia loss from **7** (Figure 4.6). This would seem to suggest that reversible

isomerization of **7** and **5**, resulting in exchange of nitrogen-bound and carbon-bound hydrogens, could occur. In previous theoretical work, a similar observation was made,[4a] and was rationalized by suggesting that the calculated barrier for rearrangement of **7** to **5** was underestimated. Our confirmation of the relative barriers at a much higher level of theory would have seemed to make this explanation less likely but we note that, due to the steep nature of the ln k vs E curve for ammonia loss from **7** (Figure 4.6), only a modest increase in the energy of the transition structure for rearrangement of **7** to **5** (via **6**) relative to the energy of the isolated allyl cation and ammonia would be required to alter the ordering of the predicted relative rates. Ammonia loss from $[CH_3CH_2CHNH_2]^+$ (**5**) also displays a strong selectivity for retention of nitrogen-bound hydrogens. Again, this is consistent with an underestimation in the calculated barrier for the rearrangement of **5** to **7**, relative to that of fragmentation

4.3.5.4 $[CH_3CH_2CHSH]^+$ (16)

On the basis of labeling studies on the metastable ion $[CH_3CH_2CHSH]^+$ (**16**), a mechanism involving incomplete exchange of the methyl hydrogens with the remaining alkyl hydrogens and only a small extent of exchange between sulfur-bound and alkyl hydrogens has been proposed.[5b] In contrast, our calculations suggest that the metastable ion **16** should undergo complete exchange of all alkyl hydrogens. Due to the low barriers to label-exchange processes such as isomerization of **16** to **17** and **16** to **15**, we would expect these processes to be rapid, resulting in a statistical distribution of labels on the alkyl chain. RRKM calculations support this conclusion, predicting that these processes should occur several orders of magnitude faster than dissociation.

We might expect that reversible isomerization of **19** to **18**, which also has a low barrier, would allow exchange between alkyl and sulfur-bound hydrogens. In the rate-constant region appropriate to metastable ions, our RRKM calculations predict that rearrangement of **19** to **18** is significantly faster than dissociation (Figure 4.8).

However, as for the related $[CH_3CH_2CHNH_2]^+$ ion, a modest increase in the calculated barrier for the rearrangement of **18** to **19** relative to the energy of the separated allyl cation and hydrogen of the predicted relative rates. This may be the reason for the apparent discrepancy between theory and experiment. Examination of the hydrogen sulfide loss from $[CH_3CH_2CHSH]^+$ (**16**) shows that again there is little exchange between the sulfur-bound and alkyl hydrogens.[5b] There is also incomplete exchange of the methyl hydrogens with the rest of the alkyl-chain, as indicated by the preference for the additional sulfur-bound hydrogen to originate from the methyl group.

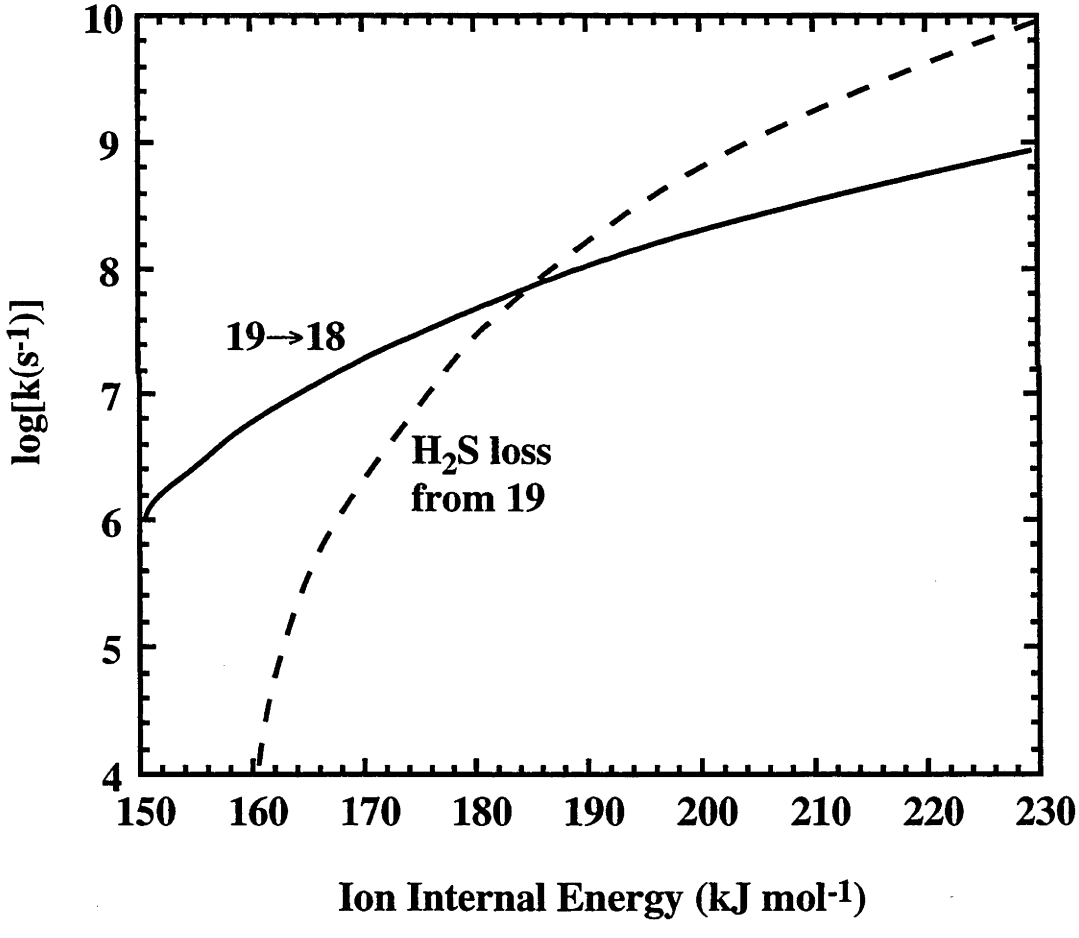

Figure 4.8 RRKM rate constants (log *k*) calculated as a function of internal energy (*E*) for the rearrangement/fragmentation processes of **19**. Energy is measured relative to **12**.

4.3.5.5 $[CH_3CHSCH_3]^+$ (13)

A mechanism to explain the results of labeling experiments associated with the loss of ethylene from $[CH_3CHSCH_3]^+$ (**13**) has previously been suggested.[5c] This mechanism involves complete exchange of all but one hydrogen, the latter originating from the sulfur-bound methyl group. The isomerization of **13** to **18** involves a hydrogen shift from exactly this methyl group to sulfur. It can be seen from Figure 4.8 that at energies above 190 kJ mol^{-1}, the energy at which RRKM calculations suggest metastable isomerization of **13** to **18** begins, H_2S loss from **19** is faster than rearrangement back to **18**. Hence, we would expect little exchange between alkyl and sulfur-bound hydrogens in such circumstances, with the result that the methyl hydrogen that has migrated to the sulfur does not participate in any further exchange processes.

4.3.5.6 $[CH_3CH_2SCH_2]^+$ (12)

As discussed in Section 4.3.4.5, ethylene elimination from $[CH_3CH_2SCH_2]^+$ (**12**) is predicted to occur to approximately equal extents via rearrangement to **14** and to **13**. This would result in about 50% β-hydrogen transfer to sulfur from isomerization of **12** to **14** and 50% exhibiting the labeling behavior of ion **13**. Such a mechanism has previously been suggested and found to be in good agreement with experimental results.[5b]

A mechanism for hydrogen sulfide loss from $[CH_3CH_2SCH_2]^+$ (**12**) that is consistent with experimental results has been proposed in which rearrangement of **12** to **18** and subsequent loss of H_2S can occur via two pathways.[5b] The first is rearrangement via **13** and **18**, as discussed for ethylene elimination above, and secondly, a direct route from **12** to **18**. Our calculations show that the first pathway is about an order of magnitude faster than direct isomerization of **12** to **18** (Figure 4.7). This does not support equal participation of the two pathways but it does suggest that isomerization of

12 to **18** could play a role in determining the resulting label distributions.

4.3.5.7 ^{13}Carbon Label Studies

The study of ^{13}C-labeled species can give insight into the skeletal rearrangements that occur during the isomerization of metastable ions. No experimental ^{13}C-labeling results have been reported for the $[C_3H_8N]^+$ ions discussed here. However, on the basis of our calculated potential surface, we would expect little ^{13}C-label exchange to occur in these systems. This type of exchange could potentially take place via reversible isomerization of protonated azeditine (**11**) and **4**. However, as discussed earlier, there are significant barriers to the formation of **4** from either $[CH_3CH_2NHCH_2]^+$ (**1**) or $[CH_3CH_2CHNH_2]^+$ (**5**), resulting in dissociation of the complex being faster than rearrangement processes, such as isomerization of **4** to **11**.

Experimental ^{13}C-labeling studies on $[C_3H_7S]^+$ ions have been performed and suggest that ^{13}C-label exchange occurs to a small extent.[5b] A mechanism to explain the results of these labeling studies suggested[5b] isomerization of $[CH_3CH_2CHSH]^+$ (**16**) to protonated methylthiirane (**18**) via the primary cation intermediate $[CH_3CH(SH)CH_2]^+$. This mechanism results in exchange of the α and β carbons within **16**. Although we find no evidence for an intermediate of this type, we do find a transition structure corresponding to it (**TS:16→18**). However, the energy requirement for this pathway is 59 kJ mol^{-1} higher than that for an alternative route via **TS:16→17** and **TS:17→18** that does not result in exchange of ^{13}C-labels. Nevertheless, the energy required for rearrangement (via **TS:16→18**) is still below the dissociation limit so, although we would not expect there to be a large amount of ^{13}C-label exchange via this pathway, it is feasible that some exchange could occur.

It is also possible that ^{13}C-label exchange can occur via reversible isomerization of protonated methylthiirane (**18**) or the complex **15** with protonated thietane (**21**). The

intervention of **TS:15→21** is distinguishable from the other possible mechanisms by virtue of the fact that it will result in exchange of all carbons. We cannot distinguish between these alternatives based on the available experimental data. While the barriers to the isomerization processes via **21** of 157 and 152 kJ mol^{-1}, respectively, are just below the dissociation threshold, they must compete with many other low-energy processes, and hence we would not expect a large extent of rearrangement to **21**. Hence, this route should also not lead to substantial ^{13}C-label exchange.

4.3.6 When Are Ion-Neutral Complexes Important?

We have noted several times in the present work that complexes that are formed with energy in excess of the dissociation limit are likely to fragment before they can be involved in any rearrangements. The principal origin of this excess energy is the presence of a reverse barrier for their formation. Hence, in order for ion-neutral complexes to be mechanistically significant intermediates, it is important that rearrangement to the complex occurs below the threshold for dissociation. We now examine some of the factors determining the relevant barriers for formation of $[CH_2CH_2{\bullet\bullet\bullet}HXCH_2]^+$ complexes.

For both X = S and NH, we find that the isomerization of $[CH_3CH_2XCH_2]^+$ to the ion-neutral complex $[CH_2CH_2{\bullet\bullet\bullet}HXCH_2]^+$ occurs above the dissociation limit, whereas for X = O the isomerization was found to occur below the dissociation threshold.[3] Since $[CH_2CH_2{\bullet\bullet\bullet}HXCH_2]^+$ is a proton-bound complex, it would be reasonable to suggest that its binding energy may in part be determined by the relative proton affinities of CH_2CH_2 and XCH_2. It can be seen from Table 4.3 that there is indeed a correlation between the binding energy of the complex and the relative proton affinities (ΔPA). More closely matched proton affinities, i.e. lower values of ΔPA, allow greater sharing of the proton and hence a greater binding energy.

It can be seen from Table 4.3 that there is also a correlation between the relative proton affinities and the barriers for rearrangement of $[CH_2CH_2{\bullet\bullet\bullet}HXCH_2]^+$ to $[CH_3CH_2XCH_2]^+$. Lower values of ΔPA are found to correspond to lower barriers. This result is not surprising when we examine the transition structures corresponding to this isomerization. It can be seen from Figures 4.1 and 4.3 that transition structures **TS:1→3** and **TS:12→14** both resemble complexes between $[CH_3CH_2]^+$ and CH_2X, as was previously found for X = O in Chapter 3.[3] A lower value of ΔPA results in the complex $[CH_3CH_2{\bullet\bullet\bullet}XCH_2]^+$, and therefore the barrier, being lower in energy relative to $[CH_2CH_2{\bullet\bullet\bullet}HXCH_2]^+$. Hence, the barrier for rearrangement of $[CH_2CH_2{\bullet\bullet\bullet}HXCH_2]^+$ to $[CH_3CH_2XCH_2]^+$ will tend to be low if the species CH_2CH_2 and XCH_2 have similar proton affinities.

Table 4.3 Relative Proton Affinities (ΔPA)[a] of CH_2X and CH_2CH_2, Binding Energies of $[CH_2CH_2{\bullet\bullet\bullet}HXCH_2]^+$ complexes[b] and Barriers for the Rearrangement of $[CH_2CH_2{\bullet\bullet\bullet}HXCH_2]^+$ to $[CH_3CH_2XCH_2]^+$ (G2, kJ mol^{-1})

X	ΔPA	Binding Energy	Barrier
O	29	73	44
S	98	41	87
NH	185	40	157

[a] ΔPA = $PA(CH_2X) - PA(CH_2CH_2)$. [b] Binding energy calculated with respect to CH_2CH_2 plus $[CH_2XH]^+$.

The rearrangement of $[CH_2CH_2{\bullet\bullet\bullet}CH_2NH_2]^+$ (**4**) to $[CH_3CH_2CHNH_2]^+$ (**5**) has a significant barrier (89 kJ mol^{-1}) and occurs above the threshold for ethylene elimination (Figure 4.2). In contrast, the corresponding rearrangements of $[CH_2CH_2{\bullet\bullet\bullet}CH_2OH]^+$

and $[CH_3CH_2{\bullet\bullet\bullet}CH_2SH]^+$ (**15**) occur with much smaller barriers (18 kJ mol^{-1} and 3 kJ mol^{-1}, respectively),[3b] i.e at energies below the dissociation limit.

We find that the barrier for rearrangement of the complex $[CH_2CH_2{\bullet\bullet\bullet}CH_2XH]^+$ to $[CH_3CH_2CHXH]^+$ can be related to the structure of the complex. The complex **15** (Figure 4.3) has relatively short bridging C–C bonds (1.860 Å and 1.786 Å) and bears some resemblance to the transition structure **TS:15→16**. Consequently, the barrier is low (3 kJ mol^{-1}). In contrast, complex **4** has very long bridging C–C bonds (2.891 Å) and its structure is quite different from that of **TS:4→5**, resulting in a larger barrier (89 kJ mol^{-1}). Intermediate behavior in relation to both the structure of the complex (bridging C–C bond lengths of 1.932 Å and 1.946 Å) and barrier height (18 kJ mol^{-1}) was observed in Chapter 3 in the case of X = O.[3b] This suggests that in situations of this type, the ion-neutral complex $[CH_3CH_2{\bullet\bullet\bullet}CH_2XH]^+$ can potentially play a more important role if it is tightly bound, i.e. if it has short bridging C–C bonds.

4.4 Concluding Remarks

Ion-neutral complexes are found not to play an important role in the fragmentation/rearrangement mechanisms of the isomeric $[C_3H_8N]^+$ and $[C_3H_7S]^+$ ions. In the case of $[C_3H_8N]^+$ systems, this is a consequence of the presence of significant reverse barriers to the formation of the important ion-neutral complexes (**3** and **4**), with the result that the complexes undergo dissociation in preference to isomerization. For the $[C_3H_7S]^+$ systems, on the other hand, the ion-neutral complexes are not mechanistically important in determining the product abundances because there are lower-energy pathways via conventionally-bonded intermediates. However, our results do suggest that the ion-neutral complex **15** could play a role in deuterium-label exchange. Apart from a few minor differences, the essential features of the mechanisms based on our potential

energy surfaces (Schemes 4.3 and 4.4) are very similar to those previously proposed solely on the basis of experimental information (Schemes 4.1 and 4.2).

The calculated potential energy surfaces together with RRKM analyses lead to predictions that are consistent with most of the observed abundances of metastable ion dissociation products and with the results of labeling experiments. Our calculated heats of formation for X = NH and barrier heights are also generally in satisfactory agreement with experiment. In the case of X = S, an experimental re-examination would be desirable.

4.5 References

(1) Bowen, R. D.; Williams, D. H. *J. Am Chem. Soc.* **1978**, *100*, 7454.

(2) For recent reviews on ion-neutral complexes see, for example: (a) Bowen, R. D. *Acc. Chem. Res.*, **1991**, *24*, 364. (b) Longevialle, P. *Mass Spectrom. Rev.* **1992**, *11*, 157. (c) McAdoo, D. J.; Morton, T. H. *Acc. Chem. Res.* **1993**, *26*, 295.

(3) (a) Bouchoux, G.; Penaud-Berruyer, F.; Audier, H. E.; Mourgues, P.; Tortajada, J. *J. Mass Spectrom.* **1997**, *32*, 188. (b) Chalk, A. J.; Radom L. *J. Am. Chem. Soc.* **1998**, *120*, 8430.

(4) (a) Bouchoux, G.; Penaud-Berruyer, F.; Tortajada, J. *Org. Mass Spectrom.* **1995**, *30*, 723. (b) Bowen, R. D. *Mass Spectrom. Rev.* **1991**, *96*, 225. (c) Bowen, R. D.; Williams, D. H.; Hvistendahl, G.; Kalman, J. R. *Org. Mass Spectrom.* **1978**, *13*, 721. (d) Bowen, R. D.; Williams, D. H. *J. Chem. Soc., Perkin Trans. 2.* **1978**, 1064. (e) Levson, K.; McLafferty, F. W. *J. Am. Chem. Soc.*, **1974**, *96*, 139. (f) Uccella, N. A.; Howe, I.; Williams, D. H. *J. Chem. Soc. (B)*, **1971**, 1933

(5) (a) Broer, W. J.; Weringa, W. D. *Org. Mass Spectrom.* **1980**, *15*, 229. (b) Broer, W. J.; Weringa, W. D. *Org. Mass Spectrom.* **1979**, *14*, 36. (c) Broer, W. J.; Weringa, W. D. *Org. Mass Spectrom.* **1977**, *12*, 326.

(6) Hudson, C. E.; McAdoo, D. J. *J. Am. Soc. Mass Spectrom.* **1998**, *9*, 138.

(7) Curtiss, L. A.; Raghavachari, K.; Pople, J. A. *J. Chem. Phys.* **1995**, *103*, 4192.

(8) Scott, A. P.; Radom, L. *J. Phys. Chem.* **1996**, *100*, 16502. The factor of 0.9427 is an optimum scale factor obtained by a least-squares procedure whereas the factor of 1.0084 is optimum for low frequencies.

(9) Lias, S. G.; Bartmess, J. E.; Liebman, J. F.; Holmes, J. L.; Levin, R. D.; Mallard, W. G. *J. Phys. Chem. Ref. Data Suppl.* **1988**, *17*.

(10) Hammerum S.; Sølling, T. I. Submitted for Publication.

(11) Holmes, J. L.; Lossing, F. P.; Mayer, P. M. *Chem. Phys. Lett.* **1992**, *198*, 285.

Chapter 5

The Involvement of Ion-Neutral Complexes in Ethylene Loss from $[PhC(CH_3)_2]^+$ and Its Isomers

5.1 Introduction

In 1956 Rylander and Meyerson suggested that the apparent equivalence of the side-chain carbons during ethylene elimination from the metastable ion $[PhC(CH_3)_2]^+$ formed from ionized *t*-butylbenzene, could be explained by the participation of 'phenylated cyclopropane' (Scheme 5.1).[1] This was a landmark paper because it was the first time an ion-neutral complex had been proposed as an intermediate for an ionic reaction. Since that time, ion-neutral complexes have been found to play an important role in numerous gas-phase ion reactions.[2]

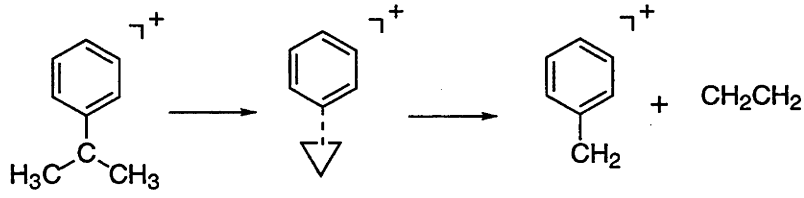

1 **2**

Scheme 5.1

More recent studies of ethylene elimination from $[PhC(CH_3)_2]^+$ (**1**), employing both ^{13}C- and deuterium-labeled analogues, have been carried out,[3-5] leading to the proposition of alternative mechanisms for ethylene elimination from **1**.[3,5] Studies of the mechanism for ethylene elimination from other labeled $[C_9H_{11}]^+$ isomers have also been

performed.[5-7] To our knowledge, there have been no relevant theoretical studies of the mechanisms for the dissociation of $[C_9H_{11}]^+$ ions.

The present work seeks, with the aid of high-level quantum chemical calculations, to examine the process of ethylene loss from $[PhC(CH_3)_2]^+$ (**1**), and to determine the mechanism for both carbon- and hydrogen-label exchange. We also investigate mechanisms for ethylene loss and label exchange for other isomeric $[C_9H_{11}]^+$ ions. Heats of formation of the relevant ions are also calculated and compared with available experimental values. Finally, we compare our findings concerning the involvement of ion-neutral complexes in the rearrangement/fragmentation behavior of the related $[C_3H_6X]^+$ ions with X = OH,[8] SH[8] or NH_2,[9] discussed in Chapters 3 and 4, with those of the present study (X = Ph).

5.2 Methods and Results

Standard ab initio calculations been performed at the G2(MP2,SVP) level, as described in Section 1.12.2. We refer to G2(MP2,SVP) in this paper simply as G2 for the sake of brevity. All MP2 calculations in this study, including the geometry optimizations, have been performed with the core electrons frozen.

Heats of formation at 298 K have been calculated using the atomization method, described in Section 1.13, using scaled (by 0.8905)[10] HF/6-31G(d) frequencies for the temperature correction.

Total G2 energies are shown in Table A3.1 in Appendix 3. MP2/6-31G(d) optimized geometries, including selected bond lengths, are displayed in Figures 5.1 and 5.4, while complete geometries in the form of GAUSSIAN archive entries are presented in Table A3.2. Schematic potential energy profiles are shown in Figures 5.2, 5.3 and

5.5. All bond lengths (Å) refer to MP2/6-31G(d) optimized values and all energies (kJ mol^{-1}) refer to G2 values at 0 K, unless otherwise stated.

5.3 Discussion

In the following discussion, all energies are quoted relative to that for $[PhC(CH_3)_2]^+$ (**1**). For species in which the phenyl ring is protonated, the position of protonation is indicated by the prefix *n*-H^+,[11] where *n* is the location of the proton on the ring relative to the side chain at position 1.

5.3.1 The Potential Surface for Ethylene Elimination From $[PhC(CH_3)_2]^+$ (1)

The metastable ion **1**, formed by radical loss from a suitable ionized neutral precursor (e.g *t*-butylbenzene),[1,5] shows a number of metastable fragmentation pathways, including loss of benzene, propyne and methane.[5] However, by far the dominant pathway (> 90%) is that corresponding to ethylene loss,[5] and we have examined this in detail with our calculations.

We find two energetically-close pathways for ethylene loss from $[PhC(CH_3)_2]^+$ (**1**) (Figure 5.1). The first, slightly higher energy pathway, proceeds initially via the transition structure **TS:1→3**, at a relative energy of 190 kJ mol^{-1} (Figure 5.2), and involves concerted methyl-cation and 1,2-hydrogen shifts. The $[PhCHCH_2CH_3]^+$ (**3**) ion that is produced lies at a relative energy of 30 kJ mol^{-1}.

The second pathway involves initial concerted phenyl-cation and 1,2-hydrogen shifts, proceeding via **TS:1→4** with a relative energy of 179 kJ mol^{-1} to give

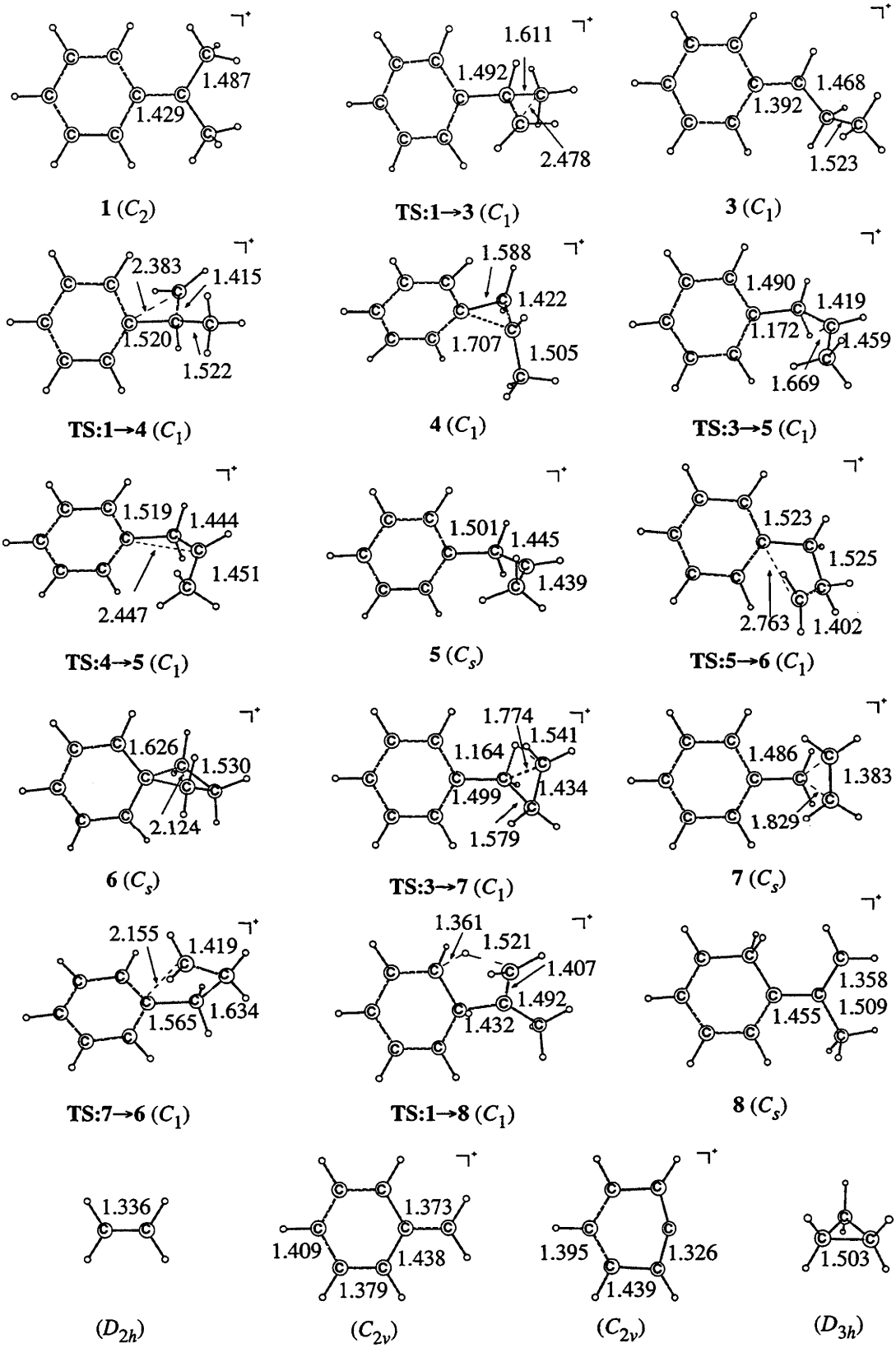

Figure 5.1 Selected MP2/6-31G(d) bond lengths (Å) of species relevant to ethylene elimination from $[PhC(CH_3)_2]^+$ (**1**).

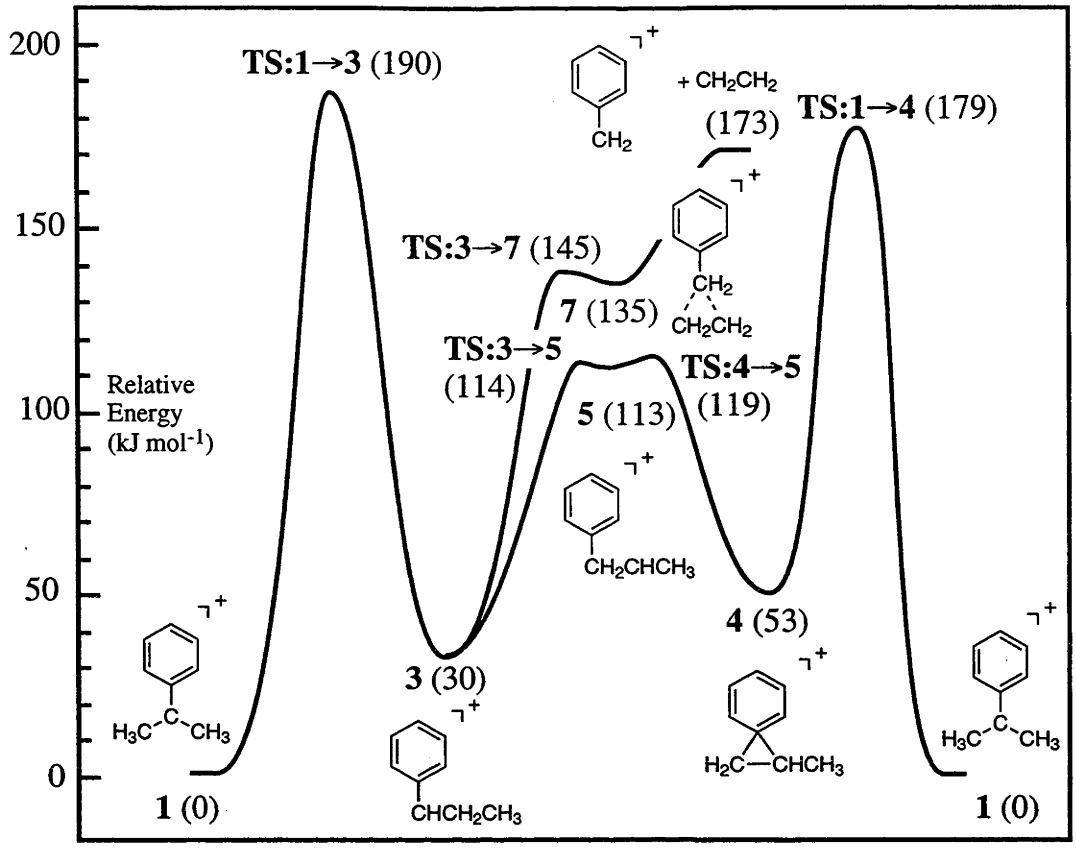

Figure 5.2 Schematic G2 potential energy profile for ethylene loss from $[PhC(CH_3)_2]^+$ (**1**). Energies relative to **1** (kJ mol^{-1}) are given in parentheses.

$[\overline{PhCH_2CH}CH_3]^+$ (**4**). This isomer lies at 53 kJ mol^{-1} and has a phenonium ion structure, with bridging C–C bond lengths of 1.588 and 1.707 Å.

Interconversion of the ions $[PhCHCH_2CH_3]^+$ (**3**) and $[\overline{PhCH_2CH}CH_3]^+$ (**4**) can occur via $[PhCH_2CHCH_3]^+$ (**5**), which lies at an energy of 113 kJ mol^{-1}. Ion **3** can rearrange to **5** via a 1,2-hydrogen shift (**TS:3→5**) at 114 kJ mol^{-1} while **4** can isomerize to **5** via a simple ring opening (**TS:4→5**) at 119 kJ mol^{-1}. Thus, ion **5** lies in a very shallow potential energy well, the barriers for its rearrangement to **3** and **4** being only 1 kJ mol^{-1} and 6 kJ mol^{-1}, respectively.

The ion $[PhCHCH_2CH_3]^+$ (**3**) can rearrange to form the ion-neutral complex $[PhCH_2{\bullet\bullet\bullet}CH_2CH_2]^+$ (**7**) via **TS:3→7** with a relative energy of 145 kJ mol^{-1}. The ion-neutral complex **7** contains an ethylene moiety linked to a benzyl cation with long bridging C-C bonds (1.829 Å). The ethylenic C=C bond is only slightly elongated compared with its value in ethylene itself while the Ph–CH_2 bond is lengthened by 0.113 Å from its value in the isolated benzyl cation. Dissociation of the complex **7** produces ethylene plus the benzyl cation at 173 kJ mol^{-1}, corresponding to a binding energy of 38 kJ mol^{-1}. An alternative pair of products, cyclopropane plus phenyl cation, is found to lie at the significantly higher energy of 405 kJ mol^{-1}.

Other pathways that could potentially be important in label exchange during ethylene elimination have also been characterized. One such process is rearrangement via $[\overline{PhCH_2CH_2CH_2}]^+$ (**6**) (Figure 5.3). This can occur by isomerization of $[PhCH_2CHCH_3]^+$ (**5**) to **6** via **TS:5→6** at 185 kJ mol^{-1}, or isomerization of $[PhCH_2{\bullet\bullet\bullet}CH_2CH_2]^+$ (**7**) to **6** via **TS:7→6** at 177 kJ mol^{-1}. Ion **6** lies at 122 kJ mol^{-1} and in some respects could be described as a complex between the phenyl cation and cyclopropane (**2**), since the C–C bond lengths linking the two components are quite long (1.626 Å). However, the three carbon atoms in **6** are by no means equivalent, as suggested for the proposed structure **2**, with our calculations indicating considerable lengthening of one bond in the 'cyclopropane' moiety (2.124 Å compared with 1.503 Å in isolated cyclopropane).

Another potentially important label-exchange pathway is rearrangement of $[PhC(CH_3)_2]^+$ (**1**) via a hydrogen transfer to the ring, resulting in $[2H^+$-$PhC(CH_3)CH_2]^+$ (**8**) at 77 kJ mol^{-1}. This occurs via **TS:1→8** at a relative energy of 185 kJ mol^{-1}.

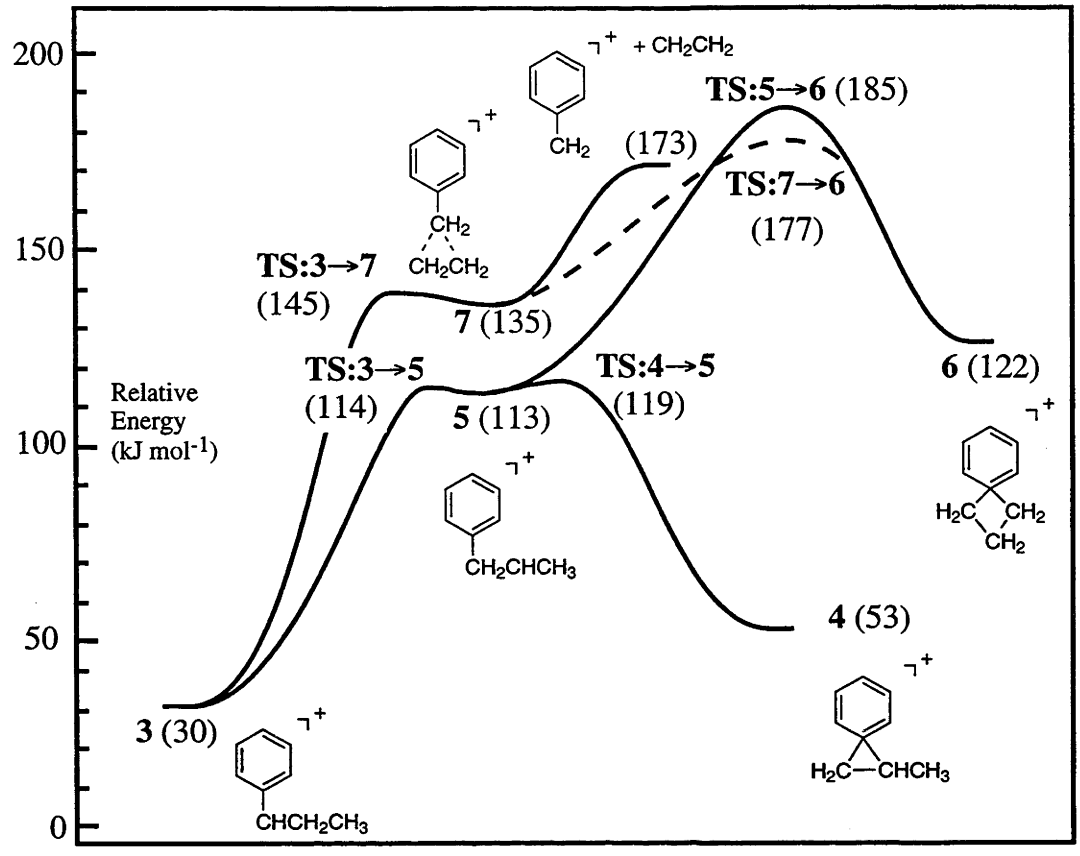

Figure 5.3 Schematic G2 potential energy profile for ethylene loss and ^{13}C exchange within $[PhCHCH_2CH_3]^+$ (**3**). Energies relative to $[PhC(CH_3)_2]^+$ (**1**) (kJ mol^{-1}) are given in parentheses.

5.3.2 The Potential Surface for Ethylene Loss From $[1H^+\text{-}PhCH_2CHCH_2]^+$ (9) or $[2H^+\text{-}PhCH_2CHCH_2]^+$ (10)

As with **1**, the ions produced by protonation of allylbenzene ($PhCH_2CHCH_2$) are also found to eliminate ethylene, and interesting results are obtained when ^{13}C-labeled allylbenzenes are examined.[7]

One of the possible products of the protonation of allylbenzene is $[1H^+$-

$PhCH_2CHCH_2]^+$ (**9**), which lies at an energy of 130 kJ mol^{-1} (Figure 5.5). In some respects, this species resembles a complex between the allyl cation and benzene, with a long C–C bond between these two components (1.680 Å). However, significant distortion of the C–C bonds in both the benzene and allyl cation moieties of **9** is observed (Figure 5.4).

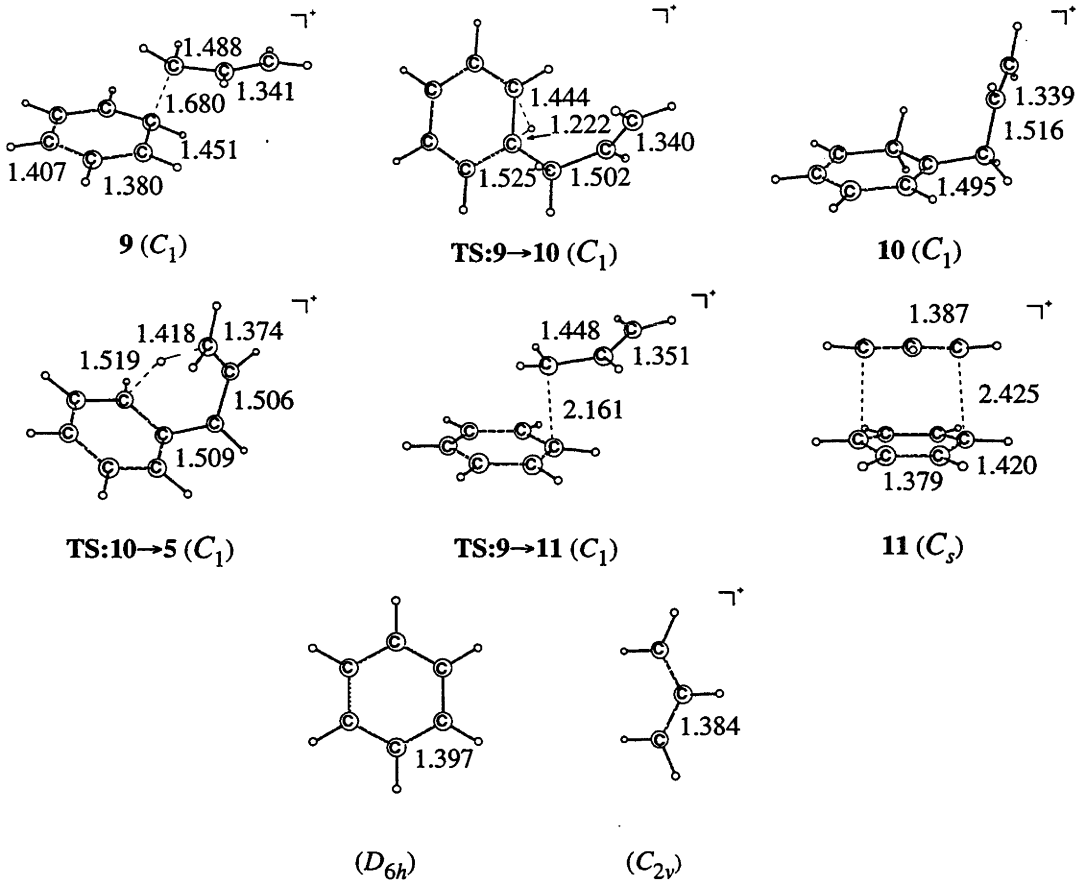

Figure 5.4 Selected MP2/6-31G(d) bond lengths (Å) of species relevant to ethylene elimination from protonated allylbenzene (**5**, **9**, or **10**).

Another possible protonation product is $[2H^+\text{-}PhCH_2CHCH_2]^+$ (**10**) which is more stable than **9**, lying at 102 kJ mol^{-1}. Interconversion of **9** and **10** can take place via **TS:9→10** at 145 kJ mol^{-1}. Alternatively, a 1,5-hydrogen shift via **TS:10→5** at 187 kJ

mol^{-1} leads to $[PhCH_2CHCH_3]^+$ (**5**). Ethylene loss from **5** can then occur, as discussed above (see Figure 5.3).

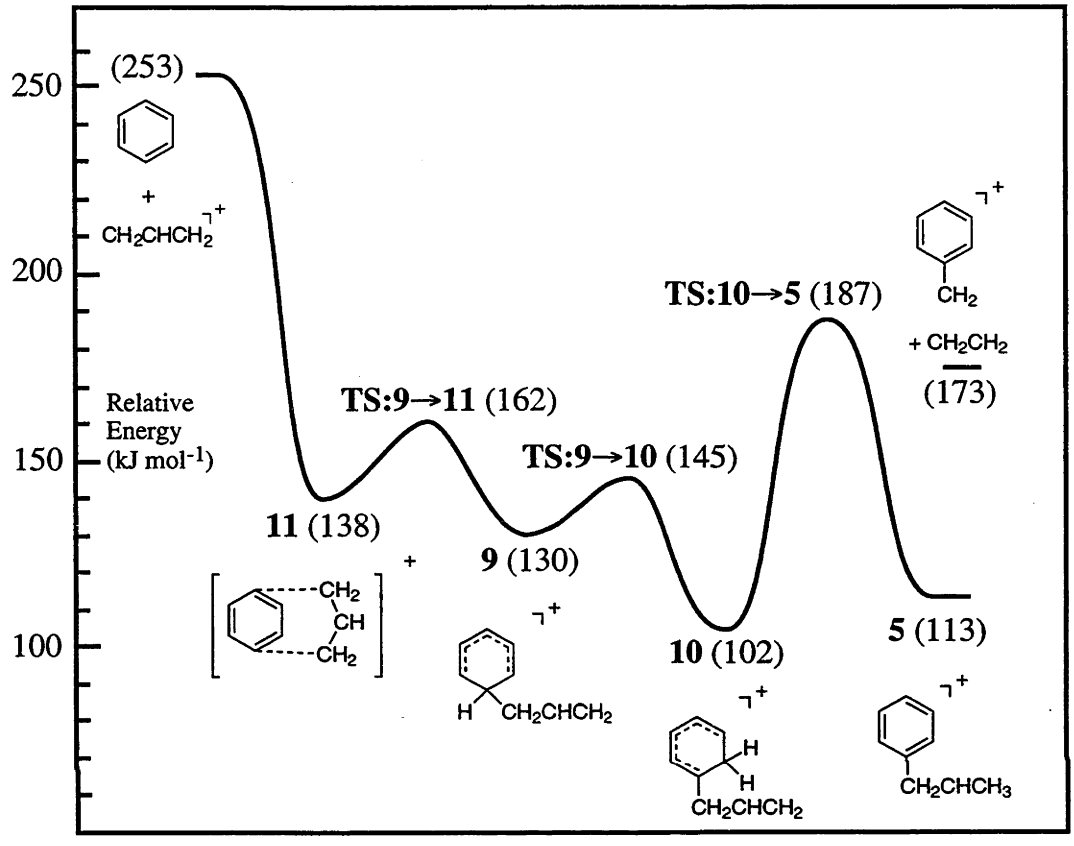

Figure 5.5 Schematic G2 potential energy profile for ethylene loss and ^{13}C exchange within $[1H^+\text{-}PhCH_2CHCH_2]^+$ (**9**). Energies relative to $[PhC(CH_3)_2]^+$ (**1**) (kJ mol^{-1}) are given in parentheses.

Cleavage of a C–C bond in $[1H^+\text{-}PhCH_2CHCH_2]^+$ (**9**) leads to the ion-neutral complex $[C_6H_6\bullet\bullet\bullet CH_2CHCH_2]^+$ (**11**), which lies at 138 kJ mol^{-1}. The transition structure for this process, **TS:9→11**, lies at 162 kJ mol^{-1}. The ion-neutral complex **11** is characterized by long C–C bonds (2.425 Å) between the allyl cation and benzene. The C–C bond lengths in the allyl cation moiety are virtually unchanged from their value in the isolated species but there is significant bond alternation in the benzene ring of **11** (Figure

5.4). The strong interaction between the components of **11** is also manifested in the large stabilization energy calculated for this complex: 115 kJ mol^{-1} relative to the isolated benzene plus allyl cation. Dissociation of **11** can give benzene plus the allyl cation at an energy of 253 kJ mol^{-1}, but this is a significantly higher energy process than loss of ethylene via **TS:10→5**. Rearrangement of **9** or **10** to the ion-neutral complex **11** is a potentially important ^{13}C-label exchange process, as discussed further below.

5.3.3 Comparison With Experimental Thermochemical Data

Our calculated heats of formation for the $[C_9H_{11}]^+$ isomers and possible fragmentation products are compared with available experimental data[12-15] in Table 5.1. It can be seen that agreement between theory and experiment is very good, the differences being well within the G2 target accuracy (± 10 kJ mol^{-1}) for all cases except $[PhCH_2CHCH_3]^+$ (**5**) and the CH_2CH_2 plus $[PhCH_2]^+$ pair, where the discrepancies are slightly greater (12 kJ mol^{-1} in each case). The G2(MP2,SVP) method has previously been found to perform particularly well in the calculation of the heats of formation for neutral hydrocarbons.[16] The present results suggest that this may be equally true for cationic hydrocarbons.[17] The good agreement between theory and experiment lends confidence to our predictions in the cases where experimental thermochemical data are not yet available.

5.3.4 Rationalization of ^{13}C-Labeling Experiments

^{13}C-labeling experiments have been previously performed on a number of $[C_9H_{11}]^+$ isomers.[1,3,6,7] We now attempt to rationalize these results in terms of our calculated potential energy surfaces.

Table 5.1 Theoretical and Experimental Heats of Formation ($\Delta_f H^\circ_{298}$)

Species		G2	Experiment[a]
$[PhC(CH_2)_2]^+$	(**1**)	774	770
$[PhCHCH_2CH_3]^+$	(**3**)	803	811[b]
$[PhCH_2CHCH_3]^+$	(**4**)	825	
$[PhCH_2CHCH_3]^+$	(**5**)	887	(899)[c]
$[PhCH_2CH_2CH_2]^+$	(**6**)	893	
$[PhCH_2 \bullet\bullet\bullet CH_2CH_2]^+$	(**7**)	909	
$[2H^+\text{-}PhC(CH_2)CH_3]^+$	(**8**)	850	
$[1H^+\text{-}PhCH_2CHCH_2]^+$	(**9**)	905	
$[2H^+\text{-}PhCH_2CHCH_2]^+$	(**10**)	876	
$[C_6H_6 \bullet\bullet\bullet CH_2CHCH_2]^+$	(**11**)	913	
$CH_2CH_2 + [PhCH_2]^+$		950	951,962[d]
$C_6H_6 + [CH_2CHCH_2]^+$		1028	1028
$C_3H_6 + [C_6H_5]^+$		1180	1179

[a] All experimental values are taken from reference 12 unless otherwise noted. [b] From reference 13. [c] Estimated in reference 14. [d] The heat of formation of $[PhCH_2]^+$ was calculated using recent values of the ionization energy[15a] and heat of formation[15b] of the benzyl radical.

5.3.4.1 $[PhC(CH_3)_2]^+$ (1)

Experiments examining ethylene loss from the labeled ion $[Ph^{13}C(CH_3)_2]^+$ (**1a**) have yielded abundances for the isotopomers of ethylene that are close to those expected (33% CH_2CH_2 and 67% $^{13}CH_2CH_2$) if complete exchange of all the side-chain carbons was occurring.[1,3,7] The ion-neutral complex **2** was initially proposed to explain this

result (Scheme 5.1).[1] However, we find that the relative energy of the separated phenyl cation and cyclopropane is 405 kJ mol^{-1} and it therefore seems unlikely that a loosely-bound complex between these two species in which the cyclopropane group is free to rotate as suggested in Scheme 5.1, could play an important role.

Previously we noted the similarities between $[\overline{PhCH_2CH_2CH_2}]^+$ (**6**) and the proposed phenylated cyclopropane **2**. It is possible that the observed near-statistical label distribution could result from reversible isomerization of **6** and $[PhCH_2{\bullet\bullet\bullet}CH_2CH_2]^+$ (**7**). Although the energy required for this rearrangement (177 kJ mol^{-1}) is slightly above the dissociation threshold, the difference is well within the uncertainty of our calculations. On the other hand, a high frequency factor process, such as dissociation, will dominate a lower frequency factor process of comparable energy, such as ring closure to form **6**. This suggests that isomerization via **6**, although not totally precluded, is unlikely to be responsible for the observed near-statistical carbon-label distribution.

A second mechanism has been proposed[3,5] whereby there is a competition between a methyl- or phenyl-cation shift in the initial isomerization of $[PhC(CH_3)_2]^+$ (**1**), subsequent to the formation, via a 1,2-hydrogen shift, of the intermediate primary cation $[PhCH(CH_3)CH_2]^+$. We find that these methyl- (**TS:1→3**) and phenyl- (**TS:1→4**) cation shifts can occur without the intermediacy of $[PhCH(CH_3)CH_2]^+$, although we note that the transition structures **TS:1→3** and **TS:1→4** bear a strong resemblance to such a species. The dominance of $^{13}CH_2CH_2$ loss from **1a** can be explained by this mechanism if the phenyl-cation shift, that will result in exchange of the carbon bonded to the ring, is preferred over the methyl-cation shift, which results in no such exchange (Scheme 5.2). This is consistent with the slightly lower calculated barrier for the phenyl-cation shift (**TS:1→4**) (Figure 5.2). Furthermore, it is found experimentally for **1a**, that greater abundances of $^{13}CH_2CH_2$ (i.e. greater than statistical) are observed when the internal energy of **1a** is decreased by going from the first to the second field-free region.[3,7] These results are most simply rationalized by Scheme 5.2. A lower-energy

process such as **TS:1→4** will become increasingly preferred as the internal energy is decreased, with the consequence that an increased proportion of $^{13}CH_2CH_2$ loss will be observed at lower internal energies.

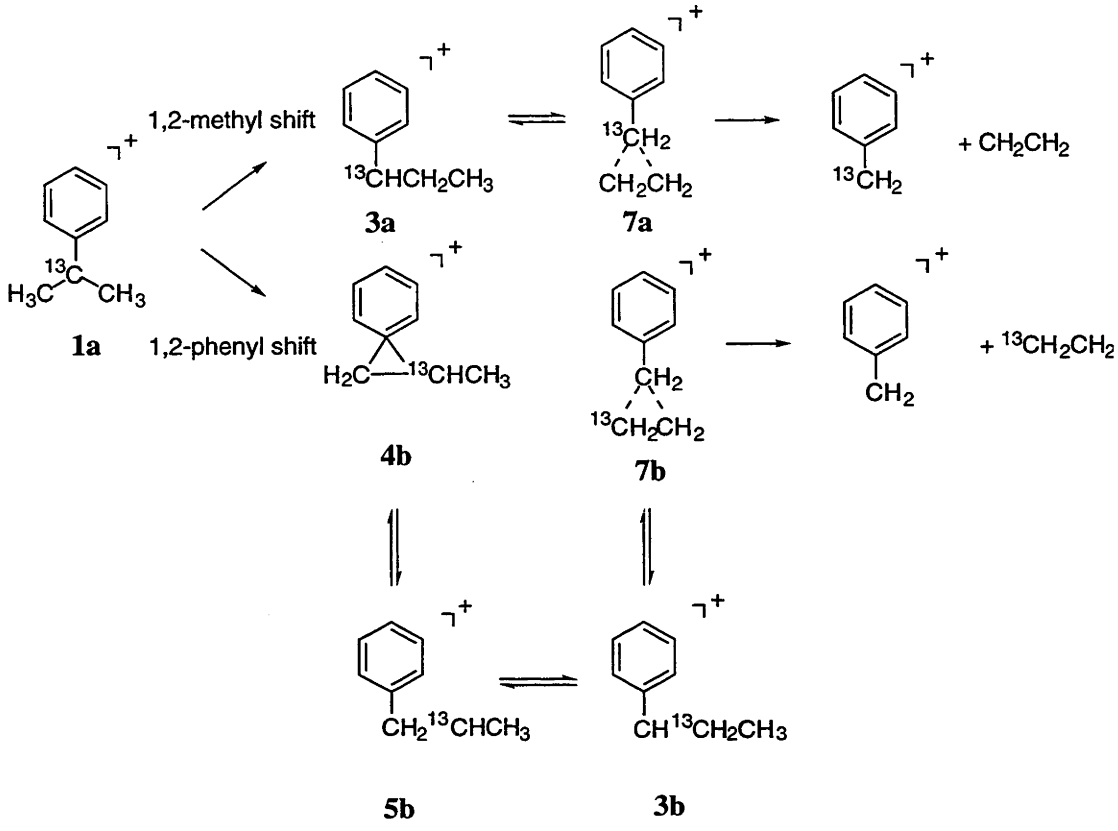

Scheme 5.2

5.3.4.2 $[PhCHCH_2CH_3]^+$ (3)

Experiments on ethylene loss from ^{13}C-labeled $[PhCHCH_2CH_3]^+$ (**3**) have also been performed.[6] These experiments find that a relatively small amount of exchange of the side-chain carbons occurs prior to ethylene loss. One process that could account for such exchange is reversible isomerization to $[\overline{PhCH_2CH_2CH_2}]^+$ (**6**). The small extent of this exchange supports our suggestion that the dissociation of $[PhCH_2{\bullet\bullet\bullet}CH_2CH_2]^+$ (**7**) is favored over isomerization to **6**.

5.3.4.3 Protonated Allylbenzene

^{13}C-label exchange accompanying ethylene loss has also been found in the dissociation of protonated allylbenzene.[7] It was concluded that around 70% of the dissociating ions rearrange by a pathway involving the exchange of α and γ carbons, while the β carbon was found to retain its identity.[7] The $[PhCH_2CH_2CH_2]^+$ (**6**) ion has been suggested as a possible intermediate involved in ^{13}C-label exchange in this system.[7] However, given the earlier discussion concerning the intermediacy of **6**, and the fact that reversible isomerization of **6** and **7** would result in exchange of all side-chain carbon atoms, it is unlikely that **6** is an important intermediate in this case.

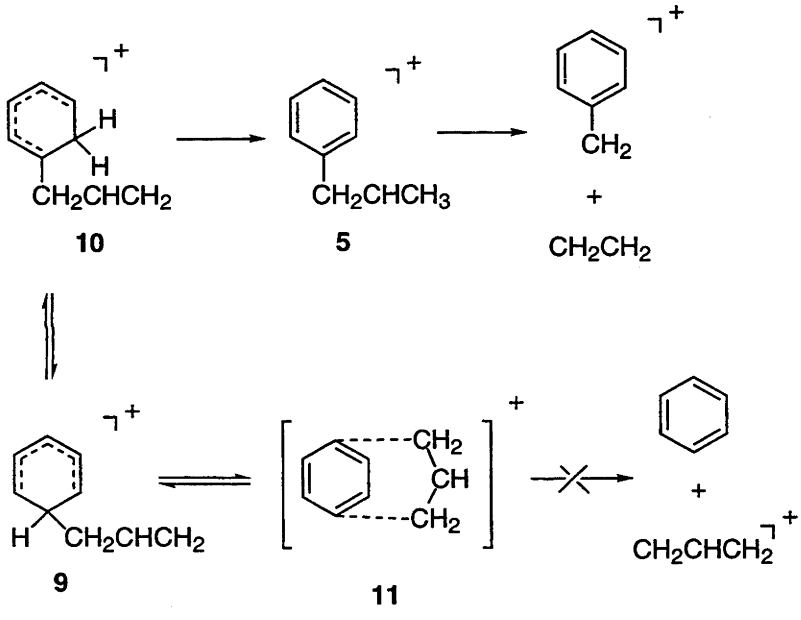

Scheme 5.3

We propose an alternative mechanism involving reversible isomerization of $[1H^+$-$PhCH_2CHCH_2]^+$ (**9**) and $[2H^+$-$PhCH_2CHCH_2]^+$ (**10**) to the intermediate ion-neutral complex $[C_6H_6 \cdots CH_2CHCH_2]^+$ (**11**) to explain the occurrence of α– and γ-carbon exchange (Scheme 5.3). Due to the symmetrical nature of **11**, it is possible for either end of the allyl cation to attack the ring, resulting in exchange of the α and γ carbons. In order for this to be a viable mechanism, two criteria must be satisfied. Firstly, this

process must be able to compete effectively with ethylene elimination. It can be seen from Figure 5.5 that this is indeed the case, the energy required for the rearrangement of **10** or **9** to **11** is significantly lower than that of the rate-limiting step (**TS:10→5**) for ethylene elimination. Secondly, ethylene loss from **11** via **TS:10→5** must occur in preference to its dissociation to benzene plus the allyl cation. The relative energies in Figure 5.5 show this condition clearly to be satisfied.

Our mechanism is consistent with the experimental observation that only the α and γ carbons are exchanged.[7] However, our calculations suggest that complete, rather than partial, exchange of these carbons will occur within $[1H^+\text{-}PhCH_2CHCH_2]^+$ (**9**) or $[2H^+\text{-}PhCH_2CHCH_2]^+$ (**10**). The barrier for rearrangement to $[C_6H_6\bullet\bullet\bullet CH_2CHCH_2]^+$ (**11**) is significantly lower than that of the rate-limiting step for ethylene elimination (**TS:10→5**), and we would therefore expect the former process and the accompanying exchange to occur prior to dissociation via **TS:10→5**.

One possible explanation for this apparent discrepancy is that a mixture of isomers might be formed during protonation of allylbenzene. On energetic grounds, ring protonation at the 2-position, resulting in $[2H^+\text{-}PhCH_2CHCH_2]^+$ (**10**), is favored over protonation at the 1-position, resulting in $[1H^+\text{-}PhCH_2CHCH_2]^+$ (**9**) (Figure 5.5, Table 5.1). However, it is also possible that protonation will occur on the side chain, resulting in $[PhCH_2CHCH_3]^+$ (**5**). This species is only slightly higher in energy than **10** (by 11 kJ mol^{-1}), making it likely that a mixture of **5** and the ring-protonated species (primarily **10**) is formed. If this is the case, the fraction formed as **10** or **9** will undergo complete exchange of the α and γ carbon atoms, while the fraction resulting in $[PhCH_2CHCH_3]^+$ (**5**) (and then $[PhCHCH_2CH_3]^+$ (**4**)) will undergo only a small proportion of exchange, as discussed for **4** above. This would be consistent with the observed incomplete exchange.[7]

5.3.5 Deuterium Exchange

Deuterium labeling studies have been performed on several $[C_9H_{11}]^+$ isomers,[3-5] and we now attempt also to rationalize these results.

5.3.5.1 $[PhC(CH_3)_2]^+$ (1)

Studies of deuterium-labeled analogues of $[PhC(CH_3)_2]^+$ (**1**) have observed that extensive exchange of the six side-chain hydrogens occurs during ethylene elimination.[3-5] This exchange of side-chain hydrogens is simply explained via reversible isomerization of $[PhCHCH_2CH_3]^+$ (**3**) with $[PhCH_2CHCH_3]^+$ (**5**), and of **3** with the ion-neutral complex $[PhCH_2\bullet\bullet\bullet CH_2CH_2]^+$ (**7**). Since the energies of **TS:3→5** and **TS:3→7** are significantly lower than that required for elimination of ethylene, we would expect these processes to result in rapid exchange of all the side-chain hydrogens, prior to dissociation.

Experiment has also found that exchange of the methyl hydrogens with up to two ring hydrogens can occur.[3] These experiments have been interpreted by a mechanism involving exchange of the side-group hydrogens with ring hydrogens at the ortho positions.[3] We find that $[PhC(CH_3)_2]^+$ (**1**) can indeed undergo a 1,4-hydrogen shift from a methyl group to the ortho position of the ring (via **TS:1→8**), resulting in $[2H^+$-$PhC(CH_3)CH_2]^+$ (**8**). The barrier to this process (185 kJ mol^{-1}) is only slightly higher than that for isomerization of **1** to $[\overline{PhCH_2CH}CH_3]^+$ (**4**) (179 kJ mol^{-1}), so we might expect that some rearrangement via this route could occur. However, since this exchange process is higher in energy than the rate-limiting step for ethylene loss from **1** (i.e **TS:1→4**), we would not expect complete exchange with the ring, consistent with experimental observations.[3]

5.3.5.2 $[PhCHCH_2CH_3]^+$ (3) and $[PhCH_2CHCH_3]^+$ (5)

When the ions $[PhCHCH_2CH_3]^+$ (**3**) and $[PhCH_2CHCH_3]^+$ (**5**) are formed directly, they are likely to have less internal energy than those formed by isomerization from $[PhC(CH_3)_2]^+$ (**1**). It would therefore not be surprising if fragmentation behavior differing from **1** was observed. There is some disagreement concerning deuterium-label exchange in **3** and **5**. One study did not observe any deuterium-label exchange with the ring in the 2,4,6-trideuterated analogue of **5**,[5] while another study found that a reasonable amount of exchange with the ring occurs in both the 2- and 4-deuterated analogues of **3**.[6] Since **3** and **5** can rapidly interconvert at the energies relevant to ethylene loss (Figures 5.2 and 5.3), we would expect similar behavior from these isomers. A pathway that could possibly allow exchange with the ring to occur is isomerization of **5** to $[2H^+$-$PhCH_2CHCH_2]^+$ (**10**). However, the energy of the transition structure for this process (187 kJ mol^{-1}) is above the dissociation threshold for ethylene loss (Figure 5.5) so we would not expect this to occur at any significant rate for metastable ions. Although it is possible that there are lower-energy pathways for this exchange, the present results are consistent with the occurrence of little or no deuterium exchange with the ring. Significant deuterium exchange within the side chain was observed in both studies,[5,6] the mechanism for this being exactly analogous to that discussed for $[PhC(CH_3)_2]^+$ (**1**) above.

5.3.6 Comparisons With Other $[C_3H_6X]^+$ Ions

The $[C_9H_{11}]^+$ ions examined here can be considered as members of the group of $[C_3H_6X]^+$ ions, where in this case X = C_6H_5. In Chapters 3 and 4, analogous studies of the loss of ethylene and HX from other ions of this type (X = OH, SH and NH_2) were performed and some general trends concerning the involvement of ion-neutral complexes

were identified (Chapter 4).[8,9] We now examine the involvement of the ion-neutral complex $[PhCH_2 \bullet\bullet\bullet CH_2CH_2]^+$ (**7**), and other species, in the light of the previous studies.

Some of the factors determining the barrier to rearrangement of $[XCH_2 \bullet\bullet\bullet CH_2CH_2]^+$ to $[XCHCH_2CH_3]^+$ have been previously noted.[9] It was found that in cases where the C–C bonds from ethylene to the bridging carbon are relatively short, a low barrier generally results.[9] In contrast, high barriers are present when these bonds are long. We find that the complex $[PhCH_2 \bullet\bullet\bullet CH_2CH_2]^+$ (**7**) has relatively short bridging C–C bond lengths, comparable to those observed for the cases X = OH[8] and SH.[9] In accord with the previously observed trends,[9] we find that the barrier for isomerization of **7** to $[PhCHCH_2CH_3]^+$ (**3**) is also relatively low (10 kJ mol^{-1}). The low value for this barrier allows reversible isomerization between **3** and **7** to occur below the dissociation threshold, making this rearrangement an important process for hydrogen-label exchange in metastable ions.

It is also of interest to compare the involvement of the $[HX \bullet\bullet\bullet CH_2CHCH_2]^+$ complexes in the various systems. In the present work, we find that the reason for the importance of $[C_6H_6 \bullet\bullet\bullet CH_2CHCH_2]^+$ (**11**) in label-exchange is, in part, because loss of ethylene from **9**, **10** and **11** is favored over the dissociation of **11**, that yields the allyl cation plus benzene. In contrast, dissociation of the complex $[HX \bullet\bullet\bullet CH_2CHCH_2]^+$ to give the allyl cation plus HX, for X = OH, SH, NH_2 is preferred to the isomerization that would be necessary for ethylene loss.[8,9] Although ethylene loss from $[HX \bullet\bullet\bullet CH_2CHCH_2]^+$ is not the favored decomposition pathway in these cases, any ethylene elimination that does occur from these species could contribute to ^{13}C-label exchange.

The involvement of ions of the type $\overline{XCH_2CH_2CH_2}^+$ as intermediates in ^{13}C-label exchange was also examined in the cases where X = OH, SH and NH_2.[8,9] It was concluded that rearrangement via $\overline{XCH_2CH_2CH_2}^+$ is unlikely to occur to any great extent

in metastable ions, a conclusion similar to that has also been reached in the present case (X = Ph).

5.4 Concluding Remarks

The potential energy surfaces associated with ethylene elimination from $[PhC(CH_3)_2]^+$ (**1**) and other $[C_9H_{11}]^+$ isomers have been characterized and the importance of ion-neutral complexes in such eliminations has been examined. Based on these results, we propose mechanisms for ethylene loss from the various ions that are found to satisfactorily account for the observed behavior of deuterium- and ^{13}C-labeled species.

We find that the ^{13}C-labeling results for ethylene elimination from $[PhC(CH_3)_2]^+$ (**1**) are more consistent with a combination of two pathways, that involve a phenyl-cation shift (leading to carbon exchange) and a methyl-cation shift (leading to no carbon exchange) (Scheme 5.2, Figure 5.2), with the former being favored, than with the originally proposed 'phenylated cyclopropane' mechanism (Scheme 5.1). However, we cannot totally discount the operation of the latter.

A number of processes in which ion-neutral complexes are important intermediates are found. The ion-neutral complex $[C_6H_6{\bullet\bullet\bullet}CH_2CHCH_2]^+$ (**11**) is likely to play a role in ^{13}C-label exchange accompanying ethylene elimination from protonated allylbenzene (Scheme 5.3). Deuterium label exchange in the side chains of $[PhC(CH_3)_2]^+$ (**1**), $[PhCHCH_2CH_3]^+$ (**3**) and $[PhCH_2CHCH_3]^+$ (**5**) can be explained by a combination of reversible isomerization of **3** to **5** and rearrangement of **3** to the ion-neutral complex $[PhCH_2{\bullet\bullet\bullet}CH_2CH_2]^+$ (**7**). In both cases, reversible rearrangement to the ion-neutral complex can occur below the threshold for dissociation, allowing isomerization to occur in preference to dissociation.

We find good agreement between experimental and calculated thermochemical data.

5.5 References

(1) Rylander, P. N.; Meyerson, S. *J. Am. Chem. Soc.* **1956**, *78*, 5799.

(2) For recent reviews on ion-neutral complexes see, for example: (a) Bowen, R. D. *Acc. Chem. Res.*, **1991**, *24*, 364. (b) Longevialle, P. *Mass Spectrom. Rev.* **1992**, *11*, 157. (c) McAdoo, D. J.; Morton, T. H. *Acc. Chem. Res.* **1993**, *26*, 295.

(3) Neeter, R.; Nibbering, N. M. M. *Org. Mass Spectrom.* **1973**, *7*, 1091.

(4) Meyerson, S.; Hart, H. *J. Am. Chem. Soc.* **1963**, *85*, 2358.

(5) Uccella, N. A.; Williams, D. H. *J. Am. Chem. Soc.* **1972**, *94*, 8878.

(6) Köppel, C.; Schwarz, H.; Bohlmann, F. *Org. Mass Spectrom.* **1973**, *7*, 869.

(7) My, N. k.; Schilling, M.; Schwarz, H. *Org. Mass Spectrom.* **1987**, *22*, 254.

(8) Chalk, A. J.; Radom, L. *J. Am. Chem. Soc.* **1998**, *120*, 8430.

(9) Chalk, A. J.; Radom, L. Submitted for Publication.

(10) Scott, A. P.; Radom, L. *J. Phys. Chem.* **1996**, *100*, 16502.

(11) Brouwer, D. M.; Mackor, E. L.; MacLean, C. in *Carbonium Ions*, (Ed. Olah, G. A.; Schleyer, P. v. R.), Wiley-Interscience, New York, 1970, Vol II, pp 841.

(12) Lias, S. G.; Bartmess, J. E.; Liebman, J. F.; Holmes, J. L.; Levin, R. D.; Mallard, W. G. *J. Phys. Chem. Ref. Data Suppl.* **1988**, *17*.

(13) Attinà, M.; Cacace, F.; Petris, G. d.; Marzio, A. D.; Giacomello, P. *Int. J. Mass Spectrom. Ion Proc.* **1989**, *93*, 185.

(14) Bowen, R. D.; Williams, D. H. *Org. Mass Spectrom.* **1977**, *12*, 475.

(15) (a) Eiden, G. C.; Weinhold, F.; Weisshaar, J. C. *J. Chem. Phys.* **1991**, *95*, 8665. (b) Hippler, H.; Troe, J. *J. Chem. Phys.* **1990**, *94*, 3803.

(16) (a) Nicolaides, A.; Radom, L. *Mol. Phys.* **1996**, *88*, 759. (b) Curtiss, L. A.; Raghavachari, K.; Redfern, P. C.; Pople, J. A. *J. Chem. Phys.* **1997**, *106*, 1063.

(17) See also: Nicolaides, A.; Radom, L. *J. Am. Chem. Soc.* **1996**, *118*, 10561.

Chapter 6

Proton-Transport Catalysis: A Systematic Study of the Rearrangement of the Isoformyl Cation to the Formyl Cation

6.1 Introduction

The isoformyl cation (HOC^+) is well known from both experimental and theoretical studies to be much less stable than its isomer, the formyl cation (HCO^+), the energy difference being about 160 kJ mol^{-1}.[1-5] However, there is a significant barrier, of about 150 kJ mol^{-1}, separating the two isomers[1,2] which ensures that both HCO^+ and HOC^+ can be observed as isolated species in the gas phase.[3-8] For example, the microwave spectra of both species have been recorded.[6,7] In addition, we note that both formyl cation and isoformyl cation are firmly established interstellar species.[9,10]

The barrier for the rearrangement of HOC^+ to HCO^+ has been found to be markedly reduced or even eliminated as a result of interaction with an external molecule.[1,5,8] More generally, the phenomenon of catalysis of proton migration by a small neutral molecule has been described by Bohme as proton-transport catalysis.[11] There have been a number of isolated examples of proton-transport catalysis reported in the literature.[11,12] However, the only systematic examination that we are aware of to date has been a very recent study of the catalysis of the interconversion of distonic radical cations and their conventional isomers.[13] Theory is ideally placed to carry out a systematic investigation of proton-transport catalysis. In this chapter, we present the results of a systematic theoretical study for the prototypical example of the rearrangement of isoformyl cation to formyl cation. Results are reported for the rearrangement of the isolated isoformyl cation to the formyl cation as well as rearrangements catalyzed by a

selection of small neutral molecules X (X = He, Ne, Ar, CO, HF, N_2, H_2O and NH_3).

6.2 Methods and Results

Standard ab initio calculations have been carried out using a variant of the G2 method (see 1.3.1 for the details of G2). Since hydrogens play a very important role in this study, we deemed it advisable to include polarization functions on hydrogen in the geometry optimizations (MP2/6-31G(d,p) instead of MP2/6-31G(d)). In addition, we have included polarization functions on hydrogen in the ZPVE calculations and carried these out at the MP2 level because several of the species under investigation are found to have different qualitative shapes at the HF and MP2 levels. Thus we have calculated the ZPVEs with MP2/6-31G(d,p) scaled by 0.9370[14] rather than HF/6-31G(d) scaled by 0.8929. We term this level of theory G2**. All electrons are correlated in the geometry optimizations and frequency calculations (i.e. MP2(full)).

Selected geometrical features of the MP2/6-31G(d) optimized geometries are shown in Figures 6.1, 6.3 and 6.5 and schematic potential energy surfaces are shown in Figures 6.2, 6.4 and 6.6. G2** total energies are shown in Table A4.1 in Appendix 4 and complete geometries in the form of GAUSSIAN archive entries can be found in Table A4.2.

6.3 Discussion

6.3.1 The Isolated Isoformyl Cation–Formyl Cation Rearrangement

The potential energy profile for the rearrangement of the isolated isoformyl cation (**1**) to the formyl cation (**3**) via transition structure **2** is included in Figure 6.2. At the

G2** level, the barrier is 147 kJ mol^{-1} and the exothermicity is 158 kJ mol^{-1}, consistent with previous results.[1-5]

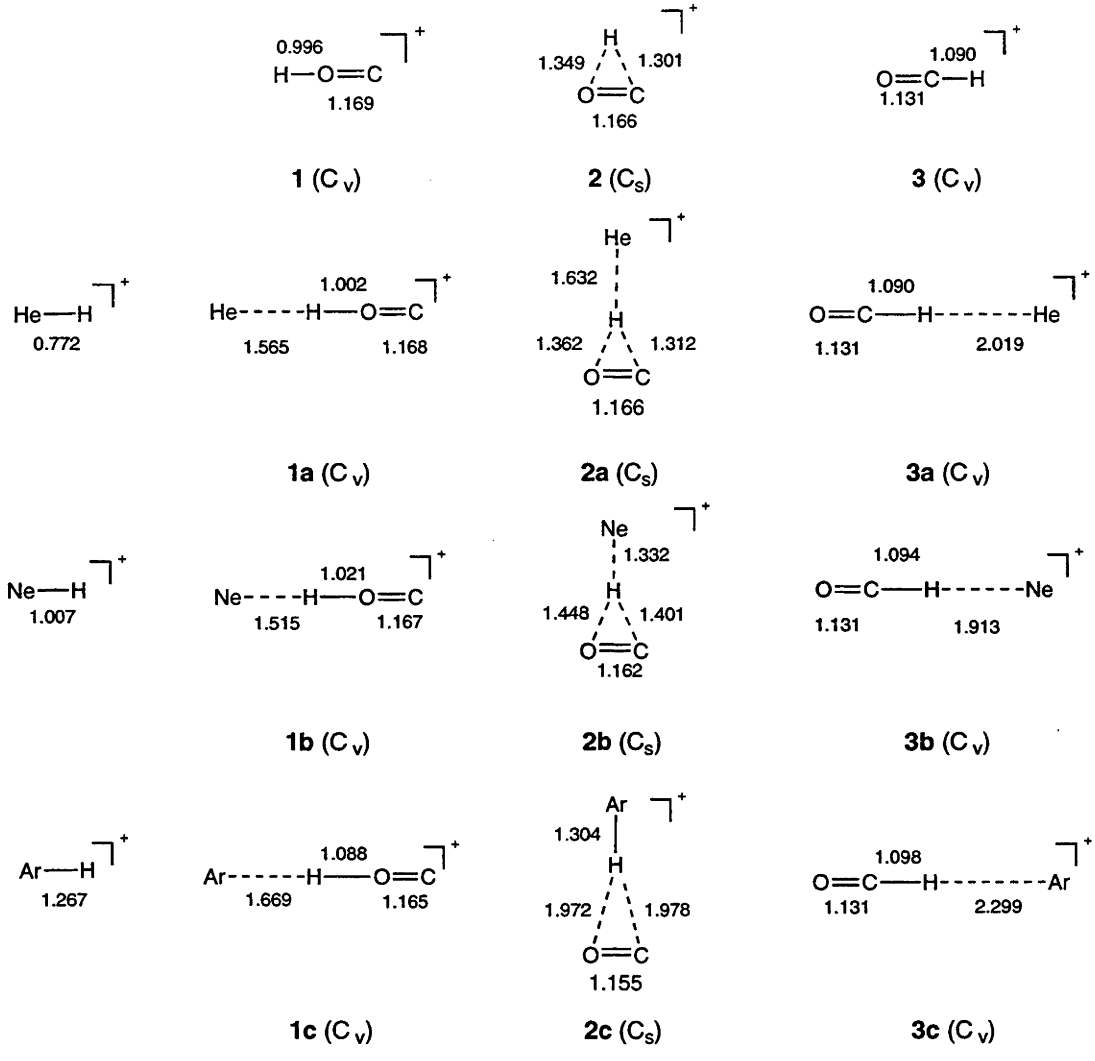

Figure 6.1 Selected MP2/6-31G(d,p) bond lengths (Å) for the isolated $[CHO]^+$ structures and for the $[X\cdots CHO]^+$ structures with X = He, Ne and Ar.

6.3.2 Interaction With Helium

The smallest perturbation to the potential energy profile is provided by interaction

with a helium atom, also included in Figure 6.2. Helium interacts weakly (by 7 kJ mol^{-1})

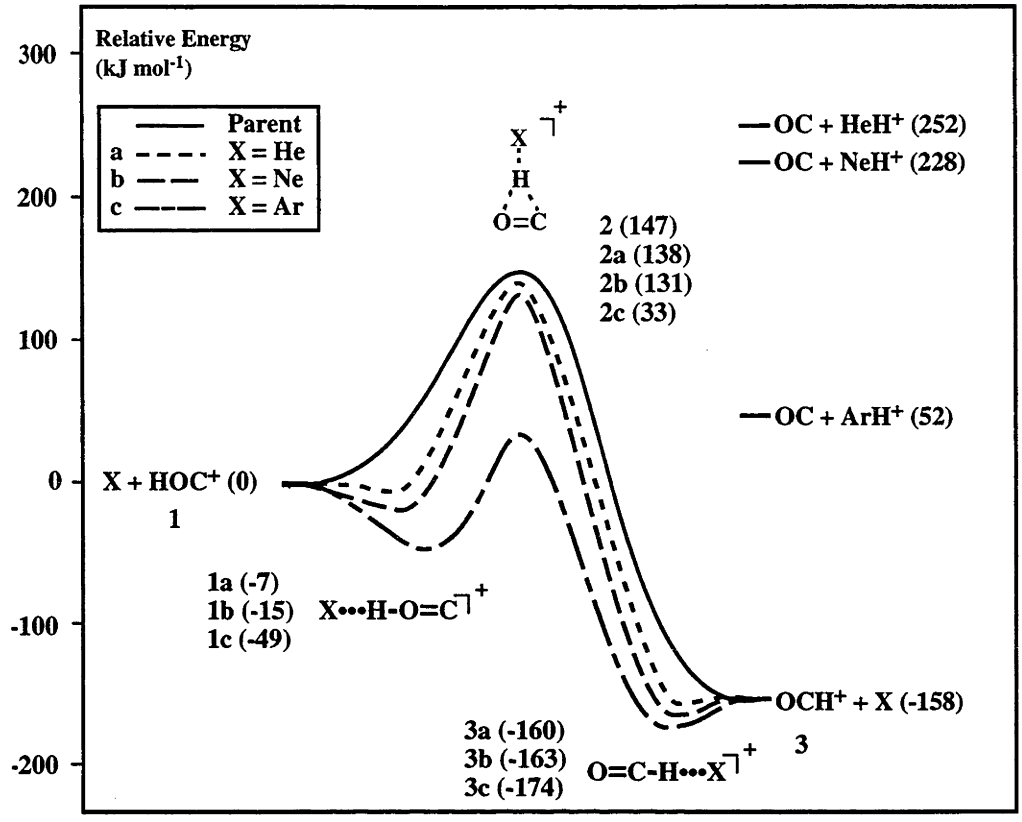

Figure 6.2 Schematic energy profile (G2**, 0 K) showing the uncatalyzed (parent) and catalyzed (X= He, Ne and Ar) isomerization of the isoformyl cation to the formyl cation.

with HOC^+, to form the complex **1a**, it interacts a little more strongly (by 9 kJ mol^{-1}) with the transition structure **2** to give the transition structure **2a**, and it interacts weakly (by 2 kJ mol^{-1}) with HCO^+ to give the product complex **3a**. We note that this ordering of interaction energies, i.e. interaction of X with the transition structure > interaction of X with HOC^+ > interaction of X with HCO^+, is observed for all X. It is readily rationalizable in that the strongest interaction should occur with the weakest bond (as in the transition structure) and the weakest interaction with the strongest bond (as in HCO^+).

The barrier to rearrangement calculated relative to the separated reactants decreases

slightly from 147 kJ mol^{-1} to 138 kJ mol^{-1}. This barrier lowering can be regarded as arising because interaction with helium weakens the H–O bond of HOC^+, thus making proton migration easier. Indeed, the bonds to the migrating proton are seen to be slightly longer in **1a** and **2a** compared with **1** and **2**, respectively (Figure 6.1).

6.3.3 Proton Affinities of X

Given this mechanism for barrier lowering, we might expect some correlation between the extent of barrier lowering and the proton affinity of the neutral molecule X: as the proton affinity of X is increased, the complex of X with HOC^+ will become stronger, the degree of bond weakening in the H–O bond of HOC^+ will be greater, the proton migration will become easier, and hence the barrier will be lower.

The G2 level of theory has been found[15] to be very successful at predicting proton affinities and this success would be expected to carry over smoothly to G2**. Comparison of calculated G2** proton affinities for the molecules X with experimental values[4,5] at 298 K (Table 6.1) shows that there is indeed good agreement between theory and experiment.[16]

6.3.4 Interaction With Neon and Argon

The proton affinities of neon and argon are greater than that of helium but smaller than that of CO at O (denoted CO*) (Table 6.1). Accordingly, we find that the interactions of Ne and Ar with the H of HOC^+ are greater and the barriers to proton migration are smaller than for He (Figures 6.1 and 6.2). However, the barriers remain positive. The barrier decreases from 147 kJ mol^{-1} in the isolated rearrangement to 138 kJ mol^{-1} for He, 131 kJ mol^{-1} for Ne and just 33 kJ mol^{-1} with Ar.

Table 6.1 Calculated and Experimental Proton Affinities (kJ mol^{-1})[a]

	QCISD[b]	MP2[c]	G2**		Expt[d]
	0 K	0 K	0 K	298 K	298 K
He		210.2	177.8	181.5	178
Ne		222.0	201.9	205.6	201
Ar		369.4	377.8	381.6	371
CO*	434.8	431.5	430.1	433.5	427[e]
HF	485.9	520.5	480.3	485.3	489.5
N_2		493.6	488.9	494.4	494.5
*CO	594.8	612.8	588.2	593.9	594
H_2O		719.2	682.3	688.3	697
NH_3		882.9	847.9	854.2	854

[a] All calculated values include a scaled MP2/6-31G(d,p) ZPVE correction. [b] 6-311+G(d,p) basis set. [c] 6-31G(d,p) basis set. [d] All experimental values taken from ref 4 unless otherwise noted. [e] From ref 5.

6.3.5 Interaction With Hydrogen Fluoride, Nitrogen and Carbon Monoxide

Molecules with proton affinities greater than He, Ne and Ar are exemplified by carbon monoxide protonating at oxygen (CO*), hydrogen fluoride, molecular nitrogen

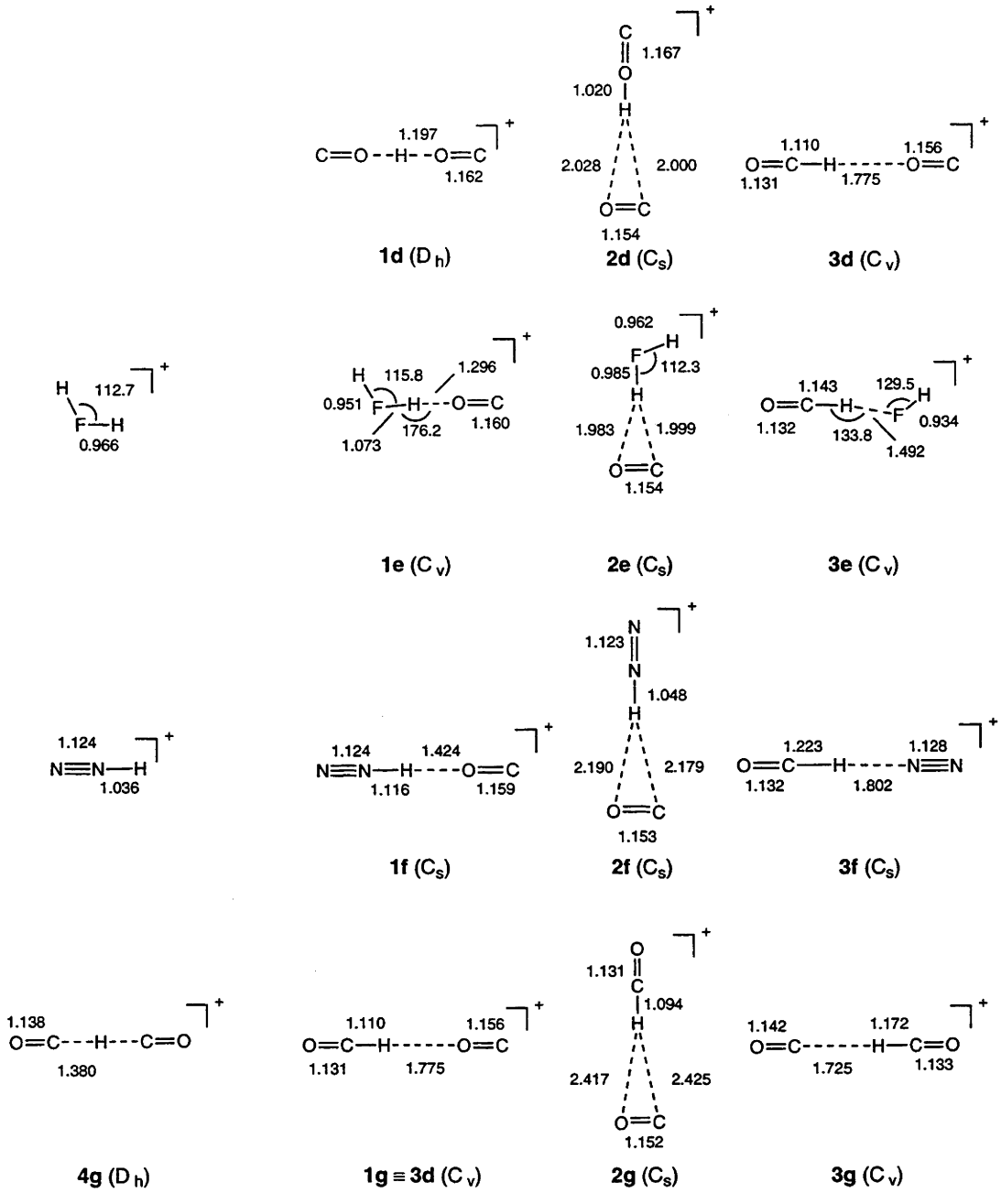

Figure 6.3 Selected MP2/6-31G(d,p) geometrical parameters for the $[X\cdots CHO]^+$ structures with X = CO*, HF, N_2 and *CO. Bond lengths in Å, bond angles in degrees.

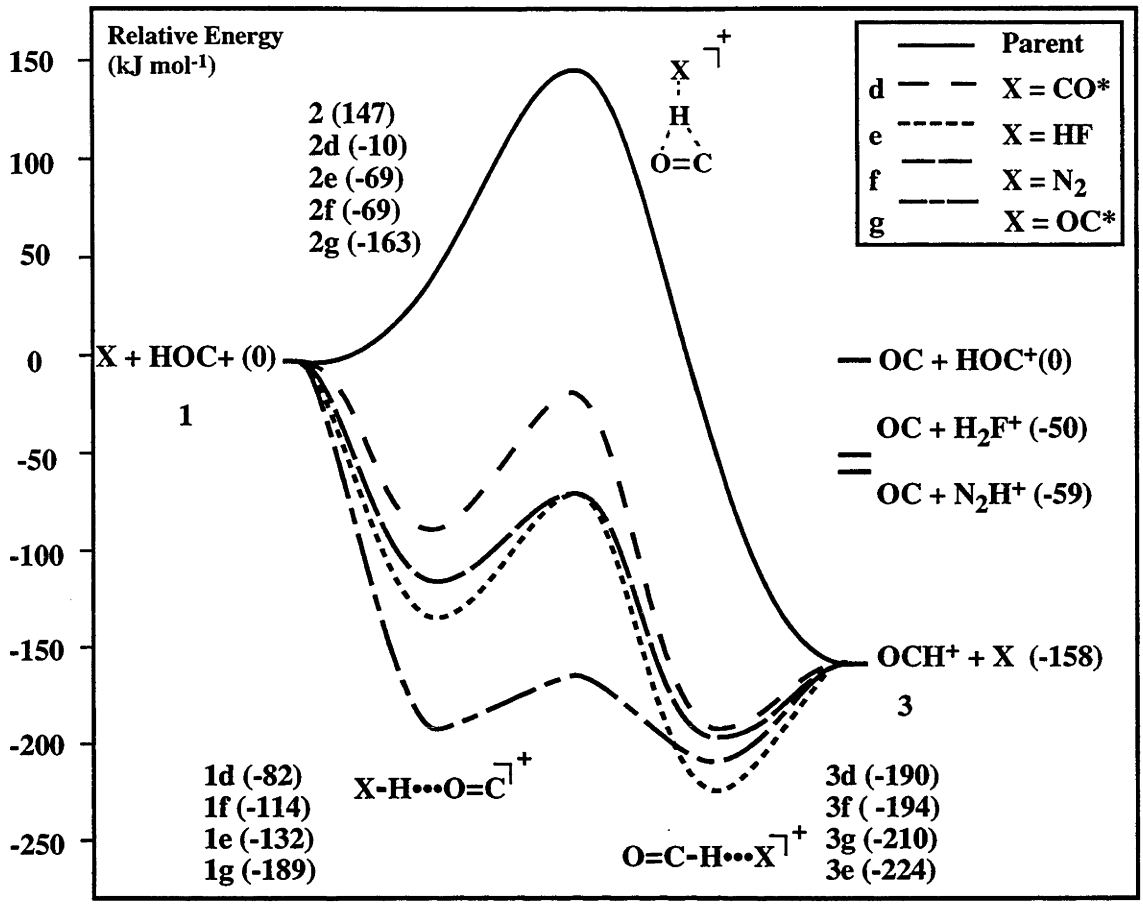

Figure 6.4 Schematic energy profile (G2**, 0 K) showing the uncatalyzed (parent) and catalyzed (X = CO*, HF, N_2 and *CO) isomerization of the isoformyl cation to the formyl cation.

and carbon monoxide protonating at carbon (denoted *CO) (Table 6.1, Figure 6.3). The potential energy profiles of Figure 6.4 show that in all these cases the transition structures for rearrangement have dropped below the energy of the reactants X + HOC^+, i.e. the barriers have become negative. So interaction with CO, HF and N_2 will allow HOC^+ to rearrange to HCO^+ without an overall barrier. We note that the interaction energy in the TS (e.g. 216 kJ mol^{-1} for X = HF) is again greater than that in either the reactant complex (132 kJ mol^{-1} for X = HF) or product complex (66 kJ mol^{-1} for X = HF).

N_2 and HF have proton affinities that lie between those of CO at oxygen and CO at carbon. They are therefore ideally placed to drag a proton from HOC^+ to X and then to re-deposit it at carbon to produce HCO^+.

In the case of *CO a subtle difference in the potential surface is observed. In contrast to all the other complexes, **3g** has a double-well potential for proton transfer between the two components of the complex. However, once ZPVE is included the transition structure for proton transfer (shown as **4g**) is predicted to be lower in energy than that of that of **3g**, indicating a very flat potential for this type of motion.

6.3.6 Interaction With Water and Ammonia

Interaction with molecules whose proton affinity is greater than that for CO at carbon is exemplified by interaction with water (Table 6.1, Figures 6.5 and 6.6). The TS for rearrangement (**2h**) moves to very low energies, the barrier becoming -258 kJ mol^{-1}. It might seem at first sight that this would lead to even better catalysis. However, a problem arises because the proton affinity of water is *too* great. The water molecule captures a proton from HOC^+ quite readily, yielding a complex that can be described as $[H_2OH{\bullet\bullet\bullet}OC]^+$ (**3h**). However, it does not want to return the proton to the carbon end of CO to give HCO^+. Instead, it is energetically profitable for the water to retain the proton and form CO + H_3O^+ at -252 kJ mol^{-1} rather than HCO^+ + water at -158 kJ mol^{-1}. We do not have successful catalysis of the rearrangement any more because *inter*molecular proton transfer to produce H_3O^+ is preferred to the desired *intra*molecular proton migration to produce HCO^+.

A similar result is found for ammonia (Figures 6.5 and 6.6). The TS for rearrangement (**2i**) is now at -419 kJ mol^{-1} but the preferred product is NH_4^+ plus CO at -418 kJ mol^{-1} rather than NH_3 plus HCO^+ at -158 kJ mol^{-1} because the energy of the

former is so much lower. Again, intermolecular proton transfer is energetically preferable to intramolecular proton migration.

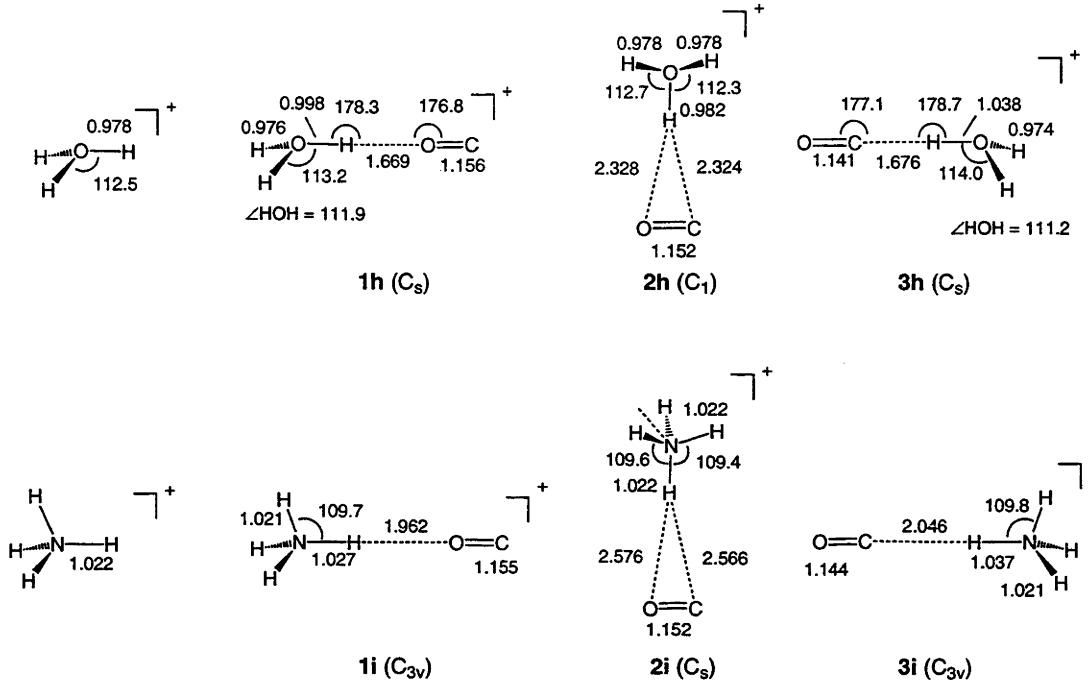

Figure 6.5 Selected MP2/6-31G(d,p) geometrical parameters for the $[X{\cdots}CHO]^+$ structures with X = H_2O and NH_3. Bond lengths in Å, bond angles in degrees.

6.3.7 General Comparisons

It is of interest to bring together some of the quantities relevant to the rearrangement process (Table 6.2). The first column of numbers lists the difference between the calculated proton affinity of X and that of CO at oxygen. The molecules are listed in order of increasing proton affinity. The next column gives the H···O distances in the initially formed complexes, $[X{\cdots}H{\cdots}OC]^+$. We can see, as expected, that the H···O distances increase relatively smoothly as the proton affinity of X increases. They start at 0.996 Å in HOC^+ itself and increase to 1.962 Å in the complex with NH_3 with its very large proton affinity. As this distance increases, we might expect the mobility of the

proton to increase also. It is less tightly held. And indeed the barrier values show an excellent correlation, decreasing from 147 kJ mol^{-1} for the isolated rearrangement to -419 kJ mol^{-1} when X = NH_3.

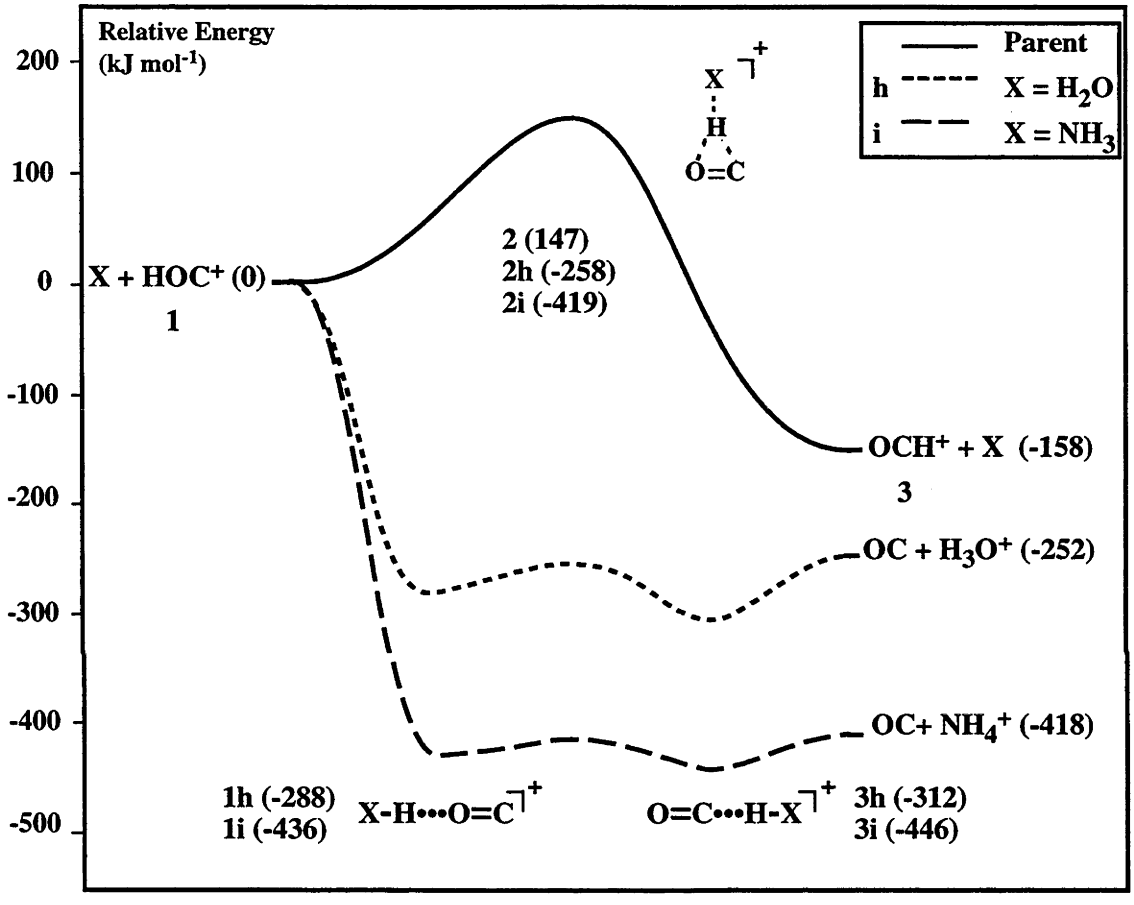

Figure 6.6 Schematic energy profile (G2**, 0 K) showing the uncatalyzed (parent) isomerization of the isoformyl cation to the formyl cation, and the formation of XH^+ in the presence of X = H_2O or NH_3.

The neutral molecules fall naturally into three groups. At the top, we have helium, neon and argon. They have proton affinities smaller than that of CO at oxygen. They reduce the barriers from the value of 147 kJ mol^{-1} in the isolated system but the

barriers remain positive. Then we have HF and N_2 which have proton affinities lying between the values for CO at oxygen and CO at carbon. They are ideally placed for catalyzing the transfer of the proton from O to C. These reactions have no overall barrier. And finally we have water and ammonia which have proton affinities greater than that of CO at carbon. They can remove the proton from HOC^+ but they don't give it back. So they are not good catalysts.

Table 6.2 Relative Proton Affinities (ΔPA, kJ mol^{-1}),[a,b] H•••O Bond Lengths in $[X•••H•••OC]^+$ Complexes (Å),[c] and Overall Reaction Barriers (kJ mol^{-1})[b,d]

X	Δ(PA)[a,b]	r (H•••O)[c]	Barrier[b,d]
-	-	0.996	147
He	-252.3	1.002	138
Ne	-228.2	1.021	131
Ar	-52.3	1.088	33
CO*	0.0	1.197	-10
HF	50.2	1.296	-69
N_2	58.8	1.424	-69
*CO	158.1	1.775	-163
H_2O	252.2	1.669	-258
NH_3	417.8	1.962	-419

[a] Δ(PA) = PA(X) - PA(CO*). [b] G2** values at 0 K. [c] MP2/6-31G(d,p) optimized values.

[d] Barrier relative to reactants X + HOC^+.

6.3.8 Theoretical Considerations

It is of importance to attempt to assess the reliability of our G2** results in the present investigation. As noted early in this paper, G2 theory has been found to be very reliable for thermochemical predictions, and a similar level of performance would be expected to hold also for G2**. Nevertheless, it is desirable to examine the performance of G2** for the specific aspects of particular relevance to the present investigation.

Proton affinities are clearly of importance in the present study. We have already commented on the good agreement between G2** proton affinities and experimental values, as listed in Table 6.1. So this aspect is well catered for.

Next we consider the level of geometry optimization. The G2** calculations correspond to high level energy calculations but these are carried out on geometries determined at the relatively modest MP2/6-31G(d,p) level of theory. MP2/6-31G(d,p) geometries would normally be expected to be quite adequate. However, the performance of MP2/6-31G(d,p) in the present study could depend in part on how well it describes the relative proton affinities of the various molecules X and CO because, for example, the geometry of the complex $[X\cdots H\cdots OC]^+$ depends very directly on the relative proton affinities of X and of CO at oxygen. A method that distorts these relativities would also distort the geometrical parameters from their true values.

The MP2/6-31G(d,p) proton affinities have been included in Table 6.1. We can see that the proton affinities at this level compare poorly with G2** values, showing deviations as large as 40 kJ mol^{-1}. In addition, these deviations vary considerably for different X, with the consequence that even the relative proton affinities compare poorly with G2** values. It is possible that the poor prediction of relative proton affinities by MP2/6-31G(d,p) may adversely affect the predicted structures, as noted above. In order to explore this possibility further, we have carried out additional calculations at the

QCISD/6-311+G(d,p) level, initially obtaining proton affinities for CO at oxygen (CO*), hydrogen fluoride, and CO at carbon (*CO). As can be seen from Table 6.1, these proton affinities are in reasonable agreement with the G2** values but, more importantly, the deviations in the three cases are similar so that the relative proton affinities are in excellent agreement with G2**. We would therefore expect the QCISD/6-311+G(d,p) geometries for the X = hydrogen fluoride structures to provide an accurate benchmark against which to test the standard MP2/6-31G(d,p) structures.

Thus, in order to examine the possible effects of geometry on the calculated energies, the G2** procedure has been applied to QCISD/6-311+G(d,p) optimized geometries for X = HF. HF was chosen because it has the largest error in its proton affinity at the MP2/6-31G(d,p) level (Table 6.1) and we would therefore expect any geometry effects to be most pronounced in this system. The largest change observed is for the H•••F bond in OCH•••FH$^+$ (**3e**) which increases from 1.492 Å (MP2/6-31G(d,p)) to 1.605 Å (QCISD/6-311+G(d,p)). However, because this is a weak bond, it does not have a large energetic effect. Indeed, the energies relative to the separated isoformyl cation and hydrogen fluoride calculated using QCISD/6-311+G(d,p) geometries for **1e** (-132.1 kJ mol^{-1}), **2e** (-70.3 kJ mol^{-1}) and **3e** (-227.5 kJ mol^{-1}) are reasonably close to the values calculated using the MP2/6-31G(d,p) geometries of -131.5 kJ mol^{-1}, -69.3 kJ mol^{-1} and -224.2 kJ mol^{-1}, respectively. We conclude from these results that the MP2/6-31G(d,p) level gives adequate geometries for our purposes.

Finally, in any ab initio study of weakly interacting systems it is important to investigate possible effects of basis set superposition error (BSSE). In the present work, we have estimated the magnitude of the BSSE for the complexes and transition structures by using the counterpoise method (see Section 1.8.4).[17] In order to apply this correction, it is necessary to divide the complexes and transition structures into two fragments. There are two obvious choices, namely X plus the appropriate [CHO]$^+$ isomer (or transition structure) or XH$^+$ plus CO. We have carried out calculations for

both possible partitionings. Before discussing the results, we note that in the counterpoise method, it is necessary to calculate the energy of each fragment in its standard basis and in the full basis of the complex. For a composite method like G2**, this requires that each component single-point calculation that makes up the G2** energy be performed in the appropriate standard and full basis sets and the results combined in the usual way to give a G2** energy.

The uncorrected and BSSE-corrected energies of the complexes and transition structures, calculated relative to isolated X plus isoformyl cation, are shown in Table 6.3. Our preferred BSSE partitioning, shown in bold in Table 6.3, corresponds to a division into the lower energy fragments since these are the fragments that the individual complexes and transition structures are most likely to resemble.[18] Interestingly, this partitioning also minimizes the BSSE correction. The effect of the BSSE correction in each case is to increase the relative energy, as expected. For our preferred partitioning, the average increases in energy relative to separated X + HOC^+ are 5, 3 and 3 kJ mol^{-1}, respectively, for $[X{\cdots}H{\cdots}OC]^+$, the TS and $[OC{\cdots}H{\cdots}X]^+$, with maximum increases of 8, 7 and 5 kJ mol^{-1}. The BSSE correction thus raises fairly uniformly the part of the potential energy surface involving the complexes and transition structure relative to separated fragments and it would therefore not affect our general conclusions.

6.4 Concluding Remarks

Rearrangement of the isoformyl cation (HOC^+) to the formyl cation (HCO^+) is impeded by a substantial barrier of 147 kJ mol^{-1}. Interaction with a neutral molecule X leads to a significant lowering of the barrier. In the cases examined in the present study, if the proton affinity of X is less than that of CO at oxygen, the barrier is reduced but remains positive. If the proton affinity of X lies between the proton affinity of CO at O and at C, the barrier becomes negative. This is the ideal situation for effective catalysis.

Table 6.3 Uncorrected and BSSE-Corrected Relative Energies (kJ mol^{-1}) [a,b]

	[X•••H•••OC]$^+$			TS			[OC•••H•••X]$^+$		
X	Uncorrected	X + HOC$^+$ [c]	XH$^+$ + OC [d]	Uncorrected	X + [HOC]$^+$ [e]	XH$^+$ + CO [d]	Uncorrected	OCH$^+$ + X [f]	OC + HX$^+$ [d]
He	-7	**-6**	-5	138	**139**	137	-160	**-159**	-161
Ne	-15	**-9**	-8	131	**138**	139	-163	**-160**	-157
Ar	-49	**-43**	-40	33	41	**36**	-174	**-172**	-169
CO*	-82	**-74**	**-74**	-10	-2	**-7**	-190	**-186**	-185
HF	-132	-122	**-124**	-69	-61	**-65**	-224	**-220**	-217
N_2	-114	-105	**-108**	-69	-61	**-66**	-194	**-189**	-188
OC*	-189	-184	**-188**	-163	-159	**-164**	-210	-206	**-207**
H_2O	-288	-280	**-283**	-258	-251	**-256**	-312	-303	**-308**
NH_3	-436	-431	**-435**	-419	-414	**-419**	-446	-440	**-445**

[a] All energies quoted are relative to separated X plus HOC$^+$. [b] Preferred BSSE partitioning shown in bold. [c] BSSE evaluated by partitioning into X + HOC$^+$. [d] BSSE evaluated by partitioning into XH$^+$ + OC. [e] BSSE evaluated by partitioning into X + [HOC]$^+$. [f] BSSE evaluated by partitioning into OCH$^+$ + X.

Finally, if the proton affinity of X lies above that of CO at carbon, the barrier is lowered further but the proton is preferentially transferred to X rather than migrating to C.

6.5 References

(1) Nobes, R. H.; Radom, L. *Chem. Phys.* **1981**, *60*, 1.

(2) See, for example, (a) Del Bene, J. E.; Frisch, M. J.; Raghavachari, K.; Pople, J. A. *J. Phys. Chem.* **1982**, *86*, 1529. (b) Dixon, D. A.; Komornicki, A.; Kraemer, W. P. *J. Chem. Phys.* **1984**, *81*, 3603. (c) DeFrees, D. J.; McLean, A. D. *J. Comp. Chem.* **1986**, *7*, 321. (d) Ma, N. L.; Smith, B. J.; Pople, J. A.; Radom, L. *J. Am. Chem. Soc.* **1991**, *113*, 7903. (e) Ma, N. L.; Smith, B. J.; Radom, L. *Chem. Phys. Lett.* **1992**, *197*, 573. (f) Yamaguchi, Y.; Richards, C. A.; Schaefer, H. F. *J. Chem. Phys.* **1995**, *101*, 8945.

(3) Harland, P. W.; Kim, N. D.; Petrie, S. A. H. *Aust. J. Chem.* **1989**, *42*, 9.

(4) Lias, S. G.; Bartmess, J. E.; Liebman, J. F.; Holmes, J. L.; Levin, R. D.;Mallard, W. G. *J. Phys. Chem. Ref. Data Suppl.* **1988**, *17*,

(5) Freeman, C. G.; Knight, J. S.; Love, J. G.; McEwan, M. J. *Int. J. Mass Spectrom. Ion Processes* **1987**, *80*, 255.

(6) Woods, R. C.; Saykally, R. J.; Anderson, T. G.; Dixon, T. A.; Szanto, P. G. *J. Chem. Phys.* **1981**, *75*, 4256.

(7) Gudeman, C. S.; Woods, R. C. *Phys. Rev. Lett.* **1982**, *48*, 1344.

(8) Wagner-Redeker, W.; Kemper, P. R.; Jarrold, M. F.; Bowers, M. T. *J. Chem. Phys.* **1985**, *83*, 1121.

(9) (a) Woods, R. C.; Gudeman, C. S.; Dickman, R. L.; Goldmsith, P. F.; Harquenin, G. R.; Irvine, W. M; Hjalmarson, Å.; Nyman L. Å.; Olofsson, H. *Astrophys. J.* **1983**, *270*, 583. (b) Ziurys, L. M.; Apponi, A. J. *Astrophys. J.* **1995**, *455*, L73.

(10) Buhl, D.; Snyder, L. E. *Nature* **1970**, *228*, 267.

(11) Bohme, D. K. *Int. J. Mass Spectrom. Ion Processes* **1992**, *115*, 95.

(12) See, for example, (a) Ferguson, E. E. *Chem. Phys. Lett.* **1989**, *156*, 319. (b) Petrie, S.; Freeman, C. G.; Meot-Ner, M.; McEwan, M. J.; Ferguson, E. E. *J. Am. Chem. Soc.* **1990**, *112*, 7121. (c) Bosch, E.; Lluch, J. M.; Bertan, J. *J. Am. Chem. Soc.* **1990**, *112*, 3868. (d) Petrie, S.; Freeman, C. G.; Meot-Ner, M.; McEwan, M. J.; Ferguson, E. E. *J. Am. Chem. Soc.* **1990**, *112*, 7121. (e) Fox, A.; Bohme, D. K. *Chem. Phys. Lett.* **1991**, *187*, 541. (f) Audier, H. E.; Millet, A.; Leblanc, D.; Morton, T. H. *J. Am. Chem. Soc.* **1992**, *114*, 2020. (g) Ruttink, P. J. A.; Burgers, P. C. *Org. Mass Spectrom.* **1993**, *28*, 1087. (h) Mourgues, P.; Audier, H. E.; Leblanc, D.; Hammerum, S. *Org. Mass. Spectrom.* **1993**, *28*, 1098. (i) Becker, H.; Schröder, D.; Zummack, W.; Schwarz, H. *J. Am. Chem. Soc.* **1994**, *116*, 1096. (j) Audier, H. E.; Leblanc, D.; Mourgues, P.; McMahon, T. B.; Hammerum, S. *J. Chem. Soc., Chem. Comun.* **1994**, 2329. (k) Chou, P. K.; Smith, R. L.; Chyall, L. J.; Kenttämaa, H. I. *J. Am. Chem. Soc.* **1995**, *117*, 4374. (l) Gauld, J. W.; Audier, H.; Fossey, J.; Radom, L. *J. Am. Chem. Soc.* **1996**, *118*, 6299.

(13) Gauld, J. W.; Radom, L. *J. Am. Chem. Soc.* **1997**, *119*, 9831.

(14) Scott, A. P.; Radom, L. *J. Phys. Chem.* **1996**, *100*, 16502.

(15) For a detailed study, see Smith, B. J.; Radom, L. *J. Am. Chem. Soc.* **1993**, *115*, 4885.

(16) The mean absolute deviation between theory and experiment is 4 kJ mol^{-1}, with a largest deviation of 11 kJ mol^{-1}.

(17) Boys, S. F.; Bernardi, F. *Mol. Phys.* **1970**, *19*, 553.

(18) Bouma, W. J.; Radom, L. *Chem. Phys. Lett.* **1979**, *64*, 216.

Chapter 7

Ion-Transport Catalysis: Catalyzed Isomerizations of NNH^+ and $NNCH_3^+$

7.1 Introduction

There have been many examples in the recent literature[1-4] of the phenomenon described by Bohme[4] as proton-transport catalysis, namely the lowering or even elimination of the barrier to a proton-transport reaction that occurs in the presence of a neutral base. However, few examples of catalysis of other ion-transport reactions have been reported. The only experimental study of which we are aware involves the isomerization of $CH_3NO_2^+$ to CH_3ONO^+, which was found to be catalyzed by both nitrogen and xenon.[5] Theoretical work on the isomerization of CH_3OC^+ to $OCCH_3^+$, that found a lowering of the barrier to methyl-cation migration by interaction with nitrogen and argon, has also been reported.[3]

In Chapter 6, it was found that the proton affinity of the added neutral molecule plays a crucial role in determining its effectiveness as a proton-transport catalyst.[2] It was concluded that the ideal catalyst should have a proton affinity lying between those of the two sites between which the proton is migrating.[2,4] In the case of degenerate rearrangements such as those that might occur in NNH^+, the two sites are the same so this condition cannot be satisfied. A study of such a system has not yet been reported.

A suggestion that the methyl-cation affinity of a neutral is important in determining its effectiveness as a methyl-cation-transport catalyst has also been made.[5] The proposed mechanism for methyl-cation transport, however, differs from that for proton transport

due to the barrier that will generally exist for transfer of a methyl cation between the two species within the initially-formed complex **a**, as shown in Scheme 7.1.[5]

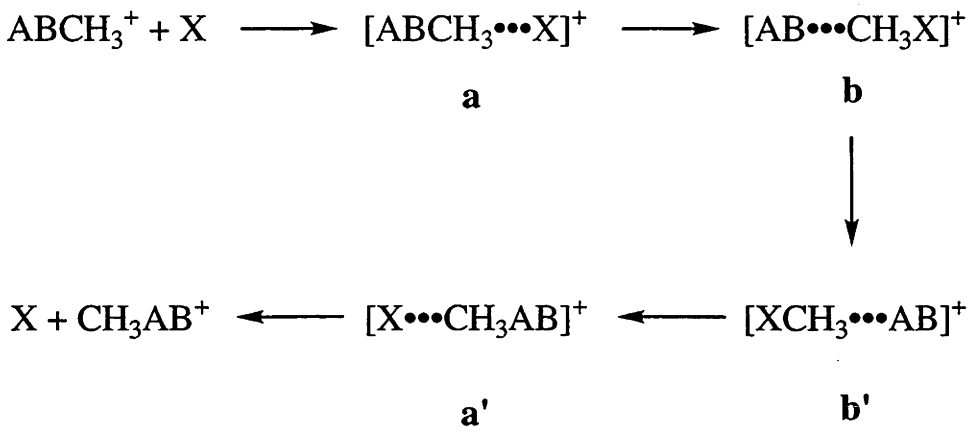

Scheme 7.1

The present work aims firstly to systematically investigate the possibility of catalysis of proton-transport reactions in a degenerate system, and secondly to make comparisons between proton transport and the corresponding methyl-cation-transport reaction. This includes a detailed investigation of the mechanism for methyl-cation-transport catalysis (Scheme 7.1). Results are reported for the isomerization of the isolated NNH^+ and $NNCH_3^+$ systems and for proton transport and methyl-cation transport catalyzed by a range of neutral molecules (Ar, HF, CO, N_2 and H_2O, or HF, H_2, N_2, HCl and H_2O).

7.2 Methods and Results

Standard ab initio molecular orbital calculations have been carried out using variants of the G2 method, which has been found to perform well in the calculation of

proton[6] and methyl-cation affinities.[7] In order to provide a better description of the hydrogens in the proton-transport reactions, polarization functions have been included (i.e. 6-31G(d,p) rather than 6-31G(d) in the geometry optimizations and ZPVE) in the calculations for these systems. In addition, ZPVE calculations have been performed at the MP2 level (and scaled by 0.9427) rather than HF. We term this level of theory G2**. The methyl-cation-transport systems have been examined using standard G2(ZPE=MP2) theory.[8]

Selected geometrical features of the proton-transport systems are given in Figures 7.1 and 7.3, while the methyl-cation transport systems are shown in Figures 7.5 and 7.7. Schematic potential energy surfaces for proton-transport are shown in Figures 7.2 and 7.4, while the methyl-cation systems are shown in Figures 7.6 and 7.8. Total G2** and G2(ZPE=MP2) energies for the proton- and methyl-cation-transport systems, respectively, are presented in Tables A5.1 and A5.2 in Appendix 5. Complete geometries are given in the form of GAUSSIAN archive files in Tables A5.3 and A5.4. Unless otherwise noted, relative energies within the text refer to G2** (proton-transport systems) or G2(ZPE=MP2) (methyl-cation-transport systems) values.

7.3 Discussion

7.3.1 The Rearrangement of the Isolated NNH^+ Cation

The potential energy profile for the degenerate rearrangement of NNH^+ (**1**) via the transition structure **TS:1→1'** is shown in Figure 7.2. A significant barrier (182 kJ mol^{-1}) is found to exist for this process at the G2** level.

7.3.2 Interaction of NNH^+ with Ar

Interaction of NNH^+ with argon leads initially to the ion-neutral complex **2** which is stabilized by 31 kJ mol^{-1} relative to the isolated species (Figure 7.2). A stronger interaction (72 kJ mol^{-1}) occurs with the transition structure **TS:2→2'** to form the rearranged product **2'**, resulting in a reduction in the overall barrier from 182 kJ mol^{-1} to 110 kJ mol^{-1}.

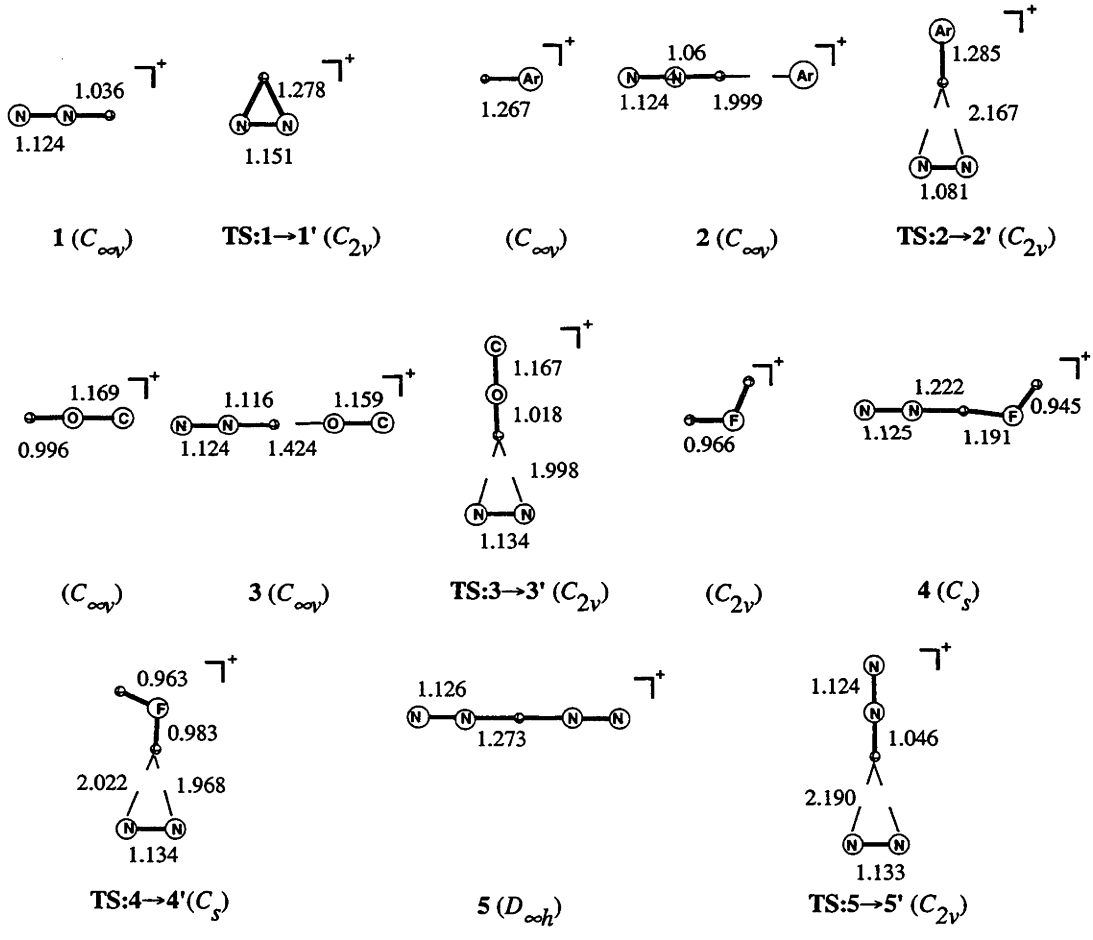

Figure 7.1 Selected MP2/6-31G(d,p) geometrical parameters for the isolated NNH^+ structures and for the $[NNH{\bullet\bullet\bullet}X]^+$ structures with X = Ar, HF, CO* and N_2.

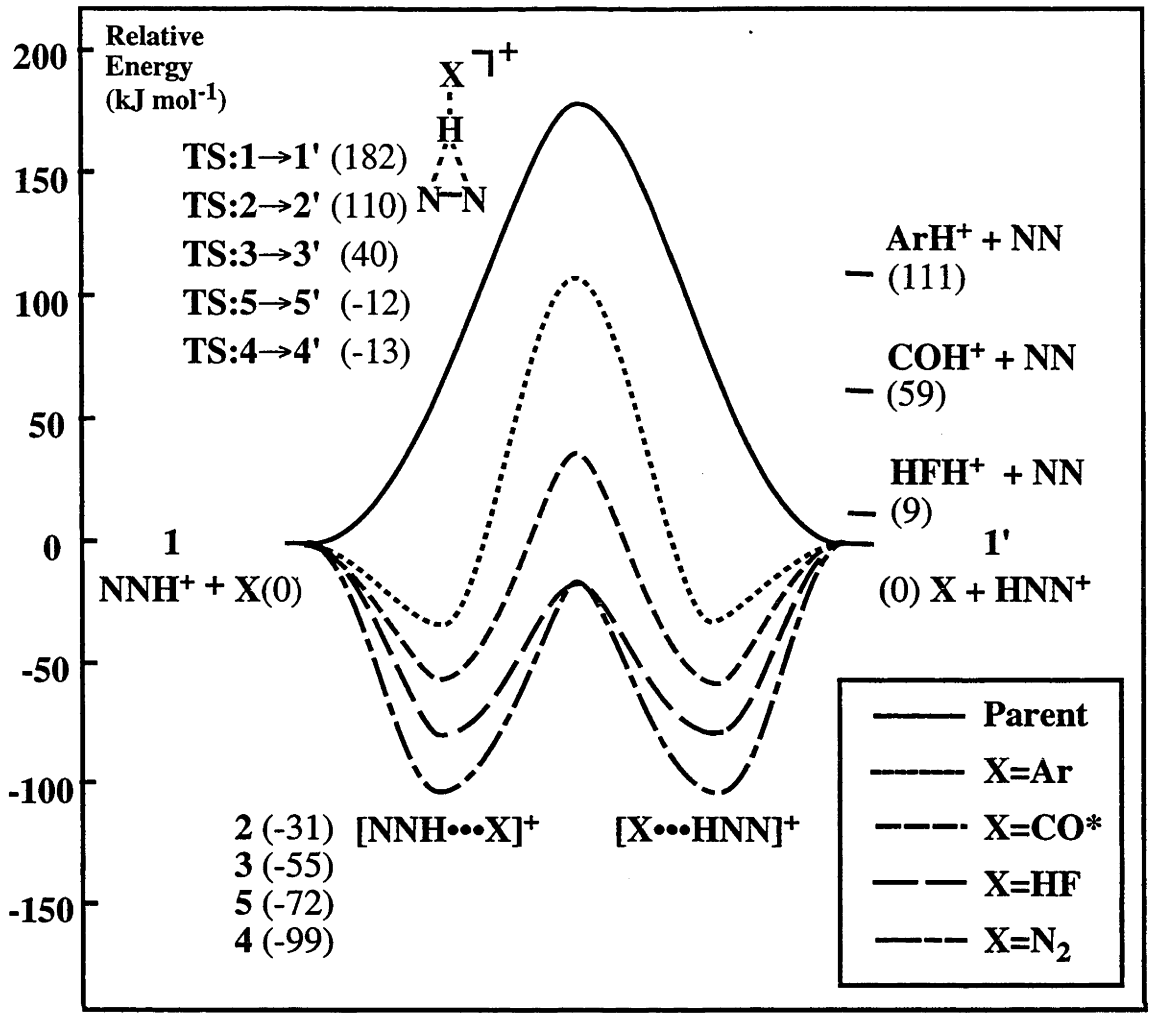

Figure 7.2 Schematic energy profile (G2**, 0 K) showing the uncatalyzed (parent) and catalyzed (X = Ar, HF, CO^* and N_2) isomerization of NNH^+.

7.3.3 Interaction of NNH^+ with CO (at O), HF and N_2

As the proton affinity of the interacting neutral molecule is increased (Table 7.1), we find a corresponding increase in the interaction energies and a decrease in the barrier to hydrogen migration (Figure 7.4), consistent with previous work.[2,3] The overall barrier decreases from its value of 182 kJ mol^{-1} in the isolated case to 40 kJ mol^{-1} in the

presence of CO* (protonating at oxygen), –13 kJ mol^{-1} in the presence of HF and –12 kJ mol^{-1} in the presence of N_2.

Table 7.1 Calculated and Experimental Proton Affinities

	G2**		Expt[a]
Species	0 K	298 K	298 K
Ar	377.8	381.6	371
CO*	430.1	433.5	427[b]
HF	480.3	485.3	489.5
N_2	488.9	494.4	494.5, 496.5[c]
*CO	588.2	593.9	594, 593.6[c]
H_2O	682.3	688.3	697, 690.2[c]

[a] From ref. 9 unless otherwise noted. [b] From ref. 1c. [c] From ref. 10.

7.3.4 Interaction of NNH^+ with CO (at C) and H_2O

The molecules *CO (protonating at carbon) and H_2O have proton affinities greater than that of nitrogen (Table 7.1). Interaction with these species results in a further lowering of the overall barriers to –105 kJ mol^{-1} (*CO) and –200 kJ mol^{-1} (H_2O) (Figure 7.4). However, the fact that these two species have proton affinities greater than that of nitrogen means that it is energetically more favorable for the neutral to retain the proton than for proton migration to occur, i.e. the protonated neutral molecule plus nitrogen will be the energetically favored products in such situations (Figure 7.4).

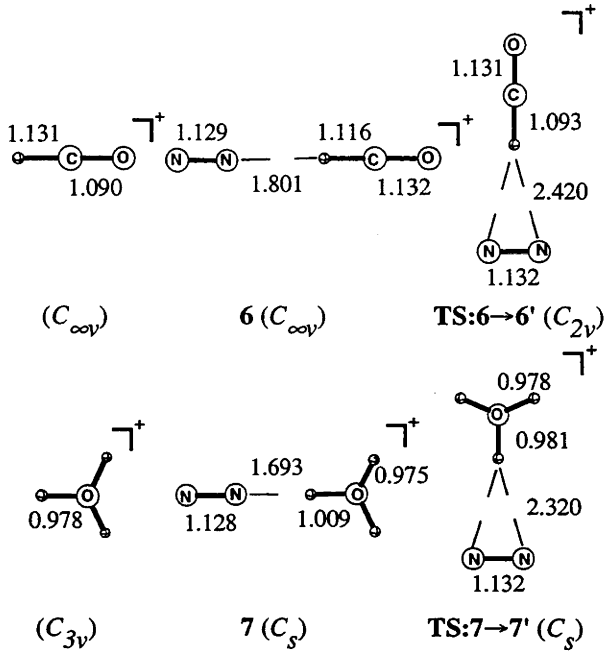

Figure 7.3 Selected MP2/6-31G(d,p) geometrical parameters for the $[NNH{\bullet\bullet\bullet}X]^+$ structures with X = *CO and H_2O.

7.3.5 The Role of Proton Affinities

In the work presented in Chapter 6 on the catalyzed isomerization of HOC^+ to OCH^+, a direct correlation between the overall barrier and the proton affinity of the neutral X and also with the H–O bond length in the initially-formed complex was found.2a Similar behavior is observed here for NNH^+ (Table 7.2). There is generally a steady decrease in the barrier from the value of 182 kJ mol^{-1} in the isolated system to –200 kJ mol^{-1} in the presence of water. A corresponding increase in the N–H bond length with increasing proton affinity of the neutral is also observed, consistent with a weakening by interaction with X of the N–H bond, thus allowing isomerization to occur more readily. There is also a stronger interaction in the transition structure than in the complex in all cases due to the fact that the weaker bonds in the transition structure allow greater interaction with the neutral, as observed previously.[2a]

7.3.6 The Rearrangement of the Isolated $NNCH_3^+$ Cation

The potential energy profile for methyl-cation migration in the isolated $NNCH_3^+$ ion (**8**) via the transition structure **TS:8→8'** is shown in Figure 7.6. There is a substantial barrier of 152 kJ mol^{-1} at the G2(ZPE=MP2) level.

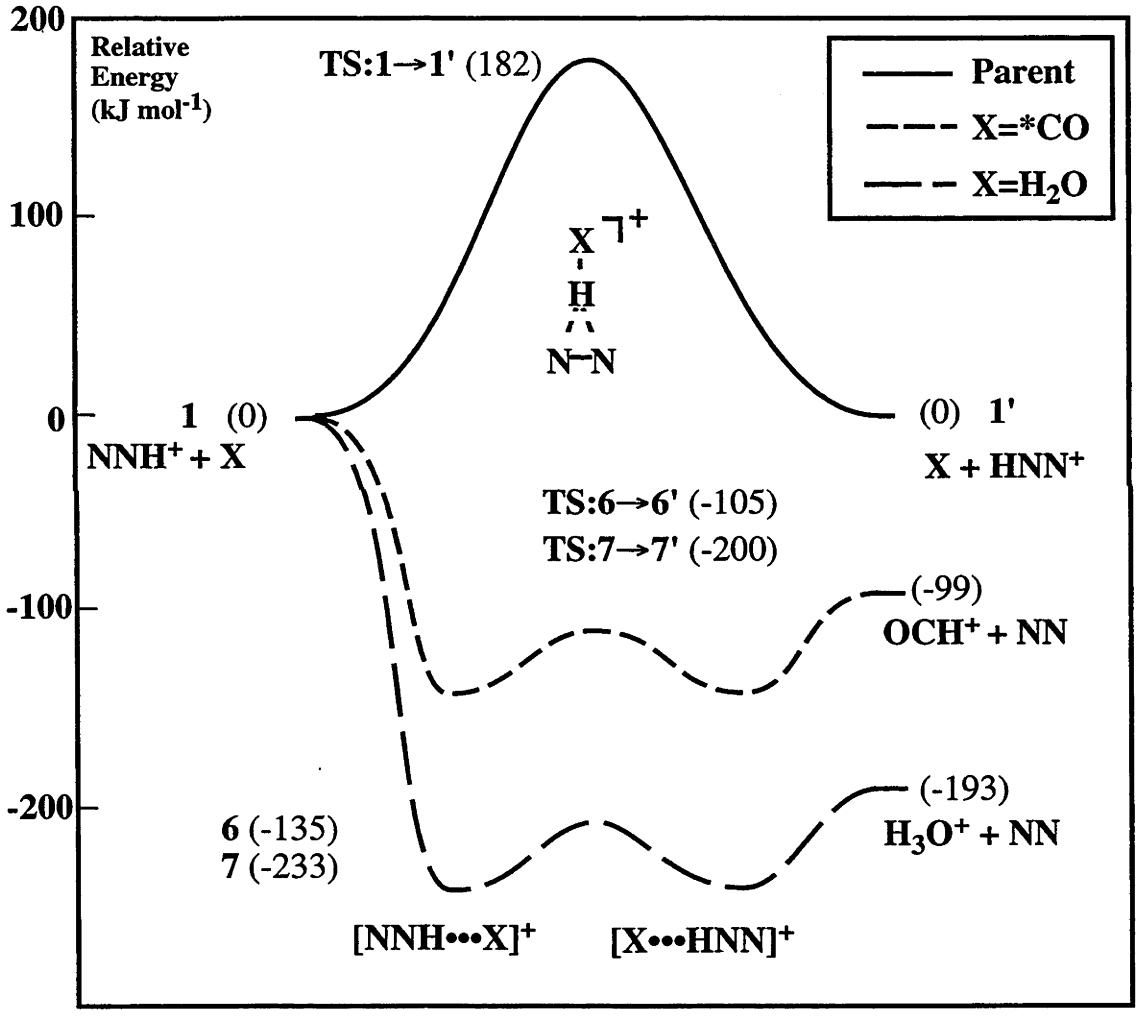

Figure 7.4 Schematic energy profile (G2**, 0 K) showing the uncatalyzed (parent) and catalyzed (X = *CO and H_2O) isomerization of NNH^+.

Table 7.2 Relative Proton Affinities (ΔPA, kJ mol–1),[a,b] N•••H bond Lengths in [NN•••H•••X]+ Complexes (Å)[c] and Overall Reaction Barriers (kJ mol^{-1})[b,d]

X	Δ(PA)	r(N•••H)	Barrier
-		1.036	182
Ar	–111	1.064	110
CO*	–59	1.116	40
HF	–9	1.222	–13
N_2	0	1.273	–12
OC*	99	1.801	–105
H_2O	193	1.693	–200

[a] Δ(PA) = PA(X) – PA(N_2). [b] G2** at 0 K. [c] MP2/6-31G(d,p) optimized geometries. [d] Barriers relative to reactants NNH^+ + X.

7.3.7 Interaction of $NNCH_3^+$ with HF

The potential energy profile showing the effect of interaction of $NNCH_3^+$ with HF, the species with the lowest methyl-cation affinity among those studied (Table 7.3), is included in Figure 7.6. The initially-formed complex **9a**, which is best described as $[NNCH_3•••FH]^+$, is stabilized by 35 kJ mol^{-1} relative to HF plus $NNCH_3^+$. Ion **9a** can undergo a methyl-cation shift to form a new complex (**9b**) via the transition structure **TS:9a→9b** which lies at 38 kJ mol^{-1}. The complex **9b** is best described as $[NN•••CH_3FH]^+$ and has a relative energy of 41 kJ mol^{-1}. This energy is actually slightly higher than that of the transition structure **TS:9a→9b** after the inclusion of ZPVE, making it likely that **9b** lies at best in a very shallow potential energy well. The components of **9b** are relatively free to undergo mutual rotation. This is reflected in the transition structure **TS:9b→9b'** for the methyl-cation migration that leads to the

equivalent complex $[HFCH_3 \bullet\bullet\bullet NN]^+$ (**9b'**) having a relative energy of just 55 kJ mol^{-1}, only 14 kJ mol^{-1} above the complex **9b**. Continuation via **TS:9b'→9a'** and the complex **9a'** gives the desired rearranged product, CH_3NN^+ (**8'**). The overall barrier for this process is 55 kJ mol^{-1}, a reduction of 97 kJ mol^{-1} from that in the isolated system.

Table 7.3 Calculated and Experimental Methyl-Cation Affinities

	MP2[a,b]	MP2[b,c]	G2(MP2=ZPE)		Expt.[d]
Species	0 K	0 K	0 K	298 K	298 K
HF		149.2	114.5	120.9	134.9
H_2		139.3	165.3	173.6	188[e]
N_2	182.9	176.6	173.1	179.4	184.2
HCl		183.9	191.7	198.1	203.6
H_2O	275.4	299.2	265.0	272.9	283.3

[a] Calculated using the 6-311+G(3df,2p) basis set. [b] Includes MP2/6-31G(d) ZPVE. [c] Calculated using the 6-31G(d) basis set. [d] From ref. 7 unless otherwise noted. [e] From ref. 9.

7.3.8 Interaction of $NNCH_3^+$ with H_2 and N_2

Both H_2 and N_2 have methyl-cation affinities higher than that of HF (Table 7.3) and it would therefore be expected that interaction with these molecules would result in a greater lowering of the overall barrier. The barriers for the methyl-cation migration step do indeed drop substantially, as reflected in the relative energy of the appropriate transition

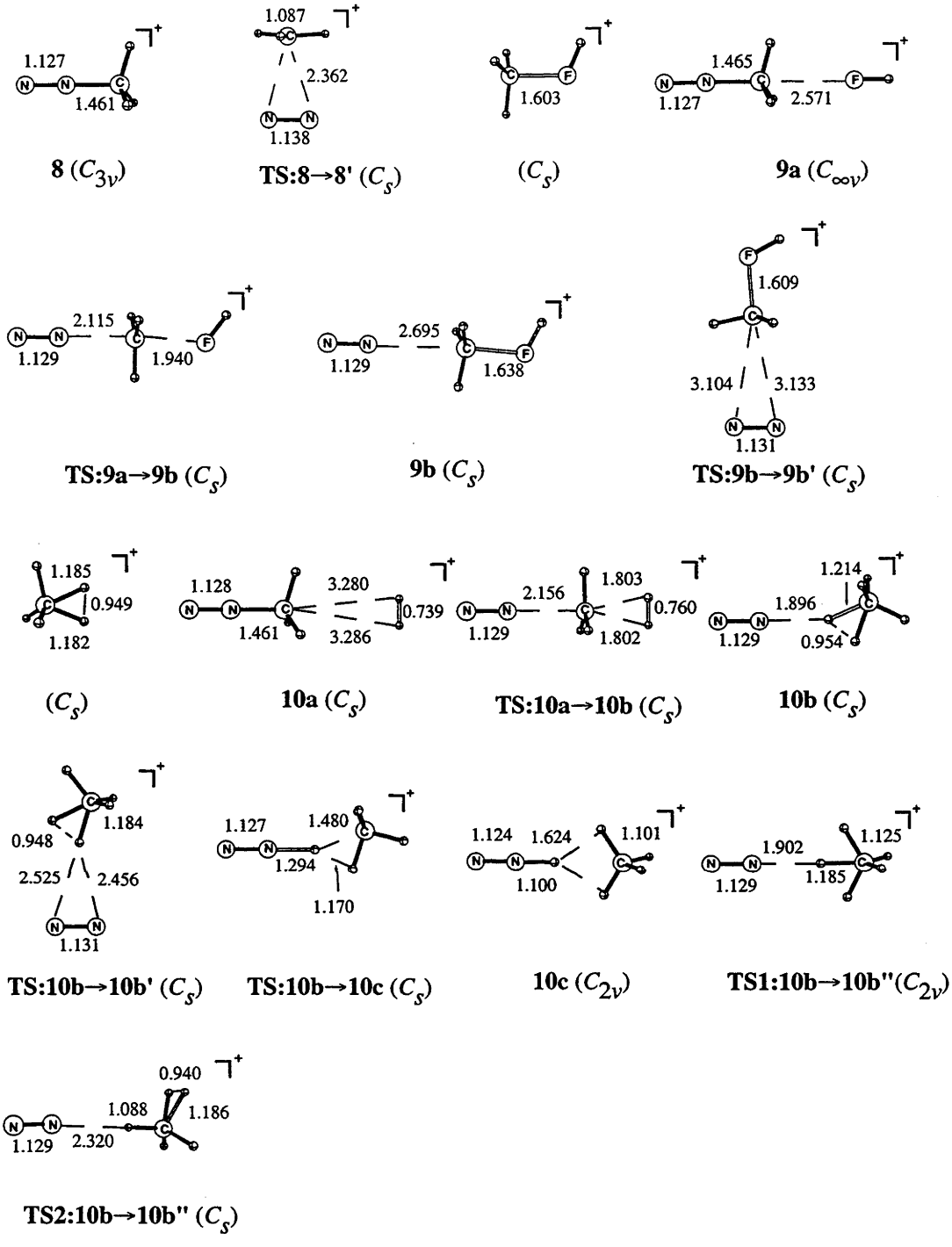

Figure 7.5 Selected MP2/6-31G(d) geometrical parameters for the isolated $NNCH_3^+$ structures and for the $[NNCH_3 \bullet\bullet\bullet X]^+$ structures with X = HF, H_2 and N_2.

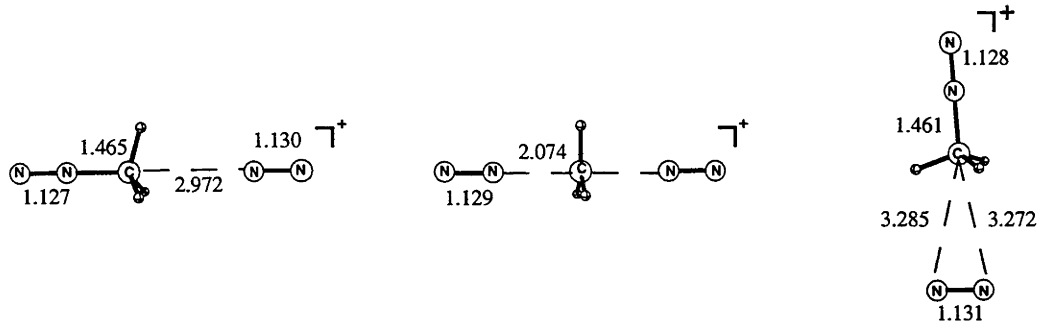

11a ($C_{\infty v}$) **TS:11a→11b** ($D_{\infty h}$) **TS:11b→11b'** (C_s)

Figure 7.5 (Cont.) Selected MP2/6-31G(d) geometrical parameters for the isolated $NNCH_3^+$ structures and for the $[NNCH_3 \bullet\bullet\bullet X]^+$ structures with X = HF, H_2 and N_2.

structure, **TS:b→b'**, for these processes which falls from 152 kJ mol^{-1} to 4 kJ mol^{-1} in the presence of hydrogen and –7 kJ mol^{-1} in the presence of nitrogen (Figure 7.6). However, the rate-limiting step for methyl-cation transport in these cases is the transformation of the $[NNCH_3 \bullet\bullet\bullet X]^+$ complex (**a**) to the $[NN \bullet\bullet\bullet CH_3X]^+$ complex (**b**). The barriers to this transformation involving hydrogen (relative energy of 73 kJ mol^{-1}) and nitrogen (relative energy of 45 kJ mol^{-1}) are quite large. Hence, the overall barriers are reduced but to a smaller extent than might otherwise be suggested, namely from 152 kJ mol^{-1} to 73 kJ mol^{-1} in the presence of hydrogen and to 45 kJ mol^{-1} in the presence of nitrogen.

7.3.9 Interaction of $NNCH_3^+$ with HCl and H_2O

Hydrogen chloride and water have methyl-cation affinities larger than nitrogen (Table 7.3) and we would therefore expect interaction with these molecules to lead to a further lowering of the barriers for methyl-cation migration. This is indeed the case, the overall barriers being reduced from 152 kJ mol^{-1} to 26 and –12 kJ mol^{-1}, respectively

(Figure 7.8). Again, the methyl-cation transfer in the complex between N_2 and X (via **TS:a→b**) is the rate-limiting step. As for the analogous case in proton transfer, the fact that the neutral has a higher methyl-cation affinity than nitrogen means that the favored products will be XCH_3^+ plus N_2 rather than the desired isomerized product, CH_3NN^+ (**8'**).

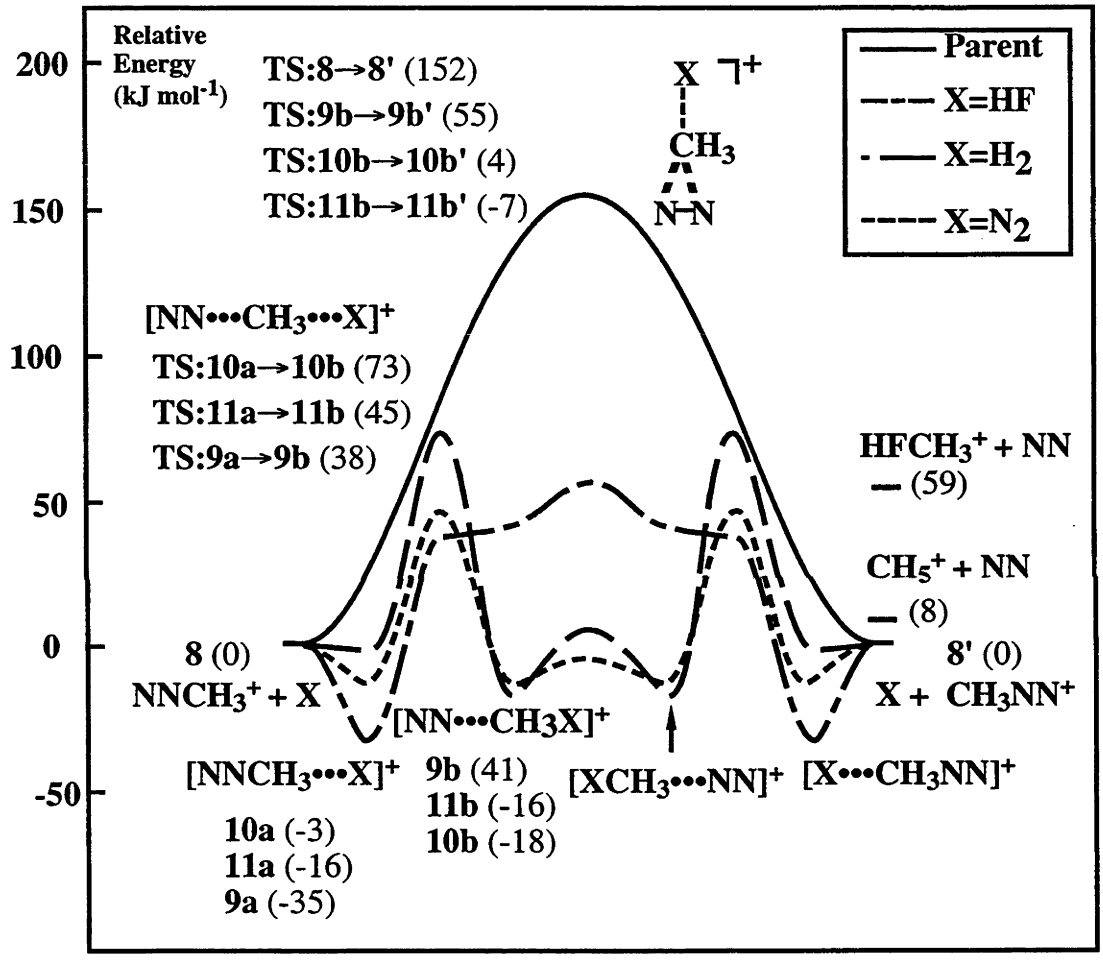

Figure 7.6 Schematic energy profile (G2(ZPE=MP2), 0 K) showing the uncatalyzed (parent) and catalyzed (X = HF, H_2 and N_2) isomerization of $NNCH_3^+$.

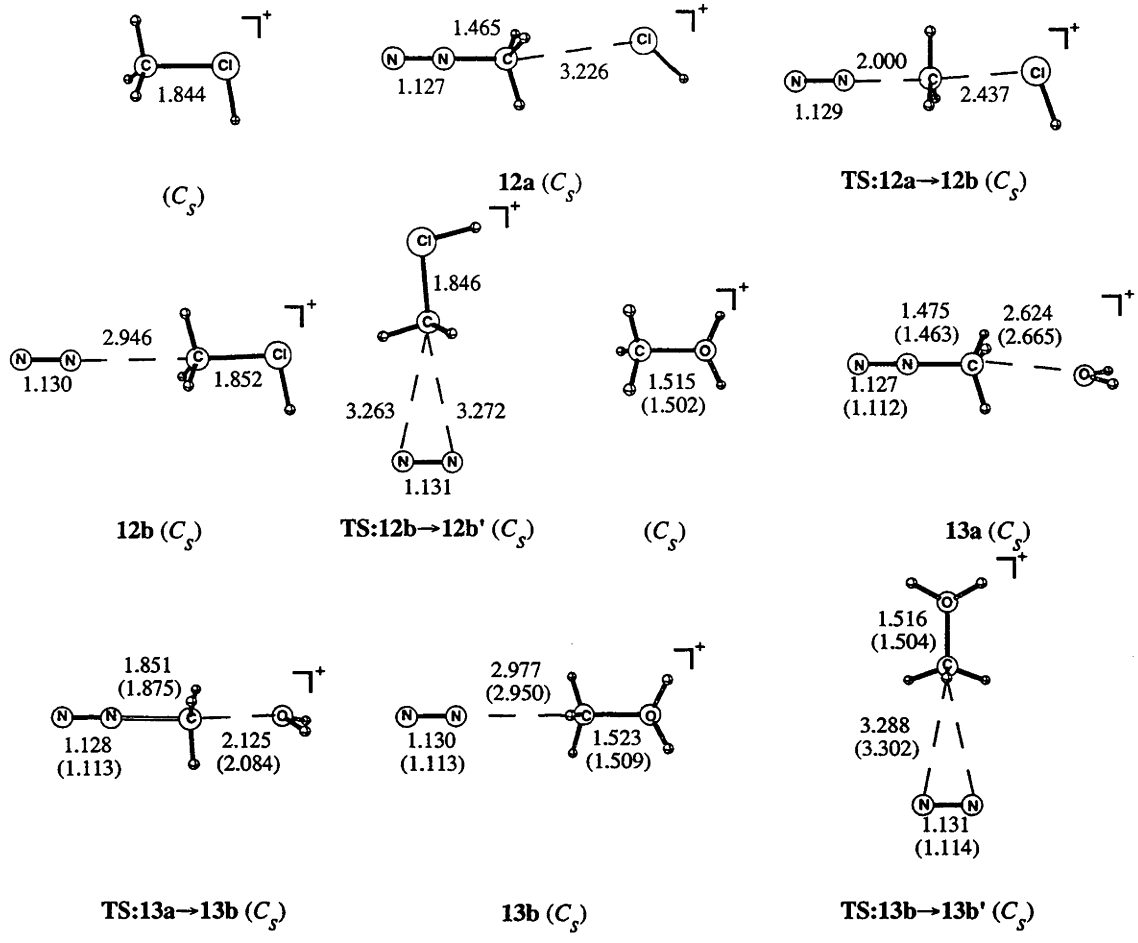

Figure 7.7 Selected MP2/6-31G(d) and MP2/6-311+G(3df,2p) (in parenthesis) geometrical parameters for the $[NNCH_3 \bullet\bullet\bullet X]^+$ structures with X= HCl and H_2O.

7.3.10 Other Reactions

In species where the neutral X contains a proton, i.e. the neutral can be described as HZ with Z = F, H, Cl or OH, there is the possibility of an additional reaction that has not been discussed above, namely proton transfer from CH_3ZH^+ to nitrogen. The reaction energies for the production of protonated nitrogen plus CH_3Z are 161 (Z = F), 56 (Z = H), 136 (Z = Cl) and 164 (Z = OH) kJ mol^{-1}. Apart from the case of Z = H (i.e. X = H_2), all these energies are significantly higher than the rate-limiting step for formation

of isomerized $NNCH_3^+$ and hence such proton-transfer will not be energetically favorable. In the case of X = H_2, however, we would expect some formation of CH_4 plus NNH^+ because the energy required to form these species (56 kJ mol^{-1}) is less than the energy of the rate-limiting step for isomerization of $NNCH_3^+$ (73 kJ mol^{-1}). CH_4 plus NNH^+ are formed from **10b**, initially via the transition structure **TS:10b→10c** at –9 kJ mol^{-1}. The latter is lower in energy than the resulting complex (**10c**) at 3 kJ mol^{-1}, indicating a very flat potential for proton transfer. Dissociation of **10c** then results in CH_4 plus NNH^+ at an energy of 56 kJ mol^{-1}.

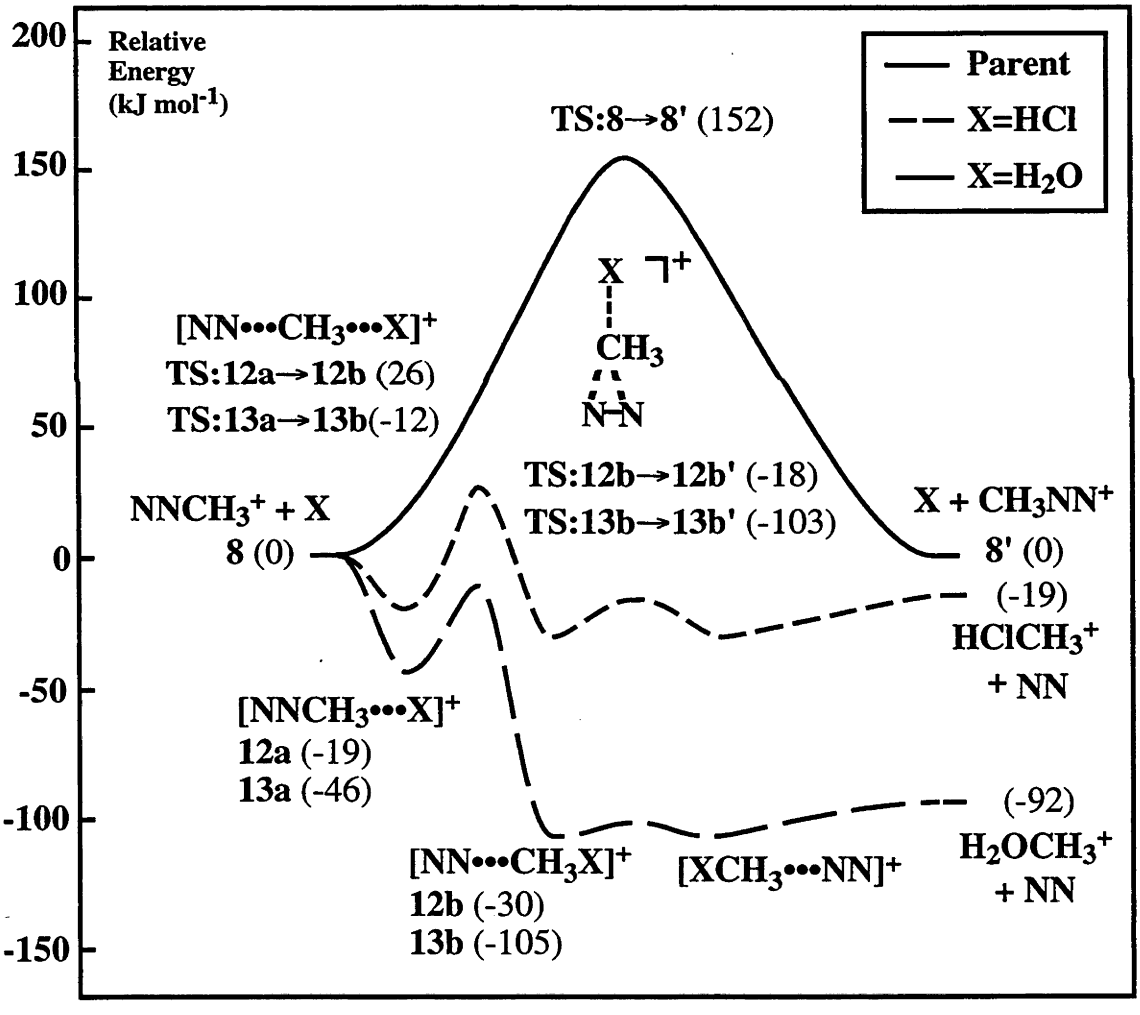

Figure 7.8 Schematic energy profile (G2(ZPE=MP2), 0 K) showing the uncatalyzed (parent) and catalyzed (X = HCl and H_2O) isomerization of $NNCH_3^+$.

For the reactions of $NNCH_3^+$ with H_2, there is also the possibility of exchange of labeled hydrogens within the complex **10b**. Recent work has shown that the CH_5^+ ion has very low barriers to internal hydrogen motions[11] and, due to the weak nature of its bonding, we would expect this property to be also exhibited in the complex **10b**. We have located two transition structures (Figure 7.5) corresponding to hydrogen exchange within **10b**. The first, **TS1:10b→10b"** at an energy of –22 kJ mol^{-1}, results in loss of identity of the three in-plane hydrogens. This energy is actually lower than that of the complex **10b**, indicating an extremely flat potential surface for such a motion. A second transition structure (**TS2:10b→10b"**) at a relative energy of –3 kJ mol^{-1} will result in exchange of in-plane with out-of-plane hydrogens. Since the energies of both these transition structures lie below the energy of the separated species, we would expect a total loss of identity of all hydrogen labels. This would mean that in the proton-transfer reaction discussed above, the transferred hydrogen should be chosen randomly from the five available hydrogens.

7.3.11 The Mechanism for Methyl-Cation-Transport

As noted above, the methyl-cation-transport process actually takes place in three steps. First, the initially-formed complex $[NNCH_3{\bullet\bullet\bullet}X]^+$ (**a**) is converted to the alternative complex $[NN{\bullet\bullet\bullet}CH_3X]^+$ (**b**). The two components in the latter are fairly weakly bound and so transformation to $[XCH_3{\bullet\bullet\bullet}NN]^+$ (**b'**) can occur with a low barrier, as suggested in Scheme 7.1. Transformation to the product-related complex $[X{\bullet\bullet\bullet}CH_3NN]^+$ (**a'**) takes place in the third step. In all but one of the cases examined here, the first methyl-cation transfer between the complexes (via **TS:a→b**) is the rate-determining step for the reaction, hence for effective catalysis to occur, we would require this barrier to be low or negative. This can certainly be achieved if the reaction is sufficiently exothermic, e.g. transfer from molecular nitrogen to water (Figure 7.8). Unfortunately, in order for a neutral X to be useful in our situation it must have a methyl-

cation affinity *lower* than that of nitrogen so that methyl-cation migration rather than methyl-cation transfer to the neutral molecule X takes place. However, this makes the methyl-cation-transfer reaction (**a**→**b**) endothermic. Thus, it would seem that it is not feasible to eliminate the barrier entirely in such degenerate methyl-cation-transport reactions, in contrast to the situation for proton transport.

7.3.12 The Importance of Dipole Moments

Proton affinities are clearly important in determining the effectiveness of a proton-transport catalyst but our calculations indicate that there are other factors to consider. For example, since nitrogen has a higher proton affinity than hydrogen fluoride (Table 7.1), we would expect on the basis of proton affinities alone that nitrogen would have a larger interaction with NNH^+ than hydrogen fluoride. In fact the opposite is observed. Nitrogen is found to have a significantly weaker interaction with NNH^+ (72 kJ mol^{-1}) than does hydrogen fluoride (99 kJ mol^{-1}). We believe that the stabilizing effect of ion-dipole interactions contributes to such apparent discrepancies. Thus the ion-dipole interaction of NNH^+ with hydrogen fluoride, which has a significant calculated dipole moment (2.0 D), is greater than that with nitrogen which has a zero dipole moment. This effect is also evident in the reaction barriers. The barrier in the presence of hydrogen fluoride (–13 kJ mol^{-1}) is very slightly lower than that observed in the presence of nitrogen (–12 kJ mol^{-1}), despite the greater proton affinity of N_2.

For proton-transport systems, we have already noted the correlation between the N–H bond lengths and the proton affinity of the interacting neutral. In contrast to this behavior, there is little correlation between the methyl-cation affinity of the interacting neutral and the N–C bond lengths in the complexes **a** and **b** involved in methyl-cation transport. It can be seen from Table 7.4 that these bond lengths are fairly constant, independent of the methyl-cation affinity of the neutral. This, and the fact that the neutral

component of the complex is always at a reasonably large distance (Figures 7.5 and 7.7), leads us to suggest that these complexes are largely electrostatically bound.

If the intermediate complexes are indeed largely electrostatically bound, we may expect that the dipole moment of the neutral molecule plays an important role in determining the stability of the ion-neutral complex. It can be seen from Table 7.4 that there does indeed appear to be a correlation between the dipole moment of the neutral and the stabilization energy of the complex (**a**). For example, HF which has a relatively high dipole moment (2.0 D) forms an initial complex (**9a**) which is stabilized by 35 kJ mol^{-1}, while H_2 with a zero dipole moment forms an initial complex (**10a**) that is stabilized by only 3 kJ mol^{-1}. N_2, which also has a zero resulting dipole moment, forms a complex (**11a**) that is stabilized by a greater amount (16 kJ mol^{-1}) due to a combination of ion–induced-dipole and ion-quadrupole interactions.[13] The magnitudes of both the polarizabilty and quadrupole moment of nitrogen are larger than those for hydrogen, resulting in the increased stabilization of the nitrogen complex. The stabilization energies increase smoothly so that H_2O, with a dipole moment of 2.3 D, forms a complex (**13a**) that is stabilized by 46 kJ mol^{-1}. However, for all cases except HF, the relative methyl-cation affinity (ΔMCA, Table 7.4) also correlates reasonably well with the stabilization energy so it is possible that ΔMCA is also important in determining the stabilization of the complex.

The overall barrier for methyl-cation transport is generally given by the relative energy of **TS:a→b**. This will be influenced by the energies, relative to the starting reactants of the complexes **a** and **b**, as shown schematically in Figure 7.9. A lowering in energy of either **a** or **b** should result in a lowering of this barrier. If electrostatic interactions are important, the stabilization energy (E_{stab}(**a**)) of the reactant complex **a** will be increased through interaction with a neutral having a large dipole moment. The energy of the product complex (**b**) is affected by both E_{stab}(**b**) and by the relative methyl-cation

Table 7.4 Relative Methyl–Cation Affinities (ΔMCA, kJ mol^{-1}),[a,b] Dipole Moments (Debye) of X,[c] N•••C bond Lengths in $[NNCH_3•••X]^+$ (**a**) and $[NN•••CH_3X]^+$ (**b**) Complexes (Å),[c] Stabilization Energies of $[NNCH_3•••X]^+$ (**a**)[d] and $[NN•••CH_3X]^+$ (**b**)[e] (E_{stab}, kJ mol^{-1})[b] and Overall Reaction Barriers (kJ mol^{-1})[b,d]

		Dipole	r(N–C)		E_{stab}		
X	Δ(MCA)	Moment	$[NNCH_3•••X]^+$	$[NN•••CH_3X]^+$	$[NNCH_3•••X]^+$	$[NN•••CH_3X]^+$	Overall Barrier
			1.461				152
HF	–59	2.01	1.465	2.695	35	18	55
H_2	–8	0.0	1.461	3.054	3	24	73
N_2	0	0.0	1.465	2.972	12	12	49
HCl	19	1.51	1.465	2.946	19	11	26
H_2O	92	2.25	1.475	2.977	46	13	–12

[a] Δ(MCA = MCA(X) – MCA(N_2). [b] G2(ZPE=MP2) at 0 K. [c] From MP2/6-31G(d,p) optimized geometries. [d] Relative to $NNCH_3^+$ + X. [e] Relative to NN + CH_3X^+.

affinity (ΔMCA), which determines the relative energy of the isolated species N_2 plus CH_3X^+ (Figure 7.9). Hence, in order to lower the barrier to the reaction, we can either choose a neutral with a larger dipole moment or choose a neutral with a less negative relative methyl-cation affinity (ΔMCA). It can be seen from Table 7.4 that an increase in the relative methyl-cation affinity does indeed result in a lowering of this barrier. On the other hand, dipole effects appear to be particularly important in the case of X = HF, where the barrier is much lower than would be expected on the basis of methyl-cation

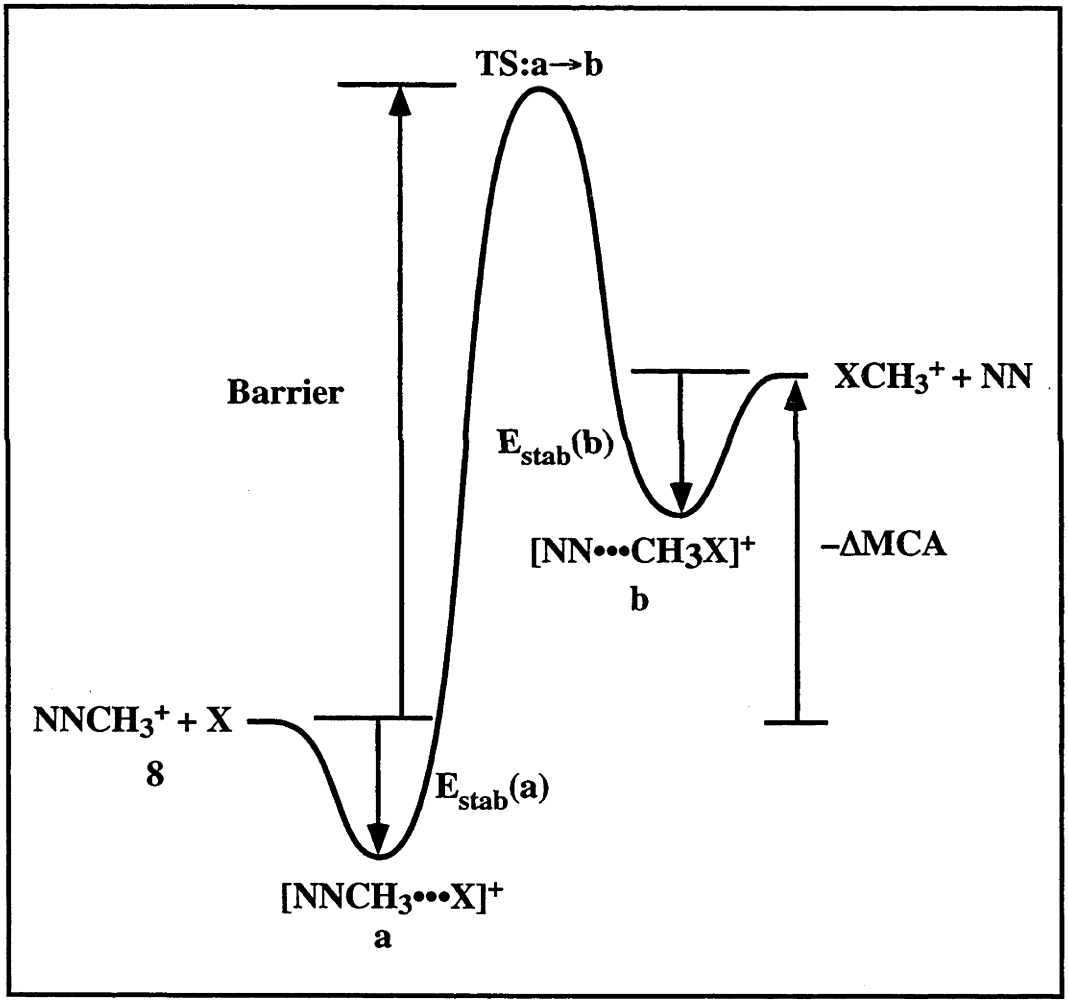

Figure 7.9 Schematic energy profile for methyl-cation transfer (**a→b**) showing the principal factors determining the barrier height.

affinities alone. We conclude that both the methyl-cation affinity and the dipole moment of the interacting neutral are important in determining its effectiveness as a catalyst for methyl-cation transport. For a non-polar neutral, the quadrupole moment and polarizability will also play a role.

7.3.13 Reliability of Theoretical Predictions

It is important to try to assess the reliability of the theoretical predictions made in the present work. Clearly the ion affinities play a very important role. As noted earlier, G2 theory has been shown to perform fairly well both for proton affinities[6] and methyl-cation affinities.[7] It would be expected that variants of G2 would perform equally well. It can be seen from Table 7.1 that there is good agreement between the G2** and experimental proton affinities.[12] It can also be seen from Table 7.3 that G2(ZPE=MP2) does not perform as well in the calculation of methyl-cation affinities. The mean absolute deviation between theory and experiment is 9.8 kJ mol^{-1} with the largest deviation being 14.4 kJ mol^{-1}. We find that the G2(ZPE=MP2) methyl-cation affinities are generally lower than the standard G2 results,[7] by as much as 4.1 kJ mol^{-1} for water. These lower values increase the deviation from experiment (Table 7.3). In the present work, methyl-cation affinities relative to that of molecular nitrogen are more important than absolute methyl-cation affinities. We find that the mean absolute deviation between theory and experiment for methyl-cation affinities relative to nitrogen is 6.3 kJ mol^{-1} with the largest deviation being 9.2 kJ mol^{-1}, a somewhat better result.

It is also important to examine the effect of the level of geometry optimization. The G2 methods used in the present study both use geometries optimized at the MP2 level with a relatively small basis set. It is possible that significant changes in the geometries of the complexes and transition structures and therefore the thermochemistry could occur if this level of optimization is not adequate. Poor geometries are most likely to occur if the level of optimization does not correctly describe the relative ion affinity values. It has

previously been shown that the MP2/6-31G(d,p) geometries used in the G2** method are sufficient to give good relative energies for proton-transport systems,[2a] so it only remains here to examine the situation for methyl-cation transport.

The MP2/6-31G(d) methyl-cation affinities are shown in Table 7.3. It can be seen that agreement with G2(ZPE=MP2) is poor at this level, the MP2/6-31G(d) results differing by as much as 35 kJ mol^{-1} from G2(ZPE=MP2). In addition, these errors vary significantly from one neutral to another, meaning that relative methyl-cation affinities are also poor. On the other hand, the methyl-cation affinities for N_2 and H_2O at the MP2/6-311+G(3df,2p) level agree reasonably well with the G2(ZPE=MP2) results (Table 7.3). More importantly, the differences from G2(ZPE=MP2) are almost the same for both molecules meaning that their relative methyl-cation affinity is also in good agreement with G2(ZPE=MP2). We might therefore expect the MP2/6-311+G(3df,2p) level to provide accurate geometries for the complexes and transition structures associated with the X = H_2O system, against which the MP2/6-31G(d) geometries can be assessed, particularly their effect on G2(ZPE=MP2) energies.

We have examined the effect of geometry optimizations for the case of X = H_2O. It can be seen in Figure 7.7 that there is little difference between the bond lengths calculated at the MP2/6–31G(d) and MP2/6–311+G(3df,2p) levels. More importantly the G2(ZPE=MP2) energies based on these new geometries for **13a** (–45.8 kJ mol^{-1}), **TS:13a→13b** (–11.3 kJ mol^{-1}), **13b** (–105.8 kJ mol^{-1}) and **TS:13b→13b'** (–102.7 kJ mol^{-1}) are in close agreement with the standard G2(ZPE=MP2) results obtained with MP2/6-31G(d) geometries of –46.2 kJ mol^{-1}, –11.6 kJ mol^{-1}, –105.4 kJ mol^{-1} and –102.5 kJ mol^{-1}, respectively. These results indicate that MP2/6–31G(d) optimized geometries provide an adequate description for the purposes of the present work.

7.4 Concluding Remarks

There are substantial barriers to the degenerate isomerizations of both NNH^+ and $NNCH_3^+$ of 182 kJ mol^{-1} and 152 kJ mol^{-1}, respectively. These barriers can be lowered significantly by interaction with an appropriate neutral molecule. It is found that species with proton affinities slightly lower than that of molecular nitrogen can act to lower the barrier to proton transfer so that it becomes negative. Interaction with species having methyl-cation affinities lower than that of nitrogen results in substantial lowering of the barriers to methyl-cation transport but in this case they remain positive. Interaction with species having ion affinities greater than that of nitrogen results in a further lowering of the barriers. However, transfer of either the proton or the methyl cation to the neutral molecule now becomes the energetically favored process. The magnitude of the dipole moment of the neutral is found to be important. Neutrals with high dipole moments are found to be more effective catalysts, especially for methyl-cation transport.

7.5 References

(1) See, for example: (a) Nobes, R. H.; Radom, L. *Chem. Phys.*, **1981**, *60*, 1. (b) Wagner-Redeker, W.; Kemper, P. R.; Jarrold, M. F.; Bowers, M. T. *J. Chem. Phys.* **1985**, *83*, 1121. (c) Freeman, C. G.; Knight, J. S.; Love, J. G.; McEwan, M. J. *Int. J. Mass Spectrom. Ion Processes* **1987**, *80*, 255. (d) Ferguson, E. E. *Chem. Phys. Lett.* **1989**, *156*, 319. (e) Petrie, S.; Freeman, C. G.; Meot-Ner, M.; McEwan, M. J.; Ferguson, E. E. *J. Am. Chem. Soc.* **1990**, *112*, 7121. (f) Bosch, E.; Lluch, J. M.; Bertran, J. *J. Am. Chem. Soc.* **1990**, *112*, 3868. (g) Petrie, S.; Freeman, C. G.; Meot-Ner, M.; McEwan, M. J.; Ferguson, E. E. *J. Am. Chem. Soc.* **1990**, *112*, 7121. (h) Fox, A.; Bohme, D. K. *Chem. Phys. Lett.* **1991**, *187*, 541. (i) Audier, H. E.; Millet, A.; Leblanc, D.; Morton, T. H. *J. Am. Chem. Soc.* **1992**, *114*, 2020. (j) Ruttink, P. J. A.; Burgers, P. C. *Org. Mass Spectrom.* **1993**, *28*, 1087. (k) Mourgues, P.; Audier, H. E.; Leblanc, D.; Hammerum, S. *Org. Mass. Spectrom.* **1993**, *28*, 1098. (l) Becker,

H.; Schröder, D.; Zummack, W.; Schwarz, H. *J. Am. Chem. Soc.* **1994**, *116*, 1096. (m) Audier, H. E.; Leblanc, D.; Mourgues, P.; McMahon, T. B.; Hammerum, S. *J. Chem. Soc., Chem. Comun.* **1994**, 2329. (n) Chou, P. K.; Smith, R. L.; Chyall, L. J.; Kenttämaa, H. I. *J. Am. Chem. Soc.* **1995**, *117*, 4374. 9831 (o) Gauld, J. W.; Audier, H.; Fossey, J.; Radom, L. *J. Am. Chem. Soc.* **1996**, *118*, 6299. (p) Ruttink, P. J. A.; Burgers, P. C.; Terlouw, J. K. *Can. J. Chem.* **1996**, *74*, 1078.

(2) (a) Chalk, A. J.; Radom, L. *J. Am. Chem. Soc.* **1997**, *119*, 7573. (b) Gauld, J.W.; Radom L. *J. Am. Chem. Soc.* **1997**, *119*, 9831.

(3) Cunje A.; Rodriquez, C. F.; Bohme, D. K.; Hopkinson, A. C. *J. Phys. Chem. A* **1998**, *102*, 478.

(4) Bohme, D. K. *Int. J. Mass Spectrom. Ion Processes* **1992**, *115*, 95.

(5) Baranov, V.; Petrie, S.; Bohme, D. K. *J Am. Chem. Soc.* **1996**, *118*, 4500.

(6) Smith, B. J.; Radom, L. *J. Am. Chem. Soc.* **1993**, *115*, 4885.

(7) Glukhovstev, M. N.; Szulejko, J. E.; McMahon, T. B.; Gauld, J. W.; Scott, A. P.; Smith, B. J.; Pross, A.; Radom, L. *J Phys. Chem.* **1994**, *98*, 13099.

(8) Curtiss, L. A.; Raghavachari, K.; Pople, J. A. *J. Chem. Phys.* **1995**, *103*, 4192.

(9) Lias, S. G.; Bartmess, J. E.; Liebman, J. F.; Holmes, J. L.; Levin, R. D.; Mallard, W. G. *J. Phys. Chem. Ref. Data Suppl.* **1988**, *17*.

(18) Szulejko, J. E.; McMahon, T. B. *J. Am. Chem. Soc.* **1993**, *115*, 7839.

(11) See, for example: (a) Schreiner, P. R.; Kim, S- J.; Schaefer, H. F.; Schleyer, P. v. R. *J. Chem. Phys.* **1993**, *99*, 3716. (b) Müller, H.; Kutzelnigg, W.; Noga, J.; Klopper, W. *J. Chem. Phys.* **1997**, *106*, 1863.

(12) The mean absolute deviation is 5 kJ mol^{-1} with a maximum deviation of 11 kJ mol^{-1}. The mean absolute deviation drops to 4.2 kJ mol^{-1} when more recent experimental values from ref. 10 for the proton affinities of N_2, *CO and H_2O are used.

(13) Henchman, M. in *Ion-Molecule Reactions*; (Ed.: Franklin, J. L.), Plenum Press: New York, 1972; Vol. I, pp 192.

Appendix 1

Table A1.1. Total G2 Energies for Chapter 3 (0 K, Hatree)

1	-193.07643	**8**	-193.09536
TS:1→2	-193.03491	**TS:8→1a**	-193.01593
TS:1→10	-192.92549	**TS:8→1b**	-192.99056
2	-193.05160	**9**	-193.06908
TS:2→3	-193.03677	**10**	-192.95003
3	-193.04793	**TS:10→11**	-192.95090
TS:3→4	-193.03108	**11**	-193.06668
TS:3→7	-193.04093	**TS:11→7**	-193.04493
TS:3→9	-193.03146	**12**	-193.12184
4	-193.05976	**TS:12→7**	-193.03310
TS:4→5	-193.03368	$[CH_3CH_2]^+$	-78.67234
5	-193.07228	CH_2CH_2	-78.41574
TS:5→6	-193.05798	CH_2O	-114.33926
6	-193.05928	$[CH_2OH]^+$	-114.60786
7	-193.09717	H_2O	-76.33232
TS:7→4	-193.06035	$[CH_2CHCH_2]^+$	-116.70832

Table A1.2. GAUSSIAN Archive Entries of MP2(full)/6-31G(d) Optimized Geometries for Chapter 3

(1)

```
1\1\ ANU-PC\FOpt\RMP2-FU\6-31G(d)\C3H7O1(1+)\AJC501\31-Oct-1996\0\\#MP
2=FULL 6-31G* OPT TEST FREQ=NORAMAN MAXDISK=250000000\\ethoxymethyl ca
tion C1\\1,1\C,0.7146207273,0.2115154058,-1.5363309508\C,0.8124803684,
0.2241815402,-0.0374144755\H,1.7337747943,0.2496662661,-1.9316557665\H
,0.24129576,-0.7003891359,-1.9029196028\H,0.174743008,1.0852216546,-1.
9028659868\H,1.2363652869,1.1402557709,0.3715994743\H,1.280674521,-0.6
59644936,0.4004505227\O,-0.6098230408,0.2694506455,0.5031901759\C,-1.0
660497102,-0.6421046939,1.221745318\H,-2.09696363,-0.5282863159,1.5498
137239\H,-0.4576137263,-1.5039819813,1.5020568776\\Version=SGI-G94RevD
.3\HF=-192.2480738\MP2=-192.8152071\RMSD=4.328e-09\RMSF=6.196e-06\Dipo
le=-0.3796569,-0.7522371,1.0860193\PG=C01 [X(C3H7O1)]\\@
```

(TS:1→2)

```
1\1\GINC-RSCQC9\FTS\RMP2-FU\6-31G(d)\C3H7O1(1+)\ACHALK\30-May-1996\1\\
#MP2=FULL 6-31G* FREQ=NORAMAN TEST OPT=(CALCFC,NORAMAN,EF,TS,Z-MATRIX)
 MAXDISK=750000000 GEOM=MODIFY\\CH3CH2OCH2+ -> [CH2CH2 HOCH2+] ts\\1,1
\C\H,1,B1\C,2,B2,1,A1\H,1,B3,2,A2,3,D1,0\H,1,B4,2,A3,4,D2,0\H,3,B5,2,A
4,1,D3,0\H,3,B6,2,A5,6,D4,0\O,2,B7,1,A6,3,D5,0\C,8,B8,1,A7,2,D6,0\H,9,
B9,8,A8,2,D7,0\H,9,B10,8,A9,10,D8,0\\B1=1.67423559\B2=1.16423481\B3=1.
08590053\B4=1.08589935\B5=1.08722185\B6=1.08721897\B7=2.03406864\B8=1.
2301672\B9=1.09651106\B10=1.09731749\A1=55.43325236\A2=110.83216464\A3
=110.8210685\A4=106.09171582\A5=106.09947454\A6=82.74025682\A7=154.163
41875\A8=120.86345107\A9=121.41311459\D1=-114.12842331\D2=-131.7326524
6\D3=-117.23390627\D4=-125.53101192\D5=180.02096771\D6=-180.63893945\D
7=-1.09635341\D8=-179.98382823\\Version=IBM-RS6000-G94RevD.1\HF=-192.2
025461\MP2=-192.7623552\RMSD=2.642e-09\RMSF=1.444e-05\Dipole=0.6062245
,0.0032742,-0.5761928\PG=C01 [X(C3H7O1)]\\@
```

(TS:1→10)

```
1\1\GINC-VPP01\FTS\RMP2-FU\6-31G(d)\C3H7O1(1+)\AJC501\02-May-1997\1\\#
MP2=(FULL,FULLDIRECT) 6-31G* OPT=(CALCFC,TS,EF,NORAMAN) FREQ=NORAMAN T
EST MAXDISK=34078720\\CH3CHOHCH2+ -> CH3CH2OCH2+ ts\\1,1\H\C,1,B1\H,2,
B2,1,A1\C,2,B3,1,A2,3,D1,0\H,2,B4,1,A3,3,D2,0\O,4,B5,2,A4,1,D3,0\H,4,B
6,2,A5,6,D4,0\H,6,B7,4,A6,2,D5,0\C,6,B8,4,A7,8,D6,0\H,9,B9,6,A8,4,D7,0
\H,9,B10,6,A9,10,D8,0\\B1=1.09313005\B2=1.09282617\B3=1.47150063\B4=1.
09926756\B5=1.45881092\B6=1.09160778\B7=1.09424131\B8=1.38369203\B9=1.
08076091\B10=1.08546084\A1=109.32304853\A2=108.62223286\A3=108.1557952
1\A4=113.77241348\A5=125.9118509\A6=74.00904944\A7=127.00071324\A8=112
.74467464\A9=115.56760238\D1=-123.13543498\D2=118.06871152\D3=160.4688
4285\D4=145.74630012\D5=-95.39612705\D6=-117.98020546\D7=151.47398448\
D8=-156.73042077\\Version=Fujitsu-VP-Unix-G94RevD.4\HF=-192.002084\MP2
=-192.6434356\RMSD=5.999e-09\RMSF=3.192e-05\Dipole=-0.0943766,-0.70255
63,-0.1370473\PG=C01 [X(C3H7O1)]\\@
```

(2)

```
1\1\GINC-RSCQC8\FOpt\RMP2-FU\6-31G(d)\C3H7O1(1+)\ACHALK\27-Nov-1995\0\
\#MP2=FULL 6-31G* OPT=CALCFC TEST FREQ MAXDISK=1000000000\\ethylene +
protonated formaldehyde complex\\1,1\C,-1.8066061124,0.,-0.4144749071\
H,0.135008511,0.,-0.3510929397\C,-1.4106431787,0.,0.8748543244\H,-2.00
25020811,-0.9262197058,-0.9474561081\H,-2.0025020811,0.9262197058,-0.9
474561081\H,-1.2955079215,0.9278348148,1.4288822089\H,-1.2955079215,-0
.9278348148,1.4288822089\O,1.1287022838,0.,-0.7055624272\C,1.996724467
7,0.,0.1922848989\H,3.0347247631,0.,-0.1307871455\H,1.7198174017,0.,1.
247541404\\Version=IBM-RS6000-G94RevD.1\State=1-A'\HF=-192.2074084\MP2
=-192.7783592\RMSD=4.699e-09\RMSF=7.037e-06\Dipole=1.5827793,0.,0.5354
384\PG=CS [SG(C3H3O1),X(H4)]\\@
```

(TS:2→3)

```
1\1\GINC-RSCQC2\FTS\RMP2-FU\6-31G(d)\C3H7O1(1+)\ACHALK\09-May-1996\1\\
#MP2=FULL 6-31G* OPT=(TS,CALCFC,EF,Z-MATRIX) TEST FREQ MAXDISK=7500000
00\\CH2CH2 HOCH2+ -> CH2CH2 CH2OH+ ts\\1,1\C\C,1,B1\H,1,B2,2,A1\H,1,B3
```

,2,A2,3,D1,0\H,2,B4,1,A3,3,D2,0\H,2,B5,1,A4,5,D3,0\C,1,B6,2,A5,3,D4,0\
O,7,B7,1,A6,2,D5,0\H,7,B8,1,A7,8,D6,0\H,7,B9,1,A8,8,D7,0\H,8,B10,7,A9,
1,D8,0\\B1=1.34326654\B2=1.08659954\B3=1.08632468\B4=1.08758723\B5=1.0
8624456\B6=3.01964667\B7=1.25783802\B8=1.08658605\B9=1.08498886\B10=0.
99342053\A1=121.42155735\A2=121.61285074\A3=121.39158558\A4=121.720458
46\A5=87.47787701\A6=93.50549846\A7=113.00892279\A8=66.43217771\A9=113
.15791026\D1=-174.05115188\D2=173.45400294\D3=-173.84652285\D4=91.9288
1951\D5=61.03808423\D6=119.39370468\D7=-123.39787182\D8=-59.59717971\\
Version=IBM-RS6000-G94RevD.1\HF=-192.1969268\MP2=-192.7610822\RMSD=9.4
73e-09\RMSF=4.092e-06\Dipole=0.2914417,-1.787622,0.0573967\PG=C01 [X(C
3H7O1)]\\@

(3)

1\1\ ANU-VP\Freq\RMP2-FU\6-31G(d)\C3H7O1(1+)\AJC501\10-Aug-1995\0\\#MP
2=(FULL,FULLDIRECT) 6-31G* FREQ TEST SCF=DIRECT GEOM=ALLCHECK\\CH2CH2.
.H2C=OH+\\1,1\C,0.5078100753,-0.4434881979,-1.1316489885\C,1.282903683
,0.1593627513,-0.1743777854\H,0.6706344625,-1.4822565307,-1.405082568\
H,-0.2138543369,0.1232643691,-1.7127273832\H,1.2250276428,1.2297112453
,-0.0020813364\H,2.0847713141,-0.3842748462,0.3169876856\C,-0.40869646
42,-0.3856351363,0.5843019792\O,-1.2822161335,0.636325999,0.5228874311
\H,-0.847946342,-1.3224907607,0.2395082024\H,0.1431051264,-0.553099939
6,1.5129357085\H,-1.0961125633,1.3171019678,1.19770901\\Version=Fujits
u-VP-Unix-G94RevB.1\HF=-192.2032182\MP2=-192.7779041\RMSD=4.684e-09\RM
SF=1.385e-05\Dipole=0.855604,-0.2541863,0.3338929PG=C01 [X(C3H7O1)]\\@

(TS:3→4)

1\1\ ANU-PC\FTS\RMP2-FU\6-31G(d)\C3H7O1(1+)\AJC501\22-May-1996\1\\#MP2
=FULL 6-31G* TEST FREQ=NORAMAN OPT=(TS,EF,Z-MATRIX,READFC)\\[CH2CH2 CH
2OH+] -> CH3CHCH2OH+ ts\\1,1\C\C,1,B1\C,2,B2,1,A1\H,1,B3,2,A2,3,D1,0\H
,1,B4,2,A3,4,D2,0\H,2,B5,1,A4,3,D3,0\H,2,B6,1,A5,3,D4,0\H,3,B7,2,A6,1,
D5,0\H,3,B8,2,A7,8,D6,0\O,3,B9,2,A8,8,D7,0\H,10,B10,3,A9,2,D8,0\\B1=1.
39622629\B2=1.60411634\B3=1.09068118\B4=1.09009005\B5=1.08858982\B6=1.
13119217\B7=1.09401064\B8=1.09187665\B9=1.38519613\B10=0.97307527\A1=1
18.3083845\A2=120.27199486\A3=123.19613768\A4=116.30293172\A5=96.84335
398\A6=106.05550516\A7=108.21647481\A8=109.23147125\A9=110.5713435\D1=
37.52158726\D2=-182.89593038\D3=142.03700984\D4=-101.54964872\D5=80.74
492064\D6=-117.90794594\D7=123.48840427\D8=263.66076473\\Version=SGI-G
94RevD.1\HF=-192.1902129\MP2=-192.7516252\RMSD=8.261e-09\RMSF=2.609e-0
5\Dipole=-0.8412466,0.6865241,-1.8053307\PG=C01 [X(C3H7O1)]\\@

(TS:3→7)

1\1\ ANU-PC\FTS\RMP2-FU\6-31G(d)\C3H7O1(1+)\AJC501\22-May-1996\1\\#MP2
=FULL 6-31G* TEST FREQ=NORAMAN OPT=(TS,EF,Z-MATRIX,READFC)\\[CH2CH2 CH
2OH+] -> CH3CHCH2OH+ ts\\1,1\C\C,1,B1\C,2,B2,1,A1\H,1,B3,2,A2,3,D1,0\H
,1,B4,2,A3,4,D2,0\H,2,B5,1,A4,3,D3,0\H,2,B6,1,A5,3,D4,0\H,3,B7,2,A6,1,
D5,0\H,3,B8,2,A7,8,D6,0\O,3,B9,2,A8,8,D7,0\H,10,B10,3,A9,2,D8,0\\B1=1.
39622629\B2=1.60411634\B3=1.09068118\B4=1.09009005\B5=1.08858982\B6=1.
13119217\B7=1.09401064\B8=1.09187665\B9=1.38519613\B10=0.97307527\A1=1
18.3083845\A2=120.27199486\A3=123.19613768\A4=116.30293172\A5=96.84335
398\A6=106.05550516\A7=108.21647481\A8=109.23147125\A9=110.5713435\D1=
37.52158726\D2=-182.89593038\D3=142.03700984\D4=-101.54964872\D5=80.74
492064\D6=-117.90794594\D7=123.48840427\D8=263.66076473\\Version=SGI-G
94RevD.1\HF=-192.1902129\MP2=-192.7516252\RMSD=8.261e-09\RMSF=2.609e-0
5\Dipole=-0.8412466,0.6865241,-1.8053307\PG=C01 [X(C3H7O1)]\\@

(TS:3→9)

1\1\ ANU-PC\FTS\RMP2-FU\6-31G(d)\C3H7O1(1+)\AJC501\12-May-1996\1\\#MP2
=FULL 6-31G* OPT=(CALCFC,TS,NORAMAN,EF) FREQ=NORAMAN TEST\\protonated
oxetane -> [CH2CH2 CH2OH]+ ts\\1,1\C\C,1,B1\C,2,B2,1,A1\O,1,B3,2,A2,3,
D1,0\H,1,B4,2,A3,4,D2,0\H,1,B5,2,A4,4,D3,0\H,3,B6,2,A5,1,D4,0\H,3,B7,2
,A6,7,D5,0\H,2,B8,1,A7,3,D6,0\H,2,B9,1,A8,3,D7,0\H,4,B10,1,A9,2,D8,0\\
B1=2.21932508\B2=1.41373521\B3=1.41776966\B4=1.09366231\B5=1.09507364\
B6=1.0924436\B7=1.08728991\B8=1.08956037\B9=1.08644548\B10=0.97715975\
A1=46.58194764\A2=76.41120429\A3=95.41825587\A4=142.90821799\A5=115.50
283808\A6=115.43297903\A7=102.48454421\A8=116.76190852\A9=110.3935968\
D1=133.83684501\D2=112.59544807\D3=-112.49623998\D4=108.88520522\D5=13
7.7080282\D6=120.60416298\D7=-110.27157504\D8=-203.19699998\\Version=S
GI-G94RevD.1\HF=-192.2005377\MP2=-192.7614552\RMSD=9.027e-09\RMSF=3.93

9e-05\Dipole=0.1440294,0.6451305,0.4939219\PG=C01 [X(C3H7O1)]\\@

(4)

1\1\GINC-RSCQC9\FOpt\RMP2-FU\6-31G(d)\C3H7O1(1+)\ACHALK\03-Jun-1996\1\
\#MP2=FULL 6-31G* OPT=Z-MATRIX TEST FREQ=NORAMAN MAXDISK=37500000\\CH3
CHCH2OH+\\1,1\C\C,1,CC1\C,2,CC2,1,CCC\O,3,CO,2,OCC,1,0.,0\H,1,CH1,2,HC
C1,3,0.,0\H,1,CH2,2,HCC2,3,HCCC,0\H,1,CH2,2,HCC2,3,-HCCC,0\H,2,CH3,3,H
CC3,1,180.,0\H,3,CH4,2,HCC4,1,HCCC2,0\H,3,CH4,2,HCC4,1,-HCCC2,0\H,4,OH
,3,HOC,2,180.,0\\CC1=1.43396794\CC2=1.44113744\CO=1.38442302\CH1=1.086
1627\CH2=1.10626131\CH3=1.09220682\CH4=1.11582707\OH=0.97432145\CCC=12
5.17947207\OCC=111.84696091\HOC=110.38314636\HCC1=114.13721041\HCC2=10
7.66141088\HCC3=115.89566511\HCC4=104.8545196\HCCC=125.46959387\HCCC2=
126.1063454\\Version=IBM-RS6000-G94RevD.1\State=1-A'\HF=-192.2230498\M
P2=-192.7836815\RMSD=3.846e-09\RMSF=6.400e-05\Dipole=-1.0631558,0.,0.6
637272\PG=CS [SG(C3H3O1),X(H4)]\\@

(TS:4→5)

1\1\ ANU-PC\FTS\RMP2-FU\6-31G(d)\C3H7O1(1+)\AJC501\29-Apr-1996\1\\#MP2
=FULL 6-31G* TEST OPT=(CALCFC,TS,EF,Z-MATRIX) FREQ GEOM=ALLCHECK\\CH3C
HCH2OH+ -> CH2CHCH2OH2+ ts\\1,1\C\C,1,B1\C,2,B2,1,A1\O,3,B3,2,A2,1,D1,
0\H,1,B4,2,A3,3,D2,0\H,1,B5,2,A4,5,D3,0\H,2,B6,1,A5,3,D4,0\H,3,B7,2,A6
,4,D5,0\H,3,B8,2,A7,4,D6,0\H,4,B9,3,A8,2,D7,0\H,4,B10,3,A9,10,D8,0\\B1
=1.36814306\B2=1.5003092\B3=1.45841727\B4=1.0934598\B5=1.08386908\B6=1
.08892261\B7=1.09489737\B8=1.09121428\B9=1.43797194\B10=0.98135007\A1=
117.88700028\A2=100.36901697\A3=122.21808765\A4=119.6583766\A5=121.172
41844\A6=112.74589036\A7=111.79920941\A8=88.0643288\A9=112.91080251\D1
=26.32961851\D2=30.30441846\D3=163.62567511\D4=-191.74505961\D5=-115.9
9706245\D6=119.07729146\D7=8.82410578\D8=131.12179776\\Version=SGI-G94
RevD.1\HF=-192.1715726\MP2=-192.7583534\RMSD=7.157e-09\RMSF=9.979e-06\
Dipole=-0.1877788,0.3774158,0.3264983\PG=C01 [X(C3H7O1)]\\@

(5)

1\1\GINC-RSCQC2\FOpt\RMP2-FU\6-31G(d)\C3H7O1(1+)\ACHALK\06-May-1996\0\
\#MP2=FULL 6-31G* OPT TEST FREQ MAXDISK=750000000\\protonated allyl al
cohol.\\1,1\C,1.7882008287,-0.3156311425,-0.1692486226\C,0.7374892518,
0.2078973227,0.4825352632\C,-0.4539334235,0.6491639851,-0.2557530871\O
,-1.6314475445,-0.3906790371,-0.0551576857\H,1.7933266676,-0.436988322
9,-1.2491929659\H,2.6868090468,-0.6123132389,0.3600537826\H,0.76430196
59,0.3595832852,1.5582832327\H,-0.9315081401,1.5657413289,0.0877096929
\H,-0.3560925334,0.6383157268,-1.3397128742\H,-2.0436976417,-0.3247208
304,0.8386978752\H,-1.292098951,-1.3127666432,-0.1597785784\\Version=I
BM-RS6000-G94RevD.1\HF=-192.2289976\MP2=-192.8040402\RMSD=3.918e-09\RM
SF=9.957e-05\Dipole=-1.1322816,-0.5316568,0.3590069\PG=C01 [X(C3H7O1)]
\\@

(TS:5→6)

1\1\ ANU-PC\FTS\RMP2-FU\6-31G(d)\C3H7O1(1+)\AJC501\15-May-1996\1\\#MP2
=FULL 6-31G* TEST FREQ OPT=(CALCFC,TS,EF)\\CH2CHCH2OH2+ -> [CH2CHCH2 O
H2]+ ts\\1,1\C\C,1,B1\C,2,B2,1,A1\O,3,B3,2,A2,1,D1,0\H,1,B4,2,A3,3,D2,
0\H,1,B5,2,A4,5,D3,0\H,2,B6,1,A5,3,D4,0\H,3,B7,2,A6,4,D5,0\H,3,B8,2,A7
,4,D6,0\H,4,B9,3,A8,2,D7,0\H,4,B10,3,A9,10,D8,0\\B1=1.37889942\B2=1.38
315049\B3=2.79916022\B4=1.085583\B5=1.08696308\B6=1.08465876\B7=1.0871
9785\B8=1.08295786\B9=0.97266116\B10=0.9722025\A1=117.14329204\A2=92.7
2121465\A3=120.582391\A4=121.7501881\A5=121.44398797\A6=121.63560689\A
7=120.85404695\A8=130.24540506\A9=118.79841173\D1=48.80222521\D2=0.226
4136\D3=-178.26572267\D4=177.58190906\D5=127.34795977\D6=-53.02530772\
D7=-144.25162009\D8=215.73924543\\Version=SGI-G94RevD.1\HF=-192.221784
8\MP2=-192.7798785\RMSD=3.065e-09\RMSF=7.004e-06\Dipole=-0.2002443,-0.
2249362,0.0839301\PG=C01 [X(C3H7O1)]\\@

(6)

1\1\GINC-RSCQC8\FOpt\RHF\6-31G(d)\C3H7O1(1+)\ACHALK\15-Dec-1995\1\\#HF
6-31G* FOPT=Z-MATRIX TEST FREQ MAXDISK=37500000\\[CH2CHCH2+ H2O] comp
lex\\1,1\C\C,1,CC\H,2,CH1,1,HCC1\C,2,CC,3,HCC1,1,180.,0\H,1,HC1,2,HCC2
,3,180.,0\H,1,HC2,2,HCC3,3,0.,0\H,4,HC1,2,HCC2,3,180.,0\H,4,HC2,2,HCC3
,3,0.,0\X,2,1.,3,90.,1,90.,0\O,2,OC,9,90.,3,180.,0\H,10,OH,2,OHC,9,0.,
0\H,10,OH,2,OHC,9,180.,0\\CC=1.37383339\CH1=1.0734354\HC1=1.07697864\H

C2=1.07566109\HCC1=121.37175939\HCC2=120.69469512\HCC3=121.21702775\OH
=0.9506901\OHC=127.35925925\OC=3.71740446\\Version=IBM-RS6000-G94RevD.
1\State=1-A1\HF=-192.228274\RMSD=3.198e-09\RMSF=2.225e-05\Dipole=0.212
462,0.,0.1295437\PG=C02V [C2(H1C1O1),SGV(C2H4),SGV'(H2)]\\@

(7)

1\1\GINC-PC\FOpt\RMP2-FU\6-31G(d)\C3H7O1(1+)\AJC501\01-Apr-1997\0\\#MP
2=FULL 6-31G* OPT TEST FREQ=NORAMAN MAXDISK=5242880000\\CH3CH2CHOH+\\1
,1\C,-0.8766820746,0.,-1.2921203743\C,-0.9213741888,0.,0.2284902384\C,
0.3612197039,0.,0.9109639846\O,1.4380600528,0.,0.2332820765\H,-1.89678
52824,0.,-1.676374695\H,-0.3691152017,-0.8869448434,-1.6740703597\H,-0
.3691152017,0.8869448434,-1.6740703597\H,-1.4713432869,0.8618585207,0.
6467224584\H,-1.4713432869,-0.8618585207,0.6467224584\H,0.4308562279,0
.,2.0022362727\H,2.2633849667,0.,0.7785745202\\Version=SGI-G94RevD.4\S
tate=1-A'\HF=-192.2634818\MP2=-192.8323147\RMSD=4.324e-09\RMSF=5.835e-
05\Dipole=0.8432463,0.,1.5706714\PG=CS [SG(C3H3O1),X(H4)]\\@

(TS:7→4)

1\1\GINC-VPP09\PTS\RMP2-FU\6-31G(d)\C3H7O1(1+)\AJC501\08-Apr-1997\1\\#
MP2=FULL 6-31G* TEST OPT=(NOFREEZE,TS,CALCALL,NORAMAN,Z-MATRIX,NOEIGEN
) MAXDISK=34078720 GEOM=CHECK GUESS=CHECK\\CH3CHCH2OH+ -> CH3CH2CHOH+
ts\\1,1\C\C,1,CC1\X,2,XC,1,XCC\H,3,HX,2,90.,1,HXCC,0\C,3,CX,4,CXH,2,CX
CC,0\O,5,CO,2,OCC,1,OCCC,0\H,6,OH,5,HOC,2,HOCC,0\H,2,CH1,5,HCC1,6,HCCO
,0\H,1,CH2,2,HCC2,5,HCCC,0\H,1,CH3,2,HCC3,5,HCCC2,0\H,1,CH4,2,HCC4,5,H
CCC3,0\H,5,CH5,2,HCC5,1,HCCC4,0\\CH5=1.09952856\HCC5=114.74900049\HCCC
4=-148.8372782\CXCC=179.8591456\CXH=125.88774038\CC1=1.43969197\XC=1.4
1456728\HX=1.14289819\CX=0.01446667\CO=1.37424036\OH=0.97485485\CH1=1.
09174182\CH2=1.08936918\CH3=1.11602189\CH4=1.09140759\XCC=123.55131791
\OCC=113.7385992\HOC=110.6509516\HCC1=116.09552996\HCC2=114.24303286\H
CC3=101.10351082\HCC4=113.1263863\HXCC=107.02645257\OCCC=-9.04763745\H
OCC=177.75392607\HCCO=173.94596359\HCCC=206.02485665\HCCC2=91.31219042
\HCCC3=-20.51087687\\Version=Fujitsu-VP-Unix-G94RevD.4\HF=-192.2210575
\MP2=-192.7843092\RMSD=9.267e-09\RMSF=2.703e-07\Dipole=-0.7919193,0.17
44898,0.7545186\Polar=38.5469568,-0.1093384,25.4540817,6.3326526,2.796
4006,40.9153872\PG=C01 [X(C3H7O1)]\\@

(8)

1\1\GINC-RSCQC8\FOpt\RMP2-FU\6-31G(d)\C3H7O1(1+)\ACHALK\11-Jul-1996\0\
\#MP2=FULL 6-31G* OPT FREQ=NORAMAN TEST MAXDISK=1000000000\\CH3CHOCH3+
\\1,1\C,-0.5322626082,0.,-1.8068745632\C,-0.5398811333,0.,-0.346271927
9\O,0.546136189,0.,0.2906021329\C,0.5745789848,0.,1.7748765285\H,0.480
2348504,0.,-2.2069952364\H,-1.0935227041,-0.8759552934,-2.1576881575\H
,-1.0935227041,0.8759552934,-2.1576881575\H,-1.4765505583,0.,0.2204698
901\H,-0.4454262293,0.,2.1567434282\H,1.1225431865,-0.8989177357,2.044
9804726\H,1.1225431865,0.8989177357,2.0449804726\\Version=IBM-RS6000-G
94RevD.1\State=1-A'\HF=-192.267175\MP2=-192.8333907\RMSD=2.952e-09\RMS
F=1.325e-04\Dipole=-0.6256075,0.,0.3160508\PG=CS [SG(C3H3O1),X(H4)]\\@

(TS:8→1a)

1\1\GINC-VPP10\Freq\RMP2-FU\6-31G(d)\C3H7O1(1+)\AJC501\11-Dec-1996\1\\
MP2=FULL 6-31G* OPT=(CALCALL,Z-MATRIX,EF,TS,NORAMAN) TEST MAXDISK=33
750000 FREQ=NORAMAN OPTCYC=99\\CH3CHOCH3+ -> CH3CH2OCH2+ ts\\1,1\C\C,1
,B1\H,1,B2,2,A1\H,1,B3,2,A2,3,D1,0\H,1,B4,2,A3,3,D2,0\H,2,B5,1,A4,3,D3
,0\H,2,B6,1,A5,6,D4,0\O,2,B7,1,A6,6,D5,0\C,8,B8,2,A7,1,D6,0\H,9,B9,8,A
8,2,D7,0\H,9,B10,8,A9,10,D8,0\\B1=1.50239016\B2=1.09119308\B3=1.092134
39\B4=1.09102351\B5=1.1535887\B6=1.09034021\B7=1.51336811\B8=1.3148326
9\B9=1.09401841\B10=1.09436782\A1=108.16995757\A2=109.44429686\A3=111.
37914961\A4=109.35118719\A5=121.12331954\A6=110.02172286\A7=79.6194490
3\A8=119.24189999\A9=119.28393984\D1=-119.21492143\D2=119.84177494\D3=
180.47099724\D4=-119.47156\D5=118.36239407\D6=-116.68498927\D7=94.3196
8266\D8=165.53061014\\Version=Fujitsu-VP-Unix-G94RevD.4\HF=-192.173142
7\MP2=-192.7461848\RMSD=9.073e-09\RMSF=9.718e-06\Dipole=-1.1955307,0.1
48143,0.6849505\PG=C01 [X(C3H7O1)]\\@

(TS:8→1b)

1\1\GINC-VPP05\FTS\RMP2-FU\6-31G(d)\C3H7O1(1+)\AJC501\29-Apr-1997\1\\#
MP2=(FULL,FULLDIRECT) OPT=(CALCFC,TS,EF,NORAMAN) FREQ=NORAMAN TEST MAX

DISK=34078720 OPTCYC=80 6-31G* GEOM=CHECK GUESS=CHECK\\1,2 1,4 CH3CHOC
H3+-> CH3CH2OCH2+ ts\\1,1\O\C,1,B1\H,2,B2,1,A1\C,2,B3,1,A2,3,D1,0\H,2,
B4,1,A3,3,D2,0\H,4,B5,2,A4,1,D3,0\C,1,B6,2,A5,3,D4,0\H,4,B7,2,A6,6,D5,
0\H,7,B8,1,A7,2,D6,0\H,7,B9,1,A8,9,D7,0\H,7,B10,1,A9,9,D8,0\\B1=1.4007
9889\B2=1.10981199\B3=1.47466981\B4=1.09866033\B5=1.08994402\B6=1.4138
2676\B7=1.09216753\B8=1.09606968\B9=1.16746966\B10=1.08891155\A1=111.3
8615841\A2=104.1937869\A3=113.77297269\A4=117.09181487\A5=103.07915416
\A6=123.93172606\A7=113.49349552\A8=106.65941499\A9=110.62135135\D1=-1
14.271631\D2=122.34174898\D3=40.68595781\D4=170.48921354\D5=165.893279
99\D6=71.51496053\D7=-114.26860459\D8=128.55887672\\Version=Fujitsu-VP
-Unix-G94RevD.4\HF=-192.1567971\MP2=-192.7158442\RMSD=3.560e-09\RMSF=1
.146e-05\Dipole=-0.5928369,-0.9636816,1.4165568\PG=C01 [X(C3H7O1)]\\@

(9)

1\1\ ANU-PC\FOpt\RMP2-FU\6-31G(d)\C3H7O1(1+)\AJC501\08-May-1996\0\\#MP
2=FULL 6-31G* OPT FREQ TEST\\protonated oxetane\\1,1\C,1.0703536971,-0
.0311247055,0.0901872606\C,-1.0703536971,-0.0311247055,0.0901872606\C,
0.,-1.1057813263,-0.0778914166\O,0.,1.0298965515,-0.1877499529\H,1.442
4323784,0.111203138,1.1046617665\H,1.8497883282,0.0771732413,-0.660077
8097\H,0.,-1.8885316176,0.679765791\H,0.,-1.5490321491,-1.0730541584\H
,-1.4424323784,0.111203138,1.1046617665\H,-1.8497883282,0.0771732413,-
0.6600778097\H,0.,1.8298230197,0.39122145\\Version=SGI-G94RevD.1\State
=1-A'\HF=-192.2362528\MP2=-192.809752\RMSD=1.966e-09\RMSF=1.610e-05\Di
pole=0.,0.532701,0.5637524\PG=CS [SG(C1H3O1),X(C2H4)]\\@

(10)

1\1\GINC-VPP04\FOpt\RMP2-FU\6-31G(d)\C3H7O1(1+)\AJC501\01-May-1997\0\\
#MP2=FULL 6-31G* OPT FREQ=NORAMAN TEST MAXDISK=34078720\\CH3CHOHCH2+\\
1,1\H,-0.1647585863,2.3777205848,-1.3060669591\C,0.3597299956,1.695819
1015,-0.6315618744\H,1.3395229226,1.491290834,-1.079239425\C,-0.463308
8609,0.4778041647,-0.5015738227\H,0.5040457329,2.2125966628,0.32654237
43\O,0.201909132,-0.6121656214,0.1506074264\H,-1.5189843916,0.43868351
47,-0.2439734954\H,1.180079375,-0.615067574,-0.0219527028\C,-0.2332316
751,-1.648785404,0.9800449519\H,0.3666397232,-2.544105618,0.8823543115
\H,-1.3009545895,-1.6128206062,1.1560209563\\Version=Fujitsu-VP-Unix-G
94RevD.4\HF=-192.0260346\MP2=-192.6751915\RMSD=6.585e-09\RMSF=6.981e-0
5\Dipole=0.3481168,-0.6835675,0.2061348\PG=C01 [X(C3H7O1)]\\@

(TS:10→11)

1\1\GINC-VPP04\FTS\RMP2-FU\6-31G(d)\C3H7O1(1+)\AJC501\01-May-1997\1\\#
MP2=(FULL,FULLDIRECT) 6-31G* TEST OPT=(CALCFC,TS,EF,NORAMAN) MAXDISK=3
4078720 FREQ=NORAMAN\\protonated methyloxirane -> CH3CHOHCH2+ ts\\1,1\
H\C,1,B1\H,2,B2,1,A1\C,2,B3,1,A2,3,D1,0\H,2,B4,1,A3,3,D2,0\O,4,B5,2,A4
,1,D3,0\H,4,B6,2,A5,6,D4,0\H,6,B10,4,A6,2,D5,0\C,6,B7,4,A7,8,D6,0\H,9,
B8,6,A8,4,D7,0\H,9,B9,6,A9,10,D8,0\\B10=0.98820559\B1=1.0933016\B2=1.0
9474807\B3=1.4682096\B4=1.10007222\B5=1.45405207\B6=1.08857215\B7=1.40
388963\B8=1.08409101\B9=1.08157812\A1=108.83052349\A2=108.1737868\A3=1
07.82407592\A4=115.13533218\A5=126.93632704\A6=120.9587996\A7=115.4435
0538\A8=115.95519604\A9=110.99772565\D1=-121.43004748\D2=117.05220133\
D3=173.42824428\D4=139.923278\D5=-81.1979344\D6=196.15947831\D7=113.49
322177\D8=-154.60595038\\Version=Fujitsu-VP-Unix-G94RevD.4\HF=-192.030
5582\MP2=-192.6692764\RMSD=3.293e-09\RMSF=1.034e-05\Dipole=-0.0492169,
-0.5420865,0.6322988\PG=C01 [X(C3H7O1)]\\@

(11)

1\1\GINC-PC\FOpt\RMP2-FU\6-31G(d)\C3H7O1(1+)\AJC501\22-Apr-1997\0\\#MP
2=FULL 6-31G* OPT FREQ=NORAMAN TEST MAXDISK=5242880000\\protonated met
hyloxirane\\1,1\H,-1.4145800249,-0.2421625833,-1.2827010502\C,-1.52455
74641,-0.1715622979,-0.1975457511\C,-0.2461200116,0.1761158983,0.48024
55275\H,-1.939981576,-1.0987319924,0.2023076363\H,-2.2384618241,0.6314
038043,0.0154671309\C,0.8786680791,0.8029961262,-0.2089371041\O,0.9921
623086,-0.6848807265,0.0876394793\H,-0.2396609753,0.2152512148,1.56560
03314\H,0.7987806795,-1.2214367081,-0.7217947968\H,1.6437542083,1.3310
613009,0.3480334359\H,0.8049074239,1.0183624163,-1.2706045553\\Version
=SGI-G94RevD.4\HF=-192.2258722\MP2=-192.804608\RMSD=7.017e-09\RMSF=8.9
05e-05\Dipole=0.1572701,0.1371309,-0.4493109\PG=C01 [X(C3H7O1)]\\@

(TS:11→7)

1\1\GINC-VPP05\FTS\RMP2-FU\6-31G(d)\C3H7O1(1+)\AJC501\22-Apr-1997\0\\#
MP2=(FULL,FULLDIRECT) 6-31G* OPT=(CALCFC,TS,NORAMAN,ADDREDUNDANT,NOEIG
EN) MAXDISK=35389440 FREQ=NORAMAN\\protonated methyloxirane -> CH3CHCH
2OH+ ts\\1,1\H,-1.9229890762,0.0890160984,-1.2217199764\C,-1.837267160
8,0.0138706157,-0.1391884758\C,-0.5149030525,0.0522100037,0.3954311419
\H,-2.4892494148,-0.7369501134,0.3171743936\H,-2.2033651353,0.98032507
37,0.3069161412\C,0.725587824,0.4588040514,-0.2986653893\O,1.660111948
5,-0.5071591093,0.1607967785\H,-0.3617446007,-0.2203985941,1.441745925
6\H,1.8209577049,-1.1613405718,-0.5437885023\H,1.0238127768,1.45905573
24,0.0538907937\H,0.6111764922,0.4982572238,-1.3860566647\\Version=Fuj
itsu-VP-Unix-G94RevD.4\HF=-192.2108051\MP2=-192.7698275\RMSD=2.175e-09
\RMSF=3.211e-06\Dipole=-1.3697272,0.2075068,-0.3105628\PG=C01 [X(C3H7O
1)]\\@

(12)

1\1\GINC-PC\FOpt\RMP2-FU\6-31G(d)\C3H7O1(1+)\AJC501\12-Feb-1998\0\\#MP
2=FULL 6-31G* OPT TEST FREQ MAXDISK=5242880000\\protonated acetone\\1,
1\H,1.8112703576,-0.2244545577,-1.1053867157\H,1.9063150228,-0.4592108
76,0.681949813\C,-0.0234668563,-0.0052652822,-0.054979128\C,-0.7548276
256,0.0249350528,1.224054236\O,-0.6280653843,-0.1301597896,-1.17620111
89\H,1.6998392626,1.1571743409,0.0162506757\C,1.4398531907,0.099159233
9,-0.1335930709\H,-1.6120704118,-0.1727235471,-1.0977581425\H,-0.61512
78403,-0.9536557428,1.7053461685\H,-1.8235605286,0.2128408874,1.104400
4363\H,-0.3114950411,0.768333785,1.8919144939\\Version=SGI-G94RevE.2\H
F=-192.2857828\MP2=-192.8546031\RMSD=3.707e-09\RMSF=8.243e-06\Dipole=-
0.5537986,0.0040965,0.3673323\PG=C01 [X(C3H7O1)]\\@

(TS:12→7)

1\1\GINC-PC\FTS\RMP2-FU\6-31G(d)\C3H7O1(1+)\AJC501\12-Feb-1998\0\\#MP2
=FULL 6-31G* OPT=(CALCFC,TS,NOEIGEN) TEST FREQ=NORAMAN MAXDISK=5242880
000\\protonated acetone 1-2 H shift ts\\1,1\H,1.709698141,-0.121219291
3,1.1935929838\H,1.4341602464,1.5131629489,0.5425839684\H,-0.645659804
3,0.4222384127,1.1964244353\C,-0.2157425289,0.0283321161,0.2297422611\
O,-0.4372908843,-1.3083727419,-0.0167785062\H,1.8179675428,0.151269222
3,-0.5690944701\C,1.3160223843,0.4468780881,0.3507030537\H,0.012909754
,-1.8632541284,0.6463325618\C,-0.864243333,0.8559993358,-0.7043944788\
H,-1.4410414536,0.4402785882,-1.5323511884\H,-0.8059264861,1.937248942
8,-0.5995652574\\Version=SGI-G94RevE.2\HF=-192.1946203\MP2=-192.755271
5\RMSD=5.089e-09\RMSF=9.515e-06\Dipole=-0.2506147,1.1583415,0.0679429\
PG=C01 [X(C3H7O1)]\\@

$[CH_3CH_2]^+$

1\1\GINC-RSCQC9\FOpt\RMP2-FU\6-31G(d)\C2H5(1+)\ACHALK\26-Apr-1996\1\\#
N GEOM=ALLCHECK GUESS=READ TEST MP2(FULL)/6-31G(D) OPT=RCFC\\bridged p
rotonated ethylene G2\\1,1\C\X,1,hCC\H,2,HX,1,90.\C,2,hCC,3,90.,1,180.
,0\H,1,CH,2,HCX,3,HCXH,0\H,1,CH,2,HCX,3,-HCXH,0\H,4,CH,2,HCX,3,HCXH,0\
H,4,CH,2,HCX,3,-HCXH,0\\hCC=0.69019666\HX=1.10711372\CH=1.08778744\HCX
=120.6555792\HCXH=90.69164329\\Version=IBM-RS6000-G94RevD.1\State=1-A1
\HF=-78.3094956\MP2=-78.5614493\RMSD=3.264e-09\RMSF=1.163e-05\Dipole=0
.3365187,0.,0.\PG=C02V [C2(H1),SGV(C2),X(H4)]\\@

CH_2O

1\1\GINC-RSCQC9\FOpt\RMP2-FU\6-31G(d)\C1H2O1\ACHALK\26-Apr-1996\0\\#N
GEOM=ALLCHECK GUESS=READ TEST MP2(FULL)/6-31G(D) OPT=RCFC\\formaldehyd
e / G2\\0,1\C,0.,0.,-0.5363605776\O,0.,0.,0.6834788192\H,0.9344720468,
0.,-1.1248335443\H,-0.9344720468,0.,-1.1248335443\\Version=IBM-RS6000-
G94RevD.1\State=1-A1\HF=-113.8637248\MP2=-114.1749576\RMSD=7.414e-09\R
MSF=2.037e-04\Dipole=0.,0.,-0.8944255\PG=C02V [C2(C1O1),SGV(H2)]\\@

CH_2CH_2

1\1\ ANU-PC\FOpt\RMP2-FU\6-31G(d)\C2H4\AJC501\29-Apr-1996\0\\#N GEOM=A
LLCHECK GUESS=READ TEST MP2(FULL)/6-31G(D) OPT=RCFC\\ethylene\\0,1\C,0
.,0.,-0.6674323544\C,0.,0.,0.6674323544\H,0.9229650954,0.,-1.237540812
1\H,-0.9229650954,0.,-1.2375408121\H,-0.9229650954,0.,1.2375408121\H,0
.9229650954,0.,1.2375408121\\Version=SGI-G94RevD.1\State=1-AG\HF=-78.0
310673\MP2=-78.2942862\RMSD=9.651e-09\RMSF=3.833e-05\Dipole=0.,0.,0.\P

G=D02H [C2"(C1.C1),SG(H4)]\\@

$[CH_2OH]^+$

1\1\GINC-RSCQC8\Freq\RMP2-FU\6-31G(d)\C1H3O1(1+)\ACHALK\28-Dec-1995\0\
\#MP2=FULL 6-31G* FREQ=NORAMAN TEST MAXDISK=37500000\\protonated forma
ldehyde\\1,1\C,0.0431713308,0.,-0.6293201055\O,0.0558055232,0.,0.62670
33421\H,1.0210304113,0.,-1.1038082556\H,-0.8886688515,0.,-1.1946993308
\H,-0.8378337301,0.,1.0608014821\\Version=IBM-RS6000-G94RevD.1\State=1
-A'\HF=-114.1546002\MP2=-114.4517952\RMSD=2.938e-09\RMSF=5.455e-05\Dip
ole=-0.6969613,0.,-0.5285295\PG=CS [SG(C1H3O1)]\\@

H_2O

1\1\GINC-RSCQC8\Freq\RMP2-FU\6-31G(d)\H2O1\ACHALK\28-Dec-1995\0\\#MP2=
FULL 6-31G* FREQ=NORAMAN TEST MAXDISK=37500000\\water\\0,1\O,0.,0.,0.1
192864545\H,0.,0.7631471968,-0.4771458179\H,0.,-0.7631471968,-0.477145
8179\\Version=IBM-RS6000-G94RevD.1\State=1-A1\HF=-76.009808\MP2=-76.19
92442\RMSD=9.400e-10\RMSF=1.993e-05\Dipole=0.,0.,-0.8655795\DipoleDeri
v=-0.7679748,0.,0.,0.,-0.4855011,0.,0.,0.,-0.3871408,0.3839874,0.,0.,0
.,0.2427505,0.0810407,0.,0.1103827,0.1935704,0.3839874,0.,0.,0.,0.2427
505,-0.0810407,0.,-0.1103827,0.1935704\Polar=2.8321445,0.,7.0595475,0.
,0.,5.2258129\PG=C02V [C2(O1),SGV(H2)]\\@

$[CH_2CHCH_2]^+$

1\1\GINC-RSCQC9\FOpt\RMP2-FU\6-31G(d)\C3H5(1+)\ACHALK\26-Apr-1996\1\\#
N GEOM=ALLCHECK GUESS=READ TEST MP2(FULL)/6-31G(D) OPT=RCFC\\ allyl c
ation\\1,1\C\C,1,CC\H,2,CH1,1,HCC1\C,2,CC,3,HCC1,1,180.,0\H,1,HC1,2,HC
C2,3,180.,0\H,1,HC2,2,HCC3,3,0.,0\H,4,HC1,2,HCC2,3,180.,0\H,4,HC2,2,HC
C3,3,0.,0\\CC=1.38237406\CH1=1.08503614\HC1=1.08821597\HC2=1.08725722\
HCC1=121.19578614\HCC2=121.01361136\HCC3=121.80839585\\Version=IBM-RS6
000-G94RevD.1\State=1-A1\HF=-116.1924969\MP2=-116.5576247\RMSD=3.505e-
09\RMSF=1.011e-05\Dipole=-0.1910957,0.,-0.1157125\PG=C02V [C2(C1H1),SG
V(C2H4)]\\@

$$\frac{d[\mathbf{1a}]}{dt} = -k_{12}[\mathbf{1a}] + k_{21}([\mathbf{2a}] + \frac{[\mathbf{2b}]}{2}) \quad \text{(A1.1)}$$

$$\frac{d[\mathbf{1b}]}{dt} = -k_{12}[\mathbf{1b}] + \frac{k_{21}[\mathbf{2b}]}{2} \quad \text{(A1.2)}$$

$$\frac{d[\mathbf{1c}]}{dt} = -k_{12}[\mathbf{1c}] + k_{21}[\mathbf{2c}] \quad \text{(A1.3)}$$

$$\frac{d[\mathbf{2a}]}{dt} = -(k_{21} + k_{23} + k_{2d})[\mathbf{2a}] + \frac{k_{12}[\mathbf{1a}]}{3} + k_{32}[\mathbf{3a}] \quad \text{(A1.4)}$$

$$\frac{d[\mathbf{2b}]}{dt} = -(k_{21} + k_{23} + k_{2d})[\mathbf{2b}] + k_{12}\left(\frac{2[\mathbf{1a}]}{3} + [\mathbf{1b}]\right) + k_{32}[\mathbf{3b}] \quad \text{(A1.5)}$$

$$\frac{d[\mathbf{2c}]}{dt} = -(k_{21} + k_{23} + k_{2d})[\mathbf{2c}] + k_{12}[\mathbf{1c}] + k_{32}[\mathbf{3c}] \quad \text{(A1.6)}$$

$$\frac{d[\mathbf{3a}]}{dt} = -(k_{32} + k_{37} + k_{3d})[\mathbf{3a}] + k_{73}[\mathbf{7d}] + k_{23}[\mathbf{2a}] \quad \text{(A1.7)}$$

$$\frac{d[3\mathrm{b}]}{dt} = -(k_{32} + k_{37} + k_{3d})[3\mathrm{b}] + k_{73}\left(\frac{2[7\mathrm{a}]}{3} + [7\mathrm{b}]\right) + k_{23}[2\mathrm{b}] \quad \text{(A1.8)}$$

$$\frac{d[\mathbf{3c}]}{dt} = -(k_{32} + k_{37} + k_{3d})[\mathbf{3c}] + k_{73}\left(\frac{[\mathbf{7a}]}{3} + [\mathbf{7c}]\right) + k_{23}[\mathbf{2c}] \quad \text{(A1.9)}$$

$$\frac{d[\mathbf{7a}]}{dt} = -(k_{73} + k_{7d})[\mathbf{7a}] + \frac{k_{37}}{2}([\mathbf{3b}] + [\mathbf{3c}]) \quad \text{(A1.10)}$$

$$\frac{d[\mathbf{7b}]}{dt} = -(k_{73} + k_{7d})[\mathbf{7b}] + \frac{k_{37}[\mathbf{3b}]}{2} \quad \text{(A1.11)}$$

$$\frac{d[\mathbf{7c}]}{dt} = -(k_{73} + k_{7d})[\mathbf{7c}] + \frac{k_{37}[\mathbf{3c}]}{2} \quad \text{(A1.12)}$$

$$\frac{d[\mathbf{7d}]}{dt} = -(k_{73} + k_{7d})[\mathbf{7d}] + k_{37}[\mathbf{3a}] + k_{12-7}[\mathbf{12d}] \quad \text{(A1.13)}$$

$$\frac{d[\mathbf{12d}]}{dt} = -k_{12-7}[\mathbf{7d}] \tag{A1.14}$$

$$\frac{d[C_2H_3D]}{dt} = k_{2d}[\mathbf{2b}] + k_{3d}[\mathbf{3b}] \tag{A1.15}$$

$$\frac{d[C_2H_4]}{dt} = k_{2d}([\mathbf{2a}] + [\mathbf{2c}]) + k_{3d}([\mathbf{3a}] + [\mathbf{3c}]) \tag{A1.16}$$

$$\frac{d[H_2O]}{dt} = k_{7d}\left(\frac{2[\mathbf{7a}]}{3} + [\mathbf{7b}] + [\mathbf{7c}]\right) \tag{A1.17}$$

$$\frac{d[HOD]}{dt} = k_{7d}\left(\frac{[\mathbf{7a}]}{3} + [\mathbf{7d}]\right) \tag{A1.18}$$

Appendix 2

Table A2.1. Total G2 Energies Relevant to the $[C_3H_8N]^+$ System from Chapter 4 (0 K, Hartree)

1	-173.25754	**TS:2→9**	-173.16951
TSa:1→2	-173.16818	**TS:2→2'**	-173.15529
TSb:1→2	-173.13797	**9**	-173.20971
2	-173.27215	**TS:1→10**	-173.14329
TS:1→3	-173.16432	**TS:2→10**	-173.15060
3	-173.22431	**10**	-173.24630
TS:3→4	-173.21736	**TS:10→5**	-173.19068
4	-173.21880	**TS:4→11**	-173.17135
TS:4→5	-173.18453	**11**	-173.24878
TS:4→6	-173.17272	$[CH_2NHCHCH_2]^+$	-172.04347
5	-173.26715	H_2	-1.16617
TS:5→6	-173.19770	$[CH_2NH_2]^+$	-94.79258
6	-173.19513	CH_2CH_2	-78.41652
TS:6→6'	236.4670742	NH_3	-56.45891
TS:6→7	-173.18461	$[CH_2CHCH_2]^+$	-116.70934
7	-173.25403	$[CH_3CH_2]^+$	-78.67288
TS:7→8	-173.18548	CH_2NH	-94.46461
8	-173.18724		

Table A2.2 Total G2 Energies Relevant to the $[C_3H_7S]^+$ System from Chapter 4 (0 K, Hartree)

12	-515.70142	**TS:16→18**	-515.64260
TSa:12→13	-515.63559	**TS:12→18**	-515.62791
TSb:12→13	-515.62270	**TS:13→18**	-515.64379
TS:12→14	-515.62365	**18**	-515.70914
13	-515.71687	**TS:18→19**	-515.64955
14	-515.65689	**19**	-515.68994
TS:14→15	-515.65112	**TS:19→20**	-515.65025
15	-515.65539	**20**	-515.65011
TS:15→16	-515.65418	**TS:15→21**	-515.64136
TS:15→17	-515.64080	**TS:17→21**	-515.64353
16	-515.70360	**21**	-515.70092
TS:16→17	-515.66536	CH_2S	-436.93501
17	-515.66602	H_2S	-398.93151
TS:17→17'	-515.63541	$[CH_2SH]^+$	-437.22472
TS:17→18	-515.66527		

Table A2.3 GAUSSIAN Archive Entries of MP2(full)/6-31G(d) Optimized Geometries Relevant to the $[C_3H_8N]^+$ system from Chapter 4

1

1\1\GINC-VPP06\FOpt\RMP2-FU\6-31G(d)\C3H8N1(1+)\AJC501\30-Oct-1996\1\\
#MP2=FULL 6-31G* FOPT=Z-MATRIX FREQ=NORAMAN TEST MAXDISK=35000000\\CH3
CH2NHCH2+ C1\\1,1\C\C,1,B1\N,2,B2,1,A1\C,3,B3,2,A2,1,D1,0\H,1,B4,2,A3,
3,D2,0\H,1,B5,2,A4,5,D3,0\H,1,B6,2,A5,5,D4,0\H,2,B7,1,A6,3,D5,0\H,2,B8
,1,A7,3,D6,0\H,3,B9,2,A8,4,D7,0\H,4,B10,3,A9,2,D8,0\H,4,B11,3,A10,11,D
9,0\\B1=1.51957155\B2=1.48120906\B3=1.28253069\B4=1.0917752\B5=1.09250
189\B6=1.09126715\B7=1.09142476\B8=1.09284491\B9=1.02551354\B10=1.0846
3002\B11=1.08497946\A1=110.12203976\A2=126.35739722\A3=108.50116689\A4
=111.63416506\A5=111.31501278\A6=112.51178881\A7=111.99957028\A8=115.8
5659659\A9=119.79425936\A10=119.37554087\D1=119.26256682\D2=179.092489
28\D3=-118.45816406\D4=119.07566079\D5=119.17520583\D6=-117.85425962\D
7=181.29591877\D8=180.99366649\D9=180.04779671\\Version=Fujitsu-VP-Uni
x-G94RevD.4\HF=-172.4672956\MP2=-173.0246944\RMSD=2.982e-09\RMSF=2.428
e-05\Dipole=0.9045749,0.0852006,0.9095973\PG=C01 [X(C3H8N1)]\\@

TSa:1→2

1\1\GINC-VPP01\FTS\RMP2-FU\6-31G(d)\C3H8N1(1+)\AJC501\16-May-1997\0\\#
MP2=FULL 6-31G* OPT=(TS,READFC,NOEIGEN,NOFREEZE) TEST FREQ=NORAMAN MAX
DISK=31457280 GEOM=CHECK GUESS=CHECK\\CH3CHNHCH3+\\1,1\H,-0.1329850304
,1.8231684807,0.1770047008\C,-0.2567718573,1.1392039088,-0.659886405\H
,1.0810520305,0.4910973692,-0.520178894\N,-1.0333631652,0.0150556867,-
0.4378366546\H,-0.0642969547,1.5165264113,-1.6668598941\H,-1.371465826
1,-0.3910523834,-1.3147617962\C,0.3825753553,-0.4155291062,-0.18267714
93\C,0.6772571514,-0.724021985,1.2606352686\H,0.7018621431,-1.10656729
58,-0.9662362551\H,0.318765976,0.076795709,1.9096801675\H,1.745909691,
-0.8766083722,1.4192083655\H,0.1363362308,-1.6366666313,1.5185699022\\
Version=Fujitsu-VP-Unix-G94RevE.2\HF=-172.3593612\MP2=-172.9252764\RMS
D=2.003e-09\RMSF=5.594e-06\Dipole=0.5764852,0.5352745,-1.1184356\PG=C0
1 [X(C3H8N1)]\\@

TSb:1→2

1\1\GINC-VPP09\FTS\RMP2-FU\6-31G(d)\C3H8N1(1+)\AJC501\22-Apr-1998\1\\#
MP2=FULL 6-31G* OPT=(TS,CALCFC,EF,Z-MATRIX) TEST FREQ=NORAMAN MAXDISK=
32768000\\CH3CHNHCH3+ 1-4 H shift TS\\1,1\N\C,1,B1\H,2,B2,1,A1\C,2,B3,
1,A2,3,D1,0\H,2,B4,1,A3,3,D2,0\H,4,B5,2,A4,1,D3,0\C,1,B6,2,A5,3,D4,0\H
,4,B7,2,A6,6,D5,0\H,7,B8,1,A7,2,D6,0\H,7,B9,1,A8,9,D7,0\H,7,B10,1,A9,9
,D8,0\H,1,B11,2,A10,7,D9,0\\B1=1.45006572\B2=1.10953197\B3=1.4663822\B
4=1.09985386\B5=1.08975775\B6=1.46269091\B7=1.09110286\B8=1.09878397\B
9=1.14699618\B10=1.09113707\B11=1.02016146\A1=112.77637206\A2=100.1629
5592\A3=117.05152581\A4=116.78166433\A5=103.22484127\A6=124.16553208\A
7=115.91191582\A8=105.18411158\A9=113.02920956\A10=113.734231\D1=-112.
17875485\D2=126.5887621\D3=47.66660095\D4=167.9141596\D5=169.89934233\
D6=64.7929676\D7=-114.77426139\D8=130.46425739\D9=122.47229358\\Versio
n=Fujitsu-VP-Unix-G94RevE.2\HF=-172.3441682\MP2=-172.8904822\RMSD=7.55
4e-09\RMSF=2.016e-05\Dipole=-0.3064964,-0.477508,1.0562542\PG=C01 [X(C
3H8N1)]\\@

2

1\1\GINC-VPP10\FOpt\RMP2-FU\6-31G(d)\C3H8N1(1+)\AJC501\15-May-1997\0\\
#MP2=FULL 6-31G* OPT FREQ=NORAMAN TEST MAXDISK=31457280\\CH3CHNHCH3+\\
1,1\C,-0.5774577773,0.,-1.8382369244\C,-0.5680051626,0.,-0.3627859435\
N,0.5072711676,0.,0.3468381095\C,0.5775122756,0.,1.8164459613\H,0.4251
298358,0.,-2.2684117973\H,-1.1280283638,-0.878354692,-2.1914834038\H,-
1.1280283638,0.878354692,-2.1914834038\H,-1.5083646523,0.,0.1861086921
\H,-0.4336181683,0.,2.2195501925\H,1.1134613292,-0.8932950838,2.137630
4767\H,1.1134613292,0.8932950838,2.1376304767\H,1.4027928671,0.,-0.149
94656\\Version=Fujitsu-VP-Unix-G94RevE.2\State=1-A'\HF=-172.4825658\MP
2=-173.0387657\RMSD=5.840e-09\RMSF=3.347e-05\Dipole=0.1616128,0.,0.095
4251\PG=CS [SG(C3H4N1),X(H4)]\\@

TS:1→3

1\1\ ANU-PC\FTS\RMP2-FU\6-31G(d)\C3H8N1(1+)\AJC501\09-Oct-1996\1\\#MP2
=FULL 6-31G* OPT=(CALCFC,Z-MATRIX,EF,NORAMAN,TS) FREQ=NORAMAN TEST MAX
DISK=250000000\\CH3CH2NHCH2+ -> [CH2CH2 H2NCH2]+ ts\\1,1\C\H,1,B1\C,2,
B2,1,A1\H,1,B3,2,A2,3,D1,0\H,1,B4,2,A3,4,D2,0\H,3,B5,2,A4,1,D3,0\H,3,B
6,2,A5,6,D4,0\N,2,B7,1,A6,3,D5,0\C,8,B8,2,A7,1,D6,0\H,9,B9,8,A8,2,D7,0
\H,9,B10,8,A9,10,D8,0\H,8,B11,9,A10,10,D9,0\\B1=1.53549026\B2=1.184112
63\B3=1.08447398\B4=1.08446751\B5=1.08602214\B6=1.08609862\B7=2.221777
07\B8=1.28500361\B9=1.08846741\B10=1.09014471\B11=1.02608309\A1=59.835
72726\A2=109.78383487\A3=110.0583078\A4=106.80373758\A5=106.64972173\A
6=84.37395548\A7=121.11280709\A8=119.20954421\A9=123.91336524\A10=110.
76660335\D1=-114.81776768\D2=-130.39722218\D3=-116.41912362\D4=-127.17
541618\D5=-179.65844319\D6=-247.50577514\D7=-30.50257731\D8=-180.02492
107\D9=179.93426905\\Version=SGI-G94RevD.3\HF=-172.366319\MP2=-172.916
7825\RMSD=4.513e-09\RMSF=1.354e-05\Dipole=0.7501372,0.1777146,-0.33603
78\PG=C01 [X(C3H8N1)]\\@

3

1\1\GINC-RSCQC9\FOpt\RHF\6-31G(d)\C3H8N1(1+)\ACHALK\08-Jun-1996\1\\#HF
6-31G* FOPT=Z-MATRIX FREQ=NORAMAN TEST OPTCYC=100 MAXDISK=37500000\\[
CH2CH2 NH2CH2+]\\1,1\C\X,1,hCC\H,2,HX,1,90.\C,2,hCC2,3,90.,1,180.,0\H,
1,CH1,2,HCX1,3,HCXH,0\H,1,CH1,2,HCX1,3,-HCXH,0\H,4,CH2,2,HCX2,3,HCXH1,
0\H,4,CH2,2,HCX2,3,-HCXH1,0\X,3,1.,2,90.,4,180.,0\N,3,HN,9,NHX,2,180.,
0\H,10,HN1,3,HNH,9,0.,0\C,10,CN,11,CNX,3,180.,0\H,12,CH3,10,HCN1,11,18
0.,0\H,12,CH4,10,HCN2,11,0.,0\\HN1=1.0047613\HNH=116.89070802\hCC=0.62
008747\hCC2=0.70505791\HX=2.3416134\HCX1=121.65389469\HCX2=121.5870759
5\NHX=92.31533757\CN=1.26102039\CH1=1.07643322\CH2=1.07667608\CH3=1.07
44472\CH4=1.07441492\HCN1=119.51199542\HCN2=120.27462311\HCXH=91.98525
558\HCXH1=92.32217133\CNX=121.4238736\HN=1.01702797\\Version=IBM-RS600
0-G94RevD.1\State=1-A'\HF=-172.4291924\RMSD=1.258e-09\RMSF=1.068e-05\D
ipole=2.7145959,0.,0.3494934\PG=CS [SG(C3H4N1),X(H4)]\\@

TS:3→4

1\1\GINC-RSCQC2\FTS\RMP2-FU\6-31G(d)\C3H8N1(1+)\ACHALK\31-Jul-1996\0\\
# MP2=FULL 6-31G* OPT=(TS,CALCFC,NORAMAN,NOEIGEN) TEST FREQ=NORAMAN MA
XDISK=750000000\\[CH2CH2 H2NCH2]+ -> [CH2CH2 CH2NH2]+ ts\\1,1\C,-0.275
9328232,1.8468529184,-0.5980889281\C,0.0767993561,2.0334592617,0.68098
96246\H,0.4661543888,1.7345345508,-1.3829897808\H,-1.3156276934,1.8742
704311,-0.91056629\H,-0.6627078985,2.2130807011,1.4554170263\H,1.11845
50968,2.0746286046,0.9844420511\C,-0.4267983359,-1.3993838701,0.003553
973\N,0.5544241385,-2.2217185992,-0.0719691911\H,-0.3831087627,-0.5638
545195,0.692424722\H,-1.2836965008,-1.5372171729,-0.6471267281\H,0.555
208107,-3.0043508932,-0.7293497267\H,1.3799451107,-2.1246313674,0.5228
050473\\Version=IBM-RS6000-G94RevD.1\HF=-172.4206156\MP2=-172.9713185\
RMSD=6.264e-09\RMSF=7.376e-07\Dipole=0.3368697,-3.1472094,-0.0805052\P
G=C01 [X(C3H8N1)]\\@

4

1\1\ ANU-PC\SP\RQCISD(T)-FC\6-311G(d,p)\C3H8N1(1+)\AJC501\29-Jun-1996\
0\\# QCISD(T,E4T) 6-311G** TEST\\[CH2CH2 CH2NH2]+ //MP2(fu)/6-31G*\\1,
1\C,0,0.8047072737,0.3962187954,-1.5025656867\C,0,1.5348518519,-0.4215
027977,-0.7270328961\H,0,-0.0144145632,0.0228818435,-2.1103497426\H,0,
1.0532127291,1.4478224583,-1.6119195327\H,0,2.4014789972,-0.0621598492
,-0.1798460434\H,0,1.3345474427,-1.4878840818,-0.6775255766\C,0,-0.586
9751056,0.453657115,1.0305848409\N,0,-1.5655406426,-0.3808810496,1.072
9212989\H,0,0.3134578016,0.2517546168,1.5956601089\H,0,-0.7083151885,1
.3948115591,0.510622702\H,0,-2.4403513054,-0.2076078621,0.5772632534\H
,0,-1.496335535,-1.2636900132,1.5797281893\\Version=SGI-G94RevD.1\HF=-
172.4729328\MP2=-173.0781515\MP3=-173.1182947\MP4D=-173.1339054\MP4DQ=
-173.1209508\MP4SDTQ=-173.149992\MP4SDQ=-173.1269609\QCISD=-173.129768
4\QCISD(T)=-173.1528383\RMSD=2.736e-09\PG=C01 [X(C3H8N1)]\\@

TS:4→5

1\1\GINC-RSCQC9\SP\RMP2-FC\6-311+G(3df,2p)\C3H8N1(1+)\ACHALK\09-May-19
97\0\\#MP2 6-311+G(3DF,2P) TEST GEOM=ALLCHECK GUESS=CHECK MAXDISK=1048
576000\\[CH2CH2 CH2NH2]+ -> CH3CH2CHNH2]+ ts\\1,1\C\C,1,1.4253788848\C
,2,1.588567929,1,72.5566009\H,3,1.1566437688,2,109.28721935,1,9.940020

68,0\N,3,1.413451149,2,110.90813364,4,-115.9410252,0\H,1,1.0870017321,
2,119.62448725,3,91.76332076,0\H,1,1.0881480884,2,120.69202504,6,167.1
4173322,0\H,2,1.0840913564,1,118.43002544,3,108.11484161,0\H,2,1.08474
23178,1,117.26391835,3,-103.68847615,0\H,3,1.097700623,2,106.28634375,
4,105.10413483,0\H,5,1.0169776744,3,113.45357937,2,171.66107593,0\H,5,
1.0164625026,3,112.48604658,11,125.25074937,0\\Version=IBM-RS6000-G94R
evE.1\HF=-172.4466339\MP2=-173.1563593\RMSD=4.360e-09\PG=C01 [X(C3H8N1
)]\\@

TS:4→6

1\1\ ANU-PC\SP\RMP2-FC\6-311+G(3df,2p)\C3H8N1(1+)\AJC501\09-Oct-1996\0
\\#MP2 6-311+G(3DF,2P) TEST MAXDISK=250000000\\[CH2CH2 CH2NH2]+ -> CH3
CHCH2NH2+ ts //MP2(fu)/6-31G*\\1,1\C\C,1,1.39700946\H,1,1.08913123,2,1
23.83613814\H,1,1.09098178,2,117.5524528,3,181.10026862,0\H,2,1.118424
28,1,100.13704243,3,112.92760634,0\H,2,1.08895356,1,116.88801271,5,-11
9.52476509,0\C,2,1.6250478,1,112.29475183,5,102.37954495,0\N,7,1.42640
659,2,109.55089996,1,-47.64633393,0\H,7,1.09184468,2,104.06618449,8,-1
23.79157077,0\H,7,1.09032218,2,105.98510078,8,121.69804312,0\H,8,1.015
32636,7,113.43439242,2,129.93085036,0\H,8,1.0157058,7,113.58149978,11,
124.94961713,0\\Version=SGI-G94RevD.3\HF=-172.4441308\MP2=-173.1362289
\RMSD=6.749e-09\PG=C01 [X(C3H8N1)]\\@

5

1\1\GINC-VPP02\FOpt\RMP2-FU\6-31G(d)\C3H8N1(1+)\AJC501\08-May-1997\1\\
#MP2=FULL 6-31G* OPT=Z-MATRIX FREQ=NORAMAN TEST MAXDISK=34078720\\CH3C
H2CHNH2+\\1,1\C\C,1,CC1\C,2,CC2,1,CCC\N,3,CN,2,NCC,1,0.,0\H,4,HN1,3,HN
C1,2,180.,0\H,4,HN2,3,HNC2,2,0.,0\H,3,CH1,2,HCC1,1,180.,0\H,2,CH2,3,HC
C2,1,HCCC1,0\H,2,CH2,3,HCC2,1,-HCCC1,0\H,1,CH3,2,HCC3,3,180.,0\H,1,CH4
,2,HCC4,3,HCCC2,0\H,1,CH4,2,HCC4,3,-HCCC2,0\\CC1=1.52214316\CC2=1.4754
7639\CN=1.28941981\HN1=1.02053322\HN2=1.02133153\CH1=1.08889909\CH2=1.
09966741\CH3=1.09044632\CH4=1.09358638\CCC=116.11008471\NCC=123.647527
51\HNC1=121.92900309\HNC2=121.15925994\HCC1=120.02017021\HCC2=106.0192
6504\HCC3=109.2197205\HCC4=111.90462657\HCCC1=124.80832521\HCCC2=61.73
586741\\Version=Fujitsu-VP-Unix-G94RevD.4\State=1-A'\HF=-172.4796594\M
P2=-173.0362175\RMSD=3.442e-09\RMSF=1.773e-05\Dipole=1.235595,0.,0.698
8779\PG=CS [SG(C3H4N1),X(H4)]\\@

TS:5→6

1\1\GINC-VPP03\FTS\RMP2-FU\6-31G(d)\C3H8N1(1+)\AJC501\13-May-1997\1\\#
MP2=FULL 6-31G* OPT=(Z-MATRIX,CALCFC,EF,TS) FREQ=NORAMAN TEST MAXDISK=
31457280\\CH3CH2CHNH2 -> CH3CHCH2NH2 ts (1-2 H shift)\\1,1\C\C,1,B1\C,
2,B2,1,A1\N,3,B3,2,A2,1,D1,0\H,1,B4,2,A3,3,D2,0\H,1,B5,2,A4,5,D3,0\H,1
,B6,2,A5,5,D4,0\H,2,B7,1,A6,3,D5,0\H,3,B8,2,A10,4,D6,0\H,3,B9,2,A7,4,D
7,0\H,4,B10,3,A8,2,D8,0\H,4,B11,3,A9,11,D9,0\\A10=89.94037364\B1=1.447
41249\B2=1.43119163\B3=1.41230544\B4=1.08985089\B5=1.0975703\B6=1.1066
324\B7=1.09152648\B8=1.15320119\B9=1.09770849\B10=1.01545579\B11=1.014
96504\A1=123.13558872\A2=118.2506727\A3=112.71673704\A4=109.21123591\A
5=108.06146574\A6=120.32260268\A7=112.65946286\A8=115.08695041\A9=112.
95077913\D1=-11.39006802\D2=166.04538074\D3=-127.53130104\D4=117.96106
141\D5=173.24827418\D6=120.98984003\D7=-137.51709373\D8=69.76103897\D9
=126.44465258\\Version=Fujitsu-VP-Unix-G94RevE.2\HF=-172.3990593\MP2=-
172.9491561\RMSD=2.412e-09\RMSF=3.288e-05\Dipole=-0.5591938,0.6483404,
0.438041\PG=C01 [X(C3H8N1)]\\@

6

1\1\GINC-RSCQC9\SP\RMP2-FC\6-311+G(3df,2p)\C3H8N1(1+)\ACHALK\14-Jun-19
96\0\\# MP2 6-311+G(3DF,2P) TEST GEOM=ALLCHECK GUESS=CHECK MAXDISK=100
0000000\\CH3CHCH2NH2+ //MP2(fu)/6-31G*\\1,1\C,0,-0.9570800936,0.003698
1957,-1.3274676747\C,0,-0.9450628324,0.0962284737,0.1190703197\C,0,0.2
521898978,0.0084000193,0.971683328\N,0,1.4774504579,-0.1369498647,0.25
12304021\H,0,-1.8974489435,-0.3649782077,-1.7157969766\H,0,-0.08385023
72,-0.4971380866,-1.7183134088\H,0,-0.8882739835,1.0609983136,-1.63364
70176\H,0,-1.8798357224,0.2715594844,0.6315034207\H,0,0.202679569,0.84
65687254,1.6729655751\H,0,0.034639171,-0.8599411427,1.6058933139\H,0,2
.006549485,0.7100981542,0.200241848\H,0,2.0631056257,-0.8584783197,0.6
188245928\\Version=IBM-RS6000-G94RevD.1\HF=-172.4724964\MP2=-173.15890
95\RMSD=5.709e-09\PG=C01 [X(C3H8N1)]\\@

TS:6→6'

1\1\GINC-VPP09\SP\RQCISD(T)-FC\6-31G(d,p)\C3H8N1(1+)\AJC501\23-Jun-199
8\0\\#QCISD(T,E4T) 6-31G** TEST GEOM=CHECK GUESS=CHECK MAXDISK=2097152
00\\CH2CH2CH2NH2+ ts //MP2(fu)/6-31G*\\1,1\H,-1.2845666204,-1.23123579
4,0.0470462452\C,-1.411059185,-0.2539232552,0.507207915\C,-0.297196173
3,0.604690436,0.7315920718\H,-2.4203936177,0.0474147076,0.7891007772\C
,0.9836263498,0.0388870266,0.1271145446\H,-0.3094982734,0.948229153,1.
787375072\H,-0.5891262868,1.5535324158,0.2230055167\H,1.3165874718,-0.
8267839393,0.7043579763\H,1.7858513418,0.7826983406,0.1558398872\N,0.5
760943007,-0.3987520253,-1.2089995694\H,1.1466001318,-1.172457661,-1.5
463156343\H,0.6696597986,0.3519417099,-1.8929000429\\Version=Fujitsu-V
P-Unix-G94RevE.2\HF=-172.3980033\MP2=-172.9724279\MP3=-173.0149263\MP4
D=-173.0283986\MP4DQ=-173.0179742\MP4SDTQ=-173.0396215\MP4SDQ=-173.022
4293\QCISD=-173.0261637\QCISD(T)=-173.0436488\RMSD=7.167e-09\PG=C01 [X
(C3H8N1)]\\@

TS:6→7

1\1\GINC-PC\SP\RMP2-FC\6-311+G(3df,2p)\C3H8N1(1+)\AJC501\07-Aug-1996\0
\\#MP2 6-311+G(3DF,2P) TEST\\CH3CHCH2NH2+ -> CH2CHCH2NH3+ ts //MP2(fu)
/6-31G*\\1,1\C\C,1,1.37963441\C,2,1.4880997,1,117.81058956\N,3,1.46408
691,2,106.85805506,1,14.86505651,0\H,1,1.09723088,2,119.97330024,3,46.
86509824,0\H,4,1.68438194,3,86.08456441,2,9.99053884,0\H,1,1.0841617,2
,119.20882763,5,148.5215896,0\H,2,1.08976727,1,122.03077241,3,-190.040
88205,0\H,3,1.09426329,2,109.2658491,4,120.66792444,0\H,3,1.10223512,2
,109.25902927,4,-123.35740068,0\H,4,1.02001352,3,112.56348033,6,128.13
599267,0\H,4,1.02014673,3,113.50291816,6,-109.55345667,0\\Version=SGI-
G94RevD.3\HF=-172.4376953\MP2=-173.1484912\RMSD=7.538e-09\PG=C01 [X(C3
H8N1)]\\@

7

1\1\GINC-RSCQC9\SP\RMP2-FC\6-311+G(3df,2p)\C3H8N1(1+)\ACHALK\08-Jul-19
96\0\\#MP2 6-311+G(3DF,2P) TEST GEOM=ALLCHECK GUESS=CHECK MAXDISK=5000
00000\\CH2CHCH2NH3+ //MP2(fu)/6-31G*\\1,1\H,0,0.1501329771,1.729521395
1,-1.4655814096\C,0,-0.425956393,0.8197109517,-1.6101717161\C,0,-0.264
9054671,-0.2553761605,-0.829493179\H,0,-1.1272135612,0.8125850429,-2.4
367239228\C,0,0.7128828186,-0.2734774324,0.2947782163\H,0,-0.827766361
1,-1.1669592831,-1.0191437232\N,0,-0.0433537167,-0.2575035854,1.622233
6863\H,0,1.3541639768,0.6095038043,0.3000211627\H,0,1.3340598001,-1.17
1573004,0.3149162774\H,0,0.5880365787,-0.2513425891,2.4351302957\H,0,-
0.6551623662,-1.0795421908,1.7085446578\H,0,-0.6449007782,0.5751877701
,1.6765209303\\Version=IBM-RS6000-G94RevD.1\HF=-172.5237017\MP2=-173.2
266741\RMSD=9.850e-09\PG=C01 [X(C3H8N1)]\\@

TS:7→8

1\1\GINC-RSCQC2\SP\RMP2-FC\6-311+G(3df,2p)\C3H8N1(1+)\ACHALK\14-Oct-19
96\0\\#MP2 6-311+G(3DF,2P) TEST MAXDISK=750000000\\[CH2CHCH2NH3+ -> [C
H2CHCH2 NH3]+ ts//MP2(fu)/6-31G*\\1,1\H,0,0.,0.,0.\C,0,0.,0.,1.087346\
C,0,1.186759,0.,1.784694\H,0,-0.963916,0.00901,1.589166\C,0,2.355809,-
0.034441,1.038287\H,0,1.204219,0.02124,2.869158\N,0,2.565651,1.808169,
-1.300103\H,0,2.334972,-0.020457,-0.048086\H,0,3.330767,-0.033465,1.52
0065\H,0,3.567693,1.940012,-1.437114\H,0,2.205842,2.731043,-1.057508\H
,0,2.19626,1.610582,-2.230159\\Version=IBM-RS6000-G94RevD.4\HF=-172.46
43537\MP2=-173.1474495\RMSD=8.748e-09\PG=C01 [X(C3H8N1)]\\@

8

1\1\GINC-PC\SP\RMP2-FC\6-311+G(3df,2p)\C3H8N1(1+)\AJC501\07-Aug-1996\0
\\#MP2 6-311+G(3DF,2P) TEST\\[CH2CHCH2 NH3]+ //MP2(fu)/6-31G*\\1,1\C\N
,1,3.89154567\C,1,1.38327994,2,56.1673879\C,1,1.38205105,2,59.05396782
,3,180.,0\H,1,1.0847897,3,122.42624199,4,180.,0\H,3,1.08713997,1,121.8
6545608,4,180.,0\H,3,1.09236498,1,118.65411557,6,180.,0\H,4,1.0870232,
1,122.05638093,3,180.,0\H,4,1.09041251,1,118.76587872,8,180.,0\H,2,1.0
2077824,1,115.56438954,3,0.,0\H,2,1.02034856,1,112.73902706,3,120.4421
7411,0\H,2,1.02034856,1,112.73902706,3,-120.44217411,0\\Version=SGI-G9
4RevD.3\State=1-A'\HF=-172.4668199\MP2=-173.150239\RMSD=7.384e-09\PG=C
S [SG(C3H6N1),X(H2)]\\@

TS:2→9

1\1\GINC-VPP07\FTS\RMP2-FU\6-31G(d)\C3H8N1(1+)\AJC501\20-May-1997\0\\#
MP2=(FULL,FULLDIRECT) 6-31G* TEST OPT=(CALCFC,TS,NOEIGEN) FREQ=NORAMAN
MAXDISK=30146560\\CH3CHNHCH3+ H2 elimination ts\\1,1\H,-2.098079675,-
0.4270856158,-1.3449832789\H,-1.0036381581,1.0403569151,-1.1915006362\
C,1.2982627823,0.6302064232,0.1353140376\N,0.4466775988,-0.1742457394,
0.7962708655\H,0.8423320438,-0.7961513812,1.5041212682\C,-0.7790168087
,-0.5123167266,0.3072022331\H,-1.2570753202,-1.3597135312,0.7857687914
\C,-1.2306865776,0.0260757518,-0.8766528822\H,1.0919183344,-0.02638738
,-1.2980179594\H,0.9110663706,1.5492625347,-0.2911611876\H,2.332159407
8,0.6226447178,0.4647446822\H,0.3232174285,-0.2469987736,-1.5980480694
\\Version=Fujitsu-VP-Unix-G94RevE.2\HF=-172.3286096\MP2=-172.9170004\R
MSD=5.821e-09\RMSF=2.091e-05\Dipole=0.4034028,-0.1074093,0.2771647\PG=
C01 [X(C3H8N1)]\\@

TS:2→2'

1\1\GINC-VPP10\SP\RMP2-FC\6-311+G(3df,2p)\C3H8N1(1+)\AJC501\02-Jul-199
8\0\\# MP2 6-311+G(3DF,2P) TEST GEOM=ALLCHECK GUESS=CHECK MAXDISK=2228
22400\\CH3CHCH2NH2+ //MP2(fu)/6-31G*\\1,1\H,-1.0760022382,0.2208449403
,-2.1992652285\C,-0.0244067011,0.1674039977,-1.9141590423\C,0.39447375
8,0.0101368634,-0.5802705429\H,0.7197413962,0.226976993,-2.7065758618\
H,1.1119342366,0.8740530958,-0.4647127027\N,-0.5388990088,-0.068397045
,0.4654243248\C,0.0415983574,-0.0410313556,1.8139879812\H,1.2167118295
,-0.7727696076,-0.6540533529\H,0.7383749442,-0.8665020567,2.0045118118
\H,-0.7748674604,-0.092676453,2.532737729\H,0.5578169347,0.9094451754,
1.9619392658\H,-1.1914090668,-0.8396498046,0.3500976889\\Version=Fujit
su-VP-Unix-G94RevE.2\HF=-172.4255672\MP2=-173.1139975\RMSD=4.657e-09\P
G=C01 [X(C3H8N1)]\\@

9

1\1\GINC-VPP07\FOpt\RMP2-FU\6-31G(d)\C3H8N1(1+)\AJC501\19-May-1997\0\\
#MP2=FULL 6-31G* OPT=CALCFC TEST FREQ=NORAMAN GEOM=CHECK GUESS=CHECK M
AXDISK=31457280\\CH2CHNHCH2 H2]+\\1,1\H,-2.0599158973,-0.6026208281,-1
.0006232952\H,-2.7116985257,0.4949005807,0.3420016104\C,1.6967278767,-
0.4143963941,0.181154256\N,0.4682535676,-0.4834068808,-0.2069545472\H,
0.2601307199,-1.0537466062,-1.0341280055\C,-0.6443130484,0.1603940017,
0.398402439\H,-0.4055344594,0.7537383236,1.2736561117\C,-1.8647588498,
0.0033023259,-0.1206160985\H,0.845840485,2.7360526527,-0.7169126702\H,
1.9471702423,0.182274193,1.0515755457\H,2.4591255402,-0.953518026,-0.3
686827886\H,1.2611710508,3.3309682747,-0.8518482568\\Version=Fujitsu-V
P-Unix-G94RevE.2\HF=-172.3961182\MP2=-172.9614655\RMSD=5.892e-09\RMSF=
9.824e-08\Dipole=0.7890136,-0.6385312,-0.1528302\PG=C01 [X(C3H8N1)]\\@

TS:1→10

1\1\GINC-PC\SP\RMP2-FC\6-311+G(3df,2p)\C3H8N1(1+)\AJC501\08-Jul-1998\0
\\#MP2 6-311+G(3DF,2P) TEST GEOM=ALLCHECK GUESS=CHECK MAXDISK=52428800
00\\CH3CH2NHCH2+ -> CH3CH(NH2)CH2+\\1,1\H,1.9504950391,1.356820553,-0.
3822013269\C,1.0073966312,1.2241032815,0.1484053493\H,1.2233440316,0.9
159688381,1.1744815255\C,0.1395938267,0.2030135721,-0.5602923572\H,0.4
757017619,2.1769193234,0.178971219\N,-0.2188422578,-1.3333649353,0.090
2278629\H,-0.2400558824,0.3397320517,-1.5773795983\C,-1.1235348031,-0.
2884730342,0.2545177165\H,0.429707429,-1.3947389535,0.8919509133\H,-2.
0364469032,-0.373583388,-0.324690109\H,-1.1846240088,0.2143824801,1.21
6827273\H,0.7730404084,-0.7338092738,-0.8653391884\\Version=SGI-G94Rev
E.2\HF=-172.3951872\MP2=-173.1118672\RMSD=6.202e-09\PG=C01 [X(C3H8N1)]
\\@

TS:2→10

1\1\GINC-VPP06\FTS\RMP2-FU\6-31G(d)\C3H8N1(1+)\AJC501\23-Apr-1998\0\\#
MP2=FULL 6-31G* OPT=(TS,CALCFC,NOEIGEN) TEST FREQ MAXDISK=28835840\\CH
3CHNHCH3+ -> ? ts\\1,1\H,0.7504165409,1.2316104451,-1.2905007367\C,0.7
730825327,1.3444154497,-0.2049535431\H,1.8073268365,1.3592856751,0.144
239453\C,0.0167887299,0.236097546,0.4646132383\H,0.3061074481,2.297151
1286,0.0545848375\H,0.2699082192,-1.9722876986,0.7503451516\N,-1.12034
06633,-0.267525206,-0.1957397724\H,-0.0349079003,0.2443769878,1.552883
5858\H,-1.789206474,-0.6893887965,0.4690633835\H,-0.6538572307,-1.5021
680126,-0.7729497417\C,0.2450279372,-1.2307192143,-0.0412455129\H,0.97

72020045,-1.1946659757,-0.8479726205\\Version=Fujitsu-VP-Unix-G94RevE.
2\HF=-172.3305758\MP2=-172.904398\RMSD=6.013e-09\RMSF=1.383e-05\Dipole
=-0.218831,-1.1745067,0.4486031\PG=C01 [X(C3H8N1)]\\@

10

1\1\GINC-RSCQC8\FOpt\RMP2-FU\6-31G(d)\C3H8N1(1+)\ACHALK\08-Dec-1996\0\
\#MP2=FULL 6-31G* OPT FREQ=NORAMAN TEST MAXDISK=1048576000\\CH3CHNH2CH
2+ N in 3-mem ring\\1,1\H,-1.5507809504,0.1307094912,-1.1515260072\C,-
1.5588221974,0.1695692833,-0.0591035403\C,-0.170226679,0.1475866618,0.
5052464661\H,-2.1523864298,-0.6599181827,0.3298641377\H,-2.0396404105,
1.1040900015,0.2399458238\C,0.9963087892,0.6443578622,-0.2500394155\N,
0.7970230208,-0.8307555018,-0.1090725734\H,-0.0808245903,0.1507251408,
1.5880434187\H,1.8657861959,1.0215651984,0.2757338554\H,0.8544342773,1
.0069436399,-1.262243927\H,0.4882619806,-1.3551273795,-0.930422806\H,1
.4324293045,-1.3527822415,0.4974924563\\Version=IBM-RS6000-G94RevE.1\H
F=-172.4528892\MP2=-173.0169012\RMSD=3.131e-09\RMSF=2.834e-05\Dipole=0
.8684604,-0.6401693,-0.0532627\PG=C01 [X(C3H8N1)]\\@

TS:10→5

1\1\GINC-VPP02\FTS\RMP2-FU\6-31G(d)\C3H8N1(1+)\AJC501\12-May-1997\1\\#
 MP2=FULL 6-31G* OPT=(TS,CALCFC,Z-MATRIX,EF) TEST FREQ=NORAMAN MAXDISK
=31457280\\methylazarinium -> CH3CHCH2NH2+\\1,1\H\C,1,B1\C,2,B2,1,A1\H
,2,B3,1,A2,3,D1,0\H,2,B4,1,A3,3,D2,0\C,3,B5,2,A4,1,D3,0\N,6,B6,3,A5,2,
D4,0\H,3,B7,2,A6,6,D5,0\H,6,B8,3,A7,7,D6,0\H,6,B9,3,A8,7,D7,0\H,7,B10,
6,A9,3,D8,0\H,7,B11,6,A10,11,D9,0\\B1=1.09057965\B2=1.43287272\B3=1.11
929494\B4=1.0931802\B5=1.46899804\B6=1.44858518\B7=1.09126702\B8=1.107
07678\B9=1.0969534\B10=1.01501334\B11=1.01511858\A1=114.92812108\A2=10
7.21613156\A3=114.43320973\A4=126.38843995\A5=104.80690041\A6=119.1641
819\A7=104.75994853\A8=112.30531465\A9=112.05480234\A10=113.61090265\D
1=-110.58714108\D2=134.33496303\D3=-20.01938291\D4=-131.4649794\D5=186
.34160871\D6=-117.70353322\D7=127.26099761\D8=101.2123898\D9=124.53116
207\\Version=Fujitsu-VP-Unix-G94RevE.2\HF=-172.3995097\MP2=-172.944406
8\RMSD=7.520e-09\RMSF=1.080e-04\Dipole=-0.4875983,0.288823,-0.3097038\
PG=C01 [X(C3H8N1)]\\@

TS:4→11

1\1\GINC-RSCQC8\SP\RMP2-FC\6-311+G(3df,2p)\C3H8N1(1+)\ACHALK\30-May-19
96\0\\#MP2 6-311+G(3DF,2P) TEST MAXDISK=1000000000\\[CH2CH2 CH2NH2]+ -
> protonated azetidine ts //MP2(fu)/6-31G*\\1,1\N,0,0.,0.,0.\C,0,0.,0.
,2.452545\H,0,1.043653,0.,2.761743\C,0,-0.676282,-1.19822,2.216613\H,0
,-0.448129,0.968998,2.263248\C,0,0.056866,-1.26834,0.703615\H,0,-1.753
946,-1.144335,2.085213\H,0,-0.314481,-2.093223,2.719848\H,0,-0.511768,
-2.10893,0.285111\H,0,0.708876,0.033821,-0.73095\H,0,1.092098,-1.57411
5,0.850973\H,0,-0.904337,0.148485,-0.445405\\Version=IBM-RS6000-G94Rev
D.1\HF=-172.4441527\MP2=-173.1391228\RMSD=4.239e-09\PG=C01 [X(C3H8N1)]
\\@

11

1\1\GINC-RSCQC8\SP\RMP2-FC\6-311+G(3df,2p)\C3H8N1(1+)\ACHALK\05-May-19
96\0\\# MP2 6-311+G(3DF,2P) TEST MAXDISK=1000000000\\protonated azetid
ine //MP2(fu)/6-31G*\\1,1\N,0,-0.116244514,0.,-1.0313424609\C,0,0.1201
115,1.0672852749,0.0376734941\H,0,1.1542463625,1.4029161364,-0.0390863
53\C,0,-0.111989539,0.,1.1181549489\H,0,-0.564809677,1.910078125,-0.04
67956676\C,0,0.1201115,-1.0672852749,0.0376734941\H,0,-1.1365887154,0.
,1.4933606736\H,0,0.5812742527,0.,1.9579088157\H,0,1.1542463625,-1.402
9161364,-0.039086353\H,0,0.5059394101,0.,-1.8490534866\H,0,-0.56480967
7,-1.910078125,-0.0467956676\H,0,-1.0851874855,0.,-1.372066358\\Versio
n=IBM-RS6000-G94RevD.1\State=1-A'\HF=-172.5193383\MP2=-173.2250428\RMS
D=9.757e-09\PG=CS [SG(C1H4N1),X(C2H4)]\\@

$[CH_2NHCHCH_2]^+$

1\1\GINC-VPP09\FOpt\RMP2-FU\6-31G(d)\C3H6N1(1+)\AJC501\16-May-1997\0\\
#MP2=FULL 6-31G* OPT TEST FREQ=NORAMAN MAXDISK=28835840\\CH2N=NHCH=CH2
+\\1,1\C,-0.5882110724,0.,-1.717862972\C,-0.6574721657,0.,-0.38415319\
N,0.5366850306,0.,0.3843525489\C,0.6198279436,0.,1.672018207\H,-1.5008
299045,0.,-2.301167281\H,0.3516669242,0.,-2.2620066514\H,1.4128119758,
0.,-0.1494804364\H,-0.2889854515,0.,2.2641772014\H,1.5965026754,0.,2.1

412525148\H,-1.5728296662,0.,0.1967445404\\Version=Fujitsu-VP-Unix-G94
RevE.2\State=1-A'\HF=-171.2692625\MP2=-171.8166999\RMSD=2.674e-09\RMSF
=1.487e-04\Dipole=0.659172,0.,0.7037411\PG=CS [SG(C3H6N1)]\\@

H_2

1\1\GINC-PC\FOpt\RMP2-FU\6-31G(d)\H2\AJC501\17-Apr-1997\0\\#MP2=FULL 6
-31G* OPT FREQ=NORAMAN TEST MAXDISK=5242880000\\H2\\0,1\H,0.,0.,-0.368
7587189\H,0.,0.,0.3687587189\\Version=SGI-G94RevD.4\State=1-SGG\HF=-1.
1267865\MP2=-1.1441408\RMSD=2.175e-12\RMSF=1.631e-06\Dipole=0.,0.,0.\P
G=D*H [C*(H1.H1)]\\@

$[NH_2CH_2]^+$

1\1\GINC-PC\FOpt\RMP2-FU\6-31G(d)\C1H4N1(1+)\AJC501\08-Aug-1996\0\\# M
P2=FULL 6-31G* OPT FREQ=NORAMAN TEST\\H2NCH2+\\1,1\C,0.,0.,-0.67902047
96\N,0.,0.,0.6025303682\H,0.9440825154,0.,-1.2131250064\H,-0.944082515
4,0.,-1.2131250064\H,0.8697900717,0.,1.1413301564\H,-0.8697900717,0.,1
.1413301564\\Version=SGI-G94RevD.3\State=1-A1\HF=-94.38198\MP2=-94.667
5883\RMSD=1.826e-09\RMSF=6.598e-05\Dipole=0.,0.,0.2096114\PG=C02V [C2(
C1N1),SGV(H4)]\\@

CH_2CH_2

1\1\ ANU-PC\FOpt\RMP2-FU\6-31G(d)\C2H4\AJC501\29-Apr-1996\0\\#N GEOM=A
LLCHECK GUESS=READ TEST MP2(FULL)/6-31G(D) OPT=RCFC\\ethylene\\0,1\C,0
.,0.,-0.6674323544\C,0.,0.,0.6674323544\H,0.9229650954,0.,-1.237540812
1\H,-0.9229650954,0.,-1.2375408121\H,-0.9229650954,0.,1.2375408121\H,0
.9229650954,0.,1.2375408121\\Version=SGI-G94RevD.1\State=1-AG\HF=-78.0
310673\MP2=-78.2942862\RMSD=9.651e-09\RMSF=3.833e-05\Dipole=0.,0.,0.\P
G=D02H [C2"(C1.C1),SG(H4)]\\@

NH_3

1\1\GINC-RSCQC2\FOpt\RMP2-FU\6-31G(d)\H3N1\ACHALK\12-Jun-1998\0\\#MP2=
FULL 6-31G* OPT TEST FREQ=NORAMAN\\ammonia\\0,1\N,0.,0.,0.1163790655\H
,0.9398774093,0.,-0.2715511528\H,-0.4699387047,-0.8139577129,-0.271551
1528\H,-0.4699387047,0.8139577129,-0.2715511528\\Version=IBM-RS6000-G9
4RevE.1\HF=-56.183841\MP2=-56.3573778\RMSD=5.520e-09\RMSF=1.040e-05\Di
pole=0.,0.,-0.7729704\PG=C03V [C3(N1),3SGV(H1)]\\@

$[CH_2CHCH_2]^+$

1\1\GINC-RSCQC9\FOpt\RMP2-FU\6-31G(d)\C3H5(1+)\ACHALK\26-Apr-1996\1\\#
N GEOM=ALLCHECK GUESS=READ TEST MP2(FULL)/6-31G(D) OPT=RCFC\\ allyl c
ation\\1,1\C\C,1,CC\H,2,CH1,1,HCC1\C,2,CC,3,HCC1,1,180.,0\H,1,HC1,2,HC
C2,3,180.,0\H,1,HC2,2,HCC3,3,0.,0\H,4,HC1,2,HCC2,3,180.,0\H,4,HC2,2,HC
C3,3,0.,0\\CC=1.38237406\CH1=1.08503614\HC1=1.08821597\HC2=1.08725722\
HCC1=121.19578614\HCC2=121.01361136\HCC3=121.80839585\\Version=IBM-RS6
000-G94RevD.1\State=1-A1\HF=-116.1924969\MP2=-116.5576247\RMSD=3.505e-
09\RMSF=1.011e-05\Dipole=-0.1910957,0.,-0.1157125\PG=C02V [C2(C1H1),SG
V(C2H4)]\\@

$[CH_3CH_2]^+$

1\1\GINC-RSCQC9\FOpt\RMP2-FU\6-31G(d)\C2H5(1+)\ACHALK\26-Apr-1996\1\\#
N GEOM=ALLCHECK GUESS=READ TEST MP2(FULL)/6-31G(D) OPT=RCFC\\bridged p
rotonated ethylene G2\\1,1\C\X,1,hCC\H,2,HX,1,90.\C,2,hCC,3,90.,1,180.
,0\H,1,CH,2,HCX,3,HCXH,0\H,1,CH,2,HCX,3,-HCXH,0\H,4,CH,2,HCX,3,HCXH,0\
H,4,CH,2,HCX,3,-HCXH,0\\hCC=0.69019666\HX=1.10711372\CH=1.08778744\HCX
=120.6555792\HCXH=90.69164329\\Version=IBM-RS6000-G94RevD.1\State=1-A1
\HF=-78.3094956\MP2=-78.5614493\RMSD=3.264e-09\RMSF=1.163e-05\Dipole=0
.3365187,0.,0.\PG=C02V [C2(H1),SGV(C2),X(H4)]\\@

CH_2NH

1\1\GINC-PC\FOpt\RMP2-FU\6-31G(d)\C1H3N1\AJC501\20-May-1997\0\\#MP2=FU
LL 6-31G* OPT FREQ=NORAMAN TEST\\HNCH2\\0,1\C,-0.0252108465,0.,-0.5921
24359\N,-0.0923210977,0.,0.6869376981\H,0.8979735114,0.,-1.1802520705\
H,-0.9544563945,0.,-1.1600287548\H,0.8539956462,0.,1.0844630927\\Versi
on=SGI-G94RevD.4\State=1-A'\HF=-94.0265381\MP2=-94.3230775\RMSD=3.190e
-09\RMSF=6.785e-05\Dipole=0.6159582,0.,-0.5434578\PG=CS[SG(C1H3N1)]\\@

Table A2.4 GAUSSIAN Archive Entries of MP2(full)/6-31G(d) Optimized Geometries Relevant to the $[C_3H_7S]^+$ system from Chapter 4

12

1\1\GINC-PC\SP\RMP2-FC\6-311+G(3df,2p)\C3H7S1(1+)\AJC501\15-Apr-1998\0
\\#MP2 6-311+G(3DF,2P) TEST MAXDISK=5242880000\\CH3CH2SCH2+ (syn) //MP
2(fu)/6-31G*\\1,1\C,0,-0.8786911944,0.,-1.3407459614\S,0,-1.0030494678
,0.,0.2652518554\H,0,0.0731925673,0.,-1.8637565775\H,0,-1.803967745,0.
,-1.9126367426\C,0,0.6947632814,0.,0.9374359981\H,0,0.7131008403,0.882
1374982,1.5858628515\H,0,0.7131008403,-0.8821374982,1.5858628515\C,0,1
.834938587,0.,-0.0602725531\H,0,2.7640815729,0.,0.5144474946\H,0,1.841
6096826,0.8948385088,-0.6861572332\H,0,1.8416096826,-0.8948385088,-0.6
861572332\\Version=SGI-G94RevE.2\State=1-A'\HF=-514.9782591\MP2=-515.6
450953\RMSD=3.866e-09\PG=CS [SG(C3H3S1),X(H4)]\\@

TSa:12→13

1\1\GINC-VPP09\SP\RQCISD(T)-FC\6-311G(d,p)\C3H7S1(1+)\AJC501\25-Jun-19
97\0\\#QCISD(T,E4T) 6-311G** TEST GEOM=CHECK GUESS=CHECK MAXDISK=22282
2400\\CH3CH2SCH2+ -> CH3CHSCH3+ 1,3 TS//MP2(fu)/6-31G*\\1,1\C\C,1,1.51
66932996\H,1,1.0904308602,2,109.82640999\H,1,1.0913642543,2,110.091202
16,3,-119.72370597,0\H,1,1.0917118273,2,111.51199283,3,119.32344627,0\
H,2,1.1105426523,1,116.91046558,3,111.00897205,0\H,2,1.1098178682,1,11
6.55039905,6,-111.5661497,0\S,2,1.9759866796,1,115.68963694,6,151.8672
365,0\C,6,1.9186587934,2,63.49427408,1,112.18340086,0\H,9,1.0888332692
,6,107.1947411,2,-86.31987784,0\H,9,1.0891375319,6,82.90688389,10,-115
.76115088,0\\Version=Fujitsu-VP-Unix-G94RevE.2\HF=-514.8802103\MP2=-51
5.4661612\MP3=-515.5063293\MP4D=-515.522285\MP4DQ=-515.5080201\MP4SDTQ
=-515.5375435\MP4SDQ=-515.5127889\QCISD=-515.5136009\QCISD(T)=-515.537
9528\RMSD=3.862e-09\PG=C01 [X(C3H7S1)]\\@

TSb:12→13

1\1\GINC-VPP10\SP\RQCISD(T)-FC\6-311G(d,p)\C3H7S1(1+)\AJC501\22-Jun-19
97\0\\#QCISD(T,E4T) 6-311G** TEST GEOM=CHECK GUESS=CHECK MAXDISK=22937
6000\\CH3CH2SCH2+ -> CH3CHSCH3+ 1,2 1,4 TS//MP2(fu)/6-31G*\\1,1\S\C,1,
1.8248088126\H,2,1.0990169748,1,109.62753408\C,2,1.465244573,1,99.9863
5688,3,-114.73967848,0\H,2,1.0905378644,1,113.38247766,3,124.31705563,
0\H,4,1.0906585902,2,117.87780353,1,65.3209081,0\C,1,1.8240161507,2,87
.64460271,3,154.698601,0\H,4,1.0912402534,2,122.77542514,6,162.8239176
2,0\H,7,1.0914680779,1,113.49408973,2,73.19615216,0\H,7,1.1434835667,1
,110.2862756,9,-119.12750452,0\H,7,1.0932154523,1,112.30147446,9,128.1
0092874,0\\Version=Fujitsu-VP-Unix-G94RevE.2\HF=-514.8825888\MP2=-515.
4457793\MP3=-515.4924012\MP4D=-515.5074722\MP4DQ=-515.4946036\MP4SDTQ=
-515.5218412\MP4SDQ=-515.5001718\QCISD=-515.5017368\QCISD(T)=-515.5241
373\RMSD=3.066e-09\PG=C01 [X(C3H7S1)]\\@

TS:12→14

1\1\GINC-PC\FTS\RMP2-FU\6-31G(d)\C3H7S1(1+)\AJC501\14-Aug-1996\0\\#MP2
=FULL 6-31G* GEOM=ALLCHECK GUESS=CHECK OPT=(TS,CALCFC,NOEIGEN) TEST FR
EQ=NORAMAN\\CH3CH2SCH2+ -> [CH2CH2 HSCH2]+ ts\\1,1\C,1.3787550991,-1.1
34327961,-0.2820876929\H,1.7525792751,0.3516059792,-0.4590488517\C,2.5
679437002,-0.4915938382,-0.6161723545\H,0.661967008,-1.4190729825,-1.0
460391253\H,1.1132951791,-1.3182476562,0.7543426369\H,3.3227978927,-0.
3299958446,0.1487421335\H,2.8698274831,-0.4312193846,-1.6583990808\S,-
0.9274002293,0.8702671187,0.1833928022\C,-2.2049786472,-0.0490583583,0
.5560694636\H,-3.1684514762,0.4091941664,0.7720640185\H,-2.1639326057,
-1.1366572329,0.6071969364\\Version=SGI-G94RevD.3\HF=-514.8282323\MP2=
-515.344817\RMSD=2.988e-09\RMSF=3.093e-06\Dipole=1.9469466,-0.0529945,
-1.4442555\Polar=82.0862689,-0.3228798,29.0148224,-0.1521009,0.4413001
,44.3931357\PG=C01 [X(C3H7S1)]\\@

13

1\1\GINC-VPP11\SP\RQCISD(T)-FC\6-311G(d,p)\C3H7S1(1+)\AJC501\23-Jun-19
97\0\\#QCISD(T,E4T) 6-311G** TEST MAXDISK=222822400\\CH3CHSCH3+ //MP2(
fu)/6-31G*\\1,1\C\C,1,1.47530128\S,2,1.62620622,1,122.69961247\C,3,1.8
0716313,2,105.27950095,1,180.,0\H,1,1.09052915,2,113.50452213,3,0.,0\H
,1,1.09714494,2,108.65271907,3,122.40016674,0\H,1,1.09714494,2,108.652
71907,3,-122.40016674,0\H,2,1.0909854,1,118.72978082,3,180.,0\H,4,1.08
99845,3,110.69291192,2,0.,0\H,4,1.09105698,3,107.72576542,2,120.885796
06,0\H,4,1.09105698,3,107.72576542,2,-120.88579606,0\\Version=Fujitsu-
VP-Unix-G94RevE.2\State=1-A'\HF=-514.9733499\MP2=-515.5435209\MP3=-515
.5873299\MP4D=-515.6026028\MP4DQ=-515.589345\MP4SDTQ=-515.6189569\MP4S
DQ=-515.5959621\QCISD=-515.5981858\QCISD(T)=-515.621029\RMSD=2.994e-09
\PG=CS [SG(C3H3S1),X(H4)]\\@

14

1\1\GINC-PC\SP\RMP2-FC\6-311+G(3df,2p)\C3H7S1(1+)\AJC501\14-Apr-1998\0
\\#MP2 6-311+G(3DF,2P) TEST MAXDISK=5242880000\\[CH2CH2 HSCH2]+ //MP2(
fu)/6-31G*\\1,1\C,0,-2.0903692932,0.,-0.7970973142\H,0,0.0015462263,0.
,-0.5746163317\C,0,-2.0893045587,0.,0.5483559333\H,0,-2.1437102297,-0.
9257138786,-1.3634262541\H,0,-2.1437102297,0.9257138786,-1.3634262541\
H,0,-2.1284253108,0.9264526247,1.1143494994\H,0,-2.1284253108,-0.92645
26247,1.1143494994\S,0,1.3809493765,0.,-0.4770636607\C,0,1.4337998925,
0.,1.1382915155\H,0,0.522183607,0.,1.7336175841\H,0,2.40059498,0.,1.63
48700205\\Version=SGI-G94RevE.2\State=1-A'\HF=-514.9303309\MP2=-515.59
05706\RMSD=3.450e-09\PG=CS [SG(C3H3S1),X(H4)]\\@

TS:14→15

1\1\GINC-RSCQC9\SP\RMP2-FC\6-311+G(3df,2p)\C3H7S1(1+)\ACHALK\07-Jul-19
96\0\\#MP2 6-311+G(3DF,2P) TEST GEOM=ALLCHECK GUESS=CHECK MAXDISK=5000
00000\\[CH2CH2 HSCH2]+ -> [CH2CH2 CH2SH]+ ts //MP2(fu)/6-31G*\\1,1\C\H
,1,3.55199981\C,1,1.34082004,2,95.71654326\H,1,1.08592599,2,109.304435
56,3,-126.44346651,0\H,1,1.08624021,2,67.91891122,3,121.91003905,0\H,3
,1.08610099,1,121.70158477,2,67.61500081,0\H,3,1.08597501,1,121.525214
15,6,175.16392804,0\S,2,1.34712064,1,106.74404254,3,16.51633422,0\C,8,
1.61996487,2,98.17323724,1,34.84985666,0\H,9,1.08505853,8,122.57388292
,2,-0.75241875,0\H,9,1.08752927,8,117.51151821,10,181.18334842,0\\Vers
ion=IBM-RS6000-G94RevD.1\HF=-514.9298384\MP2=-515.5831318\RMSD=2.715e-
09\PG=C01 [X(C3H7S1)]\\@

15

1\1\GINC-RSCQC8\SP\RMP2-FC\6-311+G(3df,2p)\C3H7S1(1+)\ACHALK\05-Feb-19
96\0\\#MP2 6-311+G(3DF,2P) TEST MAXDISK=1000000000\\[CH2CH2 CH2SH]+ //
MP2(fu)/6-31G*\\1,1\C,0,0.9079601639,-0.7040217819,-1.2697681408\C,0,1
.5701397745,-0.0030076587,-0.2789239673\H,0,1.1584760913,-1.7392219353
,-1.4837687093\H,0,0.212969207,-0.2032018834,-1.9381725521\H,0,1.47464
39471,1.075583218,-0.2147202507\H,0,2.3913966243,-0.463851788,0.260785
6425\C,0,0.0185912535,-0.6144611091,0.36141999\S,0,-1.2304431798,0.646
4619322,0.4914402194\H,0,-0.443131342,-1.5283361466,-0.0364897631\H,0,
0.4882756898,-0.9562476379,1.2876221749\H,0,-0.5756864923,1.4008285554
,1.3853326559\\Version=IBM-RS6000-G94RevD.1\HF=-514.9337293\MP2=-515.5
996932\RMSD=2.880e-09\PG=C01 [X(C3H7S1)]\\@

TS:15→16

1\1\GINC-VPP11\SP\RMP4SDTQ-FC\6-311G(2df,p)\C3H7S1(1+)\AJC501\10-Apr-1
998\0\\#MP4 6-311G(2DF,P) TEST MAXDISK=222822400\\[CH2CH2 CH2SH]+ -> C
H3CH2CHSH+ //MP2(fu)/6-31G*\\1,1\C\C,1,1.42753633\C,2,1.58410266,1,72.
68880945\H,3,1.14852123,2,111.11548402,1,1.73541785,0\S,3,1.79129136,2
,110.27954502,4,-118.30950272,0\H,1,1.08803976,2,119.80720047,3,95.262
18397,0\H,1,1.08817734,2,120.80614995,6,166.74795122,0\H,2,1.08423772,
1,118.30601712,3,106.69859886,0\H,2,1.08598649,1,117.61818779,3,-106.3
5017426,0\H,3,1.09128197,2,107.08540387,4,109.67324768,0\H,5,1.3421096
7,3,96.26834845,2,163.16758829,0\\Version=Fujitsu-VP-Unix-G94RevE.2\HF
=-514.9223362\MP2=-515.5763625\MP3=-515.6215582\MP4D=-515.6383808\MP4D
Q=-515.6207756\MP4SDQ=-515.6260602\MP4SDTQ=-515.6563047\RMSD=8.580e-09
\PG=C01 [X(C3H7S1)]\\@

TS:15→17

1\1\GINC-PC\SP\RMP2-FC\6-311+G(3df,2p)\C3H7S1(1+)\AJC501\09-Aug-1996\0

\\# MP2 6-311+G(3DF,2P) TEST\\[CH2CH2 CH2SH]+ -> CH3CHCH2SH+ ts //MP2(
fu)/6-31G*\\1,1\C\C,1,1.40499479\H,1,1.08984247,2,123.30114564\H,1,1.0
9103091,2,119.23061038,3,-180.40929137,0\H,2,1.11216791,1,104.08814371
,3,117.93196239,0\H,2,1.08934906,1,115.29852365,5,-121.27523375,0\C,2,
1.61986164,1,111.94377417,5,107.36466404,0\S,7,1.7891159,2,115.4624399
1,1,-55.37073608,0\H,7,1.08975439,2,107.36265631,8,121.35246704,0\H,7,
1.09038583,2,104.09416458,8,-124.02023475,0\H,8,1.34080949,7,96.628566
73,2,276.89845356,0\\Version=SGI-G94RevD.3\HF=-514.9270749\MP2=-515.57
65386\RMSD=4.863e-09\PG=C01 [X(C3H7S1)]\\@

16

1\1\GINC-VPP11\SP\RQCISD(T)-FC\6-311G(d,p)\C3H7S1(1+)\AJC501\10-Apr-19
98\0\\#QCISD(T,E4T) 6-311G** TEST MAXDISK=222822400\\CH3CH2CHSH+ //MP2
(fu)/6-31G*\\1,1\H,0,-2.0149919698,0.4865730444,-1.1234158852\C,0,-2.1
82011724,0.1491647567,-0.0993716282\H,0,-2.410749063,1.0097126801,0.53
20401292\C,0,-0.9580481299,-0.637716403,0.4326484812\H,0,-3.0423387413
,-0.5216430956,-0.0907350721\C,0,0.2005236494,0.2600952122,0.495850237
5\H,0,-0.7588403462,-1.5201160826,-0.180819801\H,0,-1.1736387415,-0.96
42745048,1.4591470158\H,0,0.1516207574,1.1297014728,1.1522556584\S,0,1
.5408146121,0.0392210946,-0.4187460259\H,0,2.2331215375,1.1232475764,-
0.0232981746\\Version=Fujitsu-VP-Unix-G94RevE.2\HF=-514.9642866\MP2=-5
15.5333115\MP3=-515.5776774\MP4D=-515.5928566\MP4DQ=-515.5799092\MP4SD
TQ=-515.6091021\MP4SDQ=-515.5864498\QCISD=-515.5888394\QCISD(T)=-515.6
113894\RMSD=7.106e-09\PG=C01 [X(C3H7S1)]\\@

TS:16→17

1\1\GINC-PC\FTS\RMP2-FU\6-31G(d)\C3H7S1(1+)\AJC501\30-Sep-1998\0\\#MP2
=FULL 6-31G* OPT=(CALCFC,TS,NOEIGEN) TEST FREQ=NORAMAN MAXDISK=5242880
000\\CH3CHCH2SH+ -> CH3CH2CHSH+\\1,1\H,-0.185903381,0.9510546617,-2.75
29320246\C,-0.0636411903,1.0914750478,-1.6747131984\H,0.9779838906,1.0
444774966,-1.3663287542\C,-0.9756637857,0.2678938107,-0.9016793438\H,-
0.4358332623,2.117683493,-1.4755580029\H,-0.620553621,-1.360203479,-0.
5588353045\H,-1.9983793431,0.1695870128,-1.2748418255\C,-0.6748298722,
-0.5158882387,0.2421306587\S,0.7763608066,-0.4290394485,1.2701174886\H
,-1.5492637142,-0.8055361408,0.8307880875\H,1.6749856148,-0.3133155872
,0.281399308\\Version=SGI-G94RevE.2\HF=-514.8676521\MP2=-515.3842726\R
MSD=3.298e-09\RMSF=1.685e-05\Dipole=-1.0743042,0.2175309,-1.6863396\PG
=C01 [X(C3H7S1)]\\@

17

1\1\GINC-RSCQC8\SP\RMP2-FC\6-311+G(3df,2p)\C3H7S1(1+)\ACHALK\05-Feb-19
96\0\\#MP2 6-311+G(3DF,2P) TEST MAXDISK=1000000000\\CH3CHCH2SH+ //MP2(
fu)/6-31G*\\1,1\C\C,1,1.43834748\C,2,1.43692164,1,127.96852517\S,3,1.7
9912432,2,117.56946192,1,0.,0\H,1,1.08705567,2,115.80434656,3,0.,0\H,1
,1.1061798,2,107.48992902,3,125.43214775,0\H,1,1.1061798,2,107.4899290
2,3,-125.43214775,0\H,2,1.09292668,3,115.1879934,1,180.,0\H,3,1.111973
77,2,103.99568537,1,127.31079804,0\H,3,1.11197377,2,103.99568537,1,-12
7.31079804,0\H,4,1.34004957,3,94.4729787,2,180.,0\\Version=IBM-RS6000-
G94RevD.1\State=1-A'\HF=-514.9512944\MP2=-515.600856\RMSD=7.875e-09\PG
=CS [SG(C3H3S1),X(H4)]\\@

TS:17→17'

1\1\GINC-VPP07\SP\RMP2-FC\6-311+G(3df,2p)\C3H7S1(1+)\AJC501\25-Jun-199
8\0\\#MP2 6-311+G(3DF,2P) TEST MAXDISK=13107200\\CH2CH2CH2SH+ //MP2(fu
)/6-31G*\\1,1\H,0,-1.113930777,0.,2.7017733691\C,0,-0.0652964523,0.,2.
3990900422\C,0,0.3416826935,0.,1.0518934125\H,0,0.6753015773,0.,3.1993
840075\C,0,-0.6881582653,0.,-0.0619489504\H,0,1.0969521947,-0.82827341
94,0.9753089491\H,0,1.0969521947,0.8282734194,0.9753089491\S,0,0.25929
17685,0.,-1.6121242993\H,0,-1.316162831,0.8901623764,0.0199313704\H,0,
-1.316162831,-0.8901623764,0.0199313704\H,0,-0.8009856796,0.,-2.431856
2524\\Version=Fujitsu-VP-Unix-G94RevE.2\State=1-A'\HF=-514.9235829\MP2
=-515.5708854\RMSD=8.292e-09\PG=CS [SG(C3H3S1),X(H4)]\\@

TS:17→18

1\1\GINC-RSCQC8\SP\RMP2-FC\6-311+G(3df,2p)\C3H7S1(1+)\ACHALK\16-Apr-19
96\0\\# MP2 6-311+G(3DF,2P) TEST MAXDISK=1000000000\\CH3CH3CHSH+ -> CH
3CH(SH)CH2+ ts //MP2(fu)/6-31G*\\1,1\C\C,1,1.43586857\C,2,1.45138996,1

,125.93883041\S,3,1.82523959,2,115.44217534,1,34.80492899,0\H,1,1.0886
1685,2,115.08889646,3,9.01278163,0\H,1,1.09730712,2,111.07922311,5,132
.46319792,0\H,2,1.0943538,1,116.74054736,3,-179.67955803,0\H,3,1.11291
743,2,102.38977056,4,-113.31750394,0\H,3,1.09153845,2,112.67240588,4,1
32.94136599,0\H,1,1.11453087,2,103.38280091,5,-117.66563464,0\H,4,1.34
18231,3,94.70825471,2,78.45563758,0\\Version=IBM-RS6000-G94RevD.1\HF=-
514.9534522\MP2=-515.6018857\RMSD=5.414e-09\PG=C01 [X(C3H7S1)]\\@

TS:16→18

1\1\GINC-PC\SP\RMP2-FC\6-311+G(3df,2p)\C3H7S1(1+)\AJC501\25-Jul-1998\0
\\#MP2 6-311+G(3DF,2P) TEST GEOM=ALLCHECK GUESS=CHECK MAXDISK=52428800
00\\CH3CH2CHSH+ -> protonated methylthiirane ts MP2(fu)/6-31G* with CC
exchange\\1,1\H\H,1,1.7794334902\H,1,2.4247065121,2,72.2886082\C,3,1.
0899511883,1,61.23850262,2,79.56583418,0\S,4,1.8232301236,3,111.799528
34,1,99.15927605,0\H,1,1.7919798905,2,60.43214679,3,105.42761604,0\C,6
,1.0901780403,1,34.9890152,2,-34.34180477,0\H,5,1.3422862863,4,96.6283
345,3,-124.11611623,0\C,4,1.4109262425,3,114.71985316,5,125.14670964,0
\H,9,1.0892152419,4,119.43864984,3,187.28177997,0\H,9,1.0923972159,4,1
23.17211015,10,183.07747209,0\\Version=SGI-G94RevE.2\HF=-514.9253036\M
P2=-515.5787214\RMSD=6.646e-09\PG=C01 [X(C3H7S1)]\\@

TS:12→18

1\1\GINC-VPP11\SP\RQCISD(T)-FC\6-311G(d,p)\C3H7S1(1+)\AJC501\06-Jul-19
98\0\\#QCISD(T,E4T) 6-311G** TEST GEOM=CHECK GUESS=CHECK MAXDISK=22282
2400\\CH3CH2SHCH2+ -> CH3CH(SH)CH2+ //MP2(fu)/6-31G*\\1,1\H,0.81814702
87,2.1242490236,-0.6497028664\H,-0.8376792979,2.0435632118,0.018705914
2\H,0.5072139845,2.5639466561,1.0329053375\C,0.4728309896,0.4907361011
,0.780414167\C,0.2211194009,1.8779946772,0.2276268746\S,-0.5643050626,
-1.1470069687,0.0663509452\H,1.5053565063,0.1663424022,0.899088598\C,0
.2963248116,-0.442923859,-1.1567724016\H,1.3794121168,-0.5496452637,-1
.2227699592\H,-0.1977332884,0.1070621917,-1.9590880668\H,-0.0874872605
,0.3417517616,1.7116340795\\Version=Fujitsu-VP-Unix-G94RevE.2\HF=-514.
8816654\MP2=-515.4541184\MP3=-515.4969115\MP4D=-515.5127337\MP4DQ=-515
.4987706\MP4SDTQ=-515.5291942\MP4SDQ=-515.5047483\QCISD=-515.507064\QC
ISD(T)=-515.5308505\RMSD=3.740e-09\PG=C01 [X(C3H7S1)]\\@

TS:13→18

1\1\GINC-VPP11\SP\RQCISD(T)-FC\6-311G(d,p)\C3H7S1(1+)\AJC501\25-Apr-19
98\0\\#QCISD(T,E4T) 6-311G** TEST MAXDISK=222822400\\CH3CHSCH3+ -> CH3
CH(SH)CH2+ TS//MP2(fu)/6-31G*\\1,1\C\C,1,1.50711463\S,2,1.74807828,1,1
20.64794839\C,2,1.57390863,1,116.26088981,3,-85.44578551,0\H,1,1.09179
154,2,111.49630077,3,36.73247812,0\H,1,1.092749,2,109.39342832,5,121.4
0162315,0\H,1,1.09185663,2,109.47122063,5,-120.41381001,0\H,2,1.088732
81,1,116.28335924,3,142.74357081,0\H,4,1.0893253,2,110.45202072,1,-131
.55342458,0\H,4,1.0907925,2,108.5080457,9,133.43655988,0\H,4,1.1712196
3,2,119.01436106,9,-115.23392795,0\\Version=Fujitsu-VP-Unix-G94RevE.2\
HF=-514.8898279\MP2=-515.4735922\MP3=-515.5150441\MP4D=-515.5306851\MP
4DQ=-515.5169287\MP4SDTQ=-515.5455668\MP4SDQ=-515.5217587\QCISD=-515.5
225579\QCISD(T)=-515.5462702\RMSD=3.854e-09\PG=C01 [X(C3H7S1)]\\@

18

1\1\GINC-RSCQC9\SP\RMP2-FC\6-311+G(3df,2p)\C3H7S1(1+)\ACHALK\06-Sep-19
96\0\\# MP2 6-311+G(3DF,2P) TEST GEOM=ALLCHECK GUESS=CHECK MAXDISK=500
000000\\CH3CH(SH)CH2+ //MP2(fu)/6-31G*\\1,1\C,0,1.8019598504,-0.357784
7728,-0.1431509039\C,0,0.5711539031,0.2027077825,0.5084370999\C,0,-0.2
778466943,1.1788232476,-0.176413835\S,0,-1.0553041255,-0.4998783723,-0
.1264365076\H,0,1.6845628725,-0.4550101421,-1.2250834078\H,0,2.6233051
575,0.3387192047,0.0511213953\H,0,0.5652115329,0.2339423978,1.59671860
99\H,0,-0.0271317208,1.4556145746,-1.1977797135\H,0,-0.8210862883,1.92
75129304,0.3934317276\H,0,2.065194253,-1.3287135904,0.2782750946\H,0,-
1.776792153,-0.3164889626,0.9930662503\\Version=IBM-RS6000-G94RevD.4\H
F=-514.9861369\MP2=-515.6570852\RMSD=4.230e-09\PG=C01 [X(C3H7S1)]\\@

TS:18→19

1\1\ ANU-PC\SP\RQCISD(T)-FC\6-311G(d,p)\C3H7S1(1+)\AJC501\28-Jun-1996\
0\\#QCISD(T,E4T) 6-311G** TEST\\CH3CHCH2SH+ -> CH2CHCH2SH2+ ts\\1,1\C\
C,1,1.36616761\C,2,1.50528572,1,120.44369238\S,3,1.84654159,2,103.8858

7535,1,55.76072412,0\H,1,1.09136813,2,122.22571489,3,21.98188308,0\H,1
,1.08478157,2,120.15089528,5,168.57206466,0\H,2,1.08984862,1,119.65315
319,3,-192.75946262,0\H,3,1.09363833,2,112.11182601,4,-114.55046593,0\
H,3,1.08960723,2,113.39141117,4,121.30513349,0\H,4,1.81278731,3,70.853
37179,2,-9.97558491,0\H,4,1.34563901,3,97.68381985,10,95.3345124,0\\Ve
rsion=SGI-G94RevD.1\HF=-514.8908086\MP2=-515.47089\MP3=-515.5136384\MP
4D=-515.5287994\MP4DQ=-515.5142613\MP4SDTQ=-515.5443278\MP4SDQ=-515.51
97811\QCISD=-515.5213513\QCISD(T)=-515.5463816\RMSD=5.758e-09\PG=C01 [
X(C3H7S1)]\\@

19

1\1\GINC-RSCQC9\SP\RMP2-FC\6-311+G(3df,2p)\C3H7S1(1+)\ACHALK\22-Jun-19
96\0\\#MP2 6-311+G(3DF,2P) TEST GEOM=ALLCHECK GUESS=CHECK MAXDISK=1000
000000\\CH2CHCH2SH2+ //MP2(fu)/6-31G*\\1,1\C,0,2.2344246641,-0.2470855
271,-0.1004997343\C,0,1.1620234377,0.2831755148,0.5002504963\C,0,-0.01
01027949,0.7688416602,-0.2750082271\S,0,-1.5105584267,-0.3107805021,-0
.0821544864\H,0,2.2963969491,-0.3634126411,-1.1789910669\H,0,3.0980475
645,-0.5600447683,0.4751517097\H,0,1.1352711429,0.4144823534,1.5796575
519\H,0,-0.3685020726,1.7564053245,0.0303176059\H,0,0.1653890007,0.781
2459974,-1.3542632845\H,0,-1.5575030259,-0.3773179912,1.2611542159\H,0
,-0.9182365727,-1.5084601284,-0.2470101584\\Version=IBM-RS6000-G94RevD
.1\HF=-514.9688124\MP2=-515.6309485\RMSD=8.962e-09\PG=C01 [X(C3H7S1)]\
\@

TS:19→20

1\1\GINC-PC\SP\RQCISD(T)-FC\6-311G(d,p)\C3H7S1(1+)\AJC501\25-Jul-1996\
0\\# QCISD(T,E4T) 6-311G** TEST\\CH2CHCH2SH2+ -> [CH2CHCH2 SH2]+\\1,1\
C,0,0.,0.,0.\C,0,0.,0.,1.382507\H,0,0.928505,0.,1.943736\C,0,-1.224087
,-0.000112,2.025098\H,0,-0.930593,0.011665,-0.56075\H,0,0.925572,-0.00
4342,-0.570374\H,0,-2.153031,0.011351,1.461632\H,0,-1.298974,-0.004473
,3.10972\S,0,-2.608237,2.426661,-0.191423\H,0,-2.342683,3.728721,-0.03
3084\H,0,-3.740149,2.622769,-0.877398\\Version=SGI-G94RevD.3\HF=-514.9
290948\MP2=-515.4687649\MP3=-515.5170318\MP4D=-515.5318959\MP4DQ=-515.
5190509\MP4SDTQ=-515.5455488\MP4SDQ=-515.5245055\QCISD=-515.5264589\QC
ISD(T)=-515.5482134\RMSD=2.548e-09\PG=C01 [X(C3H7S1)]\\@

20

1\1\GINC-RSCQC9\SP\RMP2-FC\6-311+G(3df,2p)\C3H7S1(1+)\ACHALK\30-Jun-19
96\0\\#MP2 6-311+G(3DF,2P) TEST GEOM=ALLCHECK GUESS=CHECK MAXDISK=1000
000000\\[CH2CHCH2 SH2]+ /MP2(fu)/6-31G*\\1,1\C\C,1,1.38296638\H,2,1.08
499375,1,121.34818835\C,2,1.38296638,3,121.34818835,1,180.,0\H,1,1.089
02782,2,120.85065926,3,180.,0\H,1,1.08729843,2,121.50771494,3,0.,0\H,4
,1.08902782,2,120.85065926,3,180.,0\H,4,1.08729843,2,121.50771494,3,0.
,0\X,2,1.,3,90.,1,90.,0\S,2,4.27696341,9,90.,3,180.,0\H,10,1.3379367,2
,132.31433405,9,0.,0\H,10,1.3379367,2,132.31433405,9,180.,0\\Version=I
BM-RS6000-G94RevD.1\State=1-A1\HF=-514.9475981\MP2=-515.5822253\RMSD=6
.281e-09\PG=C02V [C2(H1C1S1),SGV(C2H4),SGV'(H2)]\\@

TS:15→21

1\1\GINC-VPP07\SP\RQCISD(T)-FC\6-311G(d,p)\C3H7S1(1+)\AJC501\18-Apr-19
98\0\\#QCISD(T,E4T) 6-311G** TEST MAXDISK=222822400\\[CH2CH2 CH2SH]+ -
> protonated thiotane MP2(fu)/6-31G*\\1,1\C\C,1,2.00853572\C,2,1.40011
277,1,55.32598473\S,1,1.86279449,2,83.03097757,3,-193.37613896,0\H,1,1
.08729162,2,110.70424636,4,103.57797032,0\H,1,1.08920181,2,130.0589535
7,4,-108.13414125,0\H,3,1.08591351,2,118.64473181,1,103.96844187,0\H,3
,1.08568848,2,117.70585827,7,147.66626882,0\H,2,1.08649098,1,104.85049
149,3,118.23882735,0\H,2,1.08409467,1,114.04212096,3,-113.0387936,0\H,
4,1.34243266,1,96.06723759,2,-91.15015062,0\\Version=Fujitsu-VP-Unix-G
94RevE.2\HF=-514.9014214\MP2=-515.4681295\MP3=-515.5122873\MP4D=-515.5
275443\MP4DQ=-515.5142586\MP4SDTQ=-515.5421655\MP4SDQ=-515.5194525\QCI
SD=-515.5210116\QCISD(T)=-515.5440785\RMSD=4.189e-09\PG=C01 [X(C3H7S1)
]\\@

TS:18→21

1\1\GINC-VPP09\SP\RQCISD(T)-FC\6-311G(d,p)\C3H7S1(1+)\AJC501\20-Jul-19
98\0\\#QCISD(T,E4T) 6-311G** TEST MAXDISK=209715200\\CH3CH(SH)CH2+ ->
protonated thiotane//mp2/6-31G*\\1,1\S,0,-0.9669872829,0.7360446499,-0

.6930232089\H,0,-0.5598819938,0.7340095861,1.7247922985\C,0,0.02941127
47,0.5590141195,0.8240636564\C,0,0.651673768,-0.8239871145,0.825092660
6\C,0,1.3474416663,-1.1761465474,-0.3515393895\H,0,0.7965879283,1.3355
146298,0.7753774421\H,0,0.0491226074,-1.6310546396,1.2549220107\H,0,1.
6320555046,-0.9108544587,1.4267291123\H,0,1.6223574741,-2.2090770596,-
0.5669533395\H,0,1.7493880141,-0.4083308901,-1.0118269566\H,0,-1.98899
3262,-0.0402043106,-0.3003707895\\Version=Fujitsu-VP-Unix-G94RevE.2\HF
=-514.9115847\MP2=-515.4647618\MP3=-515.512545\MP4D=-515.5272406\MP4DQ
=-515.5150882\MP4SDTQ=-515.5402127\MP4SDQ=-515.5201944\QCISD=-515.5227
31\QCISD(T)=-515.5438301\RMSD=4.051e-09\PG=C01 [X(C3H7S1)]\\@

21

1\1\GINC-RSCQC2\SP\RMP2-FC\6-311+G(3df,2p)\C3H7S1(1+)\ACHALK\01-Oct-19
96\0\\#MP2 6-311+G(3DF,2P) TEST MAXDISK=750000000\\protonated thiotane
//MP2(fu)/6-31G*\\1,1\C,0,1.1413012623,-0.3610541614,0.2160613754\C,0
,-1.1413012623,-0.3610541614,0.2160613754\C,0,0.,-1.3766458435,0.02879
66229\S,0,0.,1.0017661179,-0.307705055\H,0,1.4328870735,-0.2119627431,
1.2565804096\H,0,2.0168789705,-0.4336231393,-0.4282189895\H,0,0.,-2.20
42851032,0.7391177215\H,0,0.,-1.7831841168,-0.9848204491\H,0,-1.432887
0735,-0.2119627431,1.2565804096\H,0,-2.0168789705,-0.4336231393,-0.428
2189895\H,0,0.,1.8429080969,0.7467445249\\Version=IBM-RS6000-G94RevD.4
\State=1-A'\HF=-514.9801989\MP2=-515.6488123\RMSD=5.288e-09\PG=CS [SG(
C1H3S1),X(C2H4)]\\@

CH_2S

1\1\ ANU-PC\FOpt\RMP2-FU\6-31G(d)\C1H2S1\AJC501\05-Jul-1996\1\\# MP2=F
ULL 6-31G* OPT=Z-MATRIX TEST FREQ=NORAMAN\\CH2S\\0,1\C\S,1,SC\H,1,CH,2
,HCS\H,1,CH,2,HCS,3,180.,0\\SC=1.61561263\CH=1.08999778\HCS=122.027585
32\\Version=SGI-G94RevD.1\State=1-A1\HF=-436.505944\MP2=-436.770441\RM
SD=3.174e-09\RMSF=8.732e-06\Dipole=0.,0.,-0.6682632\PG=C02V [C2(C1S1),
SGV(H2)]\\@

H_2S

1\1\ ANU-PC\FOpt\RMP2-FU\6-31G(d)\H2S1\AJC501\05-Jul-1996\1\\#MP2=FULL
6-31G* OPT=Z-MATRIX TEST\\H2S\\0,1\S\H,1,HS\H,1,HS,2,HSH\\HS=1.339410
74\HSH=93.33000615\\Version=SGI-G94RevD.1\State=1-A1\HF=-398.6671069\M
P2=-398.7986975\RMSD=9.531e-10\RMSF=1.528e-05\Dipole=0.4228653,0.,0.39
8976\PG=C02V [C2(S1),SGV(H2)]\\@

$[CH_2SH]^+$

1\1\ ANU-PC\POpt\RMP2-FU\6-31G(d)\C1H3S1(1+)\AJC501\05-Jul-1996\1\\# M
P2=FULL 6-31G* OPT=Z-MATRIX TEST FREQ=NORAMAN\\CH2SH+\\1,1\C\S,1,SC\H,
1,CH,2,HCS\H,1,CH,2,HCS,3,180.,0\H,2,HS,1,HSC,3,0.,0\\SC=1.61958681\CH
=1.08715339\HCS=120.31802767\HS=1.34644046\HSC=98.17536783\\Version=SG
I-G94RevD.1\State=1-A'\HF=-436.8064128\MP2=-437.0619517\RMSD=9.176e-09
\RMSF=2.389e-03\Dipole=0.4563722,0.,-0.4916529\PG=CS [SG(C1H3S1)]\\@

Appendix 3

Table A3.1 G2(MP2,SVP) Total Energies from Chapter 5 (0 K, Hatree)

1	-348.57776	**8**	-348.54829
TS:1→3	-348.50557	**9**	-348.52798
3	-348.56614	**TS:9→10**	-348.52260
TS:1→4	-348.50970	**10**	-348.53864
4	-348.55750	**TS:10→5**	-348.50644
TS:3→5	-348.53428	**TS:9→11**	-348.51615
TS:4→5	-348.53252	**11**	-348.52516
5	-348.53467	CH_2CH_2	-78.413321
TS:5→6	-348.50720	$[PhCH_2]^+$	-270.09824
6	-348.53124	C_6H_6	-231.77657
TS:3→7	-348.52221	$[CH_2CHCH_2]^+$	-116.70460
7	-348.52606	C_3H_6	-117.62651
TS:7→6	-348.51009	$[C_6H_5]^+$	-230.79688
TS:1→8	-348.50729		

Table A3.2 GAUSSIAN Archive Entries of MP2/6-31G(d) Optimized Geometries from Chapter 5

1

1\1\GINC-VPP08\SP\RMP2-FC\6-311+G(3df,2p)\C9H11(1+)\AJC501\05-Jul-1997
\0\\#MP2 6-311+G(3DF,2P) TEST GEOM=CHECK GUESS=CHECK MAXDISK=13107200\
\PhC(CH3)2+//MP2/6-31G*\\1,1\C,-0.5627513461,-1.228721168,0.0542458555
\C,0.1648234854,0.,0.\C,1.574820401,0.,0.\C,-0.5627513461,1.228721168,
-0.0542458555\H,-0.0410183424,-2.1769032225,0.1238539775\H,-0.04101834
24,2.1769032225,-0.1238539775\C,-1.9465102565,-1.2181322314,0.07354650
76\C,-1.9465102565,1.2181322314,-0.0735465076\H,-2.4965530083,-2.15231
84028,0.1356945186\H,-2.4965530083,2.1523184028,-0.1356945186\C,-2.639
028065,0.,0.\H,-3.7266057072,0.,0.\C,2.3823162892,-1.2439300052,-0.107
4232845\C,2.3823162892,1.2439300052,0.1074232845\H,3.3050926131,1.0382
675651,0.6579632693\H,3.3050926131,-1.0382675651,-0.6579632693\H,1.865
7690167,2.081093184,0.5717123432\H,1.8657690167,-2.081093184,-0.571712
3432\H,2.6898369911,1.5366886439,-0.9081734368\H,2.6898369911,-1.53668
86439,0.9081734368\\Version=Fujitsu-VP-Unix-G94RevE.2\State=1-A\HF=-34
7.083411\MP2=-348.5016426\RMSD=9.221e-09\PG=C02 [C2(C1C1C1H1),X(C6H10)
]\\@

TS:1→3

1\1\GINC-VPP08\SP\RMP2-FC\6-311+G(3df,2p)\C9H11(1+)\AJC501\22-Jul-1997
\0\\#MP2 6-311+G(3DF,2P) TEST GEOM=CHECK MAXDISK=13107200\\PhC(CH3)2+
-> PhCHCH2CH3+ ts //mp2/6-31G*\\1,1\H,-1.0486020627,0.1630815468,3.545
2129627\C,-0.719903538,0.1574527612,2.5097804716\C,0.1240240571,0.1459
446702,-0.1458558432\C,-1.5553319842,-0.3626640924,1.5178719554\C,0.53
95445685,0.6629733535,2.1761667854\C,0.9684601712,0.6519713745,0.84888
08793\C,-1.1327703589,-0.3755826394,0.1887604607\H,-2.5290843506,-0.76
67862148,1.7799231377\H,1.1888770443,1.0641118172,2.9491716497\H,1.949
7239898,1.0498372737,0.5927887469\H,-1.7774200115,-0.8115967599,-0.575
8953807\C,0.5773041318,0.110993939,-1.5673161046\C,-0.2843290739,0.622
9935378,-2.5528367101\H,1.4960566814,0.7283777641,-1.7733221524\H,0.00
52025454,0.6071202463,-3.6044353926\H,-1.2553280475,1.0603954777,-2.31
38565209\C,1.1650629078,-1.3168858601,-2.0261770609\H,1.954292744,-1.5
463035983,-1.3122696738\H,1.5622298082,-1.2839497338,-3.0418943431\H,0
.3616863713,-2.0474300842,-1.9410720354\\Version=Fujitsu-VP-Unix-G94Re
vE.2\HF=-347.0063704\MP2=-348.4259183\RMSD=3.178e-09\PG=C01 [X(C9H11)]
\\@

3

1\1\GINC-VPP10\SP\RMP2-FC\6-311+G(3df,2p)\C9H11(1+)\AJC501\09-Nov-1998
\0\\#MP2 6-311+G(3DF,2P) TEST MAXDISK=13107200\\PhCHCH2CH3+ //mp2/6-31
G*\\1,1\H,0,-1.2491314149,0.2278693384,3.6338979774\C,0,-0.8499848784,
0.2454779601,2.6220837141\C,0,0.1604195934,0.2861761912,0.0267544647\C
,0,-1.6529541707,-0.211717324,1.5601109917\C,0,0.4525360656,0.72278616
11,2.4061059732\C,0,0.9610328908,0.7459719963,1.1200178752\C,0,-1.1649
897465,-0.1931200034,0.2673032689\H,0,-2.6568210329,-0.5735845553,1.76
09923592\H,0,1.0512138853,1.0699748258,3.2426479975\H,0,1.9680236408,1
.1099941568,0.9262077079\H,0,-1.7832723508,-0.5421543544,-0.5538966443
\C,0,0.7194300415,0.3349311535,-1.2474766733\C,0,0.1461743147,-0.11716
569,-2.5215622686\H,0,1.7419377696,0.7173732402,-1.3109516942\H,0,0.29
38160799,0.6804489625,-3.2613679525\H,0,-0.9204982588,-0.3347979591,-2
.4583414511\C,0,0.9308961177,-1.3689331346,-2.9994610237\H,0,1.9966403
86,-1.1552267238,-3.1058540274\H,0,0.5410538477,-1.6675620989,-3.97439
09923\H,0,0.8016760799,-2.198778693,-2.3022012134\\Version=Fujitsu-VP-
Unix-G94RevE.2\HF=-347.0758509\MP2=-348.4904324\RMSD=1.503e-09\PG=C01
[X(C9H11)]\\@

TS:1→4

1\1\GINC-VPP10\SP\RMP2-FC\6-311+G(3df,2p)\C9H11(1+)\AJC501\26-Jul-1998
\0\\#MP2 6-311+G(3DF,2P) TEST GEOM=CHECK GUESS=CHECK MAXDISK=26214400\
\PhCHCH2CH3+ -> PhCH2CHCH3+ with CC exchange ts\\1,1\C\C,1,2.420763396
6\C,2,2.4293390637,1,59.53625823\C,3,1.4019288554,2,29.66992227,1,179.

51654392,0\C,3,1.3921629713,2,90.63390286,4,-179.12847599,0\C,2,1.3952
109592,1,30.44013887,3,-180.40601646,0\H,4,1.0864432707,3,119.66724015
,2,178.70114631,0\H,2,1.0863674642,1,150.34471286,3,-179.33843932,0\H,
3,1.0863865194,2,149.6433072,4,1.68931848,0\H,5,1.0884602003,3,120.256
37572,2,-179.36063102,0\H,6,1.0903403385,2,120.07163382,1,175.48732599
,0\C,1,1.51983361,2,147.06133082,3,178.66063633,0\C,12,1.4150093797,1,
108.54094113,2,57.62574256,0\H,12,1.1439866685,1,103.25660334,13,96.81
416644,0\H,13,1.0894381164,12,119.04297102,1,40.77238649,0\H,13,1.0933
509047,12,123.8516903,15,-182.73358694,0\C,12,1.5216826081,1,118.09521
82,13,-140.31531176,0\H,17,1.0912116108,12,109.47675609,1,-57.31176705
,0\H,17,1.0929538484,12,111.56298088,18,-120.60380038,0\H,17,1.0924340
302,12,109.52087174,18,118.22347444,0\\Version=Fujitsu-VP-Unix-G94RevE
.2\HF=-347.0085092\MP2=-348.4293104\RMSD=3.528e-09\PG=C01 [X(C9H11)]\\
@

4

1\1\GINC-VPP11\SP\RMP2-FC\6-311+G(3df,2p)\C9H11(1+)\AJC501\28-Jul-1998
\0\\#MP2 6-311+G(3DF,2P) TEST GEOM=CHECK GUESS=CHECK MAXDISK=26214400\
\PhCH2CHCH3+ ring structure//mp2/6-31G*\\1,1\C,-2.4269391771,0.3492226
924,-0.2615280128\C,-1.5749064244,1.3617993013,0.1854803228\C,-1.98791
05941,-0.9646435702,-0.422046212\C,-0.6838023224,-1.2690316278,-0.1320
99333\C,-0.2701469916,1.0611893737,0.4700572396\C,0.2128909844,-0.2640
375386,0.3134696578\H,-3.449922898,0.5898395574,-0.4872834224\H,-1.943
6109481,2.3620898517,0.3067270327\H,-2.6643197423,-1.723948187,-0.7641
121232\H,-0.3301718585,-2.2784159661,-0.2438747083\H,0.3898604172,1.83
19636835,0.8208011842\C,1.800276509,-0.4598760603,-0.2824521032\C,1.52
52753984,-0.7085742207,1.0898876806\H,1.7845282358,-1.3052825776,-0.94
46858923\H,1.4639751546,-1.7179868267,1.4515816555\H,1.8316807953,0.01
49418174,1.8231525176\C,2.5249773429,0.7486423998,-0.8121756477\H,2.10
62910111,1.0824587597,-1.7521310926\H,3.5523300081,0.446466827,-0.9924
747724\H,2.5410714732,1.5697285634,-0.1092619307\\Version=Fujitsu-VP-U
nix-G94RevE.2\HF=-347.058282\MP2=-348.487933\RMSD=6.636e-09\PG=C01 [X(
C9H11)]\\@

TS:3→5

1\1\GINC-VPP11\SP\RMP2-FC\6-311+G(3df,2p)\C9H11(1+)\AJC501\29-Sep-1997
\0\\#MP2 6-311+G(3DF,2P) TEST MAXDISK=13107200\\PhCH2CHCH3+ -> PhCHCH2
CH3+ ts\\1,1\C,0,-0.8513244475,1.3861622312,-0.6992850728\C,0,-0.45511
61409,0.0219732727,-0.2495932146\C,0,0.2301036308,-2.5222999733,0.6589
32803\C,0,-1.2553018632,-0.6118385149,0.7100895058\C,0,0.6737582876,-0
.6238680816,-0.7723330729\C,0,1.0134895638,-1.8971679125,-0.3141065355
\C,0,-0.9023533991,-1.8808360587,1.1682911442\H,0,-2.1437538042,-0.119
3182647,1.1008696164\H,0,1.2698969714,-0.1585096582,-1.5571485695\H,0,
1.8812305551,-2.4044147386,-0.7263148966\H,0,-1.5180971838,-2.37286200
5,1.915879505\H,0,0.494516361,-3.51541178,1.0111221576\H,0,-0.43663815
59,1.6057744637,-1.7732035871\C,0,-0.0714146895,2.5436137821,-0.442239
2534\H,0,-1.9219031174,1.5819726272,-0.8209401308\C,0,1.2902903721,2.5
769520268,0.0797190269\H,0,-0.5151972441,3.498081048,-0.7376738454\H,0
,1.204164233,3.1650591731,1.0121224259\H,0,1.9535807064,3.1700364365,-
0.5608053692\H,0,1.6994127942,1.5934480677,0.2992407093\\Version=Fujit
su-VP-Unix-G94RevE.2\HF=-347.0351582\MP2=-348.4557275\RMSD=7.628e-09\P
G=C01 [X(C9H11)]\\@

TS:4→5

1\1\GINC-VPP11\SP\RMP2-FC\6-311+G(3df,2p)\C9H11(1+)\AJC501\12-Aug-1998
\0\\#MP2 6-311+G(3DF,2P) TEST GEOM=CHECK GUESS=CHECK MAXDISK=13107200\
\PhCH2CHCH3+ ring structure -> straight chain //mp2/6-31G*\\1,1\C,-0.9
530411269,-0.5187190174,-1.9641738333\C,-0.9495319338,-0.4474545258,0.
8344416798\C,0.2604146739,-0.5388078758,-1.2754689868\C,-2.1593926461,
-0.4544181296,-1.260298589\C,-2.1577163651,-0.4301127014,0.1365969743\
C,0.2584085659,-0.5167319678,0.1243323874\H,1.1966757314,-0.6130919976
,-1.8264356683\H,-3.1015774598,-0.4446587104,-1.8010972917\H,-3.095857
4319,-0.3935281116,0.6834477692\H,-0.9564360928,-0.5568318625,-3.04998
8051\C,1.5524679598,-0.5220905868,0.9205630225\H,-0.9525978307,-0.4592
09101,1.9236988269\C,1.8528111073,0.8024000368,1.4306378806\H,2.405659
0416,-0.7321823305,0.2353619082\H,1.5945064859,-1.2832454054,1.7054807
684\C,1.634357396,2.0326729116,0.7075789942\H,2.2617701068,0.898336073
7,2.4413202928\H,2.4688287304,2.7282596307,0.867952395\H,0.7852310797,

2.5196755901,1.2328034124\H,1.361131853,1.8960473626,-0.3378015402\\Ve
rsion=Fujitsu-VP-Unix-G94RevE.2\HF=-347.0366608\MP2=-348.4536081\RMSD=
5.953e-09\PG=C01 [X(C9H11)]\\@

5

1\1\GINC-VPP07\SP\RMP2-FC\6-311+G(3df,2p)\C9H11(1+)\AJC501\08-Oct-1997
\0\\#MP2 6-311+G(3DF,2P) TEST MAXDISK=13107200\\PhCH2CHCH3+\\1,1\C,0,1
.4295552248,-0.7686196673,-0.864783195\C,0,0.3903920069,0.1950820159,-
0.3713008376\C,0,-1.5383686867,1.9577338506,0.6088665443\C,0,0.6344480
929,0.9118793824,0.8075658864\C,0,-0.8174757162,0.3608637452,-1.060015
0593\C,0,-1.7798445595,1.2440697403,-0.5675638788\C,0,-0.3307187373,1.
7951431669,1.292619289\H,0,1.5825824803,0.8044976853,1.3332211028\H,0,
-1.0026071752,-0.1770829929,-1.9891167375\H,0,-2.712760063,1.380647262
,-1.1073670564\H,0,-0.1374415243,2.3597695776,2.2005204495\H,0,-2.2858
400626,2.6500770115,0.9859908033\H,0,1.3292415753,-0.9794423499,-1.963
100558\C,0,1.3826521575,-2.119031469,-0.3521534104\H,0,2.4679857582,-0
.3966116101,-0.8226441054\C,0,0.3258016702,-2.6652685937,0.4572454438\
H,0,2.2300966957,-2.7692829556,-0.588929848\H,0,0.742270254,-2.4993484
226,1.4813556562\H,0,0.2119418873,-3.7470796408,0.3599153468\H,0,-0.60
41185411,-2.097256592,0.4072702525\\Version=Fujitsu-VP-Unix-G94RevE.2\
HF=-347.0388725\MP2=-348.4557736\RMSD=5.135e-09\PG=C01 [X(C9H11)]\\@

TS:5→6

1\1\GINC-VPP09\SP\RMP2-FC\6-311+G(3df,2p)\C9H11(1+)\AJC501\21-Oct-1997
\0\\#MP2 6-311+G(3DF,2P) TEST MAXDISK=209715200\\PhCH2CHCH3+ ring clos
ure TS\\1,1\H,0,0.6153085105,3.5331158807,0.2558646662\C,0,0.468809368
4,2.4797232871,0.034771927\C,0,0.0836054557,-0.2397933668,-0.546755826
6\C,0,1.0505228557,1.5062359615,0.8479264801\C,0,-0.2852120738,2.09512
56059,-1.0769274947\C,0,-0.4823776944,0.7404412225,-1.3634635423\C,0,0
.856881086,0.1490273639,0.5637533455\H,0,1.6663360595,1.7974992032,1.6
948246808\H,0,-0.7396217378,2.8496269059,-1.7135471589\H,0,-1.08804247
65,0.4525123132,-2.2206366982\H,0,1.4154618612,-0.5850108718,1.1462674
866\H,0,0.622549744,-2.1745600575,-1.4087288469\C,0,-0.179178494,-1.71
38568527,-0.8228839463\C,0,-0.2894220188,-2.4322731256,0.5179519375\C,
0,-0.9135373069,-1.7273241716,1.557248025\H,0,-1.100107534,-1.82867305
5,-1.4030211978\H,0,0.4934176615,-3.1334328118,0.8136109812\H,0,-1.277
2040059,-3.0622059905,0.6460420055\H,0,-0.8382722869,-2.0501571084,2.5
962981747\H,0,-1.6303728634,-0.9425499539,1.3233004756\\Version=Fujits
u-VP-Unix-G94RevE.2\HF=-347.0052784\MP2=-348.4287164\RMSD=8.415e-09\PG
=C01 [X(C9H11)]\\@

6

1\1\GINC-VPP08\SP\RMP2-FC\6-311+G(3df,2p)\C9H11(1+)\AJC501\04-Jul-1997
\0\\#MP2 6-311+G(3DF,2P) TEST GEOM=CHECK GUESS=CHECK MAXDISK=13107200\
\phCH2CH2CH2 interlocking rings //MP2/6-31G*\\1,1\H,-0.8884547997,-3.4
343931282,0.\C,-0.6472494782,-2.3729196144,0.\C,-0.0242537884,0.376976
2579,0.\C,0.7020765352,-1.9810847181,0.\C,-1.6961164659,-1.435330253,0
.\C,-1.3923478874,-0.0895171343,0.\C,1.0098903784,-0.6353543066,0.\H,1
.4864086971,-2.7318601225,0.\H,-2.7276139811,-1.774333395,0.\H,-2.1906
928122,0.6517234033,0.\H,2.0511290676,-0.3157994335,0.\H,0.8204800045,
1.1903653211,1.9685366534\C,0.3346388563,1.5547967503,1.0621634531\C,1
.1396089006,2.3065836583,0.\C,0.3346388563,1.5547967503,-1.0621634531\
H,-0.5988230926,2.0623396047,1.3146691389\H,2.1962613957,2.0307353152,
0.\H,1.0643331671,3.3948331665,0.\H,0.8204800045,1.1903653211,-1.96853
66534\H,-0.5988230926,2.0623396047,-1.3146691389\\Version=Fujitsu-VP-U
nix-G94RevE.2\State=1-A'\HF=-347.0282358\MP2=-348.4576297\RMSD=5.703e-
09\PG=CS [SG(C7H7),X(C2H4)]\\@

TS:3→7

1\1\GINC-VPP09\SP\RMP2-FC\6-311+G(3df,2p)\C9H11(1+)\AJC501\08-Oct-1997
\0\\#MP2 6-311+G(3DF,2P) TEST MAXDISK=13107200\\PhCHCH2CH3+ -> PhCH2 C
H2CH2]+ ts //mp2/6-31G*\\1,1\H,0,-1.8609281833,-0.2831122551,1.6578252
911\C,0,-1.535888846,-0.0263657161,0.6453434403\C,0,-0.0778667144,0.02
0578722,0.2982856423\C,0,-2.7887216704,0.5516616357,-0.4689637831\C,0,
-2.4435543443,-0.83557727,-0.3623232157\H,0,-1.8695002674,1.0884815889
,0.6457350588\H,0,-1.8569269387,-1.2659456083,-1.1657660749\H,0,-3.673
3749268,0.9429121604,0.0294376259\H,0,-3.1497639062,-1.5007038272,0.12
25905936\H,0,-2.3313601032,1.1633276451,-1.2432838948\C,0,2.6576462239

,0.0625841649,-0.2307497324\C,0,0.6195690936,1.235058631,0.3316562732\
C,0,0.5921089903,-1.1758936054,0.009352048\C,0,1.9625749543,-1.1495130
189,-0.2473460219\C,0,1.98677726,1.2535594493,0.0579757537\H,0,0.10743
63937,2.1662421117,0.5744821196\H,0,0.0606006488,-2.1255709711,0.00736
69549\H,0,2.4864806424,-2.0759910937,-0.4646818896\H,0,2.5277669548,2.
1953248301,0.0761573955\H,0,3.7237000034,0.0784774638,-0.4392456066\\V
ersion=Fujitsu-VP-Unix-G94RevE.2\HF=-347.0134302\MP2=-348.4506365\RMSD
=6.060e-09\PG=C01 [X(C9H11)]\\@

7

1\1\GINC-VPP11\SP\RMP2-FC\6-311+G(3df,2p)\C9H11(1+)\AJC501\15-Jul-1997
\0\\#MP2 6-311+G(3DF,2P) TEST GEOM=CHECK GUESS=CHECK MAXDISK=22282240\
\PhCH2 CH2CH2]+ //MP2/6-31G*\\1,1\H,-1.8284092935,-0.8620033858,1.3968
295489\C,-1.5119049622,0.,0.7948212876\C,-0.084284661,0.,0.3827121541\
C,-2.5913403702,0.6913567454,-0.5094370062\C,-2.5913403702,-0.69135674
54,-0.5094370062\H,-1.8284092935,0.8620033858,1.3968295489\H,-1.879099
7716,-1.2477070201,-1.1103764618\H,-3.4151793463,1.2429356084,-0.06632
56598\H,-3.4151793463,-1.2429356084,-0.0663256598\H,-1.8790997716,1.24
77070201,-1.1103764618\C,2.6168072134,0.,-0.3158440203\C,0.5936427852,
1.2155130044,0.2109224474\C,0.5936427852,-1.2155130044,0.2109224474\C,
1.9436736216,-1.2118762311,-0.1375598222\C,1.9436736216,1.2118762311,-
0.1375598222\H,0.0793557711,2.1632054223,0.36842545\H,0.0793557711,-2.
1632054223,0.36842545\H,2.4710899001,-2.1531213842,-0.2640382317\H,2.4
710899001,2.1531213842,-0.2640382317\H,3.6690674993,0.,-0.5862732468\\
Version=Fujitsu-VP-Unix-G94RevE.2\State=1-A'\HF=-347.0203918\MP2=-348.
4544009\RMSD=9.341e-09\PG=CS [SG(C3H1),X(C6H10)]\\@

TS:7→6

1\1\GINC-VPP07\SP\RMP2-FC\6-311+G(3df,2p)\C9H11(1+)\AJC501\22-May-1998
\0\\#MP2 6-311+G(3DF,2P) TEST GEOM=CHECK GUESS=CHECK MAXDISK=13107200\
\PHCH2 CH2CH2 ring closure ts //mp2/6-31G*\\1,1\H,-1.1223251459,-3.443
9162498,0.4071045372\C,-0.7997190521,-2.4282073495,0.1953745896\C,0.03
04512613,0.1823792428,-0.354871621\C,0.5595728226,-2.1540219519,0.0039
5557\C,-1.7447542664,-1.401836134,0.1023708894\C,-1.3361675118,-0.0995
560863,-0.1754218718\C,0.9776823312,-0.8564784329,-0.2753215136\H,1.29
05576362,-2.9559155585,0.0573895543\H,-2.801169266,-1.6186155311,0.233
2049196\H,-2.076953633,0.6939370389,-0.2690570478\H,2.0342015948,-0.65
03600264,-0.4447617368\H,1.231094247,0.9789700992,1.5566064223\C,0.555
2638474,1.6890338278,1.09403661\C,1.0237245759,2.6949086018,0.20945691
5\C,0.4722339791,1.5948550859,-0.864872583\H,-0.4538641767,1.725036890
2,1.4910632316\H,2.0981610643,2.8257573579,0.1239822186\H,0.4472000343
,3.6117090537,0.132701564\H,1.308719241,1.4467311651,-1.5481922803\H,-
0.3853495183,2.0602049401,-1.3482832899\\Version=Fujitsu-VP-Unix-G94Re
vE.2\HF=-347.0012318\MP2=-348.437379\RMSD=4.476e-09\PG=C01 [X(C9H11)]\
\@

TS:1→8

1\1\GINC-VPP11\SP\RMP2-FC\6-311+G(3df,2p)\C9H11(1+)\AJC501\15-Aug-1998
\0\\#MP2 6-311+G(3DF,2P) TEST GEOM=CHECK GUESS=CHECK MAXDISK=13107200\
\PhC(CH3)2+ H xchange to ring ts\\1,1\C,-0.3813924017,-1.0904372637,0.
478836007\C,0.1967538,0.2108789065,0.161909201\C,1.6230699184,0.130934
3737,0.0626421019\C,-0.6251566582,1.2847909239,-0.200526947\H,-0.03535
54418,-1.5431411517,1.4191720497\H,-0.2025743305,2.2626476114,-0.41834
2151\C,-1.7528923833,-1.3192995452,0.1807185437\C,-1.969646671,1.02379
12964,-0.455285089\H,-2.2118618031,-2.275398978,0.4192461223\H,-2.6055
248427,1.827822151,-0.818094526\C,-2.5184594908,-0.2697008018,-0.30558
87119\H,-3.5724035123,-0.424196999,-0.5206452592\C,2.0174941346,-1.097
510044,-0.4973243108\C,2.5638625063,1.1847474424,0.5438770189\H,3.5834
288201,0.7990398646,0.6071342431\H,1.5413137685,-1.4155639722,-1.42848
78443\H,2.259304716,1.5902375208,1.5113482802\H,0.712220227,-1.7220894
886,-0.0291514796\H,2.5713908402,2.0102915095,-0.1798028107\H,3.038265
033,-1.4588197971,-0.3779235068\\Version=Fujitsu-VP-Unix-G94RevE.2\HF=
-346.9738337\MP2=-348.4323435\RMSD=4.818e-09\PG=C01 [X(C9H11)]\\@

8

1\1\GINC-PC\SP\RMP2-FC\6-311+G(3df,2p)\C9H11(1+)\AJC501\16-Aug-1998\0\
\#MP2 6-311+G(3DF,2P) TEST GEOM=CHECK GUESS=CHECK MAXDISK=5242880000\\
protonated (ortho) 2-propylbenzene\\1,1\H,-1.8952202484,-0.8637231846,

-0.3088636535\C,-1.2639272413,0.,-0.5815485356\H,-1.8952202484,0.86372
31846,-0.3088636535\C,-1.1108807578,0.,-2.0505467698\C,-0.0288434752,0
.,0.2506815307\C,-0.0836855055,0.,1.7049689491\C,1.2005069175,0.,-0.41
50385035\H,-2.0197656856,0.,-2.648450046\C,0.121053917,0.,-2.641824304
3\H,2.1288291868,0.,0.1447729537\C,1.2658784218,0.,-1.8090836772\H,0.2
312693965,0.,-3.721406019\H,2.2494965374,0.,-2.2766760988\C,1.20597165
09,0.,2.4882795199\C,-1.2802690309,0.,2.3468226976\H,-1.3253037249,0.,
3.4314407729\H,-2.2367304982,0.,1.8339472456\H,0.9911954179,0.,3.55817
51839\H,1.8083102435,0.8869454227,2.2698289367\H,1.8083102435,-0.88694
54227,2.2698289367\\Version=SGI-G94RevE.2\State=1-A'\HF=-347.0500181\M
P2=-348.4675872\RMSD=4.655e-09\PG=CS [SG(C9H7),X(H4)]\\@

9

1\1\GINC-VPP11\SP\RMP2-FC\6-311+G(3df,2p)\C9H11(1+)\AJC501\22-May-1998
\0\\#MP2 6-311+G(3DF,2P) TEST GEOM=CHECK MAXDISK=13107200\\allylbenenz
e cation //mp2/6-31G*\\1,1\H,0.2968772642,-1.3243575826,1.0794052178\C
,0.2696053205,-0.6137815064,0.2463589707\C,0.2330651252,0.8456309925,1
.0775271906\C,-0.9677689391,-0.6447420659,-0.5116819361\C,1.504758357,
-0.5443245201,-0.5126310208\H,2.4488148647,-0.6088461011,0.0254147255\
C,1.4891576334,-0.2886446014,-1.869034918\H,-1.9011605881,-0.795756862
8,0.0256549056\C,-0.970914721,-0.4003848365,-1.8696964472\H,2.41449624
19,-0.1767647389,-2.4257135668\C,0.2542402536,-0.2237083041,-2.5381763
316\H,-1.9014116094,-0.3734735742,-2.4284266728\H,0.2456919815,-0.0279
648549,-3.6089712833\H,1.1789053664,0.8785484405,1.6233471802\C,-0.932
9544546,0.9034053445,2.0002231783\H,0.220800206,1.6275009627,0.3140265
536\C,-0.8101180032,0.7000769687,3.3202999714\H,-1.9010489043,1.155728
3538,1.5726686782\H,0.1461332019,0.4597555057,3.7779092091\H,-1.662521
4562,0.7844656241,3.985553108\\Version=Fujitsu-VP-Unix-G94RevE.2\HF=-3
47.0279039\MP2=-348.448357\RMSD=2.571e-09\PG=C01 [X(C9H11)]\\@

TS:9→10

1\1\GINC-VPP10\SP\RMP2-FC\6-311+G(3df,2p)\C9H11(1+)\AJC501\09-Nov-1998
\0\\#MP2 6-311+G(3DF,2P) TEST MAXDISK=13107200\\o-protonted 3-phenylpr
opene 1,2 ring H shift //mp2/6-31G*\\1,1\H,0,-1.5900887226,-0.15935036
,0.7222492157\C,0,-0.9931606654,0.0560144485,-0.1622898536\H,0,-0.1133
599527,-1.0822512904,-0.2832470461\C,0,0.4511797127,-0.0301814746,-0.0
237667888\C,0,-1.5781713621,0.3294507773,-1.4083656754\C,0,1.073614046
4,-0.0981327582,1.3665596717\C,0,1.2434731532,0.2655941226,-1.17863990
42\H,0,-2.6599777633,0.3655358807,-1.4946457038\C,0,-0.7636929783,0.60
13559354,-2.5038764454\H,0,-1.2173494189,0.8326518417,-3.4642155163\C,
0,0.6392216736,0.54889177,-2.3941435559\H,0,2.3269783114,0.244796658,-
1.0892902411\H,0,1.2549501063,0.7614155688,-3.2636810462\H,0,2.1068459
986,-0.4488971418,1.2634518434\C,0,0.3082509001,-0.9735789785,2.317628
6067\H,0,1.1159237849,0.930116922,1.7448924745\H,0,0.3737194837,-2.049
575965,2.1536539241\C,0,-0.4119439891,-0.4987267255,3.3428958501\H,0,-
0.9370672126,-1.1640698318,4.0197294175\H,0,-0.4731975618,0.5655050157
,3.5550912475\\Version=Fujitsu-VP-Unix-G94RevE.2\HF=-347.0142973\MP2=-
348.4433604\RMSD=8.973e-09\PG=C01 [X(C9H11)]\\@

10

1\1\GINC-VPP08\SP\RMP2-FC\6-311+G(3df,2p)\C9H11(1+)\AJC501\07-Nov-1998
\0\\#MP2 6-311+G(3DF,2P) TEST MAXDISK=13107200\\o-protonted 3-phenylpr
opene //mp2/6-31G*\\1,1\H,0,-1.4374520018,-1.5003570682,-0.2954493545\
C,0,-1.0900792418,-0.5365701496,0.1288326437\H,0,-1.6219204834,0.19385
78069,-0.5107894805\C,0,0.3577705885,-0.4079193093,-0.1174671541\C,0,-
1.5690116881,-0.4392886227,1.5152631868\C,0,0.8449603307,-0.3881223435
,-1.5310349041\C,0,1.2099212665,-0.2318420597,0.9615130972\H,0,-2.6371
763518,-0.5337863302,1.6978781562\C,0,-0.6893556014,-0.2543318973,2.55
07128371\H,0,-1.0337140951,-0.1859560891,3.5775128391\C,0,0.6906742754
,-0.157399328,2.2607504793\H,0,2.2822610497,-0.1469204669,0.8065942787
\H,0,1.3854639629,-0.0178156834,3.0877593039\H,0,1.9039569329,-0.66748
30909,-1.5651931842\C,0,0.6405274623,1.0093507826,-2.0814683604\H,0,0.
282258375,-1.1066571209,-2.1378475467\H,0,1.2713436362,1.7916490852,-1
.6630664709\C,0,-0.2541184705,1.2956469961,-3.035882208\H,0,-0.3643397
976,2.3059097679,-3.4151934658\H,0,-0.878414757,0.5304147781,-3.489522
7802\\Version=Fujitsu-VP-Unix-G94RevE.2\HF=-347.0435123\MP2=-348.45623
33\RMSD=6.952e-09\PG=C01 [X(C9H11)]\\@

TS:10→5

1\1\GINC-VPP09\SP\RMP2-FC\6-311+G(3df,2p)\C9H11(1+)\AJC501\11-Aug-1998
\0\\#MP2 6-311+G(3DF,2P) TEST GEOM=CHECK MAXDISK=13107200\\PhCH2CHCH3+
H xchange with ring ts//mp2/6-31G*\\1,1\H,0.9857775673,0.500776604,-2
.780433862\C,0.5929543496,0.7004633468,-1.7865511068\C,-0.3316865928,1
.2470089768,0.8142039052\C,0.9160461133,-0.1660091189,-0.7198040086\C,
-0.236824517,1.7969908371,-1.5612290834\C,-0.6657763522,2.0859481183,-
0.2612202784\C,0.4894298535,0.1456298964,0.6103250947\H,1.734043993,-0
.8775344217,-0.8627628677\H,-0.5106068098,2.4536398702,-2.3818344123\H
,-1.3008516144,2.9505158959,-0.0838793046\C,0.6293680556,-0.9713952138
,1.6150348492\H,-0.7095731254,1.4693239106,1.8098146282\H,1.6728285162
,-1.2662772401,1.7796732286\C,-0.1398955926,-2.1566177807,1.0938511472
\H,0.226834901,-0.6818023407,2.5977469082\C,-1.0834536026,-2.028381644
8,0.1038778045\H,0.1670901121,-3.1510016162,1.419069269\H,-0.100240679
3,-1.2880807476,-0.6003326888\H,-1.6735795951,-1.1126711222,-0.0032347
89\H,-1.5126935547,-2.9187132962,-0.344756051\\Version=Fujitsu-VP-Unix
-G94RevE.2\HF=-346.983552\MP2=-348.4348631\RMSD=9.000e-09\PG=C01 [X(C9
H11)]\\@

TS:9→11

1\1\GINC-VPP11\SP\RMP2-FC\6-311+G(3df,2p)\C9H11(1+)\AJC501\08-Nov-1998
\0\\#MP2 6-311+G(3DF,2P) TEST MAXDISK=13107200\\allyl addition to benz
ene//mp2/6-31G*\\1,1\H\C,1,1.08653351\C,2,2.16110905,1,100.01425092\C,
2,1.41186463,1,120.32112723,3,-116.09523864,0\C,2,1.42279855,1,118.925
7726,3,72.32317404,0\H,5,1.08792557,2,119.30041416,1,1.24301197,0\C,5,
1.41276604,2,119.6892224,6,-188.78742181,0\H,4,1.08632532,2,119.908028
42,1,5.58034105,0\C,4,1.38660424,2,119.18611674,8,-179.48235802,0\H,7,
1.08642452,5,119.9476674,2,182.02206261,0\C,9,1.4146361,4,120.68415165
,2,1.80051895,0\H,9,1.08685766,4,119.86998474,11,178.37197816,0\H,11,1
.08681656,9,119.39968377,4,-181.58942725,0\H,3,1.08854441,2,119.758537
47,1,98.18359506,0\C,3,1.44841877,2,95.74384272,14,-122.32803248,0\H,3
,1.08802276,2,90.66418162,14,118.20944127,0\C,15,1.3507414,3,120.52779
444,2,121.09071767,0\H,15,1.08696104,3,118.50366829,17,176.28368632,0\
H,17,1.08707433,15,121.73751766,3,-4.28588166,0\H,17,1.0850177,15,121.
32404943,19,178.89575961,0\\Version=Fujitsu-VP-Unix-G94RevE.2\HF=-347.
0072187\MP2=-348.4398347\RMSD=3.008e-09\PG=C01 [X(C9H11)]\\@

11

1\1\GINC-VPP07\SP\RMP2-FC\6-311+G(3df,2p)\C9H11(1+)\AJC501\10-Nov-1998
\0\\#MP2 6-311+G(3DF,2P) TEST GEOM=CHECK GUESS=CHECK MAXDISK=13107200\
\benzene allyl complex//mp2/6-31G*\\1,1\C,0.8234843477,1.3831287576,1.
2079460963\C,-0.326372856,-0.7450341899,1.386246765\H,-0.3432193102,-0
.7876494061,2.473672142\C,0.7606424274,-1.3264585418,0.6908258582\C,-1
.5169836968,-0.4063176628,0.6895279924\H,1.60062129,-1.7342359798,1.24
77957398\C,0.7604215493,-1.3256464479,-0.6926255081\H,1.600222444,-1.7
327695586,-1.2503419301\C,0.8230988503,1.3845461009,-1.2065843443\C,-0
.3268156277,-0.7434062686,-1.3870162018\H,-2.4037734632,-0.1166289672,
1.247460571\C,-1.5172038719,-0.4055081536,-0.6895201086\H,-2.404171694
8,-0.1151648049,-1.2468290117\H,-0.3440093197,-0.7847448092,-2.4744854
254\H,0.4109145462,1.727031294,-2.1526804589\H,1.8186077831,0.95145657
83,-1.2393220789\C,0.2720033616,1.7860762693,0.0010050097\H,-0.6794450
124,2.3099222779,0.001464416\H,1.8190036023,0.9500012856,1.2398574744\
H,0.411602231,1.7245029102,2.1545752086\\Version=Fujitsu-VP-Unix-G94Re
vE.2\State=1-A'\HF=-347.0041919\MP2=-348.4528443\RMSD=4.890e-09\PG=CS
[SG(C1H1),X(C8H10)]\\@

CH_2CH_2

1\1\GINC-VPP12\SP\RMP2-FC\6-311+G(3df,2p)\C2H4\AJC501\21-Jul-1997\0\\#
MP2 6-311+G(3DF,2P) TEST GEOM=ALLCHECK GUESS=CHECK MAXDISK=10485760\\e
thylene //mp2/6-31G*\\0,1\C,0.,0.,-0.6681542918\C,0.,0.,0.6681542918\H
,0.9233086081,0.,-1.23829382\H,-0.9233086081,0.,-1.23829382\H,-0.92330
86081,0.,1.23829382\H,0.9233086081,0.,1.23829382\\Version=Fujitsu-VP-U
nix-G94RevE.2\State=1-AG\HF=-78.0619064\MP2=-78.3933153\RMSD=3.585e-09
\PG=D02H [C2"(C1.C1),SG(H4)]\\@

$[PhCH_2]^+$

1\1\GINC-VPP09\SP\RMP2-FC\6-311+G(3df,2p)\C7H7(1+)\AJC501\21-Jul-1997\

0\\#MP2 6-311+G(3DF,2P) TEST GEOM=CHECK GUESS=CHECK MAXDISK=13107200\\
PhCH2+ //mp2/6-31G*\\1,1\H,0.,0.,-2.889425824\C,0.,0.,-1.801033776\C,0
.,0.,0.9747425883\C,-1.2339483548,0.,-1.1204456439\C,1.2339483548,0.,-
1.1204456439\C,1.2466252028,0.,0.2589295908\C,-1.2466252028,0.,0.25892
95908\H,-2.1623378358,0.,-1.6833926612\H,2.1623378358,0.,-1.6833926612
\H,2.1818881503,0.,0.815318324\H,-2.1818881503,0.,0.815318324\C,0.,0.,
2.3479760457\H,-0.9276190457,0.,2.9168289943\H,0.9276190457,0.,2.91682
89943\\Version=Fujitsu-VP-Unix-G94RevE.2\State=1-A1\HF=-268.9637727\MP
2=-270.0302759\RMSD=5.841e-09\PG=C02V [C2(H1C1C1C1),SGV(C4H6)]\\@

C_6H_6

1\1\GINC-RSCQC9\SP\RMP2-FC\6-311+G(3df,2p)\C6H6\ACHALK\10-Sep-1998\0\\
#MP2 6-311+G(3DF,2P) GEOM=CHECK MAXDISK=1048576000\\benzene//mp2/6-31G
*\\0,1\H,-0.0000000218,0.,2.4842191937\C,-0.0000000123,0.,1.396780307\
C,0.0000000123,0.,-1.396780307\C,-1.2096472355,0.,0.6983901429\C,1.209
6472233,0.,0.6983901642\C,1.2096472355,0.,-0.6983901429\C,-1.209647223
3,0.,-0.6983901642\H,-2.1513969413,0.,1.242109578\H,2.1513969194,0.,1.
2421096158\H,2.1513969413,0.,-1.242109578\H,-2.1513969194,0.,-1.242109
6158\H,0.0000000218,0.,-2.4842191937\\Version=IBM-RS6000-G94RevE.1\Sta
te=1-A1G\HF=-230.7734751\MP2=-231.7204518\RMSD=6.434e-09\PG=D06H [3C2'
(H1C1.C1H1)]\\@

$[CH_2CHCH_2]^+$

1\1\GINC-PC\SP\RMP2-FC\6-311+G(3df,2p)\C3H5(1+)\AJC501\10-Sep-1998\0\\
#MP2 6-311+G(3DF,2P) TEST GEOM=ALLCHECK GUESS=CHECK MAXDISK=5242880000
\\allyl cation //MP2/6-31G*\\1,1\C,-0.0048692447,0.,-1.2028102263\C,0.
4955752858,0.,0.0873832939\H,1.5643591248,0.,0.2758387212\C,-0.4159609
193,0.,1.1286065141\H,-1.0774489613,0.,-1.3882670723\H,0.6497488338,0.
,-2.0712457609\H,-1.4872861412,0.,0.9360350754\H,-0.0978435875,0.,2.16
85615466\\Version=SGI-G94RevE.2\State=1-A1\HF=-116.2307234\MP2=-116.67
75508\RMSD=1.540e-09\PG=C02V [C2(C1H1),SGV(C2H4)]\\@

C_3H_6

1\1\GINC-RSCQC8\SP\RMP2-FC\6-311+G(3df,2p)\C3H6\ACHALK\30-Apr-1998\0\\
#MP2 6-311+G(3DF,2P) TEST MAXDISK=1048576000\\cyclopropane//MP2/6-31G*
\\0,1\H,0,0.,-0.910888,1.457521\C,0,0.,0.,0.867669\C,0,0.751424,0.,-0.
433835\C,0,-0.751424,0.,-0.433835\H,0,0.,0.910888,1.457521\H,0,1.26225
1,-0.910888,-0.728761\H,0,1.262251,0.910888,-0.728761\H,0,-1.262251,-0
.910888,-0.728761\H,0,-1.262251,0.910888,-0.728761\\Version=IBM-RS6000
-G94RevE.1\State=1-A1'\HF=-117.0983517\MP2=-117.6088425\RMSD=8.924e-09
\PG=D03H [3C2(C1),3SGV(H2)]\\@

$[C_6H_5]^+$

1\1\GINC-PC\FOpt\RMP2-FC\6-31G(d)\C6H5(1+)\AJC501\27-Aug-1997\0\\# MP2
6-31G* OPT TEST MAXDISK=5242880000\\C6H5+\\1,1\H,0.,0.,2.3877792177\C
,0.,0.,-1.1809289873\C,0.,0.,1.3023104106\C,0.,1.2770043563,-0.8250758
879\C,0.,-1.2770043563,-0.8250758879\C,0.,-1.213066504,0.612631134\C,0
.,1.213066504,0.612631134\H,0.,2.1952925899,-1.4019938042\H,0.,-2.1952
925899,-1.4019938042\H,0.,-2.1770141476,1.1186284483\H,0.,2.1770141476
,1.1186284483\\Version=SGI-G94RevE.2\State=1-A1\HF=-229.7560567\MP2=-2
30.4928549\RMSD=7.411e-09\RMSF=7.403e-05\Dipole=0.,0.,-0.49845\PG=C02V
[C2(C1C1H1),SGV(C4H4)]\\@

Appendix 4

Table A4.1 G2** Total Energies (0 K, Hartree) from Chapter 6

1	-113.34174	**1d**	-226.55088	**1h**	-189.78353	H_2O	-76.33217
2	-113.28578	**2d**	-226.52329	**2h**	-189.77217	NH_3	-56.45838
3	-113.40194	**3d**	-226.59188	**3h**	-189.79266	HeH^+	-2.96775
1a	-116.24431	**1e**	-213.74200	**1i**	-169.96603	NeH^+	-128.8963
2a	-116.18920	**2e**	-213.71829	**2i**	-169.95969	ArH^+	-527.1996
3a	-116.30274	**3e**	-213.77730	**3i**	-170.02453	H_2F^+	-100.5331
1b	-242.16682	**1f**	-222.77865	He	-2.90003	N_2H^+	-109.5798
2b	-242.11145	**2f**	-222.76156	Ne	-128.81946	H_3O^+	-76.59203
3b	-242.22333	**3f**	-222.80927	Ar	-527.05570	NH_4^+	-56.78134
1c	-640.41623	**2g**	-226.59982	CO	-113.17792		
2c	-640.38486	**3g**	-226.58157	HF	-100.35017		
3c	-640.46370	**4g**	-226.60083	N_2	-109.39358		

Table A4.2 GAUSSIAN Archive Entries for MP2(full)/6-31G(d,p) Optimized Geometries for Chapter 6

(1)

```
1\1\GINC-RSCQC8\FOpt\RMP2-FU\6-31G(d,p)\C1H1O1(1+)\ACHALK\05-Jan-1996\
0\\#MP2=FULL 6-31G** OPT TEST MAXDISK=37500000\\HOC+\\1,1\O,0.,0.,-0.4
012688906\C,0.,0.,0.7678830506\H,0.,0.,-1.397147179\\Version=IBM-RS600
0-G94RevD.1\State=1-SG\HF=-112.9195275\MP2=-113.2006235\RMSD=2.278e-09
\RMSF=1.435e-06\Dipole=0.,0.,-1.0509192\PG=C*V [C*(C1O1H1)]\\@
```

(2)

```
1\1\GINC-RSCQC8\FTS\RMP2-FU\6-31G(d,p)\C1H1O1(1+)\ACHALK\05-Jan-1996\0
\\#MP2=FULL 6-31G** OPT=(CALCFC,TS) TEST MAXDISK=37500000\\HOC+ -> HCO
+ ts\\1,1\C,-0.072320637,0.,-0.6579289809\O,-0.0846434013,0.,0.5080972
239\H,1.1110710327,0.,-0.1172039053\\Version=IBM-RS6000-G94RevD.1\Stat
e=1-A'\HF=-112.8356333\MP2=-113.1398495\RMSD=7.900e-09\RMSF=1.206e-04\
Dipole=0.7237812,0.,-0.292929\PG=CS [SG(C1H1O1)]\\@
```

(3)

```
1\1\GINC-RSCQC8\FOpt\RMP2-FU\6-31G(d,p)\C1H1O1(1+)\ACHALK\05-Jan-1996\
0\\#MP2=FULL 6-31G** OPT TEST MAXDISK=37500000\\HCO+\\1,1\C,0.,0.,-0.5
304497522\O,0.,0.,0.6003082013\H,0.,0.,-1.6197670978\\Version=IBM-RS60
00-G94RevD.1\State=1-SG\HF=-112.9624546\MP2=-113.2723169\RMSD=2.519e-0
9\RMSF=1.059e-04\Dipole=0.,0.,-1.4052746\PG=C*V [C*(H1C1O1)]\\@
```

(1a)

```
1\1\ ANU-PC\FOpt\RMP2-FU\6-31G(d,p)\C1H1He1O1(1+)\AJC501\04-Jun-1996\0
\\#MP2=FULL 6-31G** OPT TEST\\[He HOC]+\\1,1\O,0.,0.,-0.0513292352\C,0
.,0.,1.1168038018\H,0.,0.,-1.0533941797\He,0.,0.,-2.6183973746\\Versio
n=SGI-G94RevD.1\State=1-SG\HF=-115.7762356\MP2=-116.0840234\RMSD=9.395
e-09\RMSF=1.863e-05\Dipole=0.,0.,-0.5375786\PG=C*V [C*(C1O1H1He1)]\\@
```

(2a)

```
1\1\ ANU-PC\FTS\RMP2-FU\6-31G(d,p)\C1H1He1O1(1+)\AJC501\04-Jun-1996\0\
\#MP2=FULL 6-31G** OPT=(CALCFC,TS) TEST\\[He HOC]+ -> [He HCO]+ ts\\1,
1\C,-0.396562964,0.,-0.6674982127\O,-0.4074586685,0.,0.4977472337\H,0.
8007061921,0.,-0.1311257191\He,2.4191704702,0.,0.0770685629\\Version=S
GI-G94RevD.1\State=1-A'\HF=-115.6919737\MP2=-116.0228088\RMSD=8.074e-0
9\RMSF=1.568e-06\Dipole=0.2728393,0.,-0.2953801\PG=CS [SG(C1H1He1O1)]\
\@
```

(3a)

```
1\1\ ANU-PC\FOpt\RMP2-FU\6-31G(d,p)\C1H1He1O1(1+)\AJC501\04-Jun-1996\0
\\#MP2=FULL 6-31G** OPT TEST\\[He HCO]+\\1,1\C,0.,0.,-0.1021739201\O,0
.,0.,1.0286132973\H,0.,0.,-1.1924044843\He,0.,0.,-3.2117291866\\Versio
n=SGI-G94RevD.1\State=1-SG\HF=-115.8185182\MP2=-116.1541613\RMSD=8.505
e-09\RMSF=2.711e-06\Dipole=0.,0.,-0.6570525\PG=C*V [C*(He1H1C1O1)]\\@
```

(1b)

```
1\1\ ANU-PC\FOpt\RMP2-FU\6-31G(d,p)\C1H1Ne1O1(1+)\AJC501\04-Jun-1996\0
\\#MP2=FULL 6-31G** OPT TEST\\[Ne HOC]+\\1,1\O,0.,0.,0.774888109\C,0.,
0.,1.9415539702\H,0.,0.,-0.2457916127\Ne,0.,0.,-1.7602637081\\Version=
SGI-G94RevD.1\State=1-SG\HF=-241.3998413\MP2=-241.8387107\RMSD=4.137e-
09\RMSF=4.302e-05\Dipole=0.,0.,0.771494\PG=C*V [C*(C1O1H1Ne1)]\\@
```

(2b)

```
1\1\ ANU-PC\FTS\RMP2-FU\6-31G(d,p)\C1H1Ne1O1(1+)\AJC501\04-Jun-1996\0\
\#MP2=FULL 6-31G** OPT=(CALCFC,TS) TEST\\[Ne HOC]+ -> [Ne HCO]+ ts\\1,
1\C,-1.0965632293,0.,-0.6495614025\O,-1.1094510832,0.,0.5125862089\H,0
.197334194,0.,-0.1112390486\Ne,1.5257653847,0.,-0.0092082208\\Version=
SGI-G94RevD.1\State=1-A'\HF=-241.3158576\MP2=-241.7807403\RMSD=2.677e-
09\RMSF=6.207e-06\Dipole=-0.4132304,0.,-0.2195893\PG=CS [SG(C1H1Ne1O1)
```

]\\@

(3b)

1\1\ ANU-PC\FOpt\RMP2-FU\6-31G(d,p)\C1H1Ne1O1(1+)\AJC501\04-Jun-1996\0
\\#MP2=FULL 6-31G** OPT TEST\\[Ne HCO]+\\1,1\C,0.,0.,0.8844604948\O,0.
,0.,2.0154080276\H,0.,0.,-0.2094268417\Ne,0.,0.,-2.1220600348\\Version
=SGI-G94RevD.1\State=1-SG\HF=-241.4409571\MP2=-241.9051315\RMSD=2.407e
-09\RMSF=1.451e-06\Dipole=0.,0.,1.0801832\PG=C*V [C*(O1C1H1Ne1)]\\@

(1c)

1\1\ ANU-PC\FOpt\RMP2-FU\6-31G(d,p)\C1H1Ar1O1(1+)\AJC501\04-Jun-1996\1
\\#MP2=FULL 6-31G** OPT=Z-MATRIX\\[Ar HOC]+\\1,1\O\C,1,CO\X,1,1.,2,90.
\H,1,OH,3,90.,2,180.,0\X,4,1.,1,90.,3,0.,0\Ar,4,ArH,5,90.,1,180.,0\\CO
=1.16489533\OH=1.08824351\ArH=1.66881772\\Version=SGI-G94RevD.1\State=
1-SG\HF=-639.6947943\MP2=-640.1342913\RMSD=3.230e-09\RMSF=6.010e-05\Di
pole=0.,0.,1.1258403\PG=C*V [C*(C1O1H1Ar1)]\\@

(2c)

1\1\ ANU-PC\FTS\RMP2-FU\6-31G(d,p)\C1H1Ar1O1(1+)\AJC501\05-Jun-1996\0\
\#MP2=FULL 6-31G** OPT=(CALCFC,TS) TEST GEOM=ALLCHECK\\[Ar HOC+] -> [A
r HCO]+ ts\\1,1\C,-1.7724389267,0.,-0.7338471569\O,-1.8121081022,0.,0.
4205214021\H,0.0949965238,0.,-0.0817504989\Ar,1.3909167697,0.,0.062259
0124\\Version=SGI-G94RevD.1\State=1-A'\HF=-639.6462289\MP2=-640.103472
9\RMSD=2.608e-09\RMSF=1.484e-05\Dipole=0.8687018,0.,-0.0271364\PG=CS [
SG(C1H1Ar1O1)]\\@

(3c)

1\1\ ANU-PC\FOpt\RMP2-FU\6-31G(d,p)\C1H1Ar1O1(1+)\AJC501\05-Jun-1996\0
\\#MP2=FULL 6-31G** OPT TEST GEOM=ALLCHECK\\[Ar HCO+]\\1,1\C,0.,0.,1.6
119705643\O,0.,0.,2.7433748791\H,0.,0.,0.5139980525\Ar,0.,0.,-1.785156
6928\\Version=SGI-G94RevD.1\State=1-SG\HF=-639.7387146\MP2=-640.197483
9\RMSD=1.864e-09\RMSF=1.734e-04\Dipole=0.,0.,2.3002941\PG=C*V [C*(O1C1
H1Ar1)]\\@

(1d)

1\1\ ANU-PC\FOpt\RMP2-FU\6-31G(d,p)\C2H1O2(1+)\AJC501\04-Jun-1996\0\\#
MP2=FULL 6-31G** OPT TEST\\[CO HOC]+\\1,1\O,0.,0.,1.1971068739\C,0.,0.
,2.3586529483\H,0.,0.,0.\O,0.,0.,-1.1971068739\C,0.,0.,-2.3586529483\\
Version=SGI-G94RevD.1\State=1-SGG\HF=-225.6866873\MP2=-226.2645254\RMS
D=3.952e-09\RMSF=2.464e-04\Dipole=0.,0.,0.\PG=D*H [O(H1),C*(C1O1.O1C1)
]\\@

(2d)

1\1\ ANU-PC\FTS\RMP2-FU\6-31G(d,p)\C2H1O2(1+)\AJC501\04-Jun-1996\0\\#M
P2=FULL 6-31G** OPT=(CALCFC,TS) TEST\\[CO HOC]+ -> [CO HCO]+\\1,1\O,0.
8251213772,-0.7331116251,-1.4304448067\C,0.897808721,0.4115619349,-1.5
564568532\H,-0.0920222382,0.1322408225,0.1595313568\O,-0.6007783183,0.
1892258599,1.0415197681\C,-1.1815957597,0.2915789484,2.0484350119\\Ver
sion=SGI-G94RevD.1\State=1-A'\HF=-225.6542021\MP2=-226.2365081\RMSD=8.
551e-09\RMSF=5.765e-05\Dipole=-0.6567416,0.2547337,1.1385386\PG=CS [SG
(C2H1O2)]\\@

(3d)

1\1\ ANU-PC\FOpt\RMP2-FU\6-31G(d,p)\C2H1O2(1+)\AJC501\05-Jun-1996\0\\#
MP2=FULL 6-31G** OPT TEST GEOM=ALLCHECK\\[CO HCO+]\\1,1\C,0.,0.,1.3579
399385\O,0.,0.,2.4891884407\H,0.,0.,0.247613636\O,0.,0.,-1.5266623152\
C,0.,0.,-2.6825770453\\Version=SGI-G94RevD.1\State=1-SG\HF=-225.714643
4\MP2=-226.3142471\RMSD=3.988e-09\RMSF=2.189e-05\Dipole=0.,0.,1.522184
4\PG=C*V [C*(C1O1H1C1O1)]\\@

(1e)

1\1\ ANU-PC\FOpt\RMP2-FU\6-31G(d,p)\C1H2F1O1(1+)\AJC501\04-Jun-1996\0\
\#MP2=FULL 6-31G** OPT TEST\\[HF HOC]+\\1,1\C,0.0044595157,0.,0.761327
8379\O,0.1358487058,0.,1.8858955973\H,-0.1186259377,0.,-0.3746846573\F
,-0.0311203763,0.,-1.8643829707\H,-0.7148374165,0.,-2.5010004126\\Vers
ion=SGI-G94RevD.1\State=1-A'\HF=-213.0042177\MP2=-213.5035184\RMSD=4.3
00e-09\RMSF=2.814e-05\Dipole=-0.6574284,0.,-0.196385\PG=CS [SG(C1H2F1O
1)]\\@

(2e)

1\1\ ANU-PC\FTS\RMP2-FU\6-31G(d,p)\C1H2F1O1(1+)\AJC501\04-Jun-1996\1\\
#MP2=FULL 6-31G** OPT=(CALCFC,TS,Z-MATRIX) TEST\\[HF HOC]+ -> [HF HCO]
+ ts\\1,1\C\O,1,CO\H,2,HO,1,HOC\F,3,FH,2,FHO,1,180.,0\H,4,HF,3,HFH,2,1
80.,0\\CO=1.15405041\HO=1.98285027\FH=0.98543814\HF=0.96244576\FHO=161
.71739518\HFH=112.30143022\HOC=73.94462679\\Version=SGI-G94RevD.1\Stat
e=1-A'\HF=-212.950295\MP2=-213.4405086\RMSD=5.573e-09\RMSF=5.130e-06\D
ipole=1.8816317,0.,-0.8567254\PG=CS [SG(C1H2F1O1)]\\@

(3e)

1\1\ ANU-PC\FOpt\RMP2-FU\6-31G(d,p)\C1H2F1O1(1+)\AJC501\05-Jun-1996\0\
\#MP2=FULL 6-31G** OPT TEST GEOM=ALLCHECK\\[HF HCO+]\\1,1\O,-0.0165406
359,0.,0.739290863\C,0.0470394162,0.,1.8972400865\H,-0.0093787324,0.,-
0.556403788\F,0.0683936236,0.,-1.6267062443\H,-0.75607529,0.,-2.101007
4364\\Version=SGI-G94RevD.1\State=1-A'\HF=-212.9835856\MP2=-213.464917
8\RMSD=8.686e-09\RMSF=8.035e-05\Dipole=-0.7599361,0.,-1.2346159\PG=CS
[SG(C1H2F1O1)]\\@

(1f)

1\1\ ANU-PC\FOpt\RMP2-FU\6-31G(d,p)\C1H1N2O1(1+)\AJC501\04-Jun-1996\0\
\#MP2=FULL 6-31G** OPT TEST\\[N2 HOC]+\\1,1\O,0.,0.,1.3065749669\C,0.,
0.,2.4656863701\H,0.,0.,-0.1173330867\N,0.,0.,-1.2329499839\N,0.,0.,-2
.3569621402\\Version=SGI-G94RevD.1\State=1-SG\HF=-221.8869959\MP2=-222
.5121021\RMSD=3.467e-09\RMSF=4.014e-06\Dipole=0.,0.,-0.7314917\PG=C*V
[C*(N1N1H1O1C1)]\\@

(2f)

1\1\ ANU-PC\FTS\RMP2-FU\6-31G(d,p)\C1H1N2O1(1+)\AJC501\04-Jun-1996\0\\
#MP2=FULL 6-31G** OPT=(CALCFC,TS) TEST\\[N2 HOC]+ -> [N2 HCO]+ ts\\1,1
\O,-1.7678708784,0.,-0.7779710964\C,-1.9436150659,0.,0.3617266297\H,0.
2236407855,0.,0.1346056198\N,1.2677943726,0.,0.2284377397\N,2.38663657
56,0.,0.3313913136\\Version=SGI-G94RevD.1\State=1-A'\HF=-221.8624552\M
P2=-222.4938765\RMSD=4.042e-09\RMSF=9.922e-07\Dipole=1.4692866,0.,0.2
854043\PG=CS [SG(C1H1N2O1)]\\@

(3f)

1\1\ ANU-PC\FOpt\RMP2-FU\6-31G(d,p)\C1H1N2O1(1+)\AJC501\04-Jun-1996\0\
\#MP2=FULL 6-31G** OPT TEST\\[N2 HCO]+\\1,1\C,0.,0.,1.4108138741\O,0.,
0.,2.542857231\H,0.,0.,0.2882780748\N,0.,0.,-1.5140857559\N,0.,0.,-2.6
424884108\\Version=SGI-G94RevD.1\State=1-SG\HF=-221.9094887\MP2=-222.5
503934\RMSD=4.530e-09\RMSF=9.266e-06\Dipole=0.,0.,1.493695\PG=C*V [C*(
N1N1H1C1O1)]\\@

(2g)

1\1\ ANU-PC\FTS\RMP2-FU\6-31G(d,p)\C2H1O2(1+)\AJC501\04-Jun-1996\0\\#M
P2=FULL 6-31G** OPT=(CALCFC,TS) TEST\\[OC HOC]+ -> [OC HCO]+\\1,1\O,-2
.0557211053,0.,-0.5129757686\C,-2.0563181783,0.,0.6392861212\H,0.29486
26696,0.,0.0463896532\C,1.3886880662,0.,0.0269401565\O,2.5195858557,0.
,0.0075073536\\Version=SGI-G94RevD.1\State=1-A'\HF=-225.6976011\MP2=-2
26.3039614\RMSD=2.917e-09\RMSF=1.570e-05\Dipole=1.8512326,0.,0.017736\
PG=CS [SG(C2H1O2)]\\@

(3g)

1\1\ ANU-PC\FOpt\RMP2-FU\6-31G(d,p)\C2H1O2(1+)\AJC501\04-Jun-1996\0\\#
MP2=FULL 6-31G** OPT TEST\\[OC HCO]+\\1,1\C,0.,0.,1.4408067599\O,0.,0.
,2.5747595501\H,0.,0.,0.2692532003\C,0.,0.,-1.4554708064\O,0.,0.,-2.59
74181653\\Version=SGI-G94RevD.1\State=1-SG\HF=-225.7112139\MP2=-226.32
63537\RMSD=9.937e-09\RMSF=4.750e-05\Dipole=0.,0.,1.1115094\PG=C*V [C*(
O1C1H1C1O1)]\\@

(4g)

1\1\ ANU-PC\FOpt\RMP2-FU\6-31G(d,p)\C2H1O2(1+)\AJC501\09-Dec-1996\0\\#
MP2=FULL 6-31G** OPT TEST GEOM=ALLCHECK\\[OC HCO+] -> [OCH CO]+ ts\\1,
1\C,0.,0.,1.3802689638\O,0.,0.,2.5185252136\H,0.,0.,0.\C,0.,0.,-1.3802
689638\O,0.,0.,-2.5185252136\\Version=SGI-G94RevD.3\State=1-SGG\HF=-22
5.7060118\MP2=-226.3248995\RMSD=7.528e-09\RMSF=8.355e-05\Dipole=0.,0.,

0.\PG=D*H [O(H1),C*(O1C1.C1O1)]\\@

(1h)

1\1\ ANU-PC\FOpt\RMP2-FU\6-31G(d,p)\C1H3O2(1+)\AJC501\04-Jun-1996\1\\#
MP2=FULL 6-31G** OPT=Z-MATRIX TEST\\[H2O HOC]+\\1,1\O\C,1,CO\X,1,1.,2,
90.\H,1,HO,3,HOX3,2,180.,0\X,4,1.,1,90.,3,0.,0\O,4,OH1,5,OHX5,1,180.,0
\X,6,1.,4,90.,5,0.,0\X,6,1.,7,X8OX7,4,180.,0\H,6,OH2,8,hHOH,7,90.,0\H,
6,OH2,8,hHOH,7,-90.,0\\CO=1.15637924\HO=1.66797306\OH1=0.99832469\OH2=
0.97556173\HOX3=93.2220638\X8OX7=44.72174686\OHX5=91.71470131\hHOH=55.
95301878\\Version=SGI-G94RevD.1\State=1-A'\HF=-189.0613661\MP2=-189.55
27035\RMSD=6.933e-09\RMSF=4.939e-05\Dipole=0.4992074,0.,-2.5654426\PG=
CS [SG(C1H1O2),X(H2)]\\@

(2h)

1\1\ ANU-PC\FTS\RMP2-FU\6-31G(d,p)\C1H3O2(1+)\AJC501\25-Nov-1996\0\\#M
P2=FULL 6-31G** OPT=(READFC,TS,NOEIGEN) TEST GEOM=ALLCHECK\\[H2O HOC+]
 -> [H2O HCO]+ ts\\1,1\C,-1.4760052989,0.1183039268,-0.4018837684\O,-1
.3357869632,-0.1137565715,0.717984621\H,0.8282951669,-0.0299035015,-0.
137917447\O,1.7968651898,-0.0537342871,-0.2999897416\H,2.0318556569,0.
2615353361,-1.1955341776\H,2.3072551574,0.3984714741,0.4007951996\\Ver
sion=SGI-G94RevD.3\HF=-189.0441697\MP2=-189.5409527\RMSD=1.329e-09\RMS
F=3.930e-06\Dipole=2.8157658,0.6232494,-0.4980511\PG=C01 [X(C1H3O2)]\\
@

(3h)

1\1\ ANU-PC\FOpt\RMP2-FU\6-31G(d,p)\C1H3O2(1+)\AJC501\04-Jun-1996\1\\#
MP2=FULL 6-31G** OPT=Z-MATRIX TEST\\[H2O HCO]+\\1,1\C\O,1,CO\X,1,1.,2,
90.\H,1,HC,3,HCX3,2,180.,0\X,4,1.,1,90.,3,0.,0\O,4,OH1,5,OHX5,1,180.,0
\X,6,1.,4,90.,5,0.,0\X,6,1.,7,X8OX7,4,180.,0\H,6,OH2,8,hHOH,7,90.,0\H,
6,OH2,8,hHOH,7,-90.,0\\CO=1.14103867\HC=1.67629863\OH1=1.03821446\OH2=
0.97396142\HCX3=91.29203614\X8OX7=45.98739875\OHX5=92.90736693\hHOH=55
.59240166\\Version=SGI-G94RevD.1\State=1-A'\HF=-189.0592176\MP2=-189.5
657689\RMSD=2.362e-09\RMSF=4.550e-05\Dipole=0.542395,0.,-2.3769989\PG=
CS [SG(C1H1O2),X(H2)]\\@

(1i)

1\1\ ANU-PC\FOpt\RMP2-FU\6-31G(d,p)\C1H4N1O1(1+)\AJC501\04-Jun-1996\0\
\#MP2=FULL 6-31G** OPT TEST\\[NH3 HOC+]\\1,1\O,0.,0.,1.0383256813\C,0.
,0.,2.1928922962\H,0.,0.,-0.9239425432\N,0.,0.,-1.9508764601\H,-0.4806
99648,0.8325962135,-2.2946271544\H,-0.480699648,-0.8325962135,-2.29462
71544\H,0.961399296,0.,-2.2946271544\\Version=SGI-G94RevD.1\HF=-169.29
08567\MP2=-169.7750761\RMSD=6.968e-09\RMSF=1.990e-05\Dipole=0.,0.,-3.2
832782\PG=C03V [C3(N1H1O1C1),3SGV(H1)]\\@

(2i)

1\1\ ANU-PC\FTS\RMP2-FU\6-31G(d,p)\C1H4N1O1(1+)\AJC501\04-Jun-1996\0\\
#MP2=FULL 6-31G** OPT=(CALCFC,TS) TEST\\[NH3 HOC+]\\1,1\C,-0.642944593
2,-1.5247890256,0.\O,0.5074505797,-1.5743303197,0.\H,0.0177504953,0.95
48165024,0.\N,-0.0181590589,1.9766661847,0.\H,0.4504974928,2.335352966
9,0.8339587539\H,-0.9935691467,2.2811909822,0.\H,0.4504974928,2.335352
9669,-0.8339587539\\Version=SGI-G94RevD.1\State=1-A'\HF=-169.279476\MP
2=-169.7679574\RMSD=9.932e-09\RMSF=1.616e-06\Dipole=0.0142786,3.461933
6,0.\PG=CS [SG(C1H2N1O1),X(H2)]\\@

(3i)

1\1\ ANU-PC\FOpt\RMP2-FU\6-31G(d,p)\C1H4N1O1(1+)\AJC501\04-Jun-1996\0\
\#MP2=FULL 6-31G** OPT TEST\\[NH3 HCO+]\\1,1\C,-0.0000001824,0.,0.9793
54689\O,0.0000005723,0.,2.1234869228\H,-0.0000014859,0.,-1.0669003525\
N,-0.0000021702,0.,-2.1038385466\H,-0.4801092699,0.8315698426,-2.44948
40065\H,-0.4801092699,-0.8315698426,-2.4494840065\H,0.9602118061,0.,-2
.4494846997\\Version=SGI-G94RevD.1\HF=-169.287954\MP2=-169.7822409\RMS
D=3.653e-09\RMSF=8.443e-06\Dipole=-0.0000019,0.,-3.2773869\PG=\\@

Appendix 5

Table A5.1 G2** Total Energies for Species Related to Proton Transport from Chapter 7 (0 K, Hatree)

Ar	-527.05570	**2**	-636.64727
ArH^+	-527.19961	**TS:2→2'**	-636.59939
CO	-113.17792	**3**	-222.77865
HOC^+	-113.34174	**TS:3→3'**	-222.74260
HCO^+	-113.40194	**4**	-209.96771
HF	-100.35017	**TS:4→4'**	-209.93473
H_2F^+	-100.53312	**5**	-219.00098
N_2	-109.39358	**TS:5→5'**	-218.97780
H_2O	-76.33217	**6**	-222.80927
H_3O^+	-76.59203	**TS:6→6'**	-222.79765
N_2H^+ **(1)**	-109.57981	**7**	-186.00064
TS:1→1'	-109.51040	**TS:7→7'**	-185.98823

Table A5.2 G2(ZPE=MP2) Total Energies for Species Related to Methyl-Cation Transport from Chapter 7 (0 K, Hatree)

CH_3^+	-39.38469	**TS:10a→10b**	-249.17520
HF	-100.35047	**10a**	-150.01162
CH_3FH^+	-139.77879	**TS:10a→10b**	-149.98271
CH_3F	-139.55383	**10b**	-150.01764
H_2	-1.16597	**TS:10b→10b'**	-150.00895
CH_5^+	-40.61363	**TS:10b→10c**	-150.01390
CH_4	-40.40930	**10c**	-150.00967
N_2	-109.39404	**TS1:10b→10b"**	-150.01891
N_2H^+	-109.58005	**TS2:10b→10b"**	-150.01191
HCl	-460.34044	**11a**	-258.24340
CH_3ClH^+	-499.79815	**TS:11a→11b**	-258.22016
CH_3Cl	-499.55321	**TS:11b→11b'**	-258.23985
H_2O	-76.33233	**12a**	-609.19255
$CH_3OH_2^+$	-115.81794	**TS:12a→12b**	-609.17521
CH_3OH	-115.53438	**12b**	-609.19650
8	-148.84468	**TS:12b→12b'**	-609.19198
TS:8→8'	-148.78662	**13a**	-225.19460
9a	-249.20838	**TS:13a→13b**	-225.18143
TS:9a→9b	-249.18053	**13b**	-225.21714
9b	-249.17970	**TS:13b→13b'**	-225.21603

Table A5.3 GAUSSIAN Archive Entries of MP2/6-31G(d,p) Optimized Geometries for Species Related to Proton Transport from Chapter 7

1

1\1\ ANU-PC\FOpt\RMP2-FU\6-31G(d,p)\H1N2(1+)\AJC501\06-Jun-1996\0\\#MP
2=FULL 6-31G** OPT TEST GEOM=ALLCHECK GUESS=CHECK\\N2H+\\1,1\N,0.,0.,-
0.6683381088\N,0.,0.,0.4552838841\H,0.,0.,1.4913795728\\Version=SGI-G9
4RevD.1\State=1-SG\HF=-109.1270568\MP2=-109.4597475\RMSD=7.886e-09\RMS
F=5.761e-05\Dipole=0.,0.,1.2750847\PG=C*V [C*(H1N1N1)]\\@

TS:1→1'

1\1\ ANU-PC\FOpt\RMP2-FU\6-31G(d,p)\H1N2(1+)\AJC501\22-Jul-1996\1\\#MP
2=FULL 6-31G** OPT=Z-MATRIX FREQ=NORAMAN TEST GEOM=ALLCHECK GUESS=CHEC
K\\N2H+ ts\\1,1\N\X,1,NX\H,2,HX,1,90.\N,2,NX,3,90.,1,180.,0\\NX=0.5754
8885\HX=1.14084735\\Version=SGI-G94RevD.1\State=1-A1\HF=-109.0520405\M
P2=-109.3764885\RMSD=5.555e-09\RMSF=9.378e-05\Dipole=0.7771012,0.,0.\P
G=C02V [C2(H1),SGV(N2)]\\@

2

1\1\ ANU-PC\FOpt\RMP2-FU\6-31G(d,p)\Ar1H1N2(1+)\AJC501\22-Jul-1996\1\\
#MP2=FULL 6-31G** OPT=Z-MATRIX FREQ=NORAMAN TEST GEOM=ALLCHECK GUESS=C
HECK\\[N2H Ar]+\\1,1\N\N,1,NN\X,2,1.,1,90.\H,2,NH,3,90.,1,180.,0\X,4,1
.,2,90.,3,0.,0\Ar,4,ArH,5,90.,2,180.,0\\NN=1.12381766\NH=1.06363004\Ar
H=1.99898783\\Version=SGI-G94RevD.1\State=1-SG\HF=-635.9045155\MP2=-63
6.3888078\RMSD=1.510e-09\RMSF=2.610e-05\Dipole=0.,0.,-1.7720568\PG=C*V
[C*(N1N1H1Ar1)]\\@

TS:2→2'

1\1\GINC-PC\FOpt\RMP2-FU\6-31G(d,p)\Ar1H1N2(1+)\AJC501\21-May-1997\1\\
#MP2=FULL 6-31G** OPT=Z-MATRIX TEST GEOM=ALLCHECK GUESS=CHECK FREQ=NOR
AMAN\\[N2H Ar]+ ts\\1,1\N\X,1,NX\H,2,HX,1,90.\N,2,NX,3,90.,1,180.,0\X,
3,1.,2,90.,1,90.,0\Ar,3,ArH,5,90.,2,180.,0\\NX=0.56707121\HX=1.9115707
2\ArH=1.29706193\\Version=SGI-G94RevD.4\State=1-A1\HF=-635.8486997\MP2
=-636.3357614\RMSD=7.659e-09\RMSF=1.147e-04\Dipole=0.9975099,0.,0.\PG=
C02V [C2(H1Ar1),SGV(N2)]\\@

3

1\1\ ANU-PC\FOpt\RMP2-FU\6-31G(d,p)\C1H1N2O1(1+)\AJC501\04-Jun-1996\0\
\#MP2=FULL 6-31G** OPT TEST\\[N2 HOC]+\\1,1\O,0.,0.,1.3065749669\C,0.,
0.,2.4656863701\H,0.,0.,-0.1173330867\N,0.,0.,-1.2329499839\N,0.,0.,-2
.3569621402\\Version=SGI-G94RevD.1\State=1-SG\HF=-221.8869959\MP2=-222
.5121021\RMSD=3.467e-09\RMSF=4.014e-06\Dipole=0.,0.,-0.7314917\PG=C*V
[C*(N1N1H1O1C1)]\\@

TS:3→3'

1\1\GINC-VPP11\FOpt\RMP2-FU\6-31G(d,p)\C1H1N2O1(1+)\AJC501\23-May-1997
\1\\# MP2=FULL 6-31G** OPT=Z-MATRIX TEST FREQ=NORAMAN MAXDISK=78643200
\\[N2H+ OC] ts\\1,1\N\X,1,NX\H,2,HX,1,90.\N,2,NX,3,90.,1,180.,0\X,3,1.
,2,90.,1,90.,0\O,3,OH,5,90.,2,180.,0\X,6,1.,3,90.,5,0.,0\C,6,OC,7,90.,
3,180.,0\\NX=0.56686744\HX=1.91543514\OH=1.01763553\OC=1.1672208\\Vers
ion=Fujitsu-VP-Unix-G94RevE.2\State=1-A1\HF=-221.8570223\MP2=-222.4694
052\RMSD=6.814e-09\RMSF=6.526e-05\Dipole=1.40436,0.,0.\PG=C02V [C2(H1O
1C1),SGV(N2)]\\@

4

1\1\GINC-PC\FOpt\RMP2-FU\6-31G(d,p)\F1H2N2(1+)\AJC501\30-Jul-1996\1\\#
MP2=FULL 6-31G** OPT=Z-MATRIX GEOM=ALLCHECK GUESS=CHECK\\[N2H FH]+\\1
,1\N\N,1,NN\X,2,1.,1,90.\H,2,NH,3,HNX,1,180.,0\X,4,1.,2,90.,3,0.,0\F,4
,HF1,5,FHX,2,180.,0\H,6,HF2,4,HFH,5,180.,0\\NN=1.12496805\NH=1.2219993
9\HF1=1.19142463\HF2=0.94481851\HNX=88.7586466\FHX=84.30156746\HFH=119
.56132814\\Version=SGI-G94RevD.3\State=1-A'\HF=-209.180519\MP2=-209.70
79877\RMSD=7.449e-09\RMSF=3.583e-05\Dipole=-0.6954274,0.,0.9203392\PG=
CS [SG(F1H2N2)]\\@

TS:4→4'

```
1\1\GINC-PC\FTS\RMP2-FU\6-31G(d,p)\F1H2N2(1+)\AJC501\30-Jul-1996\0\\#M
 P2=FULL 6-31G** TEST OPT=(CALCFC,TS,NOEIGEN) FREQ=NORAMAN GEOM=ALLCHEC
 K GUESS=CHECK\\[N2H+ FH] ts\\1,1\N,0.6271844917,-1.2106994468,0.\N,-0.
 5040198711,-1.2854909028,0.\H,0.0301209904,0.6642005584,0.\F,0.0006498
 622,1.6464499149,0.\H,-0.8981220939,1.9910826551,0.\\Version=SGI-G94Re
 vD.3\State=1-A'\HF=-209.1530215\MP2=-209.6727948\RMSD=3.792e-09\RMSF=1
 .258e-04\Dipole=-0.8696256,1.9235369,0.\PG=CS [SG(F1H2N2)]\\@
5
 1\1\ ANU-PC\FOpt\RMP2-FU\6-31G(d,p)\H1N4(1+)\AJC501\19-Jul-1996\1\\# M
 P2=FULL 6-31G** OPT=Z-MATRIX FREQ=NORAMAN TEST GEOM=ALLCHECK GUESS=CHE
 CK\\[N2 HN2]+\\1,1\N\N,1,NN1\X,2,1.,1,90.\H,2,HN1,3,90.,1,180.,0\X,4,1
 .,2,90.,3,0.,0\N,4,HN2,5,90.,2,180.,0\X,6,1.,4,90.,5,0.,0\N,6,NN2,7,90
 .,4,180.,0\\NN1=1.1260727\NN2=1.1260761\HN1=1.27326808\HN2=1.27337231\
 \Version=SGI-G94RevD.1\State=1-SG\HF=-218.0811692\MP2=-218.7522564\RMS
 D=3.303e-09\RMSF=1.412e-05\Dipole=0.,0.,-0.0002268\PG=C*V [C*(N1N1H1N1
 N1)]\\@
```

TS:5→5'

```
 1\1\ ANU-PC\Freq\RMP2-FU\6-31G(d,p)\H1N4(1+)\AJC501\19-Jul-1996\1\\#N
 GEOM=ALLCHECK GUESS=READ TEST RMP2(FULL)/6-31G(D,P) FREQ\\[N2H+ N2] ts
 \\1,1\N\X,1,NX\H,2,HX,1,90.\N,2,NX,3,90.,1,180.,0\X,3,1.,2,90.,1,90.,0
 \N,3,NH,5,90.,2,180.,0\X,6,1.,3,90.,5,0.,0\N,6,NN,7,90.,3,180.,0\\NX=0
 .56639456\HX=2.115683\NH=1.04598436\NN=1.1235067\\Version=SGI-G94RevD.
 1\State=1-A1\HF=-218.064674\MP2=-218.7268383\RMSD=5.494e-10\RMSF=5.985
 e-05\Dipole=1.5845717,0.,0.\DipoleDeriv=-0.0989721,0.,0.0758221,0.,0.0
 471032,0.,0.139539,0.,0.0655293,1.2328703,0.,0.,0.,0.3971844,0.,0.,0.,
 0.3640975,-0.0989721,0.,-0.0758221,0.,0.0471032,0.,-0.139539,0.,0.0655
 292,-0.6707977,0.,0.,0.,0.2766406,0.,0.,0.,0.2764224,0.6358716,0.,0.,0
 .,0.2319685,0.,0.,0.,0.2284216\Polar=25.4497517,0.,11.4900094,0.,0.,17
 .9748336\PG=C02V [C2(H1N1N1),SGV(N2)]\\@
```

6

```
 1\1\ ANU-PC\FOpt\RMP2-FU\6-31G(d,p)\C1H1N2O1(1+)\AJC501\04-Jun-1996\0\
 \#MP2=FULL 6-31G** OPT TEST\\[N2 HCO]+\\1,1\C,0.,0.,1.4108138741\O,0.,
 0.,2.542857231\H,0.,0.,0.2882780748\N,0.,0.,-1.5140857559\N,0.,0.,-2.6
 424884108\\Version=SGI-G94RevD.1\State=1-SG\HF=-221.9094887\MP2=-222.5
 503934\RMSD=4.530e-09\RMSF=9.266e-06\Dipole=0.,0.,1.493695\PG=C*V [C*(
 N1N1H1C1O1)]\\@
```

TS:6→6'

```
 1\1\GINC-VPP11\FOpt\RMP2-FU\6-31G(d,p)\C1H1N2O1(1+)\AJC501\23-May-1997
 \1\\# MP2=FULL 6-31G** OPT=Z-MATRIX TEST FREQ=NORAMAN MAXDISK=78643200
 \\[N2H+ OC] ts\\1,1\N\X,1,NX\H,2,HX,1,90.\N,2,NX,3,90.,1,180.,0\X,3,1.
 ,2,90.,1,90.,0\O,3,OH,5,90.,2,180.,0\X,6,1.,3,90.,5,0.,0\C,6,OC,7,90.,
 3,180.,0\\NX=0.56686744\HX=1.91543514\OH=1.01763553\OC=1.1672208\\Vers
 ion=Fujitsu-VP-Unix-G94RevE.2\State=1-A1\HF=-221.8570223\MP2=-222.4694
 052\RMSD=6.814e-09\RMSF=6.526e-05\Dipole=1.40436,0.,0.\PG=C02V [C2(H1O
 1C1),SGV(N2)]\\@
```

7

```
 1\1\ ANU-PC\POpt\RMP2-FU\6-31G(d,p)\H3N2O1(1+)\AJC501\19-Jul-1996\1\\#
 MP2=FULL 6-31G** OPT=Z-MATRIX GEOM=ALLCHECK GUESS=CHECK\\[H2O HN2]+\\1
 ,1\N\N,1,NN\X,2,1.,1,90.\H,2,HN,3,90.,1,180.,0\X,4,1.,2,90.,3,0.,0\O,4
 ,OH1,5,90.,2,180.,0\H,6,OH2,4,HOH,5,HOHX,0\H,6,OH2,4,HOH,5,-HOHX,0\\NN
 =1.12796345\HN=1.69488088\OH1=1.00897454\OH2=0.97502783\HOH=113.481655
 69\HOHX=64.5113143\\Version=SGI-G94RevD.1\State=1-A'\HF=-185.2566146\M
 P2=-185.7891983\RMSD=8.719e-09\RMSF=2.628e-04\Dipole=0.6395305,0.,2.51
 40028\PG=CS [SG(H1N2O1),X(H2)]\\@
```

TS:7→7'

```
 1\1\ ANU-PC\FOpt\RMP2-FU\6-31G(d,p)\H3N2O1(1+)\AJC501\19-Jul-1996\1\\#
 MP2=FULL 6-31G** OPT=Z-MATRIX GEOM=ALLCHECK GUESS=CHECK FREQ=NORAMAN\\
 [H2O HN2]+ ts\\1,1\N\X,1,XN\H,2,HX,1,90.\N,2,XN,3,90.,1,180.,0\X,3,1.,
 2,90.,1,90.,0\O,3,OH,5,OHX,2,180.,0\H,6,OH2,3,HOH,5,HOHX,0\H,6,OH2,3,H
 OH,5,-HOHX,0\\XN=0.56598215\HX=2.24961157\OH=0.98137873\OH2=0.97789776
 \OHX=90.74897261\HOH=112.62482688\HOHX=64.27646115\\Version=SGI-G94Rev
```

```
D.1\State=1-A'\HF=-185.2460487\MP2=-185.7740776\RMSD=1.624e-09\RMSF=7.
380e-05\Dipole=2.9110894,0.6542595,0.\PG=CS [SG(H1O1),X(H2N2)]\\@
```

Table A5.4 GAUSSIAN Archive Entries of MP2/6-31G(d) Optimized Geometries for Species Related to Methyl-Cation Transport from Chapter 7

8

1\1\GINC-PC\FOpt\RMP2-FU\6-31G(d)\C1H3N2(1+)\AJC501\27-May-1997\0\\#N
GEOM=ALLCHECK GUESS=READ TEST MP2(FULL)/6-31G(D) OPT=RCFC\\CH3NN+\\1,1
\C,0.,0.,1.1928212153\H,1.0486587588,0.,1.4954746453\H,-0.5243293794,0
.9081651251,1.4954746453\H,-0.5243293794,-0.908165125,1.4954746453\N,0
.,0.,-0.2678646587\N,0.,0.,-1.395471231\\Version=SGI-G94RevD.4\HF=-148
.2053404\MP2=-148.6661193\RMSD=2.156e-09\RMSF=4.556e-05\Dipole=0.,0.,0
.8323273\PG=C03V [C3(C1N1N1),3SGV(H1)]\\@

TS:8→8'

1\1\GINC-RSCQC2\FOpt\RMP2-FU\6-31G(d)\C1H3N2(1+)\ACHALK\09-Jan-1998\0\
\#MP2=FULL 6-31G* OPT FREQ=NORAMAN MAXDISK=786432000\\CH3N2+ ts\\1,1\C
,-0.0003481741,-0.0004233913,-1.3840094779\H,0.9394103918,0.5430406087
,-1.441503894\H,-0.0003613616,-1.0856633913,-1.4364304763\H,-0.9401355
487,0.5430406087,-1.4410310583\N,0.5687708079,0.0001516087,0.901501421
6\N,-0.5683171561,0.0001516087,0.9017874778\\Version=IBM-RS6000-G94Rev
E.1\State=1-A'\HF=-148.1651947\MP2=-148.6006459\RMSD=6.190e-09\RMSF=1.
240e-05\Dipole=-1.9188938,0.,-0.0013276\PG=CS [SG(C1H1),X(H2N2)]\\@

9a

1\1\ ANU-PC\Freq\RMP2-FU\6-31G(d)\C1H4F1N2(1+)\AJC501\11-Nov-1996\1\\#
MP2=FULL 6-31G* FREQ=NORAMAN MAXDISK=250000000\\[HF CH3 N2]+\\1,1\N\N,
1,NN\X,2,1.,1,90.\C,2,CN,3,90.,1,180.,0\H,4,CH,2,HCN,3,0.,0\H,4,CH,2,H
CN,3,-120.,0\H,4,CH,2,HCN,3,120.,0\X,4,1.,2,90.,3,0.,0\F,4,CF,8,90.,2,
180.,0\X,9,1.,4,90.,8,0.,0\H,9,FH,10,90.,5,180.,0\\NN=1.12742624\CN=1.
46459538\CH=1.0895707\CF=2.5713901\FH=0.93943659\HCN=106.31696454\\Ver
sion=SGI-G94RevD.3\HF=-248.2232632\MP2=-248.8680645\RMSD=9.029e-09\RMS
F=1.633e-05\Dipole=0.,0.,0.3167189\\PG=C03V[C3(N1N1C1F1H1),3SGV(H1)]\\@

TS:9a→9b

1\1\GINC-PC\FTS\RMP2-FU\6-31G(d)\C1H4F1N2(1+)\AJC501\09-Jan-1997\0\\#M
P2=FULL 6-31G* FREQ=NORAMAN OPT=(CALCFC,TS,NOEIGEN) MAXDISK=5000000000
\\[HF CH3N2]+ -> [HF CH3N2]+ ts\\1,1\N,-2.7090503334,-0.0070998427,0.\
N,-1.5803451899,-0.0178034099,0.\C,0.5344014727,-0.0143293999,0.\H,0.5
183523448,-0.5497510482,0.937992949\H,0.5183523448,-0.5497510482,-0.93
7992949\H,0.5183952241,1.0659906506,0.\F,2.4707171268,0.106562481,0.\H
,3.0278057726,-0.6652517152,0.\\Version=SGI-G94RevD.4\State=1-A'\HF=-2
48.2122546\MP2=-248.8433037\RMSD=7.179e-09\RMSF=1.207e-05\Dipole=1.294
9853,-0.6663427,0.\PG=CS [SG(C1H2F1N2),X(H2)]\\@

9b

1\1\GINC-PC\FOpt\RMP2-FU\6-31G(d)\C1H4F1N2(1+)\AJC501\08-Jan-1997\0\\#
MP2=FULL 6-31G* FREQ=NORAMAN OPT MAXDISK=5000000000\\[HFCH3 N2]+\\1,1\
N,0.04481866,0.,-2.9336019657\N,0.0230877231,0.,-1.8043808781\C,-0.009
1964844,0.,0.8906203315\H,1.0589382958,0.,0.7188119497\H,-0.5324381121
,-0.9269075883,0.6928213228\H,-0.5324381121,0.9269075883,0.6928213228\
F,0.044802375,0.,2.5281634622\H,-0.8174492216,0.,2.9642321614\\Version
=SGI-G94RevD.4\State=1-A'\HF=-248.2146682\MP2=-248.8477488\RMSD=3.956e
-09\RMSF=6.549e-05\Dipole=-0.771234,0.,2.6831009\PG=CS [SG(C1H2F1N2),X
(H2)]\\@

TS:9b→9b'

1\1\ ANU-PC\FOpt\RMP2-FU\6-31G(d)\C1H4F1N2(1+)\AJC501\11-Nov-1996\1\\#
 MP2=FULL 6-31G* FOPT=(Z-MATRIX,CALCFC) FREQ=NORAMAN GEOM=CHECK GUESS=
CHECK MAXDISK=250000000\\HF CH3N2]+ ts\\1,1\X\N,1,NX\C,1,CX,2,90.\N,1,
NX,3,90.,2,180.,0\X,3,1.,1,90.,2,90.,0\F,3,FC,5,FCX,1,180.,0\X,6,1.,3,
90.,5,0.,0\H,6,HF,7,HFX,3,180.,0\H,3,CH1,1,CHX1,5,0.,0\H,3,CH2,1,CHX2,
5,CHXX,0\H,3,CH2,1,CHX2,5,-CHXX,0\\NX=0.56546313\CX=3.06589088\FC=1.60
919905\HF=0.9687082\CH1=1.08330086\CH2=1.08415639\CHX1=81.23566206\CHX
2=77.79534611\CHXX=119.11339228\FCX=89.47685567\HFX=155.34789938\\Vers
ion=SGI-G94RevD.3\State=1-A'\HF=-248.2088942\MP2=-248.8414259\RMSD=2.6

85e-09\RMSF=4.994e-06\Dipole=2.7581301,0.7612811,0.\PG=CS [SG(C1H2F1),
X(H2N2)]\\@

10a

1\1\GINC-VPP12\FOpt\RMP2-FU\6-31G(d)\C1H5N2(1+)\AJC501\06-Mar-1997\0\\
MP2=FULL 6-31G* TEST OPT=CALCFC FREQ=NORAMAN MAXDISK=10485760 OPTCYC
=60\\[H2 CH3N2]+\\1,1\N,-1.7519117037,-0.0200208065,-0.0026593227\N,-0
.6245038776,-0.0030596143,-0.0006749276\C,0.8366562927,0.0187918748,0.
0018916423\H,1.1418127635,-0.0309622929,-1.0446623165\H,1.1241386154,0
.9574349117,0.4785582075\H,1.1514402812,-0.8559322546,0.5733974706\H,4
.0981245002,0.2750158377,0.2361862966\H,4.0994551526,-0.2967445052,-0.
2314897595\\Version=Fujitsu-VP-Unix-G94RevD.4\HF=-149.3325527\MP2=-149
.8108434\RMSD=5.466e-09\RMSF=8.421e-07\Dipole=0.1837941,0.0132634,0.00
06491\PG=C01 [X(C1H5N2)]\\@

TS:10a→10b

1\1\GINC-VPP08\FTS\RMP2-FU\6-31G(d)\C1H5N2(1+)\AJC501\06-Apr-1998\0\\#
MP2=FULL 6-31G* OPT=(TS,READFC,NOEIGEN) FREQ=NORAMAN TEST MAXDISK=131
07200 GEOM=CHECK\\[H2 CH3N2]+ -> [H2CH3 N2]+ ts\\1,1\N,1.8995295305,-0
.0002257102,0.0333114582\N,0.7706227349,0.0002597867,0.013500894\C,-1.
3849044712,-0.0003641513,-0.0242715842\H,-1.3641152314,1.0833458664,-0
.0361634393\H,-1.345543624,-0.5464900067,-0.9584786826\H,-1.3784675509
,-0.525617709,0.9225913838\H,-3.148461083,0.3751160651,-0.0550403077\H
,-3.1450515417,-0.3844078434,-0.0549659148\\Version=Fujitsu-VP-Unix-G9
4RevE.2\HF=-149.3108796\MP2=-149.7746718\RMSD=6.501e-09\RMSF=8.086e-07
\Dipole=2.4025626,0.0009084,0.0211297\PG=C01 [X(C1H5N2)]\\@

10b

1\1\GINC-PC\FOpt\RMP2-FU\6-31G(d)\C1H5N2(1+)\AJC501\18-Feb-1997\0\\# M
P2=FULL 6-31G* TEST OPT FREQ=NORAMAN OPTCYC=80 MAXDISK=5000000000\\[H2
CH3 N2]+\\1,1\N,-2.1154024027,-0.0684425545,0.\N,-0.9948466197,0.06862
6165,0.\C,2.0558476486,-0.0802925929,0.\H,2.0213875934,-0.6439548627,0
.9311282737\H,2.0213875934,-0.6439548627,-0.9311282737\H,0.8914616824,
0.2629237451,0.\H,2.9684242083,0.5370680361,0.\H,1.5339961879,0.968388
2276,0.\\Version=SGI-G94RevD.4\State=1-A'\HF=-149.3307232\MP2=-149.812
0496\RMSD=2.196e-09\RMSF=4.364e-05\Dipole=2.5918065,0.4569157,0.\PG=CS
[SG(C1H3N2),X(H2)]\\@

TS:10b→10b'

1\1\GINC-VPP12\FTS\RMP2-FU\6-31G(d)\C1H5N2(1+)\AJC501\07-Mar-1997\0\\#
MP2=FULL 6-31G* OPT=(CALCFC,NOEIGEN,TS) FREQ=NORAMAN TEST MAXDISK=157
28640\\[H2CH3 N2]+ N2 rotation ts\\1,1\N,-0.7659324246,-1.3854126965,0
.\N,0.3289232178,-1.670792048,0.\C,0.2136335194,2.0362871041,0.\H,-0.3
275150461,2.1732891219,-0.9355599438\H,-0.3275150461,2.1732891219,0.93
55599438\H,0.2465269658,0.8525035791,0.\H,1.08185395,2.7194230145,0.\H
,1.1039125072,1.2572057488,0.\\Version=Fujitsu-VP-Unix-G94RevD.4\State
=1-A'\HF=-149.322559\MP2=-149.8006027\RMSD=4.889e-09\RMSF=1.992e-05\Di
pole=0.8656198,2.8277793,0.\PG=CS [SG(C1H3N2),X(H2)]\\@

TS:10b→10c

1\1\GINC-VPP12\FTS\RMP2-FU\6-31G(d)\C1H5N2(1+)\AJC501\02-Apr-1998\0\\#
MP2=FULL 6-31G* OPT=(CALCFC,TS,ADDREDUNDANT,NOEIGEN) FREQ=NORAMAN TEST
MAXDISK=13107200\\CH5 N2]+ -> [CH4 HN2]+ ts\\1,1\N,-1.9543607025,-0.1
197338847,0.\N,-0.8431517751,0.067971143,0.\C,1.888446365,-0.019924814
6,0.\H,1.7770295296,-0.5990586016,0.9164351957\H,1.7770295296,-0.59905
86016,-0.9164351957\H,0.4333091067,0.2807285315,0.\H,2.893087732,0.418
7221944,0.\H,1.371453255,0.9805545564,0.\\Version=Fujitsu-VP-Unix-G94R
evE.2\State=1-A'\HF=-149.3183315\MP2=-149.8050398\RMSD=4.696e-09\RMSF=
1.052e-05\Dipole=0.8321483,0.3121779,0.\PG=CS [SG(C1H3N2),X(H2)]\\@

10c

1\1\GINC-VPP03\FOpt\RMP2-FU\6-31G(d)\C1H5N2(1+)\AJC501\27-May-1998\0\\
#MP2=FULL 6-31G* OPT=READFC TEST FREQ=NORAMAN MAXDISK=19660800\\N2H CH
4]+\\1,1\N,2.0551838908,-0.0031797759,0.\N,0.9312036228,0.0016823759,0
.\C,-2.0660050369,0.0008721291,0.\H,-1.4942431922,0.9415863363,0.\H,-2
.6760188137,0.0004938147,-0.902074577\H,-0.1692022114,0.001910105,0.\H
,-2.6760188137,0.0004938147,0.902074577\H,-1.4931993424,-0.9392350458,

0.\\Version=Fujitsu-VP-Unix-G94RevE.2\State=1-A'\HF=-149.3267877\MP2=-
149.807386\RMSD=8.170e-09\RMSF=4.618e-05\Dipole=0.3168607,0.0011617,0.
\PG=CS [SG(C1H3N2),X(H2)]\\@

TS1:10b→10b"

1\1\GINC-RSCQC8\FOpt\RMP2-FU\6-31G(d)\C1H5N2(1+)\ACHALK\30-Apr-1998\1\
\#MP2=FULL 6-31G* OPT=Z-MATRIX FREQ MAXDISK=1048576000\\N2 CH5]+ H fli
pping ts\\1,1\N\N,1,NN\X,2,1.,1,90.\H,2,NH,3,90.,1,180.,0\X,4,1.,2,90.
,3,0.,0\C,4,CH,5,90.,2,180.,0\H,6,CH1,4,HCH1,5,0.,0\H,6,CH1,4,HCH1,5,1
80.,0\H,6,CH2,4,HCH2,5,90.,0\H,6,CH2,4,HCH2,5,-90.,0\\NN=1.12895112\NH
=1.90207554\CH=1.18465781\CH1=1.12454678\CH2=1.08882339\HCH1=62.257263
33\HCH2=120.27563477\\Version=IBM-RS6000-G94RevE.1\State=1-A1\HF=-149.
3275267\MP2=-149.8116651\RMSD=8.139e-09\RMSF=5.279e-05\Dipole=0.,0.,2.
3974765\PG=C02V [C2(C1H1N1N1),SGV(H2),SGV'(H2)]\\@

TS2:10b→10b"

1\1\GINC-VPP03\FOpt\RMP2-FU\6-31G(d)\C1H5N2(1+)\AJC501\07-May-1998\0\\
#MP2=FULL 6-31G* OPT=READFC FREQ=NORAMAN MAXDISK=13107200 GEOM=CHECK G
UESS=CHECK\\[N2 CH5]+ out of plane H scrambling ts\\1,1\N,0.0800694184
,0.,-2.3361716105\N,0.0656984036,0.,-1.2068476598\H,-0.109536777,0.,1.
106399205\C,-0.1871792408,0.,2.1917444352\H,0.8044993769,0.4698308086,
2.6424131546\H,0.804499377,-0.4698308086,2.6424131546\H,-0.6983806431,
0.8680953518,2.6297213831\H,-0.6983806431,-0.8680953518,2.6297213831\\
Version=Fujitsu-VP-Unix-G94RevE.2\State=1-A'\HF=-149.3256711\MP2=-149.
8039882\RMSD=8.459e-09\RMSF=4.207e-06\Dipole=0.4225711,0.,4.317227\PG=
CS [SG(C1H1N2),X(H4)]\\@

11a

1\1\ ANU-PC\FOpt\RMP2-FU\6-31G(d)\C1H3N4(1+)\AJC501\14-Nov-1996\1\\#MP
2=FULL 6-31G* FREQ=NORAMAN FOPT=Z-MATRIX MAXDISK=5000000000\\[N2 CH3 N
2]+\\1,1\N\N,1,NN\X,2,1.,1,90.\C,2,CN,3,90.,1,180.,0\H,4,CH,2,CHN,3,0.
,0\H,4,CH,2,CHN,3,-120.,0\H,4,CH,2,CHN,3,120.,0\X,4,1.,2,90.,3,0.,0\N,
4,CN2,8,90.,2,180.,0\X,9,1.,4,90.,8,0.,0\N,9,NN2,10,90.,5,180.,0\\NN=1
.12747876\CN=1.4651149\CH=1.09031911\CN2=2.97185965\NN2=1.12981085\CHN
=106.08374057\\Version=SGI-G94RevD.3\HF=-257.1442852\MP2=-257.9336662\
RMSD=4.851e-09\RMSF=1.254e-04\Dipole=0.,0.,-2.2368634\PG=C03V [C3(N1N1
C1N1N1),3SGV(H1)]\\@

TS:11a→11b

1\1\GINC-PC\FOpt\RMP2-FU\6-31G(d)\C1H3N4(1+)\AJC501\08-Jan-1997\1\\#MP
2=FULL 6-31G* FREQ=NORAMAN FOPT=Z-MATRIX MAXDISK=5000000000\\[N2 CH3N2
]+ ts for methyl transfer\\1,1\N\N,1,NN\X,2,1.,1,90.\C,2,CN,3,90.,1,18
0.,0\H,4,CH,2,90.,3,0.,0\H,4,CH,2,90.,3,-120.,0\H,4,CH,2,90.,3,120.,0\
X,4,1.,2,90.,3,0.,0\N,4,CN,8,90.,2,180.,0\X,9,1.,4,90.,8,0.,0\N,9,NN,1
0,90.,5,180.,0\\NN=1.1287131\CN=2.07416173\CH=1.08169779\\Version=SGI-
G94RevD.4\HF=-257.1285202\MP2=-257.9070049\RMSD=2.559e-09\RMSF=3.382e-
05\Dipole=0.,0.,0.\PG=D03H [O(C1),C3(N1N1.N1N1),3C2(H1)]\\@

TS:11b→11b'

1\1\GINC-PC\FTS\RMP2-FU\6-31G(d)\C1H3N4(1+)\AJC501\09-Jan-1997\0\\# MP
2=FULL 6-31G* FREQ=NORAMAN TEST OPT=(CALCFC,TS,NOEIGEN) MAXDISK=500000
0000\\[N2 CH3N2]+ catalytic methyl transfer ts\\1,1\N,-2.7171399035,0.
,0.6793480075\C,0.4780359713,0.,-0.081440992\N,-2.7733898344,0.,-0.449
9402058\H,0.1643059576,0.,0.9639695768\H,0.1809244591,0.9075469551,-0.
6096502024\H,0.1809244591,-0.9075469551,-0.6096502024\N,1.9390760941,0
.,-0.0673331751\N,3.0665435433,0.,-0.0557922294\\Version=SGI-G94RevD.4
\State=1-A'\HF=-257.140452\MP2=-257.9292327\RMSD=8.203e-09\RMSF=2.033e
-06\Dipole=2.160972,0.,-0.1320545\PG=CS [SG(C1H1N4),X(H2)]\\@

12a

1\1\ ANU-PC\FOpt\RHF\6-31G(d)\C1H4Cl1N2(1+)\AJC501\13-Nov-1996\1\\#HF
6-31G* FREQ=NORAMAN FOPT=Z-MATRIX TEST MAXDISK=5000000000\\[HCl CH3 N2
]+\\1,1\N\N,1,NN\X,2,1.,1,90.\C,2,CN,3,CNX,1,180.,0\H,4,CH1,2,HCN1,3,0
.,0\H,4,CH2,2,HCN2,3,HCNX,0\H,4,CH2,2,HCN2,3,-HCNX,0\X,4,1.,2,90.,3,0.
,0\Cl,4,CCl,8,ClCX,2,180.,0\X,9,1.,4,90.,8,0.,0\H,9,ClH,10,HClX,5,180.
,0\\NN=1.07265116\CN=1.51169388\CH1=1.07805886\CCl=3.44794849\ClH=1.26
939304\HCN1=104.97757753\HCN2=104.9769549\CNX=89.99985773\CH2=1.078048

02\ClCX=90.08504509\HClX=86.94014512\HCNX=119.99998271\\Version=SGI-G9
4RevD.3\State=1-A'\HF=-608.2814932\RMSD=2.970e-09\RMSF=1.499e-04\Dipol
e=0.0373017,0.,-2.275994\PG=CS [SG(C1H2Cl1N2),X(H2)]\\@

TS:12a→12b

1\1\ ANU-PC\FTS\RMP2-FU\6-31G(d)\C1H4Cl1N2(1+)\AJC501\16-Dec-1996\1\\#
MP2=FULL 6-31G* FREQ=NORAMAN TEST OPT=(Z-MATRIX,READFC,TS,EF,NOFREEZE)
MAXDISK=5000000000 OPTCYC=80 GEOM=CHECK GUESS=CHECK\\[HCl CH3N2]+ ->
[HClCH3 N2]+\\1,1\N\N,1,NN\X,2,1.,1,90.\C,2,CN,3,CNX,1,180.,0\H,4,CH1,
2,HCN1,3,0.,0\H,4,CH2,2,HCN2,3,HCNX,0\H,4,CH2,2,HCN2,3,-HCNX,0\X,4,1.,
2,90.,3,0.,0\Cl,4,CCl,8,ClCX,2,180.,0\H,9,ClH,4,HClC,5,180.,0\\NN=1.12
886016\CN=2.00035875\CH1=1.081615\CCl=2.43721855\ClH=1.28789018\HCN1=9
1.37599209\HCN2=91.52153863\CNX=89.68028104\CH2=1.08073856\ClCX=87.428
71398\HClC=106.73278868\HCNX=119.67149824\\Version=SGI-G94RevD.3\State
=1-A'\HF=-608.2586274\MP2=-608.8544656\RMSD=5.794e-10\RMSF=5.339e-06\D
ipole=-0.6481996,0.,-0.2429498\PG=CS [SG(C1H2Cl1N2),X(H2)]\\@

12b

1\1\ ANU-PC\FOpt\RMP2-FU\6-31G(d)\C1H4Cl1N2(1+)\AJC501\14-Nov-1996\1\\
#MP2=FULL 6-31G* FREQ=NORAMAN FOPT=(Z-MATRIX,CALCFC,NORAMAN) TEST MAXD
ISK=5000000000\\[HCl CH3 N2]+ Cl started close to C\\1,1\N\N,1,NN\X,2,
1.,1,90.\C,2,CN,3,CNX,1,180.,0\H,4,CH1,2,HCN1,3,0.,0\H,4,CH2,2,HCN2,3,
HCNX,0\H,4,CH2,2,HCN2,3,-HCNX,0\X,4,1.,2,90.,3,0.,0\Cl,4,CCl,8,ClCX,2,
180.,0\X,9,1.,4,90.,8,0.,0\H,9,ClH,10,HClX,5,180.,0\\NN=1.129707\CN=2.
94590032\CH1=1.086902\CCl=1.85663074\ClH=1.2963669\HCN1=74.97261131\HC
N2=74.72827859\CNX=89.21461812\CH2=1.08538773\ClCX=87.67883624\HClX=16
9.40090793\HCNX=119.24471692\\Version=SGI-G94RevD.3\State=1-A'\HF=-608
.2734483\MP2=-608.8765517\RMSD=8.016e-09\RMSF=1.058e-04\Dipole=-0.6128
406,0.,2.4507342\PG=CS [SG(C1H2Cl1N2),X(H2)]\\@

TS:12b→12b'

1\1\GINC-VPP06\Freq\RMP2-FU\6-31G(d)\C1H4Cl1N2(1+)\AJC501\15-Nov-1996\
1\\# MP2=FULL 6-31G* OPT=(Z-MATRIX,CALCALL,TS,EF) TEST MAXDISK=3125000
0\\HCl CH3N2]+ ts\\1,1\N\C,1,B1\N,1,B2,2,A1\Cl,2,B3,3,A2,1,180.,0\H,4,
B4,2,A3,3,0.,0\H,2,B5,1,A4,3,180.,0\H,2,B6,1,A5,6,D4,0\H,2,B6,1,A5,6,-
D4,0\\B1=3.26260522\B2=1.13060756\B3=1.84585675\B4=1.29727161\B5=1.088
17995\B6=1.08643974\A1=80.50176634\A2=175.14517264\A3=100.58508818\A4=
61.95015667\A5=80.96832572\D4=121.68249375\\Version=Fujitsu-VP-Unix-G9
4RevD.4\State=1-A'\HF=-608.2697196\MP2=-608.8724575\RMSD=8.468e-09\RMS
F=9.957e-08\Dipole=0.1859846,0.,2.5205987\PG=CS [SG(C1H2Cl1N2),X(H2)]\
\@

13a

1\1\ ANU-PC\FOpt\RMP2-FU\6-31G(d)\C1H5N2O1(1+)\AJC501\18-Dec-1996\0\\#
MP2=FULL 6-31G* OPT TEST FREQ=NORAMAN MAXDISK=5000000000\\H2OCH3 N2]+\
\1,1\N,-0.0755022935,0.,-3.062385254\N,-0.0385748867,0.,-1.9333571733\
C,0.0168526492,0.,1.0428879188\H,1.0537095855,0.,0.7206379089\H,-0.522
9675211,0.8990338231,0.766909357\H,-0.5229675211,-0.8990338231,0.76690
9357\O,-0.0126614696,0.,2.5652952356\H,0.3954707895,0.802390102,2.9680
254853\H,0.3954707895,-0.802390102,2.9680254853\\Version=SGI-G94RevD.3
\State=1-A'\HF=-224.2756336\MP2=-224.9195791\RMSD=5.196e-09\RMSF=4.252
e-05\Dipole=0.6852352,0.,3.7377426\PG=CS [SG(C1H1N2O1),X(H4)]\\@

TS:13a→13b

1\1\GINC-VPP09\PTS\RMP2-FU\6-31G(d)\C1H5N2O1(1+)\AJC501\06-Jan-1997\1\
\#MP2=FULL 6-31G* OPT=(NOFREEZE,READFC,EF,Z-MATRIX,TS) MAXDISK=2125000
0 TEST FREQ=NORAMAN GEOM=CHECK\\H2OCH3 N2]+ -> H2O CH3N2]+ ts\\1,1\N\N
,1,NN\X,2,1.,1,90.\C,2,CN,3,CNX,1,180.,0\X,4,1.,2,90.,3,0.,0\H,4,CH1,1
,HCN1,5,0.,0\H,4,CH2,1,HCN2,5,HCNX,0\H,4,CH2,1,HCN2,5,-HCNX,0\O,4,CO,5
,OCX,2,180.,0\H,9,OH1,4,OHC1,5,OHCX,0\H,9,OH2,4,OHC2,5,-OHCX,0\\NN=1.1
2808315\CN=1.85097965\CO=2.12491213\OH1=0.97388943\OH2=0.97388943\CH1=
1.07930891\CH2=1.0798509\HCN1=94.46933932\HCN2=94.32892125\HCNX=120.41
312609\CNX=90.1948704\OCX=92.1160025\OHC1=123.38977081\OHC2=123.389770
81\OHCX=72.80954245\\Version=Fujitsu-VP-Unix-G94RevD.4\State=1-A'\HF=-
224.2342212\MP2=-224.8784935\RMSD=7.984e-09\RMSF=1.056e-05\Dipole=0.34
10597,0.,1.003631\PG=CS [SG(C1H1N2O1),X(H4)]\\@

13b

1\1\ ANU-PC\FOpt\RMP2-FU\6-31G(d)\C1H5N2O1(1+)\AJC501\03-Jan-1997\0\\#
MP2=FULL 6-31G* OPT TEST FREQ=NORAMAN MAXDISK=5000000000\\H2O CH3N2]+\
\1,1\N,-0.0766748386,0.,-2.5921808561\N,-0.0837004473,0.,-1.4647609457
\C,-0.0851303599,0.,0.0099382931\H,0.9579529555,0.,0.3196639792\H,-0.6
121708903,0.9044363669,0.3079659507\H,-0.6121708903,-0.9044363669,0.30
79659507\O,0.1814336037,0.,2.6207523873\H,0.2241645783,0.7642601533,3.
2186739375\H,0.2241645783,-0.7642601533,3.2186739375\\Version=SGI-G94R
evD.3\State=1-A'\HF=-224.236728\MP2=-224.8895247\RMSD=4.078e-09\RMSF=1
.561e-05\Dipole=-0.063802,0.,-0.1464199\PG=CS [SG(C1H1N2O1),X(H4)]\\@

TS:13b→13b'

1\1\GINC-VPP05\FTS\RMP2-FU\6-31G(d)\C1H5N2O1(1+)\AJC501\06-Jan-1997\1\
\# MP2=FULL 6-31G* OPT=(TS,CALCFC,NOFREEZE,NORAMAN,EF) MAXDISK=2750000
0 FREQ=NORAMAN TEST\\H2OCH3 N2]+ ts\\1,1\N\C,1,B1\N,1,B2,2,A1\O,2,B3,1
,A2,3,D1,0\H,4,B4,2,A3,1,D2,0\H,4,B5,2,A4,5,D3,0\H,2,B6,1,A5,4,D4,0\H,
2,B7,1,A6,4,D5,0\H,2,B8,1,A7,4,D6,0\\B1=3.28792749\B2=1.13059455\B3=1.
51626086\B4=0.98666825\B5=0.98666783\B6=1.08530794\B7=1.08531024\B8=1.
0866476\A1=80.09301245\A2=168.91973887\A3=113.69757124\A4=113.69733333
\A5=64.6308505\A6=81.65895047\A7=76.82893538\D1=-151.91515126\D2=-54.4
2947168\D3=-125.51952276\D4=4.29028399\D5=123.50236731\D6=-119.9534413
9\\Version=Fujitsu-VP-Unix-G94RevD.4\HF=-224.2723532\MP2=-224.9157332\
RMSD=7.241e-09\RMSF=6.595e-07\Dipole=-0.6348278,0.5449064,3.6194626\PG
=C01 [X(C1H5N2O1)]\\@